Acetate assisted C-H activation: Mechanism, Scope and Applications

Thesis submitted for the degree of

Doctor of Philosophy

at the University of Leicester

by

Youcef Boutadla

Department of Chemistry

University of Leicester

May 2010

Title : Acetate-assisted C-H activation: Mechanism, Scope and applications

Author Youcef Boutadla

ABSTRACT

This thesis describes mechanistic investigations of acetate assisted C-H activation, the synthesis of cyclometallated complexes containing nitrogen donor ligands *via* this method and the applications of cyclometallated complexes in terms of insertion reactions.

Chapter one introduces the synthesis, by C-H activation, of cyclometallated complexes containing C,N bidentate ligands of palladium, ruthenium, rhodium and iridium. The introduction also gives an overview on the mechanisms of C-H activation and the applications of C-H activation in catalysis, particularly in direct arylation.

Chapter two provides an introduction to the synthesis of arene ruthenium and Cp*M (M = Ir, Rh) half sandwich cyclometallated complexes). The scope of cyclometallation *via* acetate-assisted C-H activation with different directing groups (pyrazole, pyridine, imines, imidazole, oxazoline and triazole) is discussed. The methodology is extended to six membered rings, non aromatic sp^2 and sp^3 C-H bonds. Mechanistic investigations using bidentate ligands showed that chelating ligands can prevent the C-H activation process.

Chapter three describes a joint computational and experimental study of the cyclometallation reactions of dimethylbenzylamine (DMBA) with $[IrCl_2Cp^*]_2$ using a range of chelating bases. DFT calculations show that facile C-H bond cleavage occurs *via* 'ambiphilic metal ligand activation' (AMLA) and the ease of C-H activation is governed by the accessibility of the κ2-κ1 base displacement step; thus, more weakly coordinating bases promote C-H activation.

Chapter four reports the reactivity of cyclometallated half-sandwich complexes (synthesised in chapter two). Alkynes are shown to insert into the M-C bond. In some cases C-N bond formation occurs to form a heterocycle. The product formed depends on the ease of the reductive elimination step. The relevance of these results to the catalytic synthesis of hetero- and carbocycles is discussed.

Throughout the thesis all new compounds are fully characterised spectroscopically and by elemental analysis and several compounds have been structurally characterised by X-ray crystallography.

Acknowledgements

I would like to thank Dr Davies for his invaluable help, support, patience and supervision throughout this project. I would like to thank our collaborators in Heriot Watt University Prof Macgregor and Amalia Polblador for their computational work and help to understand better the mechanistic aspects of this project. I would also like to thank Dr Solan for the constructive discussions about football, chemistry, politics…

I would like to thank all the people who have been involved in this project, Dr Griffith for the low temperature NMR study and Mr Singh for the X-ray. Mr Davenport for the work on cyclometallation of oxazoline, Dr Burley for the synthesis of some ligands, Dr Stasiuk for the synthesis of a triazole. I would like to thank the students who had to face my sarcasms on a daily basis Rachel Jones, Will Browne and Sam Howe.

I would also like thank everyone I have worked with in the lab for making it such a pleasurable experience, namely Shalini, Graeme, Andy (also for proof reading some of this work), Simba, Tarn and Ginger Chris. I also want to acknowledge the people who helped me feel comfortable in a new country and had enough patience to listen to my awful French accent and who became true friends, thanks Mat, Yohan (also for some proof reading), Rob, Jeremie, Mo and Abu baker.

None of this would have been possible without the support of my family in France, my parents and my two sisters. I want to thank my wife for helping going through huge moments of stress and being patient with me.

Abbreviations

General and physical

Å	Angstroms
AMLA	Ambiphilic Metal Ligand Activation
Br s	Broad singlet
c.f.	Confer (compare)
COSY	Correlated spectroscopy
^{o}C	Degrees Centigrade
d	Doublet
dd	Doublet of doublets
dt	Doublet of triplets
δ	Delta (NMR Chemical Shift)
Da	Dalton
ΔG	Gibbs Free Energy Change
ΔH	Enthalpy Change
ΔS	Entropy Change
DFT	Density Functional Theory
EA	Electrophilic activation
e.g.	exempli gratia (for example)
Equ	Equivalents
ES-MS	Electrospray Mass Spectrometry
EtOH	Ethanol
FAB-MS	Fast Atom Bombardment Mass Spectrometry
H	Hour
Hz	Hertz
i.e.	id est (that is)
in situ	in the reaction mixture
K	Kelvin
Kcal mol^{-1}	Kilocalorie Per Mole
m	Multiplet
µl	Microlitre
µM	Micromolar

μmol	Micromole
min	Minutes
mg	Milligram
ml	Millilitre
mmol	Millimole
ms	Millisecond
MHz	Megahertz
NMR	Nuclear magnetic resonance
NOBA	Benzyl alcohol
NOE	Nuclear Overhauser *Effect*
ppm	Parts per million
OA	Oxidative addition
RT	Room temperature
SBM	Sigma bond metathesis
Sept	Septet
TS	Transition state
via	By means of

Chemical

Bn	Benzyl
^{t}Bu	t-Butyl
$CHCl_3$	Chloroform
Cod	Cyclooctadiene
Coe	Cyclooctene
Cp	Cyclopentadienyl anion
Cp*	Pentamethyl-cyclopentadienyl anion
DCM	Dichloromethane
DMAD	Dimethyl acetylenedicarboxylate
DMBA	*N,N'*-Dimethylbenzylamine
DMSO	Dimethylsulfoxide
Et	Ethyl
Et_3N	Triethylamine

EtOH	Ethanol
Me	Methyl
MeCN	Acetonitrile
MeOH	Methanol
OAc	Acetate
OTf	Triflate
PF_6	Hexafluorophosphate
Ph	Phenyl
PhCCPh	Diphenylacetylene
PhCCH	Phenylacetylene
PMe_3	Trimethylphosphine
PPh_3	Triphenylphosphine
^{i}Pr	Isopropyl
pcy	*p*-cymene
THF	Tetrahydrofuran
TMS	Trimethylsilane

List of contents

Chapter One

General introduction

1 Chapter 1

1.1 C-H activation

C-H activation is a very active area of research in organometallic chemistry, the aim of which is to make a more efficient and effective use of cheap and abundant hydrocarbon feedstocks.[1-4] It has applications in catalysis and organic synthesis.[5-9] One major goal of C-H activation research therefore, is not simply to find new C-H activation reactions but to obtain an understanding of them that will allow the development of reagents capable of selective transformations of C-H bonds into more reactive functionalized molecules. This introduction will discuss (i) the use of C-H activation in cyclometallation reactions with Pd, Ru, Ir and Rh, (ii) the different mechanisms of C-H activation and (iii) the catalytic applications of C-H activation with a focus on direct arylations.

1.2 Cyclometallation by C-H activation

The term "cyclometallation" was introduced by Trofimenko in 1973[10] to describe reactions of transition metal complexes in which a ligand undergoes an intramolecular metallation with the formation of a chelate ring containing a metal-carbon bond and a metal-donor atom bond **(Fig. 1.1)**.

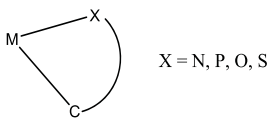

Fig. 1.1

Cyclometallated complexes have found applications in areas such as organic synthesis[11, 12], catalysis[13, 14, 15, 16, 17] and photochemistry.[19, 18] Cyclometallation was discovered in the

early 1960s[11, 12] and provides a straight forward entry to organometallic compounds with a M–C σ bond. Cyclometallation has been accomplished with a wide variety of ligand systems, including hard donor groups and soft donor groups.[13] Cyclometallated complexes can be synthesized by transmetallation reactions,[14, 15] ligand exchange,[16, 17] oxidative addition[18] or C-H activation,[19] this introduction will focus on cyclometallation by C-H activation.

Palladium has undoubtedly been the most extensively studied metal in cyclometallation chemistry. Reviews focusing specifically on cyclopalladation and on the wide application potential of palladacycles have appeared.[20, 21] Palladium(II) precursors ($Li_2[PdCl_4]$ or $Pd(OAc)_2$) are generally used for the C-H bond activation **(Fig 1.2)**.

Cyclopalladation occurs with a wide range of functional groups directing the C-H activation. **Fig. 1.2** shows some of the N-donor ligands which have been used to direct aromatic C-H activation. Amines **(1.1),**[22, 23] imines **(1.2),**[24] azobenzene **(1.3),**[24] diazobenzene **(1.4)**,[25, 26] nitrosoanilines **(1.5)**,[27-29] pyridines **(1.6),**[30] pyrimidines **(1.7**[31], **1.8**[31]), oximes **(1.9)**,[32] imidazoles **(1.10a)**,[33] oxazolines **(1.10b),**[34] thiazoles **(1.10c),**[34] triazoles **(1.11)**[35, 36] and pyrazoles **(1.12)**[10] can all direct the C-H activation of a phenyl C-H bond to form a five-membered palladacycle. In the case of amines as directing groups, C-H activation with tertiary amines was known since the 1970s however in 1968 Cope and Friedrich postulated that cyclopalladation would fail when primary amines were used.[16] In 2003 Vicente *et al.* reported that primary amines can be activated with $Pd(OAc)_2$ in MeCN at 80 °C.[23] It is believed that palladium promoted C-H activation occurs *via* an electrophilic pathway and a mechanistic study of cyclometallation of DMBA with $Pd(OAc)_2$ reported by Ryabov will be discussed further below (section 1.3.4.1).

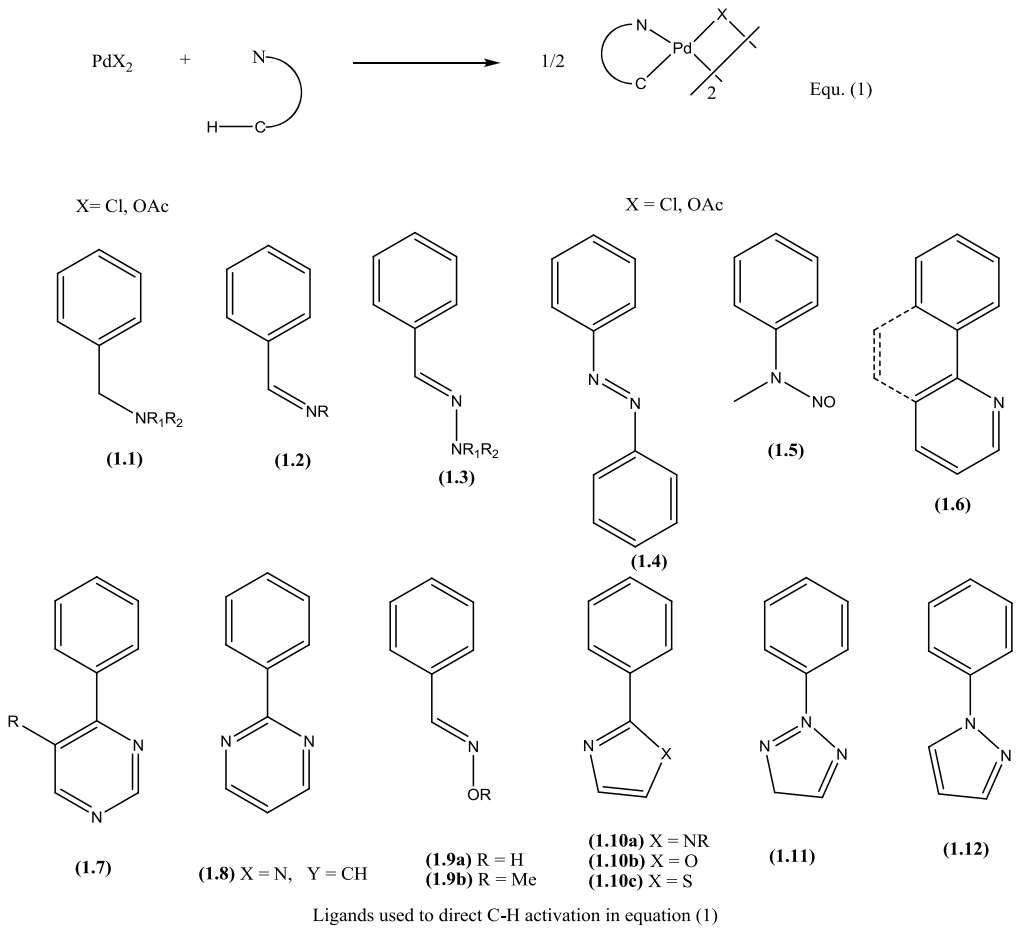

Fig. 1.2

In the case of imines, *endo* and *exo* isomers can be envisaged. The endo isomer contains the double bond of the imine in the metallocycle whereas the *exo* isomer contains the double bond of the imine outside the metallocycle. Gomez reported the reaction of imines **(1.13)** with $Pd(OAc)_2$ and showed that the formation of the *endo* five-membered ring **(1.14)** was favoured for R = H, however, when R = Me the *exo* product **(1.15)** was formed **(Scheme 1.1)**.[37]

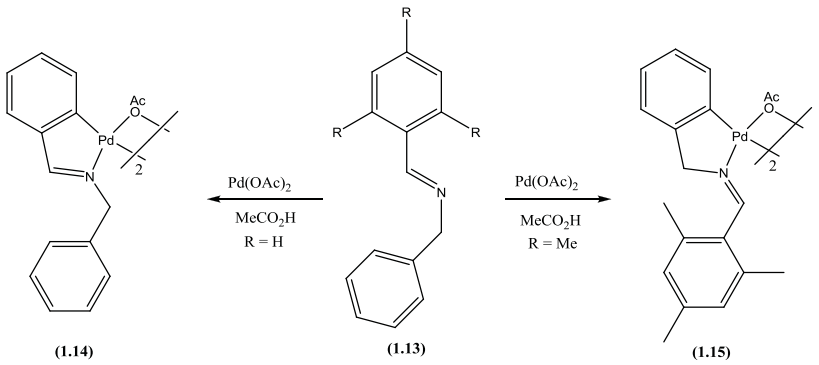

Scheme 1.1

Cyclopalladation is not restricted to five membered rings, C-H activation of aromatic C-H bonds to form six-membered rings has also been reported with different directing groups, for example, amines **(1.16**[38], **1.17**[23]**)**, amidines **(1.18)**,[39] imines **(1.19)**,[40] azonaphthalenes **(1.20),**[41] pyridines **(1.21),**[42] and pyrazoles **(1.22)**[36] **(Fig. 1.2)**. The formation of six-membered rings is known to be slower than the formation of five-membered rings **(Fig. 1.3)**.[23] In the case of **(1.22)** in presence of $Li_2[PdCl_4]$ cyclopalladation did not occur and $[Pd(LH)_2Cl_2]$ (L = **1.22**) was observed whereas in presence of $Pd(OAc)_2$ the reaction produced the desired complex. Hence, cyclopalladation is easier with $Pd(OAc)_2$ than with Li_2PdCl_4.[36]

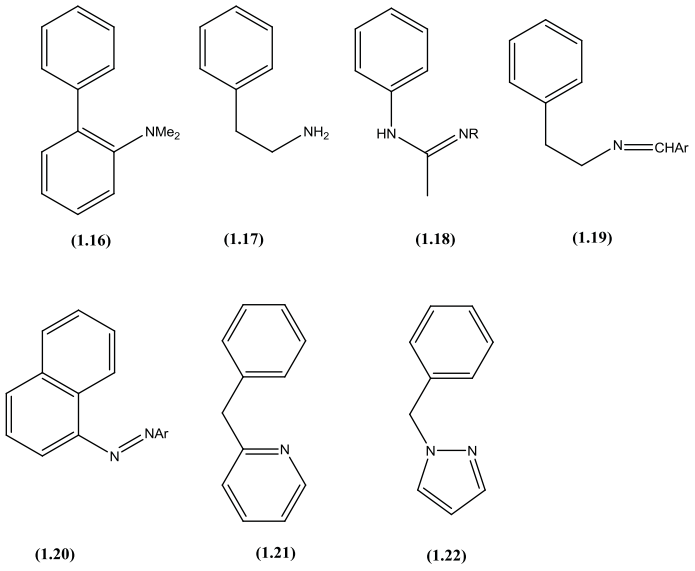

Fig 1.3

Activation of sp^3 C-H bonds has been described to form five-membered rings with hydrazones **(1.23)**,[43,44] oxazolines **(1.24)**,[45] benzothiazoles **(1.25)**[46] and six membered rings with imines **(1.26)**,[47] oximes **(1.27)**[48] and pyridines **(1.28)**[49] (**Fig. 1.4**).

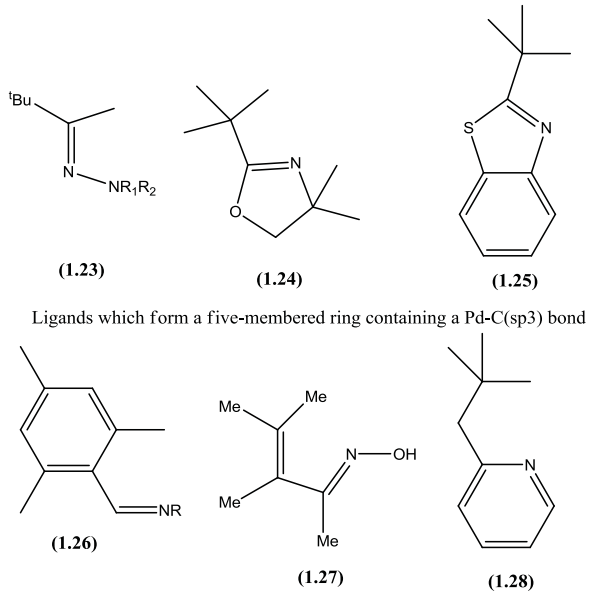

Fig. 1.4

Sokolov reported the reaction of **(1.29)** and **(1.30)** with $Li_2[PdCl_4]$ **(Scheme 1.2)**. When R = H the sp^3 C-H activation occurs to form **(1.31)**, however when R = CHNMe the sp^2 C-H activation is preferred and **(1.32)** is formed exclusively **(Scheme 1.2).**[50]

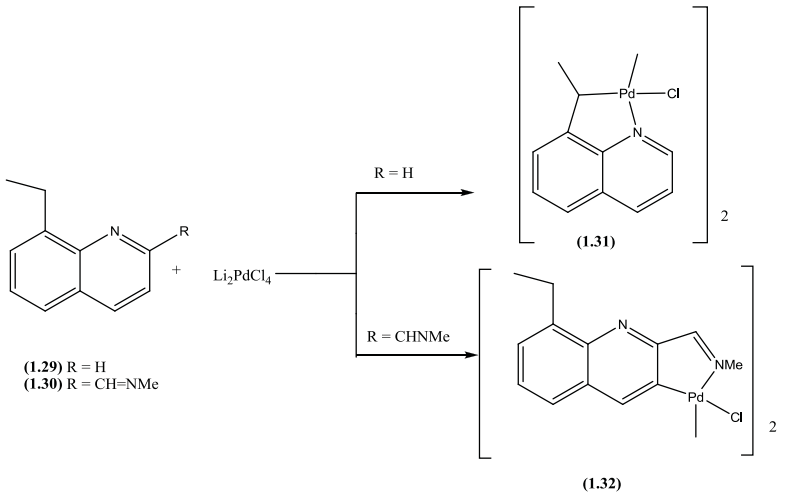

Scheme 1.2

The aim of this overview was to show that the cyclopalladation *via* C-H activation is well known with a wide range of N-donor groups, with the formation of five and six-membered rings and also different types of C-H bonds activated (sp^2, sp^3).[19, 51, 52] Cyclopalladation is easier in the presence of $Pd(OAc)_2$ than $Li_2[PdCl_4]$. The roles and effects of the carboxylate on C-H activation will be studied in Chapter 3, and the effect of the directing group on acetate-assisted C-H activation with ($[IrCl_2Cp^*]_2$, $[RuCl_2(pcy)]_2$, $[RhCl_2Cp^*]_2$) will be investigated in Chapter 3.

Cycloruthenated compounds have been much less studied than the cyclopalladated ones. A recent review by Pfeffer *et al.* [53] showed that in contrast to cyclopalladation, cycloruthenation *via* C-H activation could be achieved with a variety of Ru precursors of different oxidation states hence, it is difficult to classify cycloruthenation reactions by the mechanism of C-H activation. This section will focus on the range of N-directing groups used for cycloruthenation *via* C-H activation; the formation of half sandwich cycloruthenated C–N complexes will be discussed in Chapter 2.

Chaudret *et al.* showed that 2-phenylpyrazole, 2-phenylpyridine and benzoquinoline were cycloruthenated with $[RuH_2(H_2)_2(P^iPr_3)_2]$ to form **(1.33)** and **(1.34)**. **(Scheme 1.3).** They investigated the mechanism of this reaction and isolated an agostic intermediate **(1.35)(Scheme 1.3)**.[54]

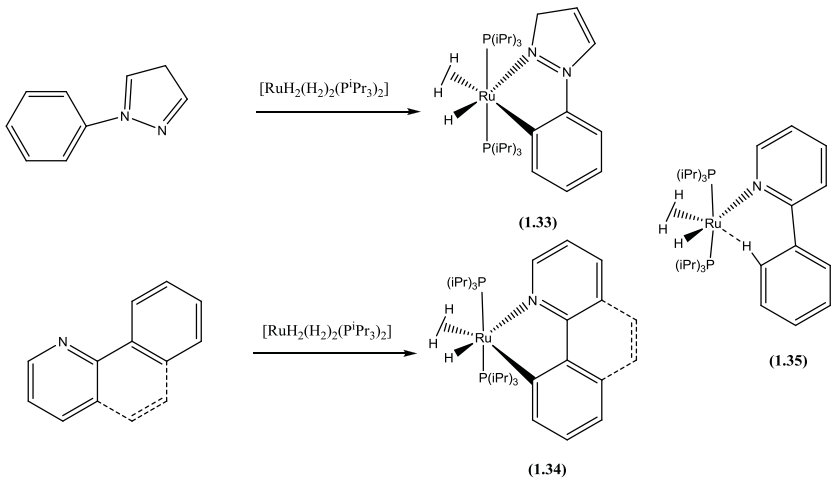

Scheme 1.3

Cyclometallation of imines with $[Ru(CO)_3Cl_2]_n$ by Bennett *et al.* produced **(1.36)** but in a very low yield (<10%) **(Scheme 1.4)**.[55] Pfeffer *et al.* concluded that the use of $[Ru(CO)_3Cl_2]_n$ required the loss of a carbonyl ligand and this accounted for the harsh conditions used and the low yields obtained.[53] The same ligand reacted with $[Ru_3(CO)_{12}]$ to produce a bis-cyclometallated complex **(1.37)** in modest yields **(Scheme 1.4)**.

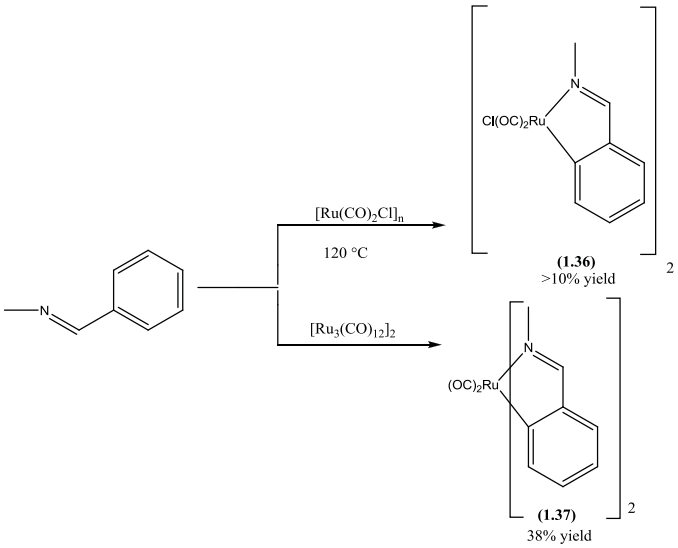

Scheme 1.4

Recent work using vinyl pyridine has shown the activation of non aromatic C-H bonds with [$RuHCl(PPh_3)_3$], although the formation of ethyl pyridine during the reaction suggested that the H_2 formed during the reaction further reacts to reduce the substrate **(Scheme 1.5)**.[56] However cycloruthenation without ligand reduction has been realized using $RuCl_2(PPh_3)_3$ as the ruthenium source.[56]

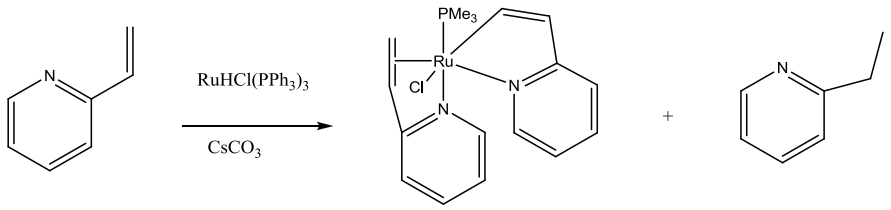

Scheme 1.5

In conclusion, despite the wider range of precursors used the scope of cycloruthenation of N-donor ligands by C-H activation is much less than cyclopalladation and cycloruthenation with Ru(CO) precursors suffers from harsh conditions and low yields. There is no easy method to cycloruthenate a wide range of N-donor ligands under mild conditions by C-H activation.

As found for Ru there are fewer examples of cyclometallation of N-donor ligands with Rh and Ir than Pd in the literature. This section will describe selected examples of C-H activation with N-donor ligands with Ir and Rh, examples involving half sandwich complexes will be discussed in more detail in Chapter 3.

For iridium and rhodium cyclometallation can occur from M(I) or M(III) oxidation states. Imine ligands have been cyclometallated with Ir(III) and Rh(III) complexes [$M(PPh_3)_2H_2(acetone)_2$] (M = Ir, Rh) to form **(1.38) (Scheme 1.6)**.[57, 58] However although an M(III) starting material is used the authors suggest reductive elimination of H_2 occurs first. The reaction then proceeds by oxidative addition of the C-H bond to the

M(I) (M = Ir, Rh) intermediate. Interestingly, only five-membered rings were formed which confirmed the easier formation of five-membered rather than six-membered rings.[57, 58] A mixture of the starting complex and the coordinated imine **(1.39)** were formed in presence of d_4-MeOH suggesting the reversibility of the C-H bond activation **(Scheme 1.6)**.[58]

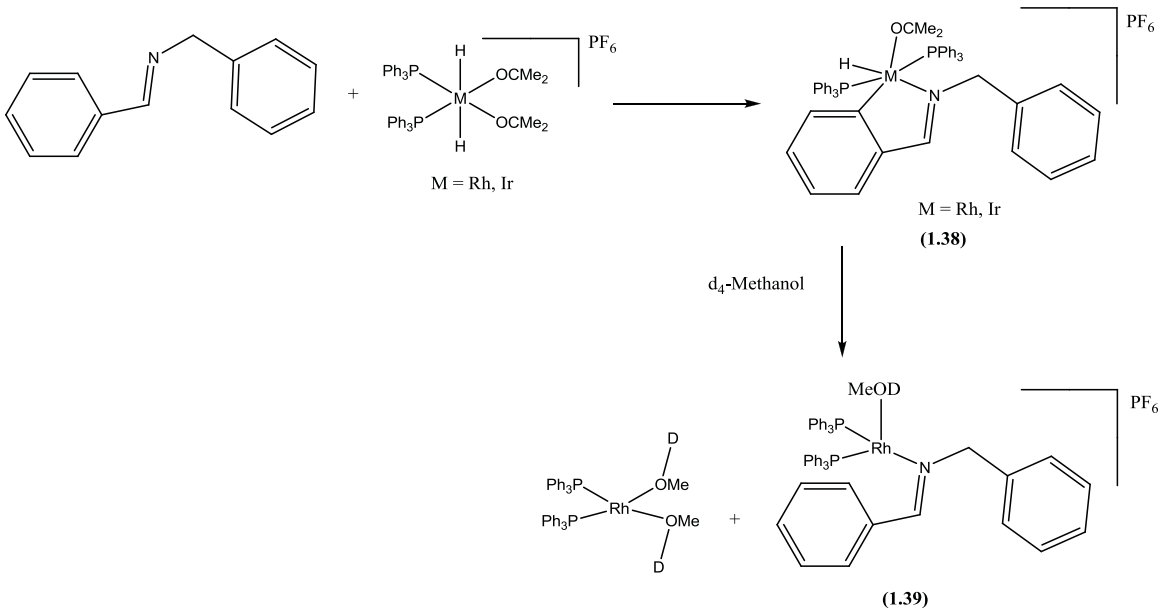

Scheme 1.6

Another example of C-H activation was described using benzoquinoline with $[Ir(PPh_3)_2(cod)]^+$ in presence of H_2 to form **(1.40)(Scheme 1.7)**.[59] A non aromatic C-H activation of an imine proton rather than an aromatic C-H activation was reported by Suggs *et al.* in 1979 **(Scheme 1.8)**. They showed that **(1.41)** selectively produced **(1.42)** in the presence of $[RhCl(PPh_3)_3]$ **(Scheme 1.8)**.

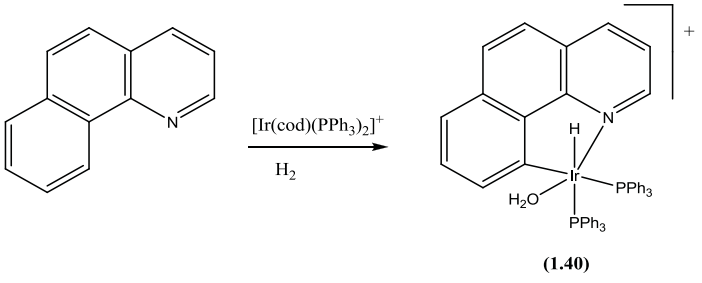

Scheme 1.7

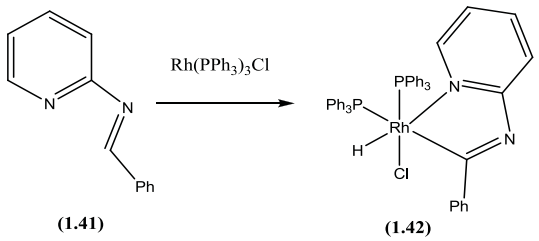

(1.41) (1.42)

Scheme 1.8

Cyclometallation with N-donor ligands was further developed with MCl_3. nH_2O (Ir, Rh). Nonoyama described the cyclometallation of 2-phenylpyridine, benzoquinoline and 2-phenylpyrazole with Ir and Rh complexes **(Scheme 1.9)**.[60] Chloro-bridged dimers **(1.43)** and **(1.44)** were formed **(Scheme 1.9)**.[60]. Alkylated and non-alkylated oximes have been used as directing groups for C-H activation, reaction with $[Rh(cod)Cl]_2$ or $RhCl_3$ $n(H_2O)$ both gave the corresponding dimeric species $[Rh(C\hat{}N)_2Cl]_2$ (C^N = cyclometallated ligand).[61] Reaction of diazobenzene with $RhCl_3$, nH_2O in the presence of NaOAc gave biscyclometallated complex **(1.45)** but this time as a monomer **(Scheme 1.10)**.[59] Complexes of type $[Ir(C\hat{}N)_3]$ and $[Ir(C\hat{}N)_2(N\hat{}N)]^+$ have recently been synthesized with a wide range of N directing groups for their luminescent applications however these reactions require harsh conditions. This field has been reviewed recently by Baranoff *et al.*[62]

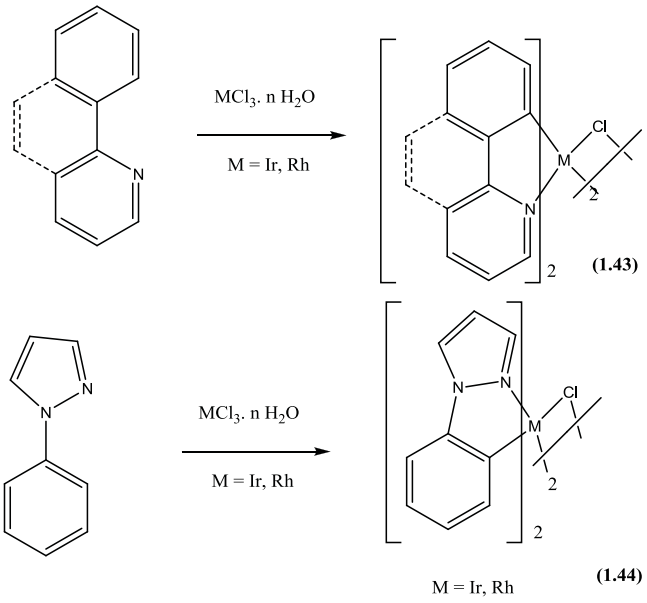

Scheme 1.9

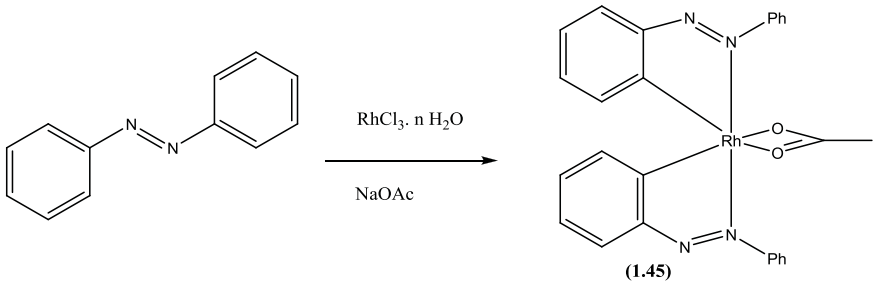

Scheme 1.10

In general C-H activation from a M(I) complex (M = Ir, Rh) proceeds *via* oxidative addition of the C-H bond into the metal. The mechanism(s) of C-H activation at M(III) are much less well defined and electrophilic, oxidative addition or metathesis mechanisms maybe possible. There are fewer examples of C-H activation with Rh and Ir in comparison to Pd and, as observed with Ru, there is no simple method which works for C-H activation with a wide range of N donor ligands under mild conditions.

From this introduction it is clear that there is not one method for cyclometallation of N-donor by C-H activation that works for all four metals Pd, Ru, Rh and Ir. Although there are many examples of cyclometallation by C-H activation with these metals there are

very few detailed mechanistic studies. Oxidative addition of a C-H bond is the most likely pathway in the case of Ir(I), Ru(0) and Rh(I) whereas Pd(II) reacts *via* an electrophilic type activation. For cyclopalladation $Pd(OAc)_2$ is a better precursor than $Li_2[PdCl_4]$ which shows that OAc may play a role in this particular reaction. In order to expand the range of cyclometallated complexes and their applications new cyclometallation reactions which occur under mild conditions are desirable. A better understanding of the mechanism(s) of cyclometallation by C-H activation may provide greater insight and hence aid progress in this area.[63] The next section will discuss mechanisms of inter and intra molecular C-H activation.

1.3 Mechanisms of C-H activation

Experimental and theoretical research has given a good understanding of the mechanisms of C-H activation and prior to 2005 five broad classes had been identified namely (i) oxidative addition (OA) with electron rich low valent transition metal, (ii) σ-bond metathesis (SBM) at electrophilic early transition metal centres (iii) 1,2 addition, (iv) electrophilic-activation (EA) at electron deficient late transition metal centres and (v) radical mechanisms, which will not be discussed in this thesis. Distinguishing between these possibilities experimentally can be extremely difficult; however, insight can often be gained from computational methods which can even lead to proposals of novel mechanisms for C-H activation.[20,64] This section will give an overview of these four classes of C-H activation and recent work on ambiphilic activation[65] which has some similarities to electrophilic activation and 1,2-addition.

1.3.1 Oxidative addition

Oxidative addition is a mechanism where an electron rich metal reacts with a C-H bond to form a M–C and M–H bond *via* a three membered transition state **(Scheme 1.11)**.

Early experimental studies were reported by Graham *et al.*[66], Bergman *et al.*[67] and Jones *et al.*[68] using d^8 fragments Cp*ML (M = Rh, Ir, and L= PMe_3, CO). Further studies showed that the formation of reactive 16-electron complexes prior to the C-H activation was a common feature for this reaction.[69-72]

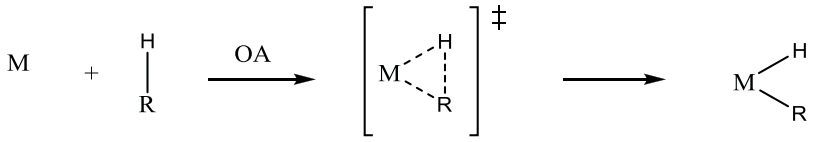

Scheme 1.11

In early work, many metal complexes were shown to activate the strong arene C-H bond (110 kcal/mol) but few reported the activation of the weaker alkane C-H bond (96-102 kcal/mol).[67,69] Bergman *et al.* described activation of cyclohexane to form **(1.46)** under mild conditions **(Scheme 1.12)**.[73]

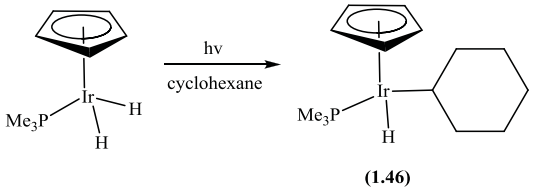

(1.46)

Scheme 1.12

Bergman *et al*. reported that photolysis of **(1.47)** leads to loss of H_2 to give **(1.48)** which undergoes oxidative addition of methane *via* a proposed three–centre transition state **(1.49)** to give the Ir^{III} complex **(1.50) (Scheme 1.13).**[74] The electron-donating Cp* and the electron rich metal centre were necessary for oxidative addition of a C-H bond. An indication that less electron-rich systems might function well in this reaction has been provided by Graham and Hoyano, who found that Cp'Ir(CO) also activates methane.[66]

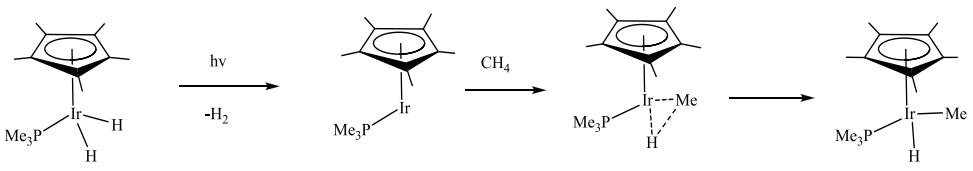

(1.47) **(1.48)** **(1.49)** **(1.50)**

Scheme 1.13

The same group demonstrated C-H activation of alkanes, methane and ethane with the Ir^{III} complex [IrMe(PMe_3)(OTf)Cp*] **(1.51)** under mild conditions.[75] Two possible mechanisms were proposed: (i) a nucleophilic pathway *via* oxidative addition, proceeding through an Ir(V) intermediate then reductive elimination; or (ii) σ-bond metathesis **(Scheme 1.17)**. The reaction was dependent on the ease of dissociation of OTf to form a 16-electron species. Hence, complex **(1.52)** reacts faster than **(1.51)** because the dissociation of DCM to form a 16-electron species **(Scheme 1.14)** is easier than dissociation of triflate **(Scheme 1.15)**.

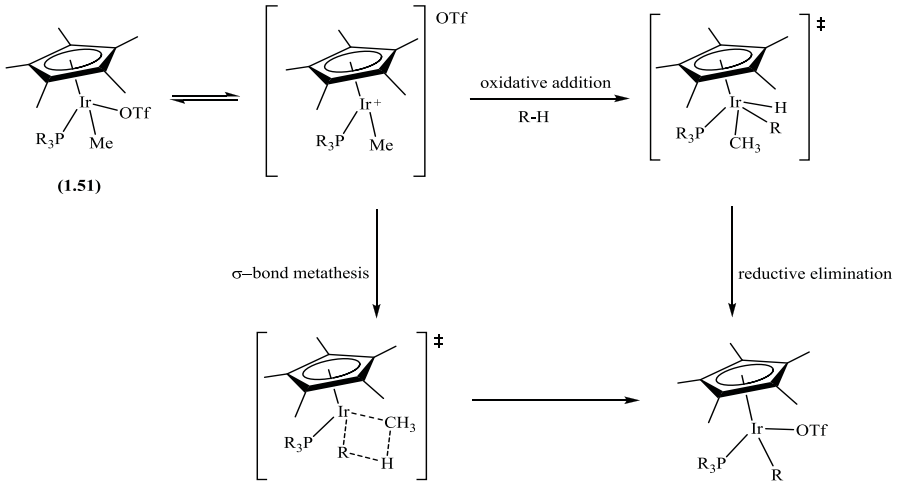

Scheme 1.14

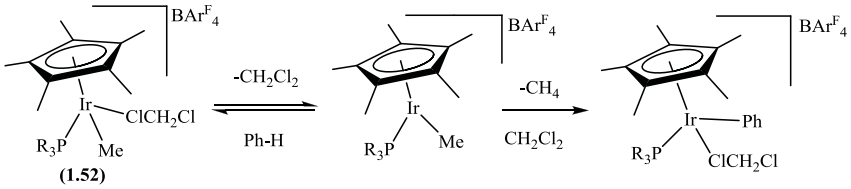

Scheme 1.15

For iridium the reaction of the more electron donating PMe_3 complex is thirty times faster than with the $P(OMe)_3$ one whereas in the case of the Rh analogs the rates of the reaction were about the same for PMe_3 and $P(OMe)_3$ and about 1000 times slower than with Ir.[76] The authors suggested this was due to a more difficult dissociation of triflate

in the case of Rh than Ir.[77] This suggests that the rate determining step is the dissociation and not the C-H activation.

This experimental study from Bergman *et al.* could not distinguish between an OA and SBM mechanism so computational chemistry was used to probe the mechanism involved. Hall *et al.* considered the reaction of methane with $[IrMe(PMe_3)Cp]^+$ *via* the two probable mechanisms (OA, SBM) and showed that OA was the lower energy pathway.[78] Despite a careful search, no transition state for SBM pathway could be found. Hence, in this case computational chemistry allowed the distinction between an oxidative addition and a SBM mechanism.

1.3.2 σ-Bond metathesis

SBM is a one step reaction by which two σ-bonds are broken and two new σ-bonds are formed in a concerted manner without change of the metal oxidation state **(Scheme 1.16)**. This process is known for early d^0 transition metal complexes where a change in the oxidation state is not possible and Watson *et al*. described the SBM mechanism for the exchange of $^{13}CH_4$ with the methyl group of **(1.53) (Scheme 1.17)**.[79] Methane may coordinate very weakly to the electrophilic Lu centre *via* a C-H bond. This is followed by a rearrangement *via* **(1.54)**, which results in methyl group exchange to give **(1.55) (Scheme 1.20)**. Bercaw *et al.*[80] suggested that the transition state may be relatively non-polar and suggested the term "σ-bond metathesis mechanism", however a computational study of Eisenstein suggested a more polar TS.[64] This topic has been recently reviewed by Lin.[81]

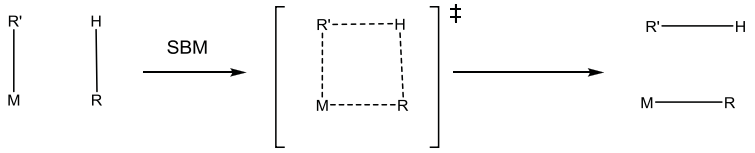

Scheme 1.16

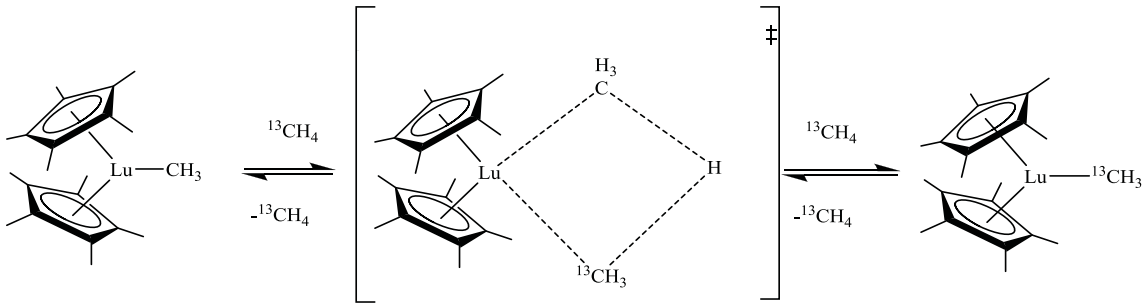

(1.53) **(1.54)** **(1.55)**

Scheme 1.17

Lin, and Eisenstein previously computed methane activation with {TpM(PH_3)(CH_3)} (M = Fe, Ru, Os; Tp = tris(pyrazolyl)borate) fragments *via* four membered ring transition states. They showed that the activation barrier increased in the order Os< Ru< Fe **(Fig. 1.5)** with a change in the nature of the C-H process showing a dramatic effect of the nature of the metal centre.[82] With M = Os a 3-centred oxidative addition was computed, but with the Ru and Fe analogues, 4-centred transition states were seen. For M = Ru a very shallow Ru(IV)−H intermediate was located, while for M = Fe, C−H activation was clearly a one-step process *via* a transition state featuring a short Fe-H distance of only 1.53 Å showing some Fe-H bonding which suggested an oxidative character. With late transition metals the computed transition states often show a M–H bond. Lin called these mechanisms oxidatively added transition states (OATS).

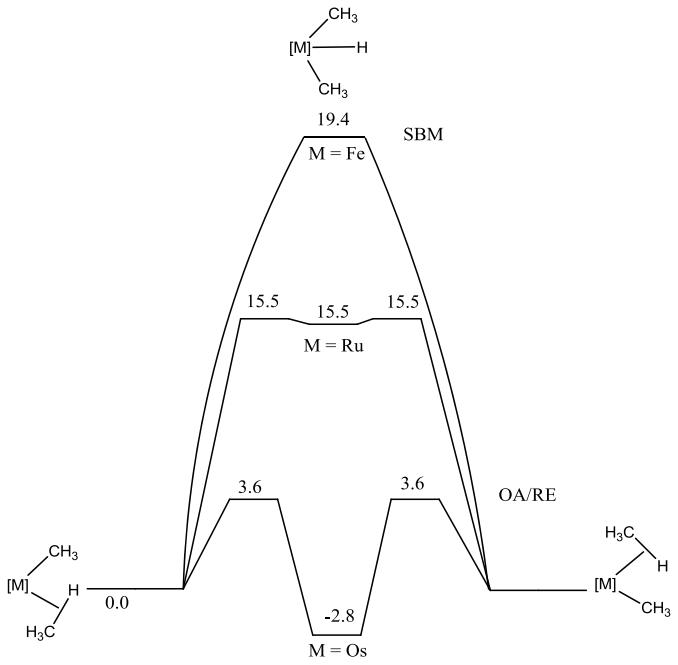

Fig. 1.5 Energy in Kcal/mol, [M] = TpM(PH_3) with M = Fe, Ru, Os.

In 2003, using DFT calculations Periana and Goddard showed that C-H activation catalysed by [IrPh(acac)$_2$(pyridine)] goes *via* SBM type of mechanism rather than OA.[83] In the transition state the Ir-H distance is short (1.58 Å) which implies an oxidation at the metal centre during the process, the authors called this mechanism an oxidative hydrogen migration (OHM). They rationalised the difference in mechanism in comparison to Bergman's system [Ir(CH_3)(PMe_3)(OTf)Cp*] by two main factors. They speculated that in Bergman's complex the Cp* is less bulky than the bis-acac making the seven coordinated Ir(V) intermediate more favoured, and the more electron donating ligands (Me, PMe_3) also make the OA more favoured.

Gunnoe *et al*. described an experimental and computational study on the C-H activation of arenes (C_6H_5X) with [TpRu(L)(C_6H_5X)Me] (L = PMe_3, CO) investigating the effect of substituents on the arene and other ligands. The calculations showed a short Ru-H bond distance (between 1.592 and 1.677 Å) in the transition state which is similar to Goddard's observations for OHM, moreover the reaction showed a lower energy barrier for L = PMe_3 than L = CO, consistent with the more donating ligand stabilizing the

"oxidative character" in the transition state.[84,85] More recently they studied the impact of the acidic character of the C-H bond being activated by varying the substrate (CH_3NO_2, CH_3CN, $(CH_3)_2CO$, THF). An easier activation of more acidic C-H bonds was observed (CH_3NO_2 > CH_3CN > $(CH_3)_2CO$ > THF). These results showed that the 16 electron fragment {$TpRu(PMe_3)R$} can activate sp^3 C-H bonds and confirmed a degree of heterolytic character in the transition state with the C-H activation resembling an intramolecular proton transfer.[86]

Recently Hall *et al*. reported[87] a computational study summarising all the different mechanisms reported in the literature for a SBM type of mechanism (SBM, OHM (Goddard), OATS (Lin)) and showing a "spectrum of mechanisms for metal-mediated hydrogen transfer" **(Fig. 1.6)**. Macgregor and Davies suggest that a continuum of structures will be formed as more computational data become available on SBM processes.[88] Hence, whilst computation has provided some insights into different mechanisms the ability to distinguish between some of these mechanisms without computation has become almost impossible.

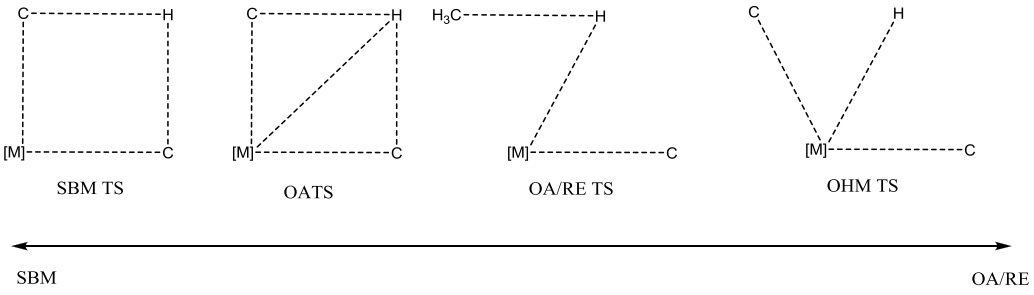

Fig. 1.6

1.3.3 1,2 addition

Bergman[89] **(Scheme 1.18a)** and Wolczanski[90] **(Scheme 1.18b)** independently reported in 1988 that transient Zr(IV) imido complexes could activate a C-H bond *via* 1,2-

addition **(Scheme 1.18)**. Computational studies have also been reported on these systems by Wolczanski *et al.*[91, 92] which confirm the 1,2 addition mechanism.

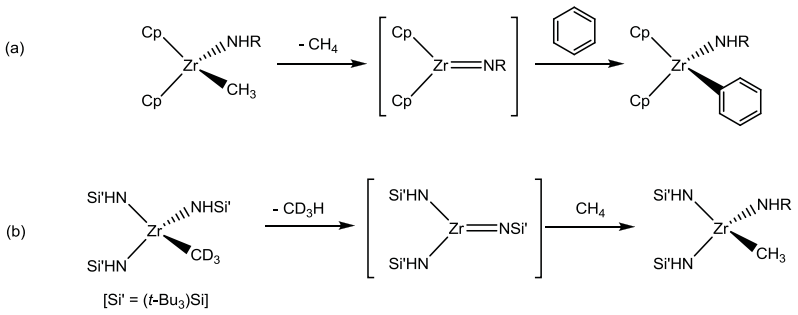

Scheme 1.18

In 2005, Periana[93] and Gunnoe[94] reported the first experimental studies of 1,2-addition of a C-H bond to an M-X (X = O, N) single bond. Gunnoe reported H/D exchange with benzene using [TpRu(PMe_3)$_2$(OH)] as catalyst in the presence of D_2O at 100°C.[94] Kinetic studies suggested that dissociation of PMe_3 occurs before the coordination of benzene. The selective *ortho* and *meta* deuterium incorporation into toluene suggested the metal is involved in the process.

More recently Gunnoe *et al.* studied the effect of substituting the hydroxyl group with OPh, NHPh, SH, Cl and OTf. H/D exchange was only observed with NHPh as a substituent.[95] They suggested that C-H activation was related to the basicity of the group receiving the hydrogen and that non-dative heteroatom-based ligands on low oxidation late transition metals would have lower activation barriers for C-H activation than similar metal-alkyl or aryl bonds. They proposed that the mechanism of C-H(D) activation steps for (X = OH, NH_2)[96] involved coordination of the C-H(D) bond to the metal centre followed by a net heterolytic cleavage in a process that resembles σ-bond metathesis.[96,95] Further computational studies on benzene activation with 16 electron {Ru(PH_3)X} (X = Me, OH, NH_2) showed substantial differences in the transition states with a lower activation barrier for X = NH_2, OH than X = Me, the latter showing a

shorter M–H bond distance. The authors explained this by the presence of a lone pair on NH_2/OH and a less efficient bridging for the proton transfer with X = Me **(Fig. 1.7)**.[96]

Fig. 1.7

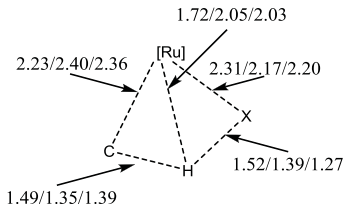

[Ru] = $Ru(PH_3)(Tab)$
Tab $HB(NNH)_3$
bond distances in the transition state for X= Me/NH_2/OH

Periana *et al.* showed the formation of **(1.59)** *via* C-H activation of benzene with $[Ir(acac)_2(OMe)L]$ (L = MeOH, pyridine) **(Scheme 1.19)**.[93] In the presence of C_6D_6, MeOD was produced *via* H/D exchange. A computational study of the system showed that the reaction proceeds *via* a SBM (four-membered TS **(1.57)**) rather than an OA (three-membered ring TS). As with Gunnoe's observation on $[TpRu(PMe_3)_2(OH)]$, **(1.56)** catalyses the H/D exchange in presence of D_2O *via* an Ir-OH intermediate.[97] Oxgaard *et al.* further analysed the 1,2 addition across the Ir-OMe bond by computing the localised orbitals. They observed an electrophilic metal attacking the benzene generating a positively charged hydrogen, which was transferred to the coordinated hydroxide which they termed an internal electrophilic substitution mechanism (IES).[98]

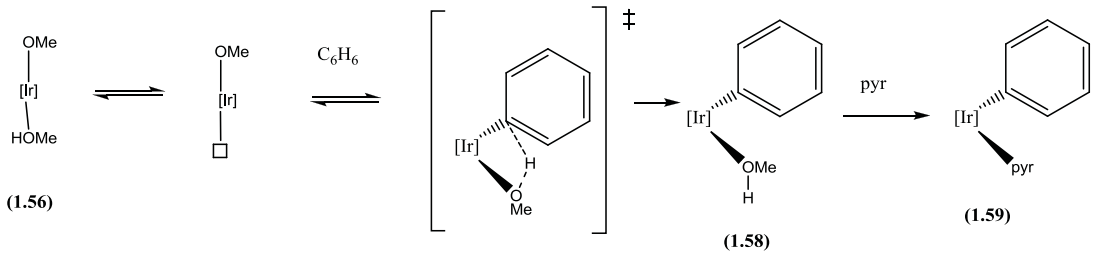

Scheme 1.19

Goddard *et al.* concluded that the net 1,2 addition of C-H bonds to an M-X bond (X = O, N) occurs *via* a four-membered transition state however there is no M–H bonding interaction and the forming X-H bond and the cleaving M-X bond are not based on the same orbital, which makes the process fundamentally different to SBM. Davies and Macgregor viewed the process as concerted, involving an electron-deficient metal and a basic ligand acting together to cause a heterolytic scission of the C-H bond, they called this an AMLA process (ambiphilic metal ligand activation).[88]

1.3.4 Electrophilic activation

1.3.4.1 Intramolecular C-H activation

As mentioned in section 1.2.1, Ryabov *et al.* studied the mechanism of cyclopalladation of DMBA (DMBA = N,N' dimethylbenzylamine) in the presence of $Pd(OAc)_2$.[20, 22] Detailed kinetic studies led the authors to propose a Wheland intermediate and an electrophilic C-H activation since in the case of substituted DMBA the rate constants of the reaction increased as the donor strength of the ring substituent increased. The activation parameters of the rate-limiting step, ΔH* and ΔS* (11 kJ/mol and -254 J/(K mol) respectively) were in accord with a highly ordered six-membered transition state **(Fig. 1.8)** in which the leaving hydrogen is abstracted by the second arm of the acetate and not the external amine.

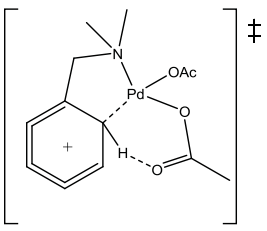

Fig. 1.8

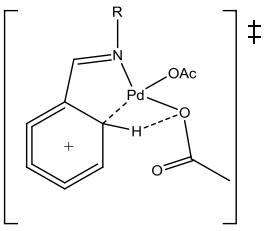

Fig. 1.9

A similar mechanistic investigation of cyclopalladation of imines with $Pd(OAc)_2$ was carried out by Gomez *et al.*[99] The rate of the reaction was measured at different temperatures and pressures and the authors suggested a highly ordered transition state, but this time with the bound oxygen of a monodentate acetate acting as a proton acceptor *via* a four-membered transition state **(Fig 1.9)**. This is closely related to the transition states proposed by Gunnoe[94] and Periana[98] as discussed earlier where the basic heteroatom plays an important role in the proton transfer in a four-membered transition state.

Davies and Macgregor studied the cyclometallation of DMBA with $Pd(OAc)_2$ computationally, they considered three possible mechanisms namely oxidative addition, sigma bond metathesis, related to the pathway proposed by Gomez *et al.*[37] and electrophilic activation *via* a six membered transition state as suggested by Ryabov.[20, 22] The most favoured pathway was an H-transfer process *via* a six-membered transition state involving an agostic C-H interaction, rather than the Wheland intermediate proposed by Ryabov with hydrogen bonding to the free arm of acetate **(Fig. 1.8)**. The displacement of one arm of the acetate to form the agostic intermediate was the rate determining step with an activation barrier of 13 kcal/mol.[100]

The computed activation barrier of 13 kcal/mol for the H-transfer was lower than that computed for OA (+34.3 kcal/mol) or SBM (+25.7 kcal/mol). A small KIE was computed (1.2) which is consistent with a low KIE experimentally observed by Ryabov.[22,20] Davies and Macgregor suggested an ambiphilic activation by an electrophilic metal centre and an intramolecular base, they also suggested a small influence of the metal which implied that this process could be extended to other metal centres.[100]

Davies had already shown experimentally that acetate-assisted cyclometallation of amines, imines and oxazolines with $[MCl_2Cp^*]_2$ (M = Ir, Rh) and $[RuCl_2(pcy)]_2$ occurred at room temperature. Subsequently, the acetate assisted C-H activation of DMBA with $[IrCl_2Cp^*]_2$ was computationally investigated and again a six membered transition state was the most favoured transition state and this will be further discussed in Chapter 2. Following this, Jones *et al.* carried out an experimental study of acetate assisted cyclometallation of phenylimines [PhN=CH(p-C_6H_4R)], (R = OMe, CH_3, F, CO_2Me, CF_3 and CN). Kinetic measurements showed that the reaction with $[Cp^*IrCl_2]_2$ was 2-4 times faster than the reaction with $[Cp^*RhCl_2]_2$ for a given substrate; also the reactions with the substrate bearing a *p*-methoxy substituent was over 10 times faster than the reaction with the *p*-trifluoromethyl substrate, consistent with an electrophilic type activation.[101]

Echavarren and Maseras have studied palladium catalysed intramolecular arylation using a combined experimental and theoretical approach.[102] Treatment of **(1.60)** with $Pd(OAc)_2$ led to the formation of **(1.61)** and **(1.62)(Scheme 1.20)**. The ratio of the regioisomers formed (1:1) was independent of the electronic nature of the substituent which ruled out an S_EAr mechanism and kinetic results showed a high KIE ($K_{H/D}$=5) which was consistent with a proton transfer being the rate determining step.

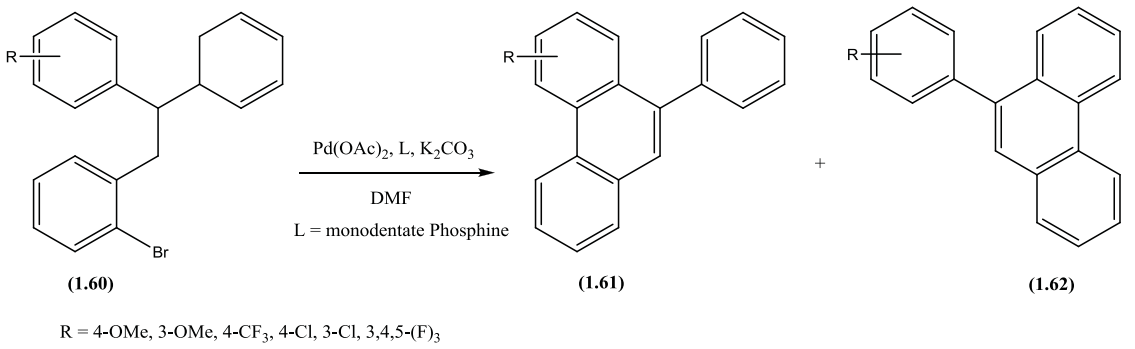

(1.60) **(1.61)** **(1.62)**

R = 4-OMe, 3-OMe, 4-CF_3, 4-Cl, 3-Cl, 3,4,5-$(F)_3$

Scheme 1.20

Three different transition states were envisaged by DFT computations, TS1 involving a four membered transition state where the bromide acts as an acceptor, TS2 involving external carbonate as base, or TS3 with bound carbonate as base **(Fig. 1.10)**. TS1 showed the highest activation energy (43.5 kcal/mol) but whether the inter TS2 or intramolecular TS3 pathway was favoured depended on the substituent on the phenyl ring with small differences between the two (6 kcal/mol). A bidentate phosphine was also tried, the DFT computations showed the intermolecular pathway to be favoured and confirmed previous observations in which electron withdrawing substituents made the reaction lower in energy.

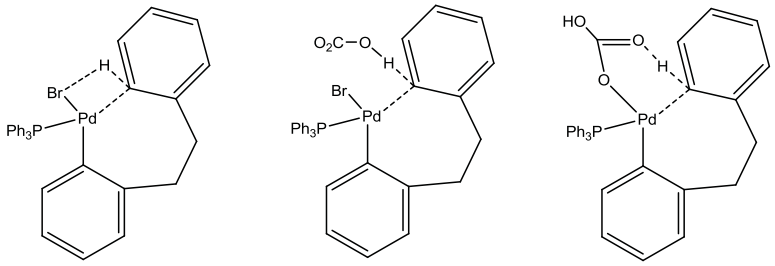

TS1 TS2 TS3

Fig. 1.10

A similar experimental and theoretical study of the sp^3 C-H activation shown in **Scheme 1.21** was carried out by Fagnou *et al.*.[103] The reaction selectively produced one regioisomer **(1.63)(Scheme 1.21)**. The DFT calculation showed a six-membered transition state with an agostic interaction between the Pd and the C-H being activated **(Fig. 1.11).** The regioselectivity observed experimentally was confirmed computationally showing a lower activation barrier for the primary C-H activation in comparison to the other isomers.

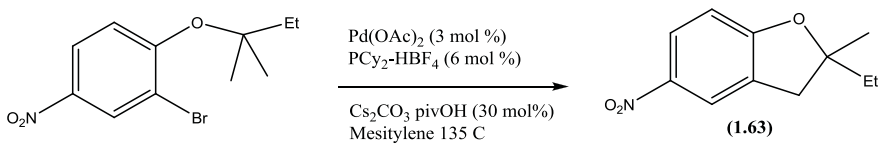

(1.63)

Scheme 1.21

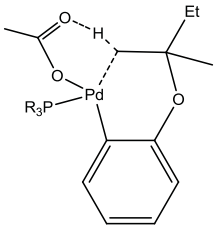

Fig. 1.11

Baudoin, Clot *et al.* reported the formation of benzocyclobutenes by sp^3 C-H activation catalysed by $Pd(OAc)_2$ to produce **(1.64)(Scheme 1.22).**[104] The reaction showed a high KIE ($K_{H/D}$ = 5.8) which suggested that C-H activation was the rate determining step **(Scheme 1.22)**. Two possible isomers could be formed from the first step (C-Br oxidative addition) and a computational study showed that **(1.66)** previously reported by Hartwig *et al.*[105] was more stable than **(1.67) (Fig. 1.12)**. Calculations of the C-H activation step from **(1.66)** showed a higher activation barrier than the one reported by Fagnou, moreover the overall process was *endo*thermic and acetate showed a lower activation barrier than carbonate which is opposite to the experimental results. However when the C-H activation process was computed from **(1.65)** the C-H activation proceeds *via* (κ^1O_2CX)Pd complexes with an agostic interaction with one C-H bond of the ^{t}Bu group of the aromatic ring. The proton transfer now occurs in a plane perpendicular to the P-Pd-Ph plane and the lower activation barrier is calculated with carbonate as observed experimentally and the reaction is now exothermic. This study demonstrated that the carboxylate does not need to be located cis to the site being activated in the square planar complex.

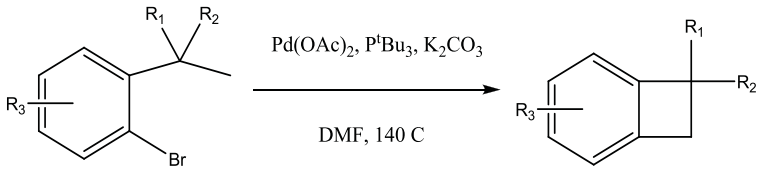

R_1 = Me
R_2 = CO_2Me

(1.64)

Scheme 1.22

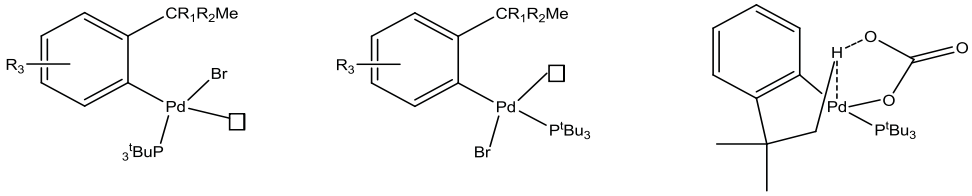

(1.65) **(1.66)** **(1.67)**

Fig. 1.12

1.3.4.2 Intermolecular C-H activation

In 2000, an early computational study of C-H bond activation of benzene and methane by $Pd(O_2CH)_2$ and $Pd(PH_3)_2$ was reported by Sakaki *et al.*[106] C-H activation of benzene, *via* OA, with $Pd(PH_3)_2$ has a high activation energy and is significantly endothermic whilst C-H activation of benzene with $Pd(OCOH)_2$ has moderate activation energy (16-20 kcal/mol) due to assistance by formate and is exothermic. They showed that the processes involved an η^1-η^2 displacement of one arm of the formate by the C-H bond. Subsequent electrophilic attack of the metal occurs in concert with the abstraction of the proton by the formate ligand to give a heterolytic fission of the C-H bond **(Fig 1.13)**.

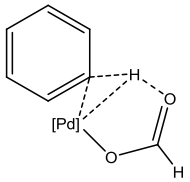

Fig. 1.13

Further development of mechanistic studies on direct arylation with perfluorobenzenes in the presence of $Pd(OAc)_2$ was reported by Fagnou *et al.* in 2006.[107] Interestingly, the reaction was easier in the case of electron deficient arenes which contrasts with a purely electrophilic activation mechanism. However a computational study located a transition state with a six membered ring similar to that in **Fig. 1.13**, showing that hydrogen bonding to acetate plays a key role. Fagnou called this process a concerted metallation deprotonation (CMD) to describe that the hydrogen is abstracted by the coordinated base at the same time as the M–C bond is formed. The faster reaction of electron deficient arenes is therefore due to the greater acidity of the proton being abstracted. They reported the advantage of using pivalate for the C-H activation experimentally and theoretically. [108]

Goddard *et al.* studied the activation of benzene and methane by $[Ir(acac)_2(OAc)]$ computationally.[109] They showed that a six-membered ring transition state was lower in energy for both methane and benzene activation than the four membered ring transition states. Very recently they reported a combined experimental and computational study of C-H activation of benzene with $[Ir(acac)_2(\kappa 2\text{-}OAc)]$.[110] Experimentally deuterium incorporation in benzene was observed in the presence of CD_3CO_2D and CF_3CO_2D. Monodeuteration was observed with CF_3CO_2D whereas multideuteration occurred in CH_3CO_2D. The authors showed that in acetic acid, the rate-determining step is the displacement of one arm of the bidentate acetate followed by benzene coordination resulting in rapid H/D exchange *via* a six-membered acetate-assisted transition state. In contrast, in trifluoroacetic acid, C-H bond cleavage becomes rate determining, resulting in the formation of only monodeuterated benzene.

Computation has helped shed light on mechanisms and influence of ligands. However it also allows more fine distinctions between mechanisms, for example CMD, IES both involving electrophilic type of activation with an intramolecular base, or OHM as a process between OA and SBM. Davies and Macgregor in a recent review commented on the importance of the lone pair of the heteroatom involved in the four and six membered ring transition states involved in the proton transfer. They emphasized the little influence of the M–H bonding interaction during the C-H activation at M-X (X = O, N) and therefore the difference to the SBM at M–H, M–C and M–B. They viewed these processes as variants of concerted ambiphilic activation in which an electron deficient metal and a basic ligand cause a heterolytic cleavage of a C-H bond, they termed these AMLA mechanisms (ambiphilic metal ligand activation) which would include CMD, IES and OHM processes. They suggested to specify an AMLA(4) and AMLA(6) for four and six-membered transition states. This section has shown the variety of mechanisms and approaches to C-H activation. The next section will attempt to give an overview of the applications of C-H activation in catalysis with a focus on direct arylation.

1.4 Applications of C-H activation in C–C bond formation

The development of methods for the direct conversion of C-H bonds into C–O, C–N and C–C bonds remains a critical challenge in organic chemistry.[7] The aim of this brief introduction is to describe some advances in catalytic processes involving C-H activation followed by C–C bond formation. The C–C bond formation step can either be an insertion, e.g. with an alkene or alkyne, or a reductive elimination with another M–C bond on the same metal. Cases of alkyne insertion are specifically dealt with in Chapter

4, so this section will focus on direct arylation reactions, where the C–C bond forming step is reductive elimination involving a M–C bond of an arene or heterocycle.

The classical methods of creating an Ar–Ar bond have involved the reaction of aryl organometallics of B, Sn, Si, Mg with a wide range of aryl halides in the presence of a transition metal **(Scheme 1.23 (iii))**.[111, 112] While high yields and selectivities can now be obtained by these traditional methods, they still suffer from drawbacks. Both coupling partners need to be preactivated, which is wasteful since it necessitates the installation and subsequent disposal of stoichiometric activating agents. The coupling of two aryl C−H bonds to give the corresponding biaryl product would seem ideal **(Scheme 1.23 (i))**. However, given the strength of the C−H bond, these processes are thermodynamically disfavoured. A chemical compromise with the substitution of one preactivated species with a simple arene **(Scheme 1.23 (ii))** and there have been considerable advances in the last five years with now several reviews on the subject.[6, 7, 113]

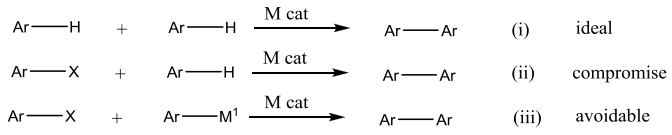

Scheme 1.23

This introduction will focus on use of Pd, Ru, Ir and Rh to couple a C-H bond with an Ar-X precursor and the more difficult, and hence rarer, coupling of two aryl C-H bonds. For each metal the different possibilities involving C-H activation (i.e. type (i) and (ii) in **Scheme 1.23)** will be classified according to inter or intramolecular processes and to the directing functional groups.

1.4.1 Palladium catalysed direct arylation

1.4.1.1 Palladium catalysed direct arylation with halogenated substrates

Early examples of palladium catalysed intramolecular direct arylation were reported by Ames *et al.*[114,115] In an attempt to investigate the Heck reaction, they observed the arylation of a C-H bond **(1.73)** instead of the product from the Heck reaction **(Scheme 1.24)**. Further investigation of this reaction showed it could be extended to a variety of benzofurans.[116]

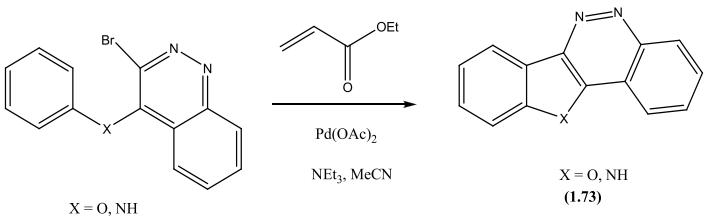

Scheme 1.24

Fagnou *et al.* recently studied the formation of **(1.75)** starting from **(1.74)** with $Pd(OAc)_2$ as catalyst **(Scheme 1.25)**.[117] The reaction produced the cyclised product **(1.26)** with high yields with all three halogens (Cl, Br, I) and the authors initially suggested an electrophilic proton abstraction mechanism for the C-H activation related to that computed by Maseras[102] (See section 1.3.4.2).

The nature of the base and its counterion have a significant impact on catalyst reactivity and selectivity.[118] For example, while K_2CO_3 gave optimal results, both Na_2CO_3 and Cs_2CO_3 were less effective, giving lower conversion and leading to a higher proportion of (**1.76)** whilst KOAc gave good selectivity but lower conversion and alkoxide bases led to an increased amount of **(1.76)**. Organic bases such as Et_3N, Cy_2MeN, and diisopropylethylamine (DIPEA) gave **(1.76)** as the major product and very low conversion. More recently a more detailed experimental study combined with DFT

calculations[119] showed a lower energy barrier for a CMD pathway using pivalate as an intramolecular base (see section 1.3.4.2). This approach has also been applied to sp^3 C-H activation as described earlier **(Scheme 1.25** in section 1.3.4.2**)**.[103] The mechanism of the overall process goes *via* an oxidative addition of the CX bond to Pd(0) followed by a C-H activation then reductive elimination to generate the desired product and the Pd(0) catalyst.

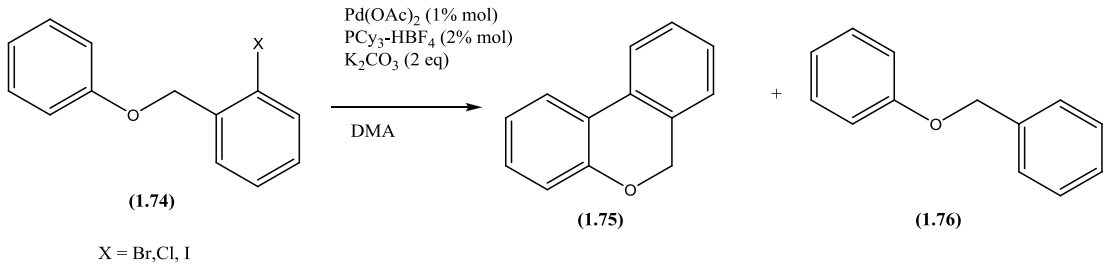

(1.74)

X = Br,Cl, I

(1.75) **(1.76)**

Scheme 1.25

Weak N-donor functional groups can direct arylation such as (benz)oxazoles,[120] indoles,[121] pyroles[122, 123] (benz)imidazoles,[123, 124]and undergo arylation with arylhalides. In these cases the C-H activation nominally proceeds *via* a three membered ring interaction between the N-atom and the metal centre. As expected three membered rings are not very stable so the M–N bond is not retained in the products, this may be a factor in allowing catalytic turnover. These transformations are an improvement on both partners being activated, however they usually suffer from the use of an excess of one of the aryl partners. Fagnou *et al.* investigated the possibility of using a 1:1 ratio of the two coupling partners and one set of conditions which could be applied for a wide range of ligands.[123] They showed that the use of a catalytic amount of pivalic acid (30%) and excess $CaCO_3$ afforded optimal results even with a 1:1 ratio between the two aromatic groups and these conditions could be applied to a wide range of substrates. The benefit of using pivalic acid was also applied to a wide range of heterocycles.[125]

As observed with weak N-donor directing groups, S-donor groups can direct arylation with benzothiophenes[123, 126-128] and benzothiazoles[129-131] and O-donor with furans [132, 133] again nominally *via* a three membered ring interaction. Fagnou *et al.* recently reported a mechanistic investigation of the arylation of benzothiophenes in the presence of pivalic acid **(Scheme 1.26)**. In a competition between **(1.77)** and **(1.78)** arylation occurred preferentially on the fluorinated benzothiophene **(1.78)** which is not consistent with a S_EAr mechanism however it is consistent with a CMD mechanism since the C-H bond is more acidic in this case. A computational study also agreed with a CMD mechanism.

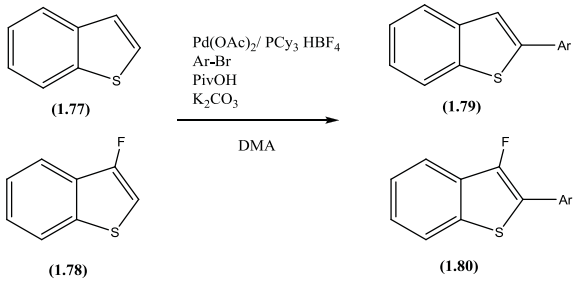

Scheme 1.26

Pyridine N-oxide can be used as substrate to direct arylation catalysed by $Pd(OAc)_2$ in presence of $CsCO_3$ **(Scheme 1.27)**.[134,135] The reaction is compatible with electron donating and electron withdrawing substituents. In all cases the arylation selectively takes place in the position ortho to the N-oxide which implies a weak interaction between the oxide and the Pd centre presumably *via* a four membered ring for the C-H activation step. The reaction is compatible with bromides, chlorides, iodides and triflates[136, 137] the latter has also been used for sp^3 arylation **(Scheme 1.27)**.[138, 139]

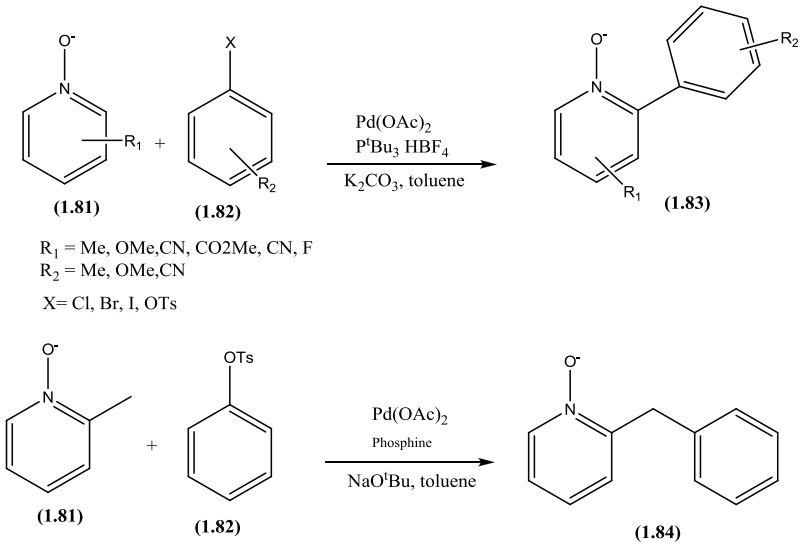

Scheme 1.27

Direct arylation *via* a five membered ring intermediate has been reported for weak donor groups e.g. ketones[140], aldehydes[141, 142], amides[143] and nitrobenzene[144]. However, direct arylation with arylhalides with strong N-donor groups, using Pd(II)/Pd(0) catalysts does not seem to be favourable probably due to a difficult reductive elimination from a stable cyclometallated intermediate (see below). Phenolates which are strong O-donors have been reported for direct arylation with aryl iodide *via* a six-membered ring cyclometallated intermediate to form **(1.85) (Scheme 1.28)**.[145] Note, in this case, unlike the previous cases involving the smaller rings, no phosphine ligand is used, presumably the strong chelating atom blocks one site hence a phosphine could not remain bonded throughout the catalytic cycle.

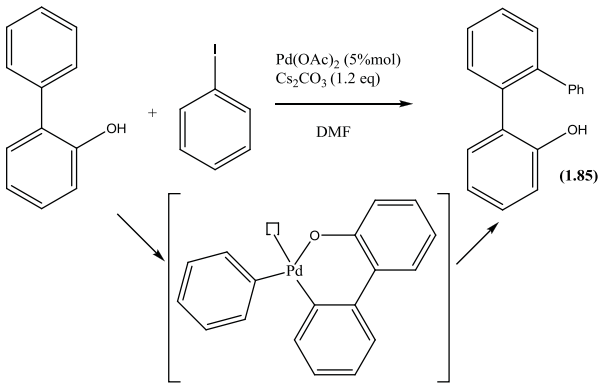

Scheme 1.28

As mentioned above, strong N-directing groups giving five or six membered rings have not been reported for the direct arylation with arylhalides with Pd(II)/Pd(0) catalysts. An alternative for the direct arylation of strong N-directing groups (arylpyridines, quinolines, pyrrolidinones, oxazolidinones, and benzodiazepines) has been reported by Sanford *et al.* in presence of $Pd(OAc)_2$ and diphenyliodonium salts. These reactions were proposed to proceed by a Pd(II)/Pd(IV) mechanism with (i) C-H activation at Pd(II) followed by (ii) oxidative addition of the iodonium salt and (iii) reductive elimination to form the desired product and regenerate the Pd(II) catalyst **(Scheme 1.29)**.[7, 146, 147] Generally, faster reaction rates and higher yields were observed with electron-deficient aryl groups.

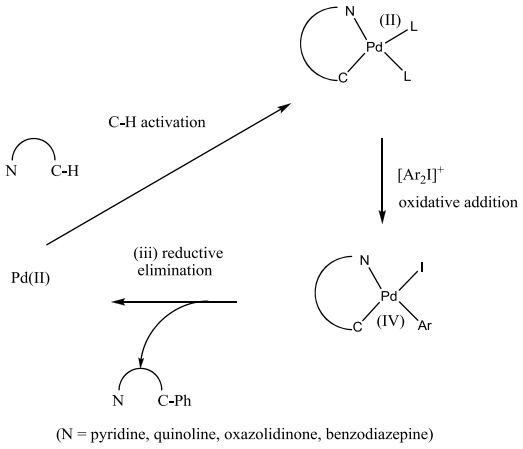

Scheme 1.29

In conclusion, Pd-catalysed direct arylation with halogenated substrates has been described with O-donor and weak N-donor directing groups *via* a Pd(0)/Pd(II) mechanism. The absence of reports showing arylation of strong directing groups *via* this mechanism suggests the reductive elimination step from a cyclometallated intermediate is difficult. Another method was to use a Pd(II)/Pd(IV) catalytic cycle where the reductive elimination from a Pd(IV) intermediate is much easier than from a Pd(II) intermediate.

1.4.1.2 Palladium catalysed direct arylation with non-halogenated substrates

Sanford *et al.* reported the Pd-catalysed coupling of two aryl C-H bonds with quinoline, pyridine, pyrazole, and pyrimidine which are strong directing groups in the presence of $AgCO_3$ and benzoquinone **(Scheme 1.30)**.[148] The order of C-H activations is different to the systems involving an aryl halide. No phosphine is present and in this case the cyclometallation occurs first whereas with aryl halides the oxidative addition occurs first. They showed that the presence of benzoquinone was essential; no conversion was observed without it. Mechanistic studies showed that the benzoquinone ligand is bound to the Pd centre during the second C-H activation probably making the the Pd(II) centre more electrophilic. The easier dissociation of the benzoquinone in comparison to phosphine probably helps the reductive elimination. They proposed that these transformations proceed *via* the (*i*) ligand-directed C-H activation to afford a cyclometallated intermediate, (*ii*) benzoquinone-assisted C-H activation of the arene, (*iii*) C–C bond forming reductive elimination, and (*iv*) oxidation of the Pd(0) to Pd(II) by Ag_2CO_3 **(Scheme 1.31)**.[148]

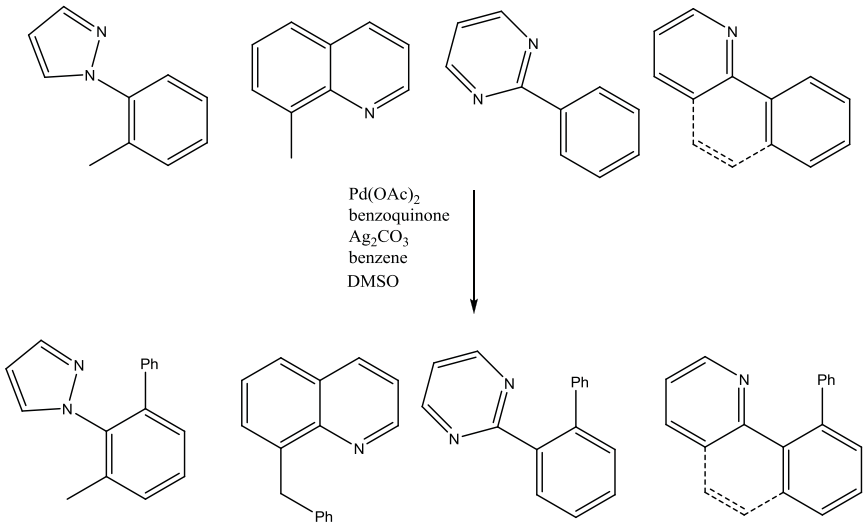

Scheme 1.30

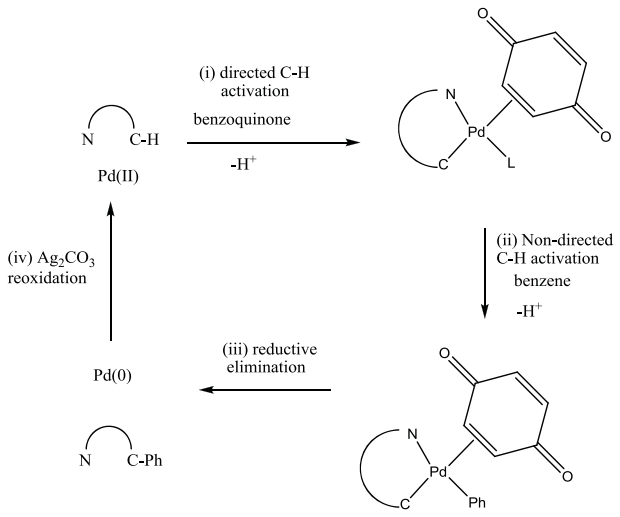

Scheme 1.31 Mechanism proposed by Sanford *et al*. for the arylation of strong directing group.[148]

C–C bond forming reactions involving C-H bonds on each coupling partner are rare, particularly those at inactivated sp^3 positions, however, Fagnou has described the development of arene-alkane coupling.[149,150] In the absence of a halogenated ligand an external oxidising agent is needed to make the catalytic cycle turnover. Fagnou showed that the use of an air atmosphere at ambient pressure provided superior outcomes compared to the use of other common oxidants such as copper(II) acetate and silver(I) acetate. The reaction could be applied to the formation of five-membered rings e.g. **(1.87)** *via* an sp^3 C-H activation **(Scheme 1.32)** and to sp^2 C-H activation to form a six-membered ring **(1.89)(Scheme 1.32)**, with optimum conditions using ^{t}BuONa in pivalic acid. This also showed that esters could direct the arylation *via* a five membered ring in an intramolecular process.[150]

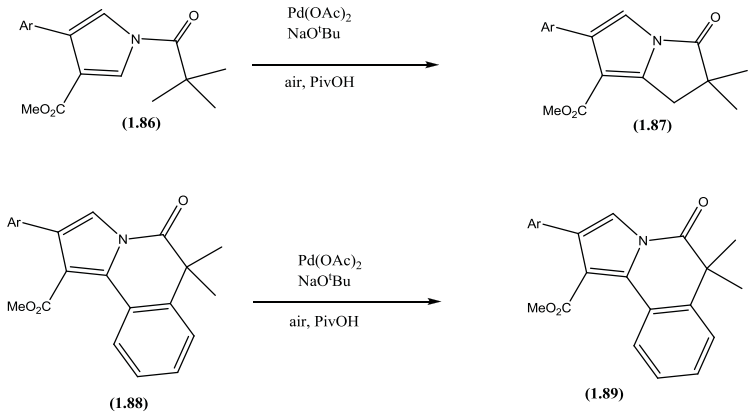

Scheme 1.32

Intermolecular coupling of two sp^2 C-H bonds has been reported using O-directing groups with pyridine N-oxide and Ag(OAc) as an oxidising reagent **(Scheme 1.33)**.[151] No homocoupled product was observed which implies that the oxygen directs the C-H activation *via* a four membered ring. In this case oxidative addition of the C-H bond of the pyridine N-oxide with Pd(0).

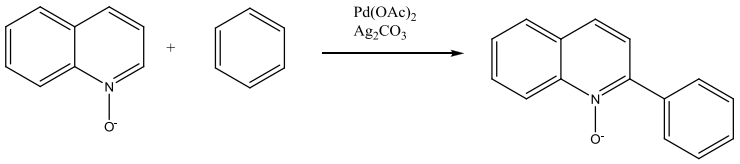

Scheme 1.33

1.4.1.3 Palladium catalysed direct arylation with no directing group

The direct arylation of a triazole with ArCl[152], ArBr[153] and ArOTs[120] has been recently reported. Interestingly the arylation selectively took place in the heterocyclic ring to form **(1.90)** and not on the aromatic ring which showed that a cyclometallated triazole complex could not be an intermediate of this reaction, this is therefore an example of a non directed arylation **(Scheme 1.34)**.

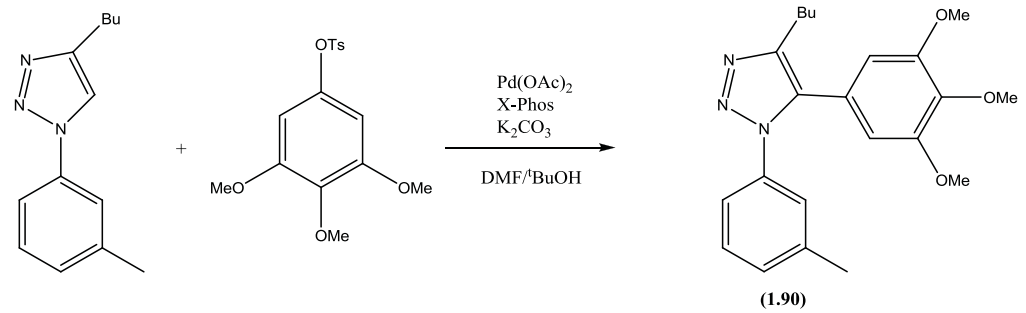

Scheme 1.34

In 2006, Fagnou reported the arylation with no directing groups of electron deficient perfluorobenzenes **(1.91)** with ArBr **(1.92)** to form **(1.93) (Scheme 1.35)**. The reaction was favoured with C-H acidic benzenes i.e. a selectivity opposite to a S_EAr pathway. Computational studies revealed that the key C-H bond functionalisation step occurred *via* a CMD mechanism. The same group extended this reaction to Cl.[154] The authors concluded that the C-H activation depended on the acidity of the C-H bond rather than the nucleophilicity. They also showed direct arylation of non fluorinated benzenes, [108] interestingly a catalytic amount of pivalic acid was needed for the reaction to proceed in this case.[108]

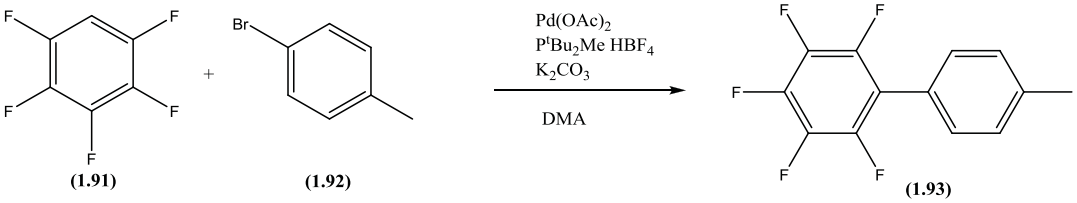

Scheme 1.35

As mentioned earlier the ideal situation is the intermolecular coupling of two C-H bonds without preactivation and directing group. Lu *et al.* reported the direct arylation of benzene with mesitylene.[155] They showed that the ratio of the concentrations of TFA/$K_2S_2O_8$ was important to achieve the formation of **(1.94)(Scheme 1.36)**.

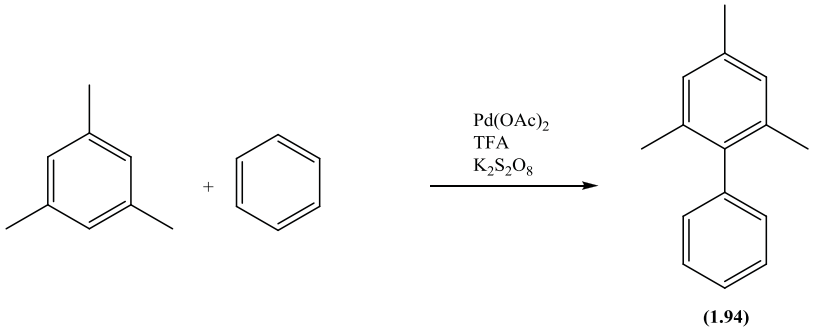

(1.94)

Scheme 1.36

In the case of palladium the intra and intermolecular direct arylation with no preactivation and no directing group could be achieved, however there are currently only a few examples. On the other hand, direct arylation of halogenated rings can be achieved with a wide range of directing groups. The understanding of the mechanism allowed further use of this reaction specially the use of pivalic acid to produce arylation of electron deficient aryl halide groups.

1.4.2 Ruthenium catalysed direct arylation

2-phenylpyridine has been described as directing group for direct arylation using halogenated aryl groups. Monoarylated product **(1.95)** was the major product in the presence of $[RuCl_2(C_6H_6)]_2$, PPh_3 with aryl chlorides, bromides and iodides.[156] Monoarylation was also observed in the case of tosylates with 2-phenylpyridine using $[RuCl_2(pcy)]_2$ and $HPOR_2$ in presence of $CsCO_3$[157] however diarylation **(1.96)** was observed in the case of aryl chlorides and bromides.[157, 158] Ackermann improved this methodology by using $RuCl_3(H_2O)_n$ as a catalyst in the presence of K_2CO_3 without phosphine, however, diarylated products were the major products **(Scheme 1.37)**.[159] This method have also been described with aryliodide using peroxides instead of K_2CO_3 **(Scheme 1.37)**.[160]

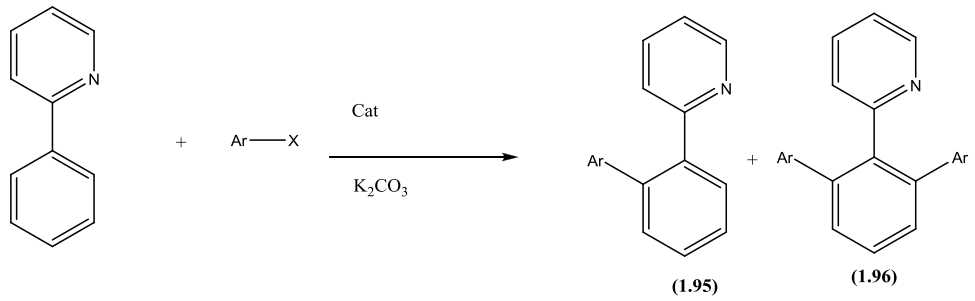

(1.95) **(1.96)**

Catalyst	additive	major product formed: monoarylation	major product formed: diarylation
$[RuCl_2(arene)]_2$ arene = C_6H_6	+ PPh_3	X = Br, Cl, I ref 161	
$[RuCl_2(arene)]_2$ arene = pcy	+ $HP(O)R_2$	X = OTs ref 162	X = Cl, Br ref 163
$RuCl_3$ n(H_2O)			X = Br ref 164
$RuCl_3$ n(H_2O)	+ peroxides		X = I ref 165

Scheme 1.37

Pyridine can also direct a non-aromatic sp^2 C-H arylation **(1.97)** catalysed by $[RuCl_2(C_6H_6)]_2$ in the presence of K_2CO_3 and PPh_3 **(Scheme 1.38)**. The authors proposed a mechanism which involved (i) an oxidative addition of the aryl halide to a ruthenium complex to give an aryl ruthenium intermediate, (ii) C-H activation of the alkene, directed by coordination of the pyridyl group to the ruthenium atom and finally (iii) reductive elimination to afford the arylated product (**1.98)** with the simultaneous regeneration of the initial ruthenium complex.[161]

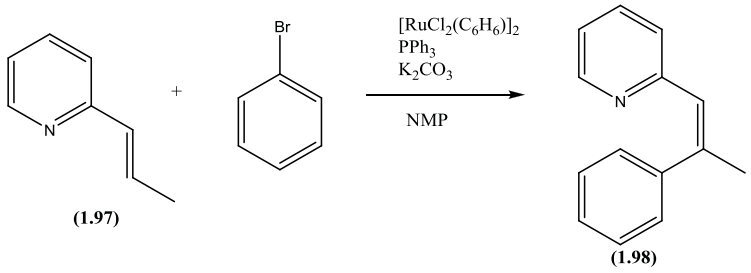

Scheme 1.38

Ackermann also reported arylation of a cyclohexene directed by a pyridine with an arylchloride.[162] The same group expanded the area of the functional groups directing the arylation to imines[157], oxazolines[163], pyrazoles[159] and triazoles[159]. They suggested an AMLA type of transition state.

Interestingly in the case of triazoles the regioselectivity is different to the Pd-catalysed direct arylation. In this case the formation of **(1.99)(Scheme 1.39)** suggests a five membered ring cyclometallated intermediate.[163, 164]

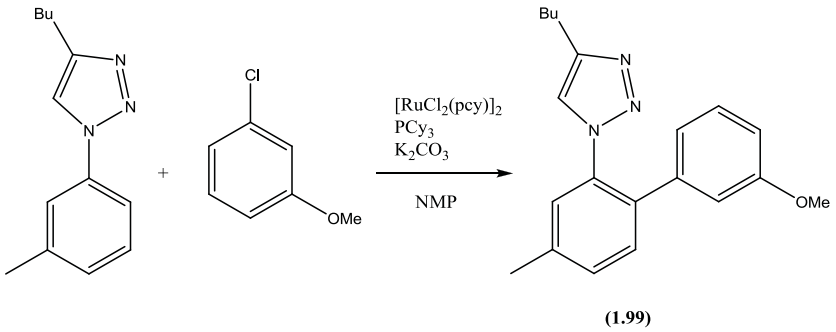

Scheme 1.39

Hence, direct arylation with aryl halides using ruthenium catalysts is efficient with strong N-directing groups. Mechanistic work showed cyclometallated intermediates, in those reactions which involve carboxylate activation of the C-H bond probably proceeds *via* an AMLA type of mechanism. It is noticeable that the type of directing group (strong donor) is different and complementary to Pd catalysts (weak donors). Direct

arylation without a directing group or without prehalogenated aryl groups has not yet been reported in the case of ruthenium catalysts.

1.4.3 Rhodium catalysed direct arylation

Rhodium shows good catalyst properties for the application of C-H activation and the area has been reviewed recently by Bergman *et al.*[6] Phenols are good directing groups for arylation, as observed with palladium catalysts, thus the reaction of **(1.100)** and **(1.101)** in presence of a Rh(I) catalyst produced **(1.102)(Scheme 1.40)**.

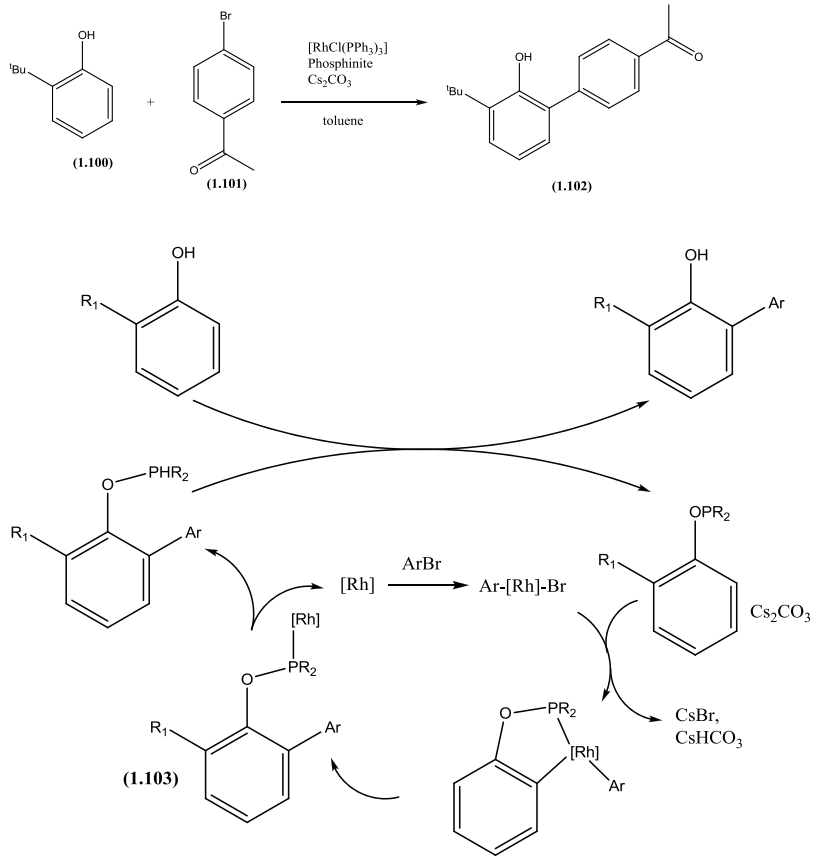

Scheme 1.40

The proposed mechanism **(Scheme 1.40)** starts with an oxidative addition of the aryl bromide to the rhodium(I) catalyst, followed by ortho-metallation of the phosphinite. Reductive elimination then occurs to give intermediate **(1.103)**. The catalytically active species is regenerated through dissociation of the phosphinite which undergoes

transesterification with the corresponding phenol to give desired the 2-arylated phenol.[9, 165-167]

Pyridines and quinolines can direct arylation with acid chlorides in the presence of $[RhCl(CO)_2]_2$ as a catalyst with Na_2CO_3 and no phosphine.[168] The authors proposed a mechanism involving oxidative addition of the acyl chloride, followed by decarbonylation to give a Rh(III)-aryl species and then chelation-assisted C-H activation followed by reductive elimination to give **(1.104)(Scheme 1.41)**. In the absence of a protective group double arylation was observed to form **(1.105)**. Subsequently, Bergman *et al.* reported a similar reaction using an aryl bromide in place of the acyl chloride.[169]

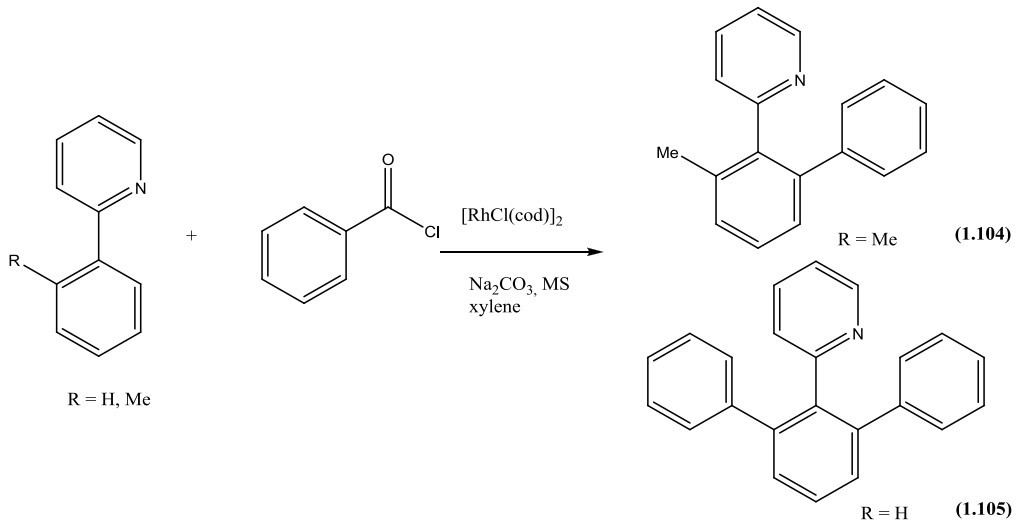

Scheme 1.41

Direct arylation of a wide range of heterocycles with aryl iodides occurs in the presence of $[RhCl(coe)]_2$, PCy_3 and NEt_3 **(Scheme 1.42)**. The proposed mechanism (**Scheme 1.43)** involves coordination of the heterocycle to form **(1.106)** followed by tautomerisation by proton transfer from the C-H to make the carbene complex **(1.107)**. Oxidative addition of aryl halides occurs followed by elimination of HI to produce

(1.108). Finally, reductive elimination of the desired arylated product would regenerate the Rh catalyst. [169, 170]

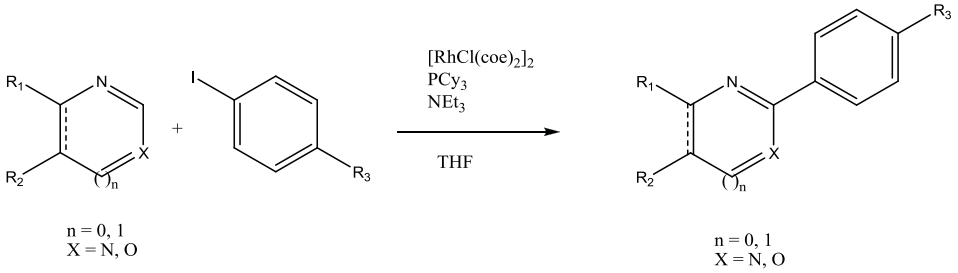

Scheme 1.42

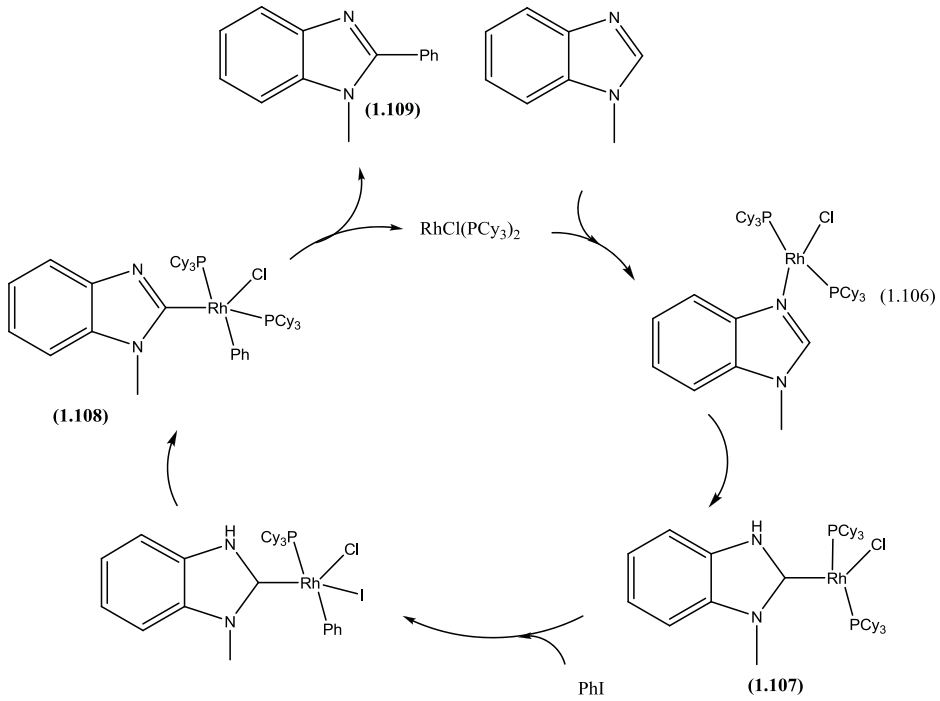

Scheme 1.43

Indoles could not be arylated under the conditions described by Bergman in **Scheme 1.42**. However, Sames *et al.* showed the arylation of indole using [$RhCl(PCy_3)_2$] as catalyst precursor, however, electron deficient phosphines and pivalate were both necessary to convert **(1.110)** into **(1.111)(Scheme 1.44)**.[171] An electrophilic C-H activation assisted by the pivalate *via* Rh(III) intermediate **(1.112)** was proposed **(Scheme 1.45)**. This methodology was later extended to thiophenes by Itami *et al.*[172, 173]

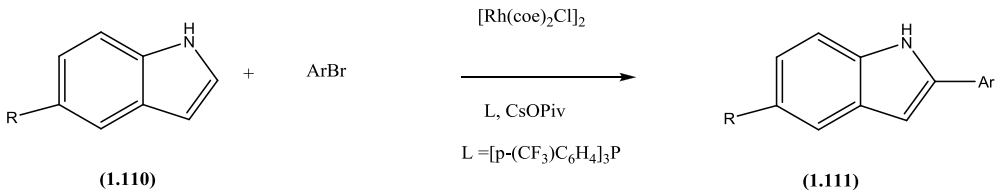

Scheme 1.44

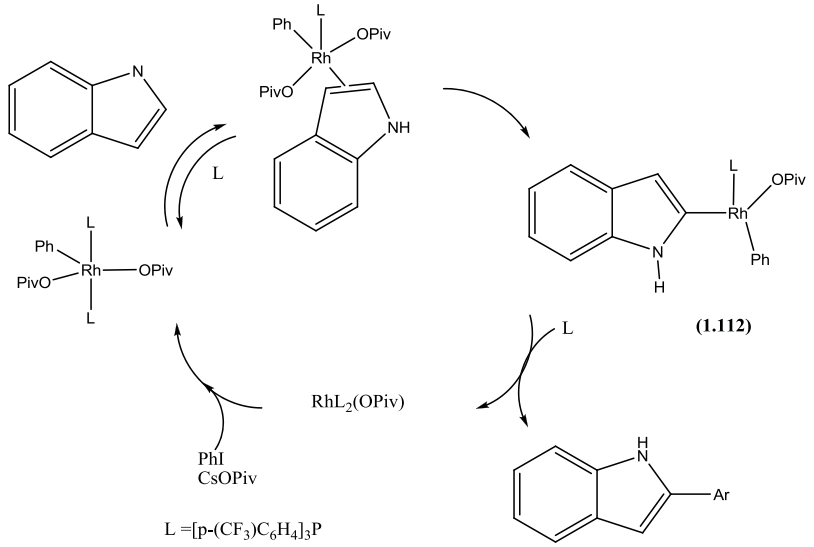

Scheme 1.45

The only example of a direct arylation of benzene was achieved in the synthesis of **(1.113)** (X= Cl, Br, I) catalysed by $[RhCl(cod)]_2$ **(Scheme 1.46)** by Kempe *et al.* in 2007. However, in this case a radical mechanism was proposed.

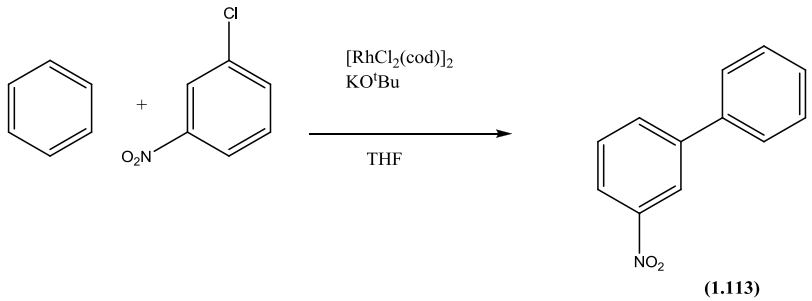

Scheme 1.46

All the examples above involve oxidative addition of an aryl halide to a Rh(I) species. However as mentioned in section 1.2 oxidative addition of a C-H bond is also possible

at Rh(I). This type of reaction has also been used in catalytic C–C bond forming reactions, for example in the hydroiminoacylation of an alkene with aldimine **(1.114)** catalysed by [$RhCl(PPh_3)_3$]. The mechanism involves the oxidative addition of a C-H bond to form the intermediate cyclometallated species **(1.115)**, followed by an alkene insertion into the Rh-H bond and reductive elimination to produce **(1.116)(Scheme 1.47)**.[174] Note reactions involving insertion of alkenes and alkynes into the M–C bond of a cyclometallated intermediate is also possible and examples of these reactions will be discussed further in Chapter 4.

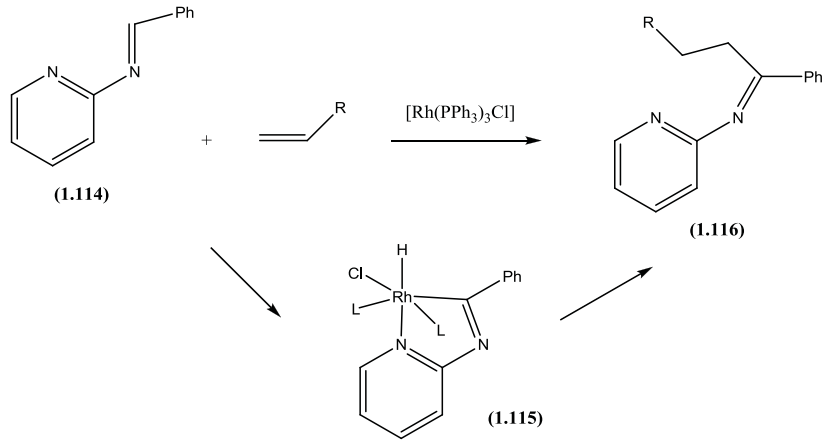

Scheme 1.47

In conclusion, Rh-catalysed direct arylation is an efficient process with O-or N-donor directing groups, however the variety of directing groups is not as wide as with Pd. Notably more than one mechanism is possible even when Rh(I)/Rh(III) cycles are involved, the C-H activation can occur at Rh(I) or at Rh(III). In addition processes involving a carbene intermediate are also possible. Hence though the overall synthetic scope of Rh-catalysed CH activation is perhaps not yet as great as Pd, Rh-catalysis has more mechanistic variety. So far the only example of a Rh-catalysed intermolecular direct arylation with no directing group is a radical based process.

1.4.4 Iridium catalysed direct arylation

Examples of direct arylation with iridium are very rare in the literature. In 2004, Yamaguchi *et al.* showed the direct arylation of benzene using aryl iodides as substrates with $[Cp^*IrHCl]_2$ as a catalyst and KO^tBu as a base.[175] The regioselectivity observed in the case of PhOMe (anisole) (*ortho*: *meta*: *para*, 6:1:1) led the authors to suggest that the mechanism goes *via* a radical mechanism **(Scheme 1.48)**.

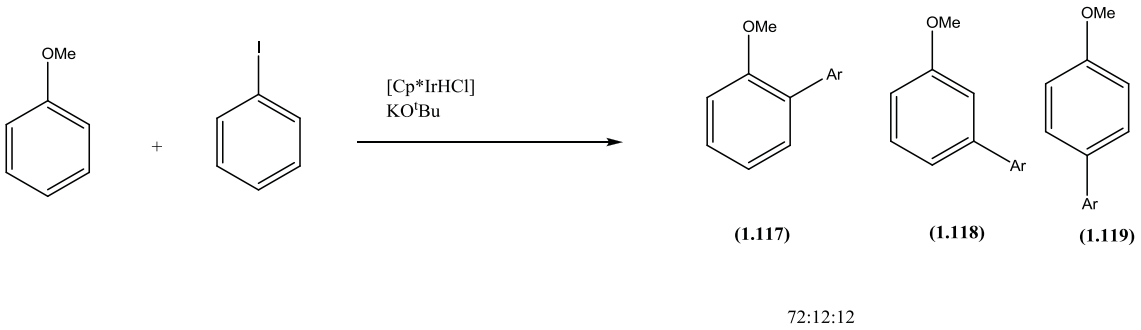

Scheme 1.48

Itami *et al.* described the Ir-catalysed direct arylation of electron rich thiophenes using aryl iodides.[176] Thiophene **(1.120)** reacted with the iodobenzene in the presence of $[Ir(cod)(py)PCy_3][PF_6]$ as a catalyst and Ag_2CO_3 **(Scheme 1.49)**. In this case the authors suggested an electrophilic metallation process.

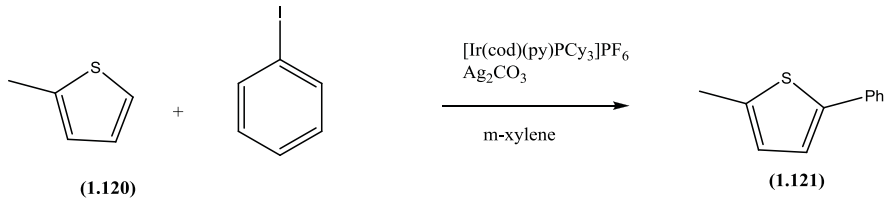

Scheme 1.49

In conclusion, iridium shows similar reactivity to rhodium in the case of cyclometallation (see section 1.2) but it is clear that it is less reactive in term of catalysis and only aryl iodides which undergo oxidative addition most easily can be used so far. However, for iridium as for Rh and Pd a strongly bound directing group is clearly not

necessary. Other examples of Rh- or Ir-catalysis involving C-H activation and C–C bond formation will be discussed in Chapter 4. These involve $[MCl_2Cp^*]_2$ precursors and reactions with alkenes or alkynes.

From this section catalytic C-H activation has a considerable range of applications particularly in direct arylation. Pd is currently the most versatile metal, however complementary results on selectivity could be obtained with Rh and Ru. Catalytic C-H activation can occur by more than one mechanism, with AMLA type activations now being the most common. This section has emphasised the importance of understanding the mechanism of C-H activation to be able to apply it to a broader range of applications in direct arylation with the ultimate aim to be able to selectively couple two “inert” C-H bonds.

1.5 Conclusion

The aim of this introduction was to describe the areas of stoichiometric and catalytic C-H activation with Pd, Ru, Rh and Ir transition metal complexes. Synthesis of cyclometallated complexes with Pd(II) is the most versatile method with a broad range of N-directing groups. From Ru, Rh and Ir it is noticeable that there is no single method which can produce the cyclometallated complexes by C-H activation with a wide range directing groups. There are different mechanisms for C-H activation, OA, SBM, AMLA(4) or AMLA(6) mechanisms and computational studies often allowed one to distinguish between these. Catalytic C-H activation has great synthetic potential and in terms of direct arylation complementary results could be obtained with different transition metal catalysts. This thesis will focus in acetate assisted C-H activation (AMLA(6)) with half sandwich complexes of iridium, rhodium and ruthenium. Chapter 2 will focus on scope and the effect of the directing group will be investigated in Chapter 2. The role(s) of the carboxylate in the reaction will be discussed in Chapter 3 and Chapter 4 will describe the results obtained from the insertion of alkynes into the M–C bond of cyclometallated complexes in the context of catalytic C–C bond formation already described by Miura[177,178,179,180,181] and Fagnou.[182]

1.6 Bibliography

1 R. G. Bergman, *Nature*, 2007, **446**, 391.
2 R. H. Crabtree, *J. Chem. Soc., Dalton Trans.*, 2001, 2437.
3 J. A. Labinger and J. E. Bercaw, *Nature*, 2002, **417**, 507.
4 A. E. Shilov and G. B. Shul'pin, *Chem. Rev.*, 1997, **97**, 2879.
5 S. Murai, F. Kakiuchi, S. Sekine, Y. Tanaka, A. Kamatani, M. Sonoda, and N. Chatani, *Nature*, 1993, **366**, 529.
6 D. A. Colby, R. G. Bergman, and J. A. Ellman, *Chem. Rev.*, 2009, **110**, 624.
7 T. W. Lyons and M. S. Sanford, *Chem. Rev.*, 2010, **110**, 1147.
8 G. P. Chiusoli, M. Catellani, M. Costa, E. Motti, N. Della Ca, and G. Maestri, *Coord. Chem. Rev.*, 2010, **254**, 456.
9 J. C. Lewis, R. G. Bergman, and J. A. Ellman, *Acc. Chem. Res.*, 2008, **41**, 1013.
10 S. Trofimenko, *Inorg. Chem.*, 1973, **12**, 1215.
11 J. P. Kleiman and M. Dubeck, *J. Am. Chem. Soc.*, 1963, **85**, 1544.
12 A. C. Cope and R. W. Siekman, *J. Am. Chem. Soc.*, 1965, **87**, 3272.
13 M. Catellani, *Angew. Chem., Int. Ed.*, 2009, **48**, 2636.
14 Y. Wu, S. Huo, J. Gong, X. Cui, L. Ding, K. Ding, C. Du, Y. Liu, and M. Song, *J. Organomet. Chem.*, 2001, **637-639**, 27.
15 Y. J. Wu, Y. H. Liu, K. L. Ding, H. Z. Yuan, and X. A. Mao, *J. Organomet. Chem.*, 1995, **505**, 37.
16 A. C. Cope and E. C. Friedrich, *J. Am. Chem. Soc.*, 1968, **90**, 909.
17 A. D. Ryabov and A. K. Yatsimirsky, *Inorg. Chem.*, 1984, **23**, 789.
18 D. M. Grove, G. Van Koten, H. J. C. Ubbels, R. Zoet, and A. L. Spek, *Organometallics*, 1984, **3**, 1003.
19 V. Ritleng, C. Sirlin, and M. Pfeffer, *Chem. Rev.*, 2002, **102**, 1731.
20 A. D. Ryabov, *Chem. Rev.*, 1990, **90**, 403.
21 J. Dupont, M. Pfeffer, and J. Spencer, *Eur. J. Inorg. Chem.*, 2001, **2001**, 1917.
22 A. D. Ryabov, I. K. Sakodinskaya, and A. K. Yatsimirsky, *J. Chem. Soc., Dalton Trans.*, 1985, 2629.
23 J. Vicente, I. Saura-Llamas, J. Cuadrado, and M. C. Ramirez de Arellano, *Organometallics*, 2003, **22**, 5513.
24 I. R. Girling and D. A. Widdowson, *J. Chem. Soc. Perkin Trans*, 1988, 1317.
25 P. Espinet, G. Garcia, F. J. Herrero, Y. Jeannin, and M. Philoche-Levisalles, *Inorg. Chem.*, 1989, **28**, 4207.
26 J. Granell, R. Moragas, J. Sales, M. Font-Bardía, and X. Solans, *J. Organomet. Chem.*, 1992, **431**, 359.
27 A. Albinati, S. Affolter, and P. S. Pregosin, *J. Organomet. Chem.*, 1990, **395**, 231.
28 M. Waldo, J. K. Alfred, and R. Paul, *Helv. Chim. Acta*, 1992, **75**, 2531.
29 S. Affolter and P. S. Pregosin, *J. Organomet. Chem.*, 1990, **398**, 197.
30 J. Selbin and M. A. Gutierrez, *J. Organomet. Chem.*, 1983, **246**, 95.
31 G. B. Caygill, R. M. Hartshorn, and P. J. Steel, *J. Organomet. Chem.*, 1990, **382**, 455.
32 H. Onoue, K. Minami, and K. Nakagawa, *Bull. Chem. Soc. Jpn.*, 1970, **43**, 3480.
33 K. Hiraki, Y. Fuchita, H. Nakaya, and S. Takakura, *Bull. Chem. Soc. Jpn.*, 1979, **52**, 2531.
34 M. R. Churchill, H. J. Wasserman, and G. J. Young, *Inorg. Chem.*, 1980, **19**, 762.

[35] A. A. Watson, D. A. House, and P. J. Steel, *J. Organomet. Chem.*, 1986, **311**, 387.
[36] G. B. Caygill and P. J. Steel, *J. Organomet. Chem.*, 1987, **327**, 115.
[37] M. Gomez, J. Granell, and J. Martinez, *J. Chem. Soc., Dalton Trans.*, 1998, 37.
[38] J. Dupont, M. Pfeffer, M. A. Rotteveel, A. De Cian, and J. Fischer, *Organometallics*, 1989, **8**, 1116.
[39] J. Barker, N. D. Cameron, M. Kilner, M. M. Mahmoud, and S. C. Wallwork, *J. Chem. Soc., Dalton Trans.*, 1991, 3435.
[40] J. Albert, M. Gomez, J. Granell, J. Sales, and X. Solans, *Organometallics*, 1990, **9**, 1405.
[41] K. Gehrig, M. Hugentobler, A. J. Klaus, and P. Rys, *Inorg. Chem.*, 1982, **21**, 2493.
[42] K. Hiraki, Y. Fuchita, and K. Takechi, *Inorg. Chem.*, 1981, **20**, 4316.
[43] B. Galli, F. Gasparrini, B. E. Mann, L. Maresca, G. Natile, A. M. Manottilanfredi, and A. Tiripicchio, *J. Chem. Soc., Dalton Trans.*, 1985, 1155.
[44] B. Galli, F. Gasparrini, L. Maresca, G. Natile, and G. Palmieri, *J. Chem. Soc., Dalton Trans.*, 1983, 1483.
[45] G. Balavoine and J. C. Clinet, *J. Organomet. Chem.*, 1990, **390**, C84.
[46] K. Hiraki, Y. Fuchita, M. Nakashima, and H. Hiraki, *Bull. Chem. Soc. Jpn.*, 1986, **59**, 3073.
[47] J. Albert, J. Granell, J. Sales, X. Solans, and M. Font-Altaba, *Organometallics*, 1986, **5**, 2567.
[48] A. G. Constable, W. S. McDonald, L. C. Sawkins, and B. L. Shaw, *J. Chem. Soc., Dalton Trans.*, 1980, 1992.
[49] V. A. Polyakov and A. D. Ryabov, *J. Chem. Soc., Dalton Trans.*, 1986, 589.
[50] V. I. Sokolov, T. A. Sorokina, L. L. Troitskaya, L. I. Solovieva, and O. A. Reutov, *J. Organomet. Chem.*, 1972, **36**, 389.
[51] I. Omae, *Chem. Rev.*, 1979, **79**, 287.
[52] M. Albrecht, *Chem. Rev.*, 2009, **110**, 576.
[53] J. P. Djukic, J. B. Sortais, L. Barloy, and M. Pfeffer, *Eur. J. Inorg. Chem.*, 2009, 817.
[54] A. J. Toner, S. Grundemann, E. Clot, H. H. Limbach, B. Donnadieu, S. Sabo-Etienne, and B. Chaudret, *J. Am. Chem. Soc.*, 2000, **122**, 6777.
[55] R. L. Bennett, M. I. Bruce, F. G. A. Stone, M. Z. Iqbal, and B. L. Goodall, *J. Chem. Soc., Dalton Trans.*, 1972, 1787.
[56] L. Zhang, L. Dang, T. B. Wen, H. H. Y. Sung, I. D. Williams, Z. Lin, and G. Jia, *Organometallics*, 2007, **26**, 2849.
[57] P. Marcazzan, B. O. Patrick, and B. R. James, *Russian Chemical Bulletin*, 2003, **52**, 2715.
[58] P. Marcazzan, B. O. Patrick, and B. R. James, *Organometallics*, 2005, **24**, 1445.
[59] M. Lavin, E. M. Holt, and R. H. Crabtree, *Organometallics*, 1989, **8**, 99.
[60] M. Nonoyama and K. Yamasaki, *Inorganic and Nuclear Chemistry Letters*, 1971, **7**, 943.
[61] H. Onoue and I. Moritani, *J. Organomet. Chem.*, 1972, **44**, 189.
[62] E. Baranoff, J.-H. Yum, M. Graetzel, and M. K. Nazeeruddin, *J. Organomet. Chem.*, 2009, **694**, 2661.
[63] D. L. Davies, O. Al-Duaij, J. Fawcett, M. Giardiello, S. T. Hilton, and D. R. Russell, *Dalton Trans.*, 2003, 4132.
[64] D. Balcells, E. Clot, and O. Eisenstein, *Chem. Rev.*, 2010, **110**, 749.

[65] D. L. Davies, S. M. A. Donald, O. Al-Duaij, J. Fawcett, C. Little, and S. A. Macgregor, *Organometallics*, 2006, **25**, 5976.
[66] J. K. Hoyano, A. D. McMaster, and W. A. G. Graham, *J. Am. Chem. Soc.*, 1983, **105**, 7190.
[67] A. H. Janowicz and R. G. Bergman, *J. Am. Chem. Soc.*, 1982, **104**, 352.
[68] W. D. Jones and F. J. Feher, *J. Am. Chem. Soc.*, 1984, **106**, 1650.
[69] W. D. Jones and F. J. Feher, *Acc. Chem. Res.*, 1989, **22**, 91.
[70] B. A. Arndtsen, R. G. Bergman, T. A. Mobley, and T. H. Peterson, *Acc. Chem. Res.*, 1995, **28**, 154.
[71] R. H. Crabtree, *Chem. Rev.*, 1985, **85**, 245.
[72] R. H. Crabtree, *Chem. Rev.*, 1995, **95**, 987.
[73] A. H. Janowicz and R. G. Bergman, *J. Am. Chem. Soc.*, 1983, **105**, 3929.
[74] B. A. Arndtsen and R. G. Bergman, *J. Organomet. Chem.*, 1995, **504**, 143.
[75] P. Burger and R. G. Bergman, *J. Am. Chem. Soc.*, 1993, **115**, 10462.
[76] D. M. Tellers, C. M. Yung, B. A. Arndtsen, D. R. Adamson, and R. G. Bergman, *J. Am. Chem. Soc.*, 2002, **124**, 1400.
[77] B. K. Corkey, F. L. Taw, R. G. Bergman, and M. Brookhart, *Polyhedron*, 2004, **23**, 2943.
[78] S. Niu and M. B. Hall, *J. Am. Chem. Soc.*, 1998, **120**, 6169.
[79] P. L. Watson and G. W. Parshall, *Acc. Chem. Res.*, 1985, **18**, 51.
[80] M. E. Thompson, S. M. Baxter, A. R. Bulls, B. J. Burger, M. C. Nolan, B. D. Santarsiero, W. P. Schaefer, and J. E. Bercaw, *J. Am. Chem. Soc.*, 1987, **109**, 203.
[81] Z. Y. Lin, *Coord. Chem. Rev.*, 2007, **251**, 2280.
[82] W. H. Lam, G. C. Jia, Z. Y. Lin, C. P. Lau, and O. Eisenstein, *Chem. Eur. J.*, 2003, **9**, 2775.
[83] J. Oxgaard, R. P. Muller, W. A. Goddard, and R. A. Periana, *J. Am. Chem. Soc.*, 2004, **126**, 352.
[84] N. A. Foley, M. Lail, T. B. Gunnoe, T. R. Cundari, P. D. Boyle, and J. L. Petersen, *Organometallics*, 2007, **26**, 5507.
[85] N. J. DeYonker, N. A. Foley, T. R. Cundari, T. B. Gunnoe, and J. L. Petersen, *Organometallics*, 2007, **26**, 6604.
[86] N. A. Foley, T. B. Gunnoe, T. R. Cundari, P. D. Boyle, and J. L. Petersen, *Angew. Chem., Int. Ed.*, 2008, **47**, 726.
[87] B. A. Vastine and M. B. Hall, *J. Am. Chem. Soc.*, 2007, **129**, 12068.
[88] Y. Boutadla, D. L. Davies, S. A. Macgregor, and A. I. Poblador-Bahamonde, *Dalton Trans.*, 2009, 5820.
[89] P. J. Walsh, F. J. Hollander, and R. G. Bergman, *J. Am. Chem. Soc.*, 1988, **110**, 8729.
[90] C. C. Cummins, S. M. Baxter, and P. T. Wolczanski, *J. Am. Chem. Soc.*, 1988, **110**, 8731.
[91] T. R. Cundari, T. R. Klinckman, and P. T. Wolczanski, *J. Am. Chem. Soc.*, 2002, **124**, 1481.
[92] L. M. Slaughter, P. T. Wolczanski, T. R. Klinckman, and T. R. Cundari, *J. Am. Chem. Soc.*, 2000, **122**, 7953.
[93] W. J. Tenn, K. J. H. Young, G. Bhalla, J. Oxgaard, W. A. Goddard, and R. A. Periana, *J. Am. Chem. Soc.*, 2005, **127**, 14172.
[94] Y. Feng, M. Lail, K. A. Barakat, T. R. Cundari, T. B. Gunnoe, and J. L. Petersen, *J. Am. Chem. Soc.*, 2005, **127**, 14174.

[95] Y. Feng, M. Lail, N. A. Foley, T. B. Gunnoe, K. A. Barakat, T. R. Cundari, and J. L. Petersen, *J. Am. Chem. Soc.*, 2006, **128**, 7982.
[96] T. R. Cundari, T. V. Grimes, and T. B. Gunnoe, *J. Am. Chem. Soc.*, 2007, **129**, 13172.
[97] W. J. Tenn, K. J. H. Young, J. Oxgaard, R. J. Nielsen, W. A. Goddard, and R. A. Periana, *Organometallics*, 2006, **25**, 5173.
[98] J. Oxgaard, W. J. Tenn, R. J. Nielsen, R. A. Periana, and W. A. Goddard, *Organometallics*, 2007, **26**, 1565.
[99] M. Gomez, J. Granell, and M. Martinez, *Organometallics*, 1997, **16**, 2539.
[100] D. L. Davies, S. M. A. Donald, and S. A. Macgregor, *J. Am. Chem. Soc.*, 2005, **127**, 13754.
[101] L. Li, W. W. Brennessel, and W. D. Jones, *Organometallics*, 2009, **28**, 3492.
[102] D. Garcia-Cuadrado, A. A. C. Braga, F. Maseras, and A. M. Echavarren, *J. Am. Chem. Soc.*, 2006, **128**, 1066.
[103] M. Lafrance, S. I. Gorelsky, and K. Fagnou, *J. Am. Chem. Soc.*, 2007, **129**, 14570.
[104] M. Chaumontet, R. Piccardi, N. Audic, J. Hitce, J.-L. Peglion, E. Clot, and O. Baudoin, *J. Am. Chem. Soc.*, 2008, **130**, 15157.
[105] J. P. Stambuli, C. D. Incarvito, M. Buhl, and J. F. Hartwig, *J. Am. Chem. Soc.*, 2004, **126**, 1184.
[106] B. Biswas, M. Sugimoto, and S. Sakaki, *Organometallics*, 2000, **19**, 3895.
[107] M. Lafrance, C. N. Rowley, T. K. Woo, and K. Fagnou, *J. Am. Chem. Soc.*, 2006, **128**, 8754.
[108] M. Lafrance and K. Fagnou, *J. Am. Chem. Soc.*, 2006, **128**, 16496.
[109] D. H. Ess, S. M. Bischof, J. Oxgaard, R. A. Periana, and W. A. Goddard, *Organometallics*, 2008, **27**, 6440.
[110] S. M. Bischof, D. H. Ess, S. K. Meier, J. Oxgaard, R. J. Nielsen, G. Bhalla, W. A. Goddard, and R. A. Periana, *Organometallics*, 2010, **29**, 742.
[111] N. Miyaura and A. Suzuki, *Chem. Rev.*, 1995, **95**, 2457.
[112] J.-P. Corbet and G. r. Mignani, *Chem. Rev.*, 2006, **106**, 2651.
[113] L. Ackermann, R. Vicente, and A. Kapdi, R, *Angew. Chem., Int. Ed.*, 2009, **48**, 9792.
[114] D. E. Ames and D. Bull, *Tetrahedron*, 1982, **38**, 383.
[115] D. E. Ames and A. Opalko, *Tetrahedron*, 1984, **40**, 1919.
[116] D. E. Ames and A. Opalko, *Synthesis*, 1983, 234.
[117] L. C. Campeau and K. Fagnou, *Chem. Commun.*, 2006, 1253.
[118] L. C. Campeau, M. Parisien, A. Jean, and K. Fagnou, *J. Am. Chem. Soc.*, 2006, **128**, 581.
[119] M. Lafrance, D. Lapointe, and K. Fagnou, *Tetrahedron*, 2008, **64**, 6015.
[120] L. Ackermann, A. Althammer, and S. Fenner, *Angew. Chem., Int. Ed.*, 2009, **48**, 201.
[121] N. Lebrasseur and I. Larrosa, *J. Am. Chem. Soc.*, 2008, **130**, 2926.
[122] R. D. Rieth, N. P. Mankad, E. Calimano, and J. P. Sadighi, *Org. Lett.*, 2004, **6**, 3981.
[123] B. Liegault, D. Lapointe, L. Caron, A. Vlassova, and K. Fagnou, *J. Org. Chem.*, 2009, **74**, 1826.
[124] F. Bellina, S. Cauteruccio, A. Di Fiore, C. Marchetti, and R. Rossi, *Tetrahedron*, 2008, **64**, 6060.
[125] Z. Dongbing, W. Weida, L. Shuang, Y. Fei, L. Jingbo, and Y. Jingsong, *Chem. Eur. J.*, 2009, **15**, 1337.

[126] T. Okazawa, T. Satoh, M. Miura, and M. Nomura, *J. Am. Chem. Soc.*, 2002, **124**, 5286.
[127] B. Glover, K. A. Harvey, B. Liu, M. J. Sharp, and M. F. Tymoschenko, *Org. Lett.*, 2003, **5**, 301.
[128] J. Roger and H. Doucet, *Organic & Biomolecular Chemistry*, 2008, **6**, 169.
[129] A. Yokooji, T. Okazawa, T. Satoh, M. Miura, and M. Nomura, *Tetrahedron*, 2003, **59**, 5685.
[130] M. Parisien, D. Valette, and K. Fagnou, *J. Org. Chem.*, 2005, **70**, 7578.
[131] L. G. Aditya and D. Henri, *Eur. J. Inorg. Chem.*, 2007, **2007**, 3629.
[132] M. S. McClure, B. Glover, E. McSorley, A. Millar, M. H. Osterhout, and F. Roschangar, *Org. Lett.*, 2001, **3**, 1677.
[133] A. Gottumukkala, L and H. Doucet, *Adv. Synth. Catal.*, 2008, **350**, 2183.
[134] L. C. Campeau, S. Rousseaux, and K. Fagnou, *J. Am. Chem. Soc.*, 2005, **127**, 18020.
[135] L.-C. Campeau, D. R. Stuart, J.-P. Leclerc, M. g. Bertrand-Laperle, E. Villemure, H.-Y. Sun, S. Lasserre, N. Guimond, M. Lecavallier, and K. Fagnou, *J. Am. Chem. Soc.*, 2009, **131**, 3291.
[136] J.-P. Leclerc and K. Fagnou, *Angew. Chem., Int. Ed.*, 2006, **45**, 7781.
[137] D. J. Schipper, M. El-Salfiti, C. J. Whipp, and K. Fagnou, *Tetrahedron*, 2009, **65**, 4977.
[138] L. C. Campeau, D. J. Schipper, and K. Fagnou, *J. Am. Chem. Soc.*, 2008, **130**, 3266.
[139] D. J. Schipper, L.-C. Campeau, and K. Fagnou, *Tetrahedron*, 2009, **65**, 3155.
[140] Y. Terao, Y. Kametani, H. Wakui, T. Satoh, M. Miura, and M. Nomura, *Tetrahedron*, 2001, **57**, 5967.
[141] D. Öznur, G. Nevin, Idot, Ö. smail, and Ç. Bekir, *Heteroatom Chemistry*, 2008, **19**, 569.
[142] I. Özdemir, S. Demir, and B. Çetinkaya, *Tetrahedron*, 2005, **61**, 9791.
[143] Y. Kametani, T. Satoh, M. Miura, and M. Nomura, *Tetrahedron Lett.*, 2000, **41**, 2655.
[144] L. Caron, L.-C. Campeau, and K. Fagnou, *Org. Lett.*, 2008, **10**, 4533.
[145] T. Satoh, Y. Kawamura, M. Miura, and M. Nomura, *Angew. Chem., Int. Ed.*, 1997, **36**, 1740.
[146] D. Kalyani, N. R. Deprez, L. V. Desai, and M. S. Sanford, *J. Am. Chem. Soc.*, 2005, **127**, 7330.
[147] N. R. Deprez and M. S. Sanford, *Inorg. Chem.*, 2007, **46**, 1924.
[148] K. L. Hull and M. S. Sanford, *J. Am. Chem. Soc.*, 2007, **129**, 11904.
[149] Y. Rong, R. Li, and W. Lu, *Organometallics*, 2007, **26**, 4376.
[150] B. Liegault, D. Lee, M. P. Huestis, D. R. Stuart, and K. Fagnou, *J. Org. Chem.*, 2008, **73**, 5022.
[151] S. H. Cho, S. J. Hwang, and S. Chang, *J. Am. Chem. Soc.*, 2008, **130**, 9254.
[152] S. Chuprakov, N. Chernyak, A. S. Dudnik, and V. Gevorgyan, *Org. Lett.*, 2007, **9**, 2333.
[153] L. Ackermann, R. Vicente, and R. Born, *Adv. Synth. Catal.*, 2008, **350**, 741.
[154] M. Lafrance, D. Shore, and K. Fagnou, *Org. Lett.*, 2006, **8**, 5097.
[155] R. Li, L. Jiang, and W. Lu, *Organometallics*, 2006, **25**, 5973.
[156] S. Oi, S. Fukita, N. Hirata, N. Watanuki, S. Miyano, and Y. Inoue, *Org. Lett.*, 2001, **3**, 2579.
[157] L. Ackermann, *Org. Lett.*, 2005, **7**, 3123.

[158] L. Ackermann, A. Althammer, and R. Born, *Angew. Chem., Int. Ed.*, 2006, **45**, 2619.
[159] L. Ackermann, A. Althammer, and R. Born, *Tetrahedron*, 2008, **64**, 6115.
[160] K. Cheng, B. Yao, J. Zhao, and Y. Zhang, *Org. Lett.*, 2008, **10**, 5309.
[161] S. Oi, K. Sakai, and Y. Inoue, *Org. Lett.*, 2005, **7**, 4009.
[162] L. Ackermann, R. Born, and P. Álvarez-Bercedo, *Angew. Chem., Int. Ed.*, 2007, **46**, 6364.
[163] L. Ackermann, R. Vicente, and A. Althammer, *Org. Lett.*, 2008, **10**, 2299.
[164] L. Ackermann, R. Born, and R. Vicente, *ChemSusChem*, 2009, **2**, 546.
[165] R. Bedford, B. , S. Coles, J. , M. Hursthouse, B. , and M. Limmert, E. , *Angew. Chem., Int. Ed.*, 2003, **42**, 112.
[166] J. C. Lewis, J. Wu, R. G. Bergman, and J. A. Ellman, *Organometallics*, 2005, **24**, 5737.
[167] S. H. Wiedemann, J. C. Lewis, J. A. Ellman, and R. G. Bergman, *J. Am. Chem. Soc.*, 2006, **128**, 2452.
[168] X. Zhao and Z. Yu, *J. Am. Chem. Soc.*, 2008, **130**, 8136.
[169] A. M. Berman, J. C. Lewis, R. G. Bergman, and J. A. Ellman, *J. Am. Chem. Soc.*, 2008, **130**, 14926.
[170] J. C. Lewis, S. H. Wiedemann, R. G. Bergman, and J. A. Ellman, *Org. Lett.*, 2003, **6**, 35.
[171] B. S. Lane, M. A. Brown, and D. Sames, *J. Am. Chem. Soc.*, 2005, **127**, 8050.
[172] S. Yanagisawa, T. Sudo, R. Noyori, and K. Itami, *J. Am. Chem. Soc.*, 2006, **128**, 11748.
[173] S. Yanagisawa, T. Sudo, R. Noyori, and K. Itami, *Tetrahedron*, 2008, **64**, 6073.
[174] C. H. Jun, C. W. Moon, and D. Y. Lee, *Chem. Eur. J.*, 2002, **8**, 2423.
[175] K.-i. Fujita, M. Nonogawa, and R. Yamaguchi, *Chem. Commun.*, 2004, 1926.
[176] B. Join, T. Yamamoto, and K. Itami, *Angew. Chem., Int. Ed.*, 2009, **48**, 3644.
[177] S. Miyamura, H. Tsurugi, T. Satoh, and M. Miura, *J. Organomet. Chem.*, 2008, **693**, 2438.
[178] T. Fukutani, N. Umeda, K. Hirano, T. Satoh, and M. Miura, *Chem. Commun.*, 2009, 5141.
[179] N. Umeda, H. Tsurugi, T. Satoh, and M. Miura, *Angew. Chem., Int. Ed.*, 2008, **47**, 4019.
[180] S. Mochida, K. Hirano, T. Satoh, and M. Miura, *J. Org. Chem.*, 2009, **74**, 6295.
[181] M. Shimizu, K. Hirano, T. Satoh, and M. Miura, *J. Org. Chem.*, 2009, **74**, 3478.
[182] N. Guimond and K. Fagnou, *J. Am. Chem. Soc.*, 2009, **131**, 12050.

Chapter Two

Scope of the acetate assisted C-H activation reaction

2 Chapter 2

2.1 Cyclometallation of monodentate ligands

2.1.1 Introduction

Chapter 1 contained a brief overview of cyclometallation reactions of N-donor ligands by CH activation with Pd and with non-half sandwich complexes of Ru, Rh and Ir. This introduction will focus on half sandwich cyclometallated complexes of Ru, Rh and Ir with N-donor ligands, very few examples of which were present in the literature prior to 2003. The two main methods to make such complexes are transmetallation and C-H activation.

2.1.1.1 Transmetallation

The first method to prepare cyclometallated C–N half sandwich complexes was by transmetallation reactions. In 1993, Pfeffer *et al.* developed a transmetallation with organomercury and organozinc reagents for the preparation of areneruthenium cyclometallated amine complexes **(Scheme 2.1),**[1] the yields being much better with the organomercury reagents. They later showed that the transmetallation with organomercury reagents was sensitive to steric factors,[2] an increase in the number of alkyl substituents in the π-ligand or the presence of bulky groups *ortho* to Hg in the starting materials led to a significant decrease of the yields. Moreover, the toxicity of mercury reagents could be a problem from a synthetic perspective. The use of organolithium reagents did not afford the cyclometallated complexes which is consistent with the results reported later by Davies *et al.* where a Li derivative of 4(S)-isopropyl-2-oxazolinylbenzene failed to cyclometallate $[RuCl_2(mes)]_2$ and $[RhCl_2Cp^*]_2$.[3]

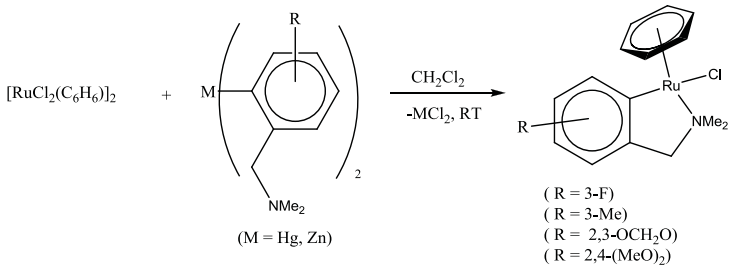

Scheme 2.1

Other types of N-donor ligands have been used for transmetallation of Ru(*p*-cymene) complexes. For example transmetallation of phenylpyridine has also been reported by Pfeffer **(Scheme 2.2)**.[4] More recently substituted 2-phenylpyridines have also been cyclometallated *via* transmetallation with $[RuCl_2(NO)Cp^*]$ **(Scheme 2.3)**.[5]

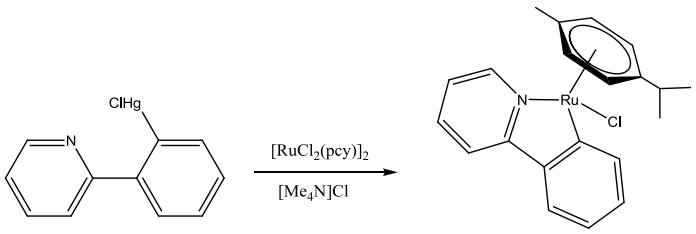

Scheme 2.2

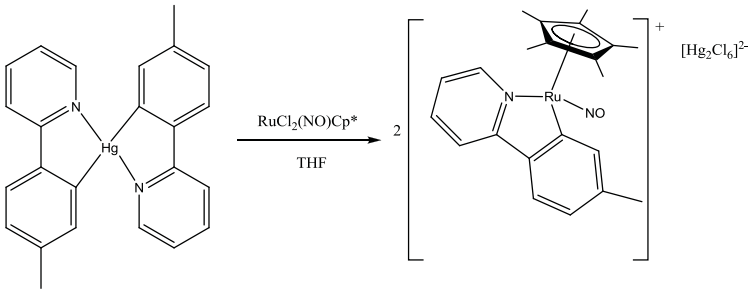

Scheme 2.3

To date no transmetallation of iridium and rhodium half sandwich complexes to form cyclometallated C,N complexes have been reported. However, preparation of a C,O cyclometallated complex of rhodium was described by Vicente in 1990, *via* transmetallation with a mercury reagent **(Scheme 2.4)**.[6]

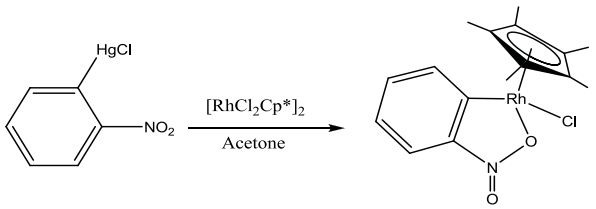

Scheme 2.4

Hence, transmetallation is not a very general method for the synthesis of cyclometallated C–N half sandwich complexes. It has only been used for Ru complexes and still requires the use of toxic mercury reagents. However, C–N cyclometallated half sandwich complexes are useful for investigation of the reactivity of cyclometallated complexes.[1] Hence there was a need for a better and more generally applicable synthesis for C–N half sandwich cyclometallated complexes of Ir, Rh and Ru and this led to the investigation of C-H activation as a greener and cheaper alternative.

2.1.1.2 C-H activation

In 1993, in addition to the transmetallation route, Pfeffer *et al.* reported the first cyclometallation by CH activation of N-donor ligands, tertiary amines, with $Ru(C_6H_6)$ complexes **(Scheme 2.5)**,[1] however this method produced the desired complexes in lower yields than by the transmetallation method described above.

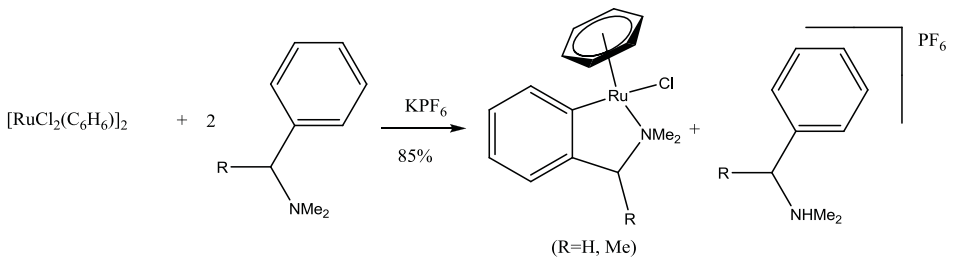

Scheme 2.5

Improvements on the C-H activation method were achieved by the same group, using MeCN as a solvent and heating the mixture to 45°C with NaOH as base **(Scheme 2.6)**,[7] hence, only one equivalent of ligand was needed to produce cyclometallated cationic complexes, and in better yields. An sp^3 C-H activation was observed with 8-methylquinoline **(Scheme 2.7)**, however the extension of this reaction to other N donor ligands was not very successful. Use of 2-phenylpyridine or 2-benzylpyridine led to cyclometallated complexes in which the arene had been displaced by acetonitrile ligands giving $[Ru(L)(MeCN)_4]PF_6$ (L= 2-phenylpyridine, 2-benzylpyridine).[7]

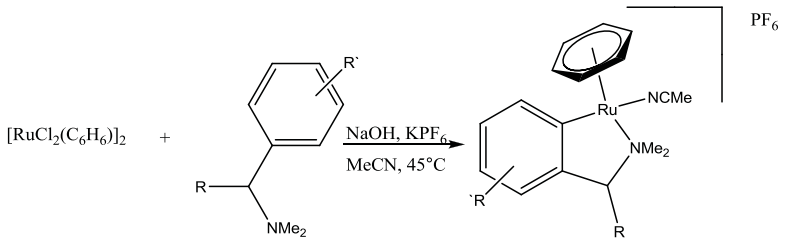

R = R`=H
R = Me, R`= H
R = H, R`= 2,3-$(OMe)_2$
R = H, R`= 3-NO_2

Scheme 2.6

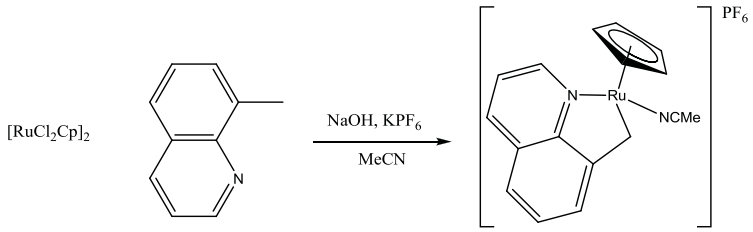

Scheme 2.7

The authors proposed a mechanism for the C-H activation reaction **(Scheme 2.8)**, with the formation of cationic intermediates **(2.1)** and **(2.2)** and an electrophilic C-H activation step.[7]

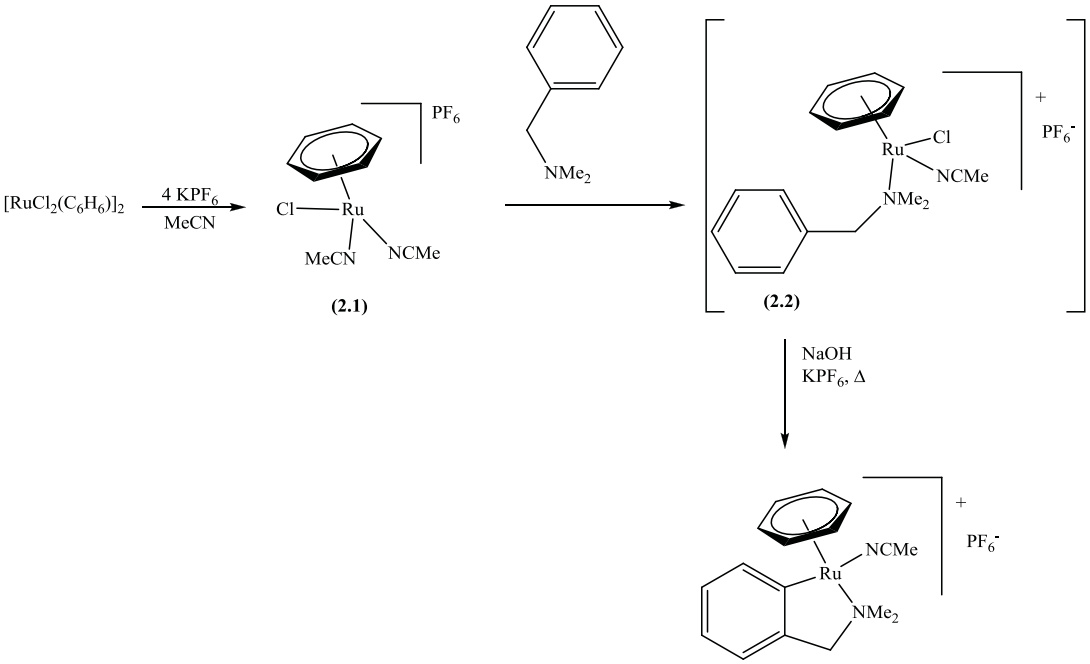

Scheme 2.8

In 2007, the same group extended this reaction to primary amines, particularly substituted benzylamines **(Fig 2.1)**. They also isolated **(2.4) (Fig 2.2)** which is a neutral analogue of the intermediate **(2.2) (Scheme 2.8)** and which subsequently reacted to afford the cyclometallated product in the presence of NaOH.[8] In the same paper they described the C-H activation of benzylamine and DMBA to form IrCp* and RhCp* half sandwich complexes *via* the same route shown in **(Scheme 2.6)**. The tertiary amine (DMBA) has also been cyclometallated with IrCp* *via* acetate assisted C-H activation at room temperature by Davies *et al.* and will be discussed below.[9] Pfeffer *et al.* during the course of our study, also reported the acetate assisted C-H activation of 2-phenylpyridine and it is discussed in more detail in the results and discussion section.[10]

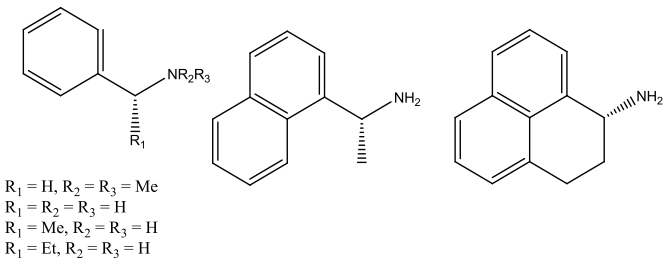

Fig. 2.1

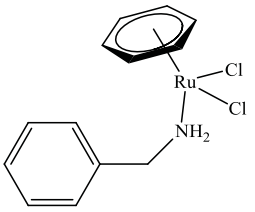

(2.4)

Fig. 2.2

Boncella *et al.* also showed an easy C-H activation with a cationic intermediate, in the cyclometallation of benzylidene aniline with $[RuCl_2(PMe_3)(C_6H_6)]$ in the presence of $AgBF_4$ **(Scheme 2.9).**[11] This shows that imines can also be cyclometallated by C-H activation. Benzodiazepine which is a substituted imine has also been cyclometallated with $[RuCl_2(p\text{-cymene})]_2$ in the presence of NEt_3 and $NaBPh_4$ **(Scheme 2.10)**.[12]

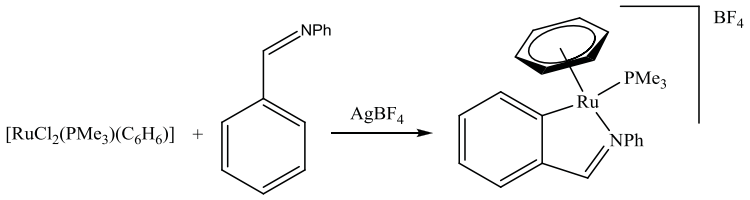

Scheme 2.9

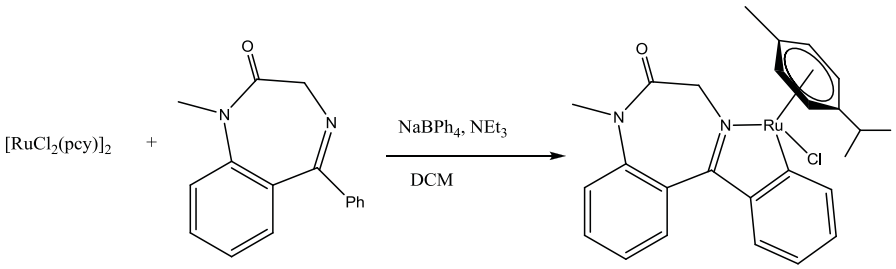

Scheme 2.10

These reactions involve cationic species which suggests an electrophilic C-H activation and they often require an external base. This method is so far limited to a small number of N-donor amines and imines.

Prior to 2003, complexes of Cp*M (M = Ir, Rh) with cyclometallated nitrogen donor ligands were rare in the literature. In 2002, Tilset *et al.* described C-H activation with an imine

directing group **(Scheme 2.11)**, interestingly instead of the formation of the N–N coordinated complex, an sp^3 C-H activation occurred to form **(2.3)** which subsequently afforded **(2.4)**.[13]

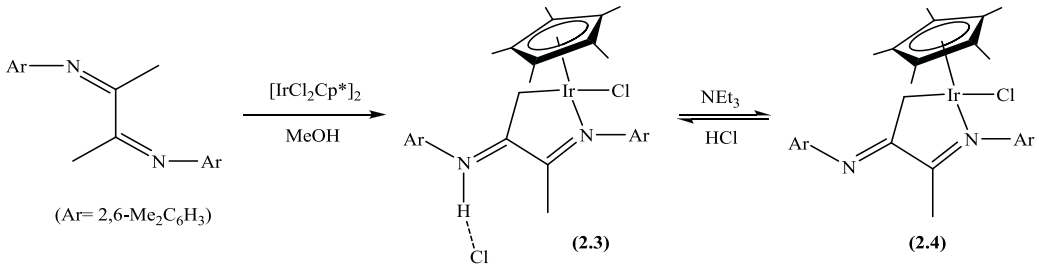

Scheme 2.11

In 1998, Beck *et al.* reported C-H activation of a nitrogen donor ligand (an oxazolone) **(2.5)** with $[IrCl_2Cp^*]_2$ in the presence of NaOAc.[14] This reaction occurred under very mild conditions, room temperature in DCM. This was the first acetate assisted C-H activation with $[IrCl_2Cp^*]_2$. The substituent on the oxazolone affected the product formed. Thus, when R = Me the cyclometallated complex **(2.6)** was produced, as a mixture of two diasteromers, but when R = H a dimeric species **(2.7)** was obtained via an sp^3 C-H activation **(Scheme 2.12)**.[14]

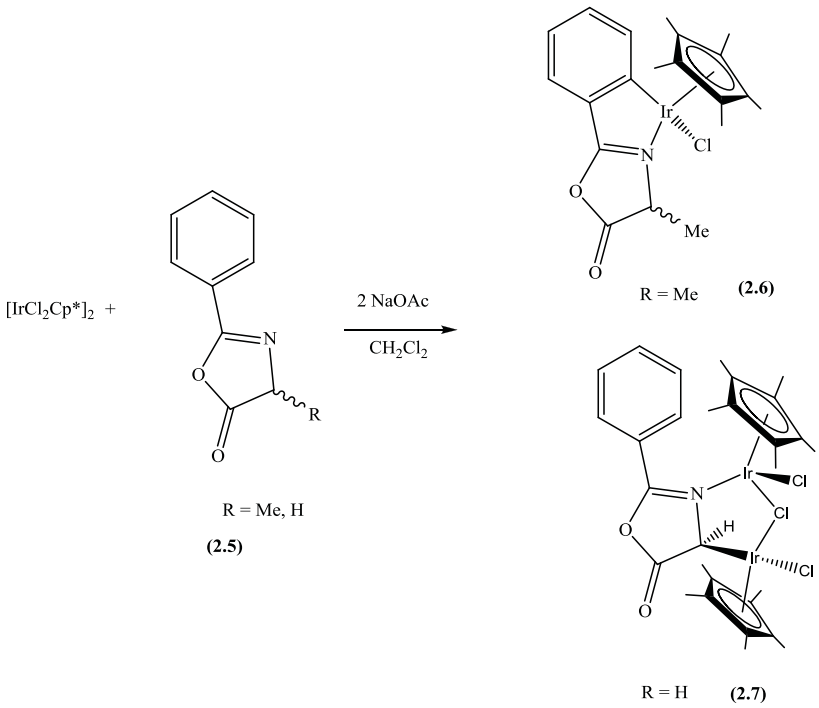

Scheme 2.12

In 2003, Davies *et al.* investigated the scope of acetate assisted C-H activation with a wider range of N-donor atoms with the three complexes $[IrCl_2Cp^*]_2$, $[RhCl_2Cp^*]_2$, and [Ru(*p*-cymene)Cl_2]$_2$. DMBA could be cyclometallated *via* this method with $[IrCl_2Cp^*]_2$ but not with [Ru(*p*-cymene)Cl_2]$_2$ or $[RhCl_2Cp^*]_2$.[9] Different imines were investigated **(Scheme 2.13)**, when R = alkyl, C-H activation occurred with all three metals. This showed that acetate assisted C-H activation could be extended to the three different metals (Ir, Rh, Ru). However, when R = Ph the corresponding Ru(*p*-cymene) complex could not be obtained, which contrasts with the results described by Boncella *et al.* described earlier **(Scheme 2.9)** where the same imine could be cyclometallated with Ru using $AgBF_4$.[11]

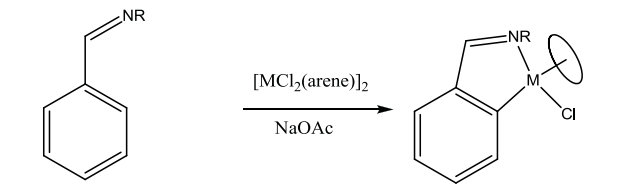

Scheme 2.13

4,4-Dimethyl-2-oxazolinylbenzene was also used as a donor ligand for the acetate assisted C-H activation by Davies *et al.* and only the cyclometallated IrCp* complex could be obtained **(Scheme 2.14)**.[9] The Ru complex could be synthesised by transmetallation, hence the failure of the cyclometallation reaction with Ru was not due to the lack of stability of the product.

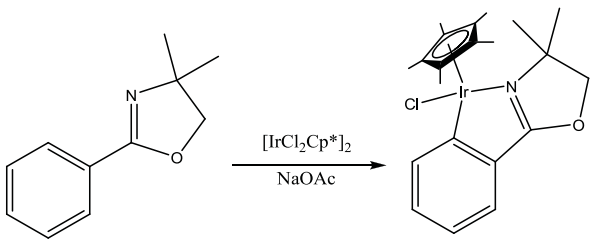

Scheme 2.14

More recently Ikariya *et al*. showed an acetate assisted C-H activation of a primary amine with $[IrCl_2Cp^*]_2$ **(Scheme 2.15)**. They also investigated the mechanism of this reaction by

reacting the ligand with a non isolated "$Ir(OAc)_2Cp^*$" to afford the cyclometallated complex, the authors suggested that "$Ir(OAc)_2Cp^*$" is a key intermediate during the reaction.[15] In 2006, they reported a C-H activation assisted by a benzoate in the case of a sulfonylimido bridged complex **(2.8)** and they proposed an η1 coordinated carboxylate as an intermediate **(Scheme 2.16)**.[16]

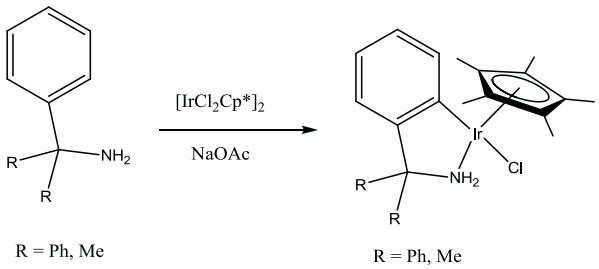

Scheme 2.15

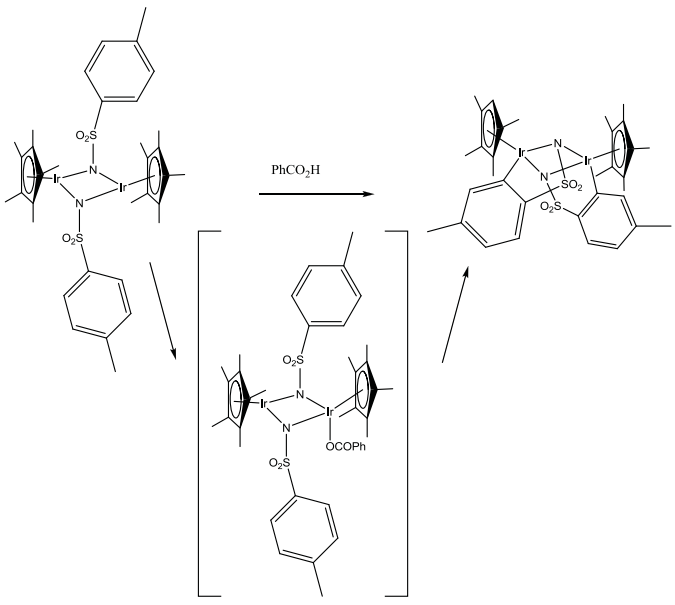

Scheme 2.16

In 2008, during the course of our study, Jones *et al.* independently reported the extension of the acetate assisted C-H activation to different imines, pyridine and benzoquinoline donor ligands with $[MCl_2Cp^*]_2$ (M = Ir, Rh) to form **(2.9)**, **(2.10)** and **(2.11) (Scheme 2.17).** They used these to study formation of isoquinolinium salts by insertion reactions.[17] These

applications will be discussed further in Chapter 4, and the imine **(2.9)** and pyridine **(2.10)** complexes will be discussed further in section 2.1.2.

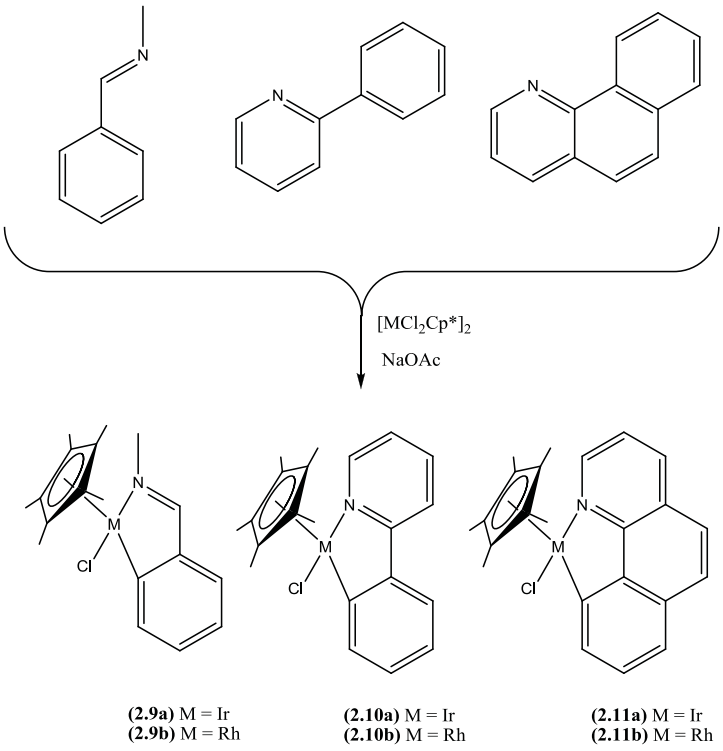

Scheme 2.17

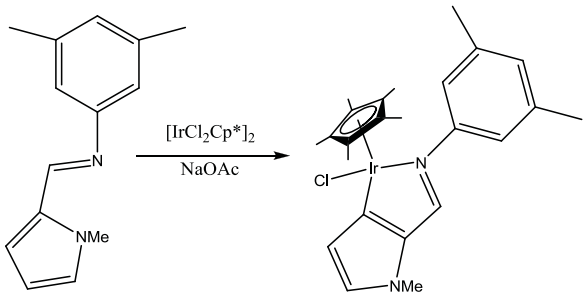

Scheme 2.18

In 2006 Davies *et al.* reported the activation of an sp^2 C-H bond of a pyrrole at iridium using an imine as a directing group **(Scheme 2.18)**.[18] As with Beck previously,[14] this demonstrates that acetate assisted C-H activation is not limited to phenyl groups.

Acetate assisted C-H activation is a promising method for cyclometallation of different N donor ligands at Cp*M (M = Ir, Rh) and arene ruthenium moieties, though the results would suggest that Ir is better than Rh and Ru for this reaction. Different types of C-H bonds can be activated, sp^2 (aromatic and pyrrole), and sp^3. From these preliminary results acetate assisted C-H activation seems to be a general method for cyclometallation of C–N ligands with half sandwich complexes. The aim of this chapter is to study further the scope of acetate assisted C-H activation in terms of: (i) the N-donor atom, (ii) the type of C-H bond activated, (iii) the size of the ring formed (iv) the metal centre. The aim is to have a better understanding of the process and the reasons for differences in reactivity between different ligands and metals. Note, the effect of changing the acetate will be covered in Chapter 3.

2.1.2 Results and discussion

Complexes were routinely characterised using ^{1}H, ^{13}C, and 2-D (NOESY, COSY, DEPT) NMR spectroscopy, FAB and ES mass spectrometry and elemental analysis. Several complexes were also characterised by single crystal X-ray diffraction (Note these were performed by Mr K.Singh).

To investigate the effect of the directing group in acetate assisted C-H activation a range of N-donor groups were tested, namely pyridine, pyrazole, oxazoline, imidazole, imine and triazole. 2-phenylpyridine (L1) has been widely used as a ligand for cyclometallation. However, before the start of this work on the cyclometallated phenylpyridine complexes (**2.10a-c)** only (**2.10c)** had been reported and this was made by a transmetallation route. **(Scheme 2.2)**.[4] In order to probe the generality of the acetate assisted C-H activation, L1 was reacted with the three dimers ($[IrCl_2Cp^*]_2$, $[RhCl_2Cp^*]_2$, $[RuCl_2(p\text{-cymene})]_2$) in the presence of NaOAc **(Scheme 2.19)**.

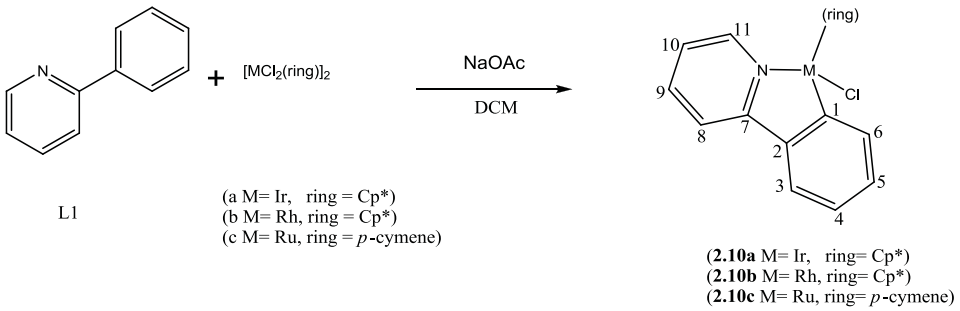

Scheme 2.19

All the reactions were carried out in DCM at room temperature and gave **(2.10a-c)** in good yields (>50%) after 4 hours. The ^{1}H NMR spectrum of **(2.10a)** shows signals for only eight protons in the aromatic region, as expected for an orthometallated phenyl and a N–coordinated pyridine, and these are in a 1:1 ratio to the Cp* which is a singlet at δ 1.68. The pyridine protons could be distinguished from the phenyl ones by a H-H COSY experiment with the exception of H^9 and H^3 having very close chemical shifts. The pyridine protons give rise to four signals, two doublets at δ 8.70 H^{11} and δ 7.82 H^8, a multiplet at δ 7.65 H^9 and a triplet of doublets at δ 7.02 H^{10}. The assignment of H^{11} and H^8 was determined by NOESY spectroscopy. Thus, an NOE correlation is observed between H^{11} and the Cp* signal, whilst H^8 shows an NOE with the phenyl multiplet at δ 7.65 which is therefore assigned as H^3. The phenyl system gives a similar arrangement namely, a doublet at δ 7.82 H^6, a multiplet at δ 7.65 for H^3 and two triplets of doublets at δ 7.20 H^5 and δ 7.07 H^4. The assignment of the phenyl protons is further confirmed by the observation of an NOE between H^6 and the Cp* signal. In the ^{13}C NMR spectrum, the expected number of quaternary and C-H carbons is observed and the metallated carbon is at δ 167.36. Further ^{1}H NMR studies of the coordination of L1 with $[IrCl_2Cp^*]_2$ will be described below (see section 2.3).

The FAB-MS spectrum showed ions at *m/z* 517 and 482 due to $[M]^+$ and $[M\text{-}Cl]^+$. Crystals of this compound were obtained from DCM/hexane and were suitable for single X-ray crystallography. The structure is shown in **Fig. 2.3** with selected bonds distances and angles

in **Table 2.1,** the metal has the expected piano stool geometry with the Cp* occupying 3 facial sites of an octahedron. The crystal structure is discussed further below.

The same ligand, L1, was also reacted with $[RhCl_2Cp^*]_2$ in DCM in the presence of NaOAc to give **(2.10b)** in 75% yield. The ^1H NMR spectrum of **(2.10b)** is similar to that of **(2.10a)**, showing eight different proton signals and a Cp* signal at δ 1.68 the same chemical shift as observed for **(2.10a)**. All the ^1H NMR signals are very close (within 0.05 ppm) to the ones of **(2.10a)**. The pyridine gives rise to two doublets at δ 8.75 and 7.77 for H^{11} and H^8 and two triplets of doublets at δ 7.77 and 7.06 for H^9 and H^{10} respectively. The phenyl group gives rise to two doublets of doublets δ 7.81 and 7.60 for H^6 and $H^3$and two triplets of doublets at δ 7.23 and 7.13 for H^5 and H^4 respectively, the assignment being done by analogy to **(2.10a)**. The metallated carbon is observed at δ 178.68 as a doublet (*J* 128 Hz) due to the coupling to Rh, a coupling can also be seen between Rh and the Cp* carbons (C_5Me_5) at δ 96.97 (*J* 24 Hz). The easy assignment of the metallated carbon for **(2.10b)** provides confirmation of the assignment of the metallated carbon of **(2.10a)** at δ 167.36. The FAB-MS spectrum showed ions at *m/z* 427 and 392 due to $[M]^+$ and $[M\text{-}Cl]^+$ respectively. The structure of **(2.10b)** was determined by X-ray diffraction and a view is shown below **(Fig. 2.3)** with selected bond distances and angles in **Table 2.1**.

As mentioned above, during the course of our study Pfeffer *et al.*[10] in 2007 and Jones *et al.*[17] in 2008 described the cyclometallation of L1 with $[IrCl_2Cp^*]_2$ and $[RhCl_2Cp^*]_2$, *via* the acetate assisted C-H activation method. The spectroscopic and the crystallographic data are identical to the ones described above.

The reaction of L1 with $[RuCl_2(p\text{-cymene})]_2$ in DCM in the presence of NaOAc proceeded analogously to give **(2.10c)** in 61% yield. As above, the expected signals for the cyclometallated ligand are present in the ^1H NMR spectrum. The pyridine group gives rise to

a doublet at δ 9.23 for H^{11}, a triplet at δ 7.06 for H^{10}, and the protons H^9 and H^8 are observed as overlapping multiplets at δ 7.69. The phenyl group gives rise to two doublets at δ 8.15 and 7.61 for H^6 and H^3 and two triplets at δ 7.19 and 7.02 for H^5 and H^4 respectively. The *p*-cymene gives rise to three doublets at δ 5.57 (2 H), 5.17 (1 H) and 4.98 (1 H), arising from the aromatic protons. The isopropyl group is observed as a septet at δ 2.44 and two doublets at δ 0.88 and 0.97 for the inequivalent methyl groups. The fact that the four aromatic protons are inequivalent as well as the two methyl groups of the isopropyl group is consistent with the metal centre being chiral and epimerisation being slow on the NMR timescale. The ^{13}C NMR spectrum shows the expected signals for the cyclometallated ligand with the metallated carbon at δ 181.4 and the expected ten signals for the *p*-cymene. The FAB-MS spectrum shows a molecular ion at *m/z* 425 $[M]^+$ and a fragment ion at *m/z* 390 $[M\text{-}Cl]^+$. Crystals of **(2.10c)** were suitable for X-ray diffraction and the structure is shown below **(Fig. 2.3)** with selected bonds distances and angles given in **Table 2.1**.

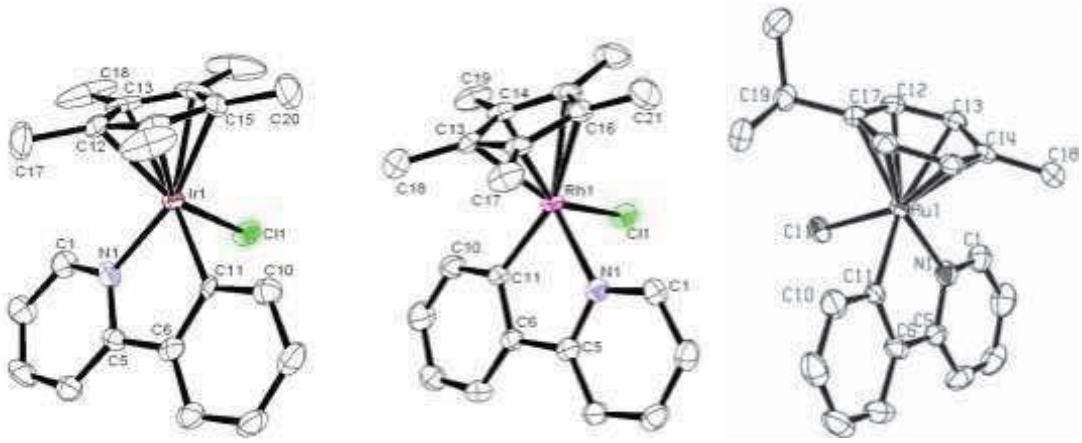

Fig. 2.3 Molecular structure of **(2.10a, b, c)**

Table 2.1 Selected bond distances (Å) and bond angles [˚] for **(2.10a, b, c)**

	2.10a	**2.10b**	**2.10c**
M-C(11)	2.058(5)	2.035(3)	2.060(3)
M-N	2.074(5)	2.099(3)	2.077(3)
M-Cl	2.4046(15)	2.3919(9)	2.4170(9)
M-C(ring)	2.173(5)	2.159(3)	2.175(3)
	2.176(6)	2.160(3)	2.201(3)
	2.185(6)	2.162(3)	2.225(3)
	2.210(6)	2.240(3)	2.243(3)
	2.221(6)	2.262(3)	2.264(3)
			2.189(3)
N-C(5)	1.382(7)	1.360(4)	1.362(4)
C(5)-C(6)	1.449(8)	1.464(4)	1.458(8)
C(6)-C(11)	1.388(7)	1.394(4)	1.389(4)
C(11)-M-N	78.0(2)	78.71(12)	77.80(12)
C(11)-M-Cl(1)	86.45(14)	88.32(9)	85.72(9)
N(1)-M-Cl(1)	87.97(13)	88.12(7)	83.65(8)

Complexes **(2.10a)** and **(2.10b)** show similar bond distances and angles. The M-N bonds for **(2.10a)** and **(2.10b)** [2.0745(2) and 2.099(3) Å respectively] are longer than the M-C(1) bonds [2.058(5) and 2.035(3) Å respectively]. The Cp* ring bond is bonded asymmetrically to the metal centre with two long M-C bonds [2.210(6) to 2.262(3) Å] and three short ones

[2.159(3) to 2.185(6) Å]. The chelate bite angle of **(2.10a)** and **(2.10b)** is 78.0(2)° and 78.71(12)° respectively. The phenyl and pyridine rings are almost coplanar, the dihedral angle between them, C(11)C(6)C(5)N(1), is 5.47° and 2.95° in **(2.10a)** and **(2.10b)** respectively; moreover, the C(5)-C(6) bond is short [1.449(8) and 1.464(4) Å for **(2.10a)** and **(2.10b)** respectively] suggesting some electronic delocalisation across the two aromatic rings. The crystal structure of **(2.10c)** has previously been reported[4] and showed bond distances and angles similar to those in Table 2.1.

These reactions show that pyridine is a good N-donor ligand for acetate-assisted C-H activation. Cyclometallation to form a five-membered ring occurred in good yields for the three metal complexes used, $[IrCl_2Cp^*]_2$, $[RhCl_2Cp^*]_2$, and $[RuCl_2(p\text{-cymene})]_2$. Hence, pyridine should be a good candidate as a directing group for formation of a six-membered ring. This possibility was tested by attempting the cyclometallation of 2-benzylpyridine (L2).

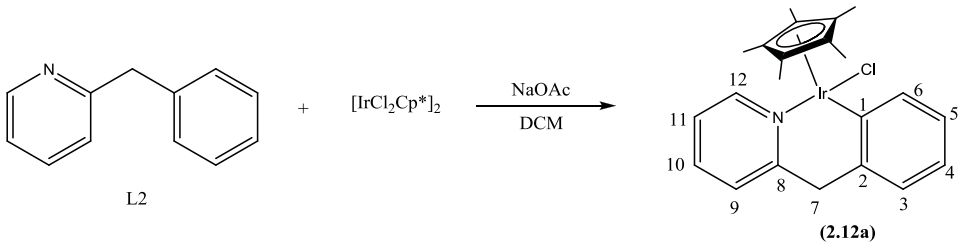

(2.12a)

Scheme 2.20

The reaction of L2 with $[IrCl_2Cp^*]_2$ and NaOAc in DCM led to the formation of **(2.12a)** after 20 hours in 80% yield **(Scheme 2.20)**. The ^1H NMR spectrum of **(2.12a)** shows a 1:1 ratio between the Cp* and the ligand signals, eight aromatic protons are observed showing that cyclometallation has occurred. The Cp* signal is observed at δ 1.56 (cf. δ 1.68 for **2.10a**). The cyclometallated L2 shows two mutually coupled doublets for the benzyl protons at δ 3.77 and 3.88 and two sets of four aromatic protons identified by a COSY experiment. The pyridine group gives rise to two doublets at δ 9.05 and 7.31 for H^{12} and H^9, a triplet of doublets at δ 7.53 for H^{10} and a triplet at δ 7.03 for H^{11}. The cyclometallated phenyl ring

gives two doublets at δ 7.59, 7.07 for H^2 and H^5, a triplet of doublets at δ 6.81 for H^4 and a triplet at δ 6.97 for H^3. The expected number of C-H and quaternary carbons is observed in the ^{13}C NMR spectra with the metallated carbon being at δ 162.36. The ES-MS showed two peaks at m/z 496 and 537 assigned as $[M\text{-}Cl]^+$ and $[M\text{-}Cl+MeCN]^+$. Crystals suitable for X-ray analysis were obtained from DCM/hexane. The structure contains two independent molecules in the unit cell one of which is shown in **(Fig. 2.4)** with selected bonds distances and angles, and is discussed below.

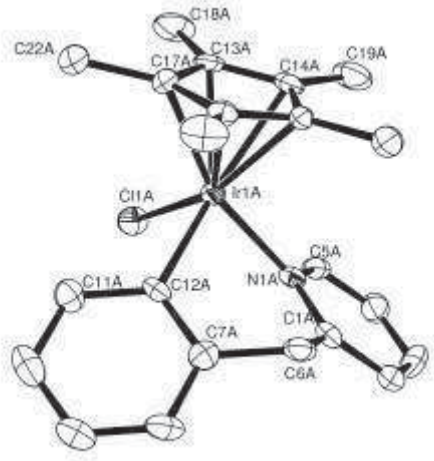

Fig.2.4 X-ray structure of **(2.12a)**

Selected bond lengths and angles: M-N 2.109(5) Å, M-C(12) 2.049(7) Å, M-Cl 2.4084(18) Å, N(1)-C(1) 1.336(8) Å, C(12)-M-N 84.4(2)˚, C(12)-M-Cl(1) 88.67(19)˚, N(1)-M-Cl(1) 88.99(16)˚

The crystal structure of **(2.12a)** shows a six-membered cyclometallated ring with a three legged piano stool structure. The C-M-N chelate angle in **(2.12a)** [84.4(2)˚] is larger than that [78.0(2)˚] in **(2.10a)** due to the increased ring size. Jones *et al*. recently independently reported the synthesis of **(2.12a)** with identical ^1H NMR, ^{13}C NMR and crystallographic data.[17]

The cyclometallation of L2 shows that acetate assisted C-H activation can be extended to the formation of six-membered rings, however the reaction is slower (20 hours) than for the formation of the five-membered ring. Jones *et al.* reported an attempt to make the analogous

RhCp* complex but no C-H activation occurred. This suggests that cyclometallation is easier with iridium than rhodium as found previously by Davies *et al.*[9]

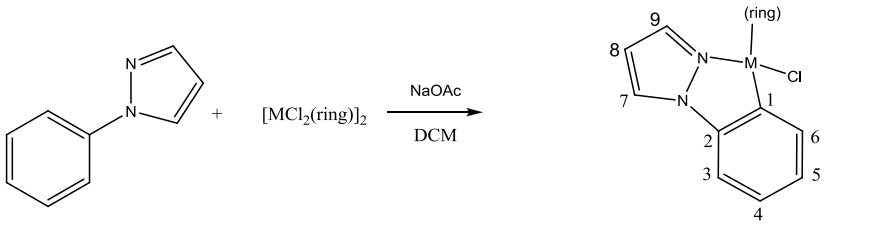

L3

(a M = Rh, ring = Cp*)
(b M = Ir, ring = Cp*)
(c M = Ru, ring = p-cymene)

(**2.13a** M = Ir, ring = Cp*)
(**2.13b** M = Rh, ring = Cp*)
(**2.13c** M = Ru, ring = p-cymene)

Scheme 2.21

Pyrazole was also investigated as a donor group for the acetate assisted C-H activation, thus, 2-phenylpyrazole (L3) was reacted with the three metal complexes $[IrCl_2Cp^*]_2$, $[RhCl_2Cp^*]_2$ and $[RuCl_2(p\text{-cymene})]_2$. The reaction of L3 with $[IrCl_2Cp^*]_2$ in DCM in the presence of NaOAc led to the formation of **(2.13a)** after 4 hours in 50% yield **(Scheme 2.21)**. The ^1H NMR spectrum of **(2.13a)** shows a 1:1 ratio between the Cp* and the ligand, cyclometallation is confirmed by the observation of only four different protons in the aromatic region and three from the pyrazole group. The Cp* signal is observed at δ 1.66, close to that at δ 1.68 observed for **(2.10a)**. The pyrazole gives rise to two doublets at δ 7.81 H^7 and δ 7.60 H^9, and a triplet at δ 6.43 H^8. The phenyl system is composed of four protons, two doublets of doublets at δ 7.67 and at δ 7.18 for H^6 and H^3, and two triplets of doublets at δ 7.02 and δ 6.93 for H^5 and H^4 respectively. In comparison to free L3 the signals are observed with similar chemical shifts (within 0.20 ppm). The signals for H^9 and H^6 were assigned by ^1H NOESY spectroscopy, both of these protons show an NOE correlation to the Cp* signal while another NOE effect can be seen between H^7 and H^3. In the ^{13}C NMR spectrum, the expected number of quaternary and C-H carbons can be seen and the metallated carbon is observed at δ 144.52. The FAB-MS spectrum showed ions at *m/z* 506 and 471 due to $[M]^+$ and $[M\text{-}Cl]^+$ respectively. Crystals suitable for X-ray diffraction were obtained from

chloroform/hexane. The X-ray structure is shown in **Fig 2.5** and the selected bond distances and angles given in **Table 2.2** are discussed further below.

The corresponding reaction of L3 with $[RhCl_2Cp^*]_2$ in DCM in the presence of NaOAc gave **(2.13b)** in a good yield (61%) after 4 hours **(Scheme 2.21)**. In the ^1H NMR spectrum the Cp* signal is observed at δ 1.68 which is very close to that of **(2.13a).** The pyrazole group gives rise to two doublets at δ 7.81 and δ 7.95 assigned as H^9 and H^7 respectively and a triplet at δ 6.50 assigned to H^8, with similar chemical shifts to **(2.13a)**(within 0.20 ppm). The phenyl group shows a doublet of doublets at δ 7.76 for H^6, a multiplet integrating for two protons at δ 7.15 for H^3 and H^5 and a triplet of doublets at δ 7.04 for H^4. In the ^{13}C NMR spectrum the metallated carbon is coupled to Rh and gives a doublet (*J* 129 Hz) at δ 159.17. The FAB-MS spectrum showed ions at *m/z* 416 and 381 due to $[M]^+$ and $[M\text{-}Cl]^+$. Crystals suitable for X-ray diffraction were obtained from DCM/hexane. The structure is shown **(Fig 2.5)** with selected bonds distances and angles given in **Table 2.2** and is discussed further below.

The reaction of L3 with $[RuCl_2(p\text{-cymene})]_2$ in DCM in the presence of NaOAc gave **(2.13c)** in 64% yield after 4 hours **(Scheme 2.21)**. As described for **(2.13a,b)** the expected signals for a cyclometallated product are present in the ^1H NMR spectrum. The pyrazole group shows two doublets at δ 7.90 and 8.05 for H^7 and H^9 and a triplet at δ 6.48 for H^8. The isopropyl of the *p*-cymene gives rise to two inequivalent doublets at δ 0.96 and at δ 0.92 and a septet at δ 2.44, all the four aromatic protons are also inequivalent and are observed as four doublets between δ 5.07 and 5.55 and the remaining methyl is a singlet at δ 2.04. These data are consistent with the metal centre being chiral and epimerisation being slow on the NMR timescale. The ^{13}C NMR spectrum shows the expected number of signals with the metallated carbon at δ 140.75. The FAB-MS shows a molecular ion at *m/z* 414 $[M]^+$ and a fragment ion

at *m/z* 379 $[M\text{-}Cl]^+$. Crystals of **(2.13c)** were suitable for X-ray diffraction, the structure is shown **(Fig 2.5)** with selected bonds distances and angles in **(Table 2.2)**.

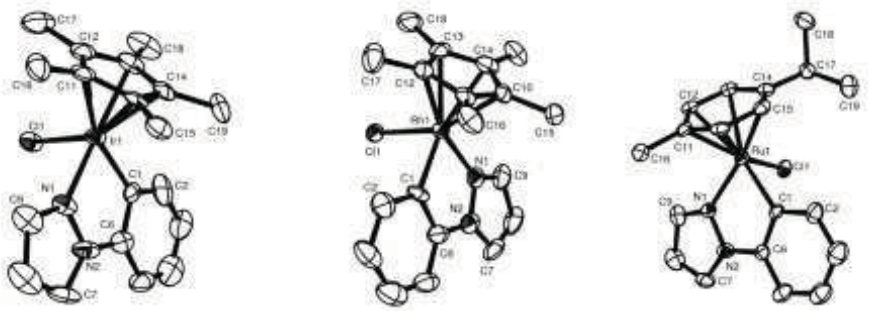

Fig. 2.5 Molecular Structures of **(2.13a, b, c)**

Table 2.2 Selected bond distances (Å) and bond angles [°] for (2.13a, b, c)

	2.13a	**2.13b**	**2.13c**
M-C(1)	2.061(9)	2.027(7)	2.074(3)
M-N(1)	2.073(7)	2.083(8)	2.066(3)
M-Cl	2.409(2)	2.407(2)	2.4207(10)
M-ring	2.152(8)	2.258(8)	2.165(3)
	2.162(7)	2.148(8)	2.185(3)
	2.164(9)	2.159(8)	2.187(3)
	2.223(9)	2.221(9)	2.203(3)
	2.236(8)	2.126(9)	2.252(3)
			2.243(3)
N(1)-N(2)	1.357(10)	1.366(12)	1.369(4)
N(2)-C(6)	1.413(13)	1.422(14)	1.423(4)
C(6)-C(1)	1.382(12)	1.401(14)	1.375(5)
C(1)-M-N	77.5(3)	78.5(3)	77.38(12)
C(1)-M-Cl(1)	87.2(2)	88.3(2)	84.97(9)
N(1)-M-Cl(1)	87.9(2)	90.8(2)	84.40(8)

The structures of **(2.13a,b,c)** each show the expected piano stool geometry. The M-C(1) [2.061(9) Å] and M-N(1) [2.073(7) Å] bond distances are similar in **(2.13a)** and these are similar to the corresponding distances for **(2.13c)** [2.074(3) Å] and [2.066(3) Å] respectively, however, the Rh-C(1) bond length [2.027(8) Å] is noticeably shorter than the Rh-N length [2.083(8) Å] in **(2.13b)**. The C-M-N angle is similar for the three complexes, 77.5(3)°, 78.5(3)° and 77.38(12)° for **(2.13a)**, **(2.13b)** and **(2.13c)** respectively.

The scope of the reaction was extended to oxazolines as an N-donor ligand. As described in the introduction, oxazolines have been examined as N-donor ligands for acetate assisted C-H activation.[9] 4,4-Dimethyl-2-oxazolinylbenzene only afforded the cyclometallated complex in the case of IrCp* **(Scheme 2.14)**. It is known that steric factors are very important in the coordination of N-donor ligands to arene ruthenium complexes[2, 19] and, as mentioned in the introduction, in the preparation of cyclometallated half-sandwich complexes of ruthenium.[7] Hence it was thought that a monosubstituted oxazoline may cyclometallate more easily. To test this hypothesis acetate-assisted cyclometallation of 4(S)-isopropyl-2-oxazolinylbenzene (L4) was attempted.

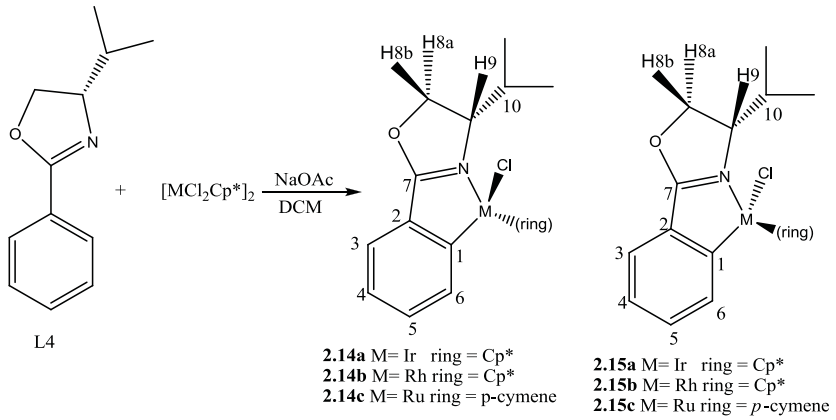

Scheme 2.22

L4 was reacted with $[IrCl_2Cp^*]_2$ in presence of NaOAc **(Scheme 2.22)** and after 26 hours, the ^1H NMR spectrum of the solid showed two sets of signals with a ratio 1:8. Since L4 is homochiral two diastereomers may be formed on cyclometallation which differ in chirality at the metal centre i.e. S_CR_{Ir} **(2.14a)**, S_CS_{Ir} **(2.15a)** with the priority Cp* > Cl > N_{ox} > C_{ph}.[20] The Cp* signal of the major product is observed at δ 1.73 with the minor one at δ 1.71. Four aromatic protons are observed as expected for a cyclometallated product. These are seen as a doublet at δ 7.73 for H^6, a triplet of doublets δ 7.20 for H^5, a triplet at δ 6.97 for H^4 and a

doublet of doublets at δ 7.36 for H^3 with ^4J coupling observed for this proton. The chemical shifts of the aromatic protons and the Cp* signal are very close to those observed for 4-dimethyl-2-oxazolinylbenzene described by Davies *et al.*(within 0.1 ppm).[9] The isopropyl group gives rise to a multiplet at δ 2.31 H^{10} and two 3H doublets at δ 0.89 and 0.97. The CH_2 group gives to two non-equivalent mutually coupled protons H^{8a} and H^{8b} at δ 4.63 and 4.71 respectively both of which also couple to H^9 which is observed as a multiplet at δ 4.16. The assignment of H^{8a} and H^{8b} was established by en NOESY experiment, a cross peak was observed between H^{8b} and H^9 whereas H^{8a} couples with H^{10}. In the NOESY spectrum a cross peak between the Cp* and H^9 allowed the unambiguous assignment to **(2.15a)** rather than **(2.14a)**. The favoured diastereomer **(2.15a)** is the S_CS_{Ir} with the isopropyl group pointing away from the Cp* to limit the steric hindrance. ^{13}C NMR spectra show the expected number of C-H and quaternary carbons with C^1 observed at δ 163.59. The other set of signals (presumably due to the minor diastereomer) showed two doublets at δ 0.85 and 1.02 and a Cp* at δ 1.71. Unfortunately the other signals could not be distinguished from the main product. The two diastereomers could not be separated from each other, however the mixture gave satisfactory microanalytical data as expected for two isomers. The FAB-MS spectrum shows two peaks at m/z 551 and 516 for $[M]^+$ and $[M\text{-}Cl]^+$ respectively.

The same reaction was attempted with $[RhCl_2Cp^*]_2$ **(Scheme 2.22)**. The reaction was very slow and showed little conversion after 6 hours (6%). In order to have a better conversion the reaction was repeated in a more polar solvent (MeOH) and showed a 15% conversion after 4 hours, when the mixture was refluxed for 5 days the conversion reached 50% but this did not increase even after longer times (2 more days). The reaction mixture was filtered through celite to remove NaCl by-product and excess NaOAc and then evaporated and washed with hexane. The ^1H NMR spectrum shows one set of signals which agree with the formation of **(2.14b)** or **(2.15b)** and other RhCp* signals due to the reaction of the $[RhCl_2Cp^*]_2$ with

NaOAc. The signals assigned to the major product occur at similar chemical shifts to those for **(2.15a).** The Cp* is observed at δ 1.66 and the four aromatic protons give rise to a doublet for H^6 at δ 7.74, two triplets of doublets for H^5 and H^4 at δ 7.26 and 7.00 and a doublet of doublets at δ 7.33 for H^3. The CH_2 group gives overlapping multiplets for H^{8a} and H^{8b} at δ 4.60. The isopropyl group gives rise to two 3H doublets at δ 0.88 and 0.98 and a multiplet at δ 2.24. Unfortunately the product could not be completely separated from the mixture of other "RhCp*" products by chromatography, however a single crystal selected from one batch was suitable for crystallography. The structure is shown below in **Fig. 2.6** with selected angles and bond distances and discussed below.

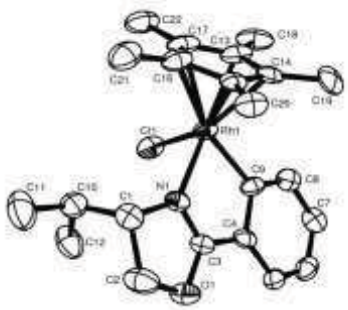

Fig.2.6 Molecular Structure of **(2.15b)**

Selected bond lengths and angles: M-N(1) 2.104(4) Å, M-C(9) 2.029(5) Å, M-Cl(1) 2.3929(14) Å, N(1)-C(3) 1.278(6) Å, C(4)-C(3) 1.431(7) Å, C(9)-C(4) 1.410(7) Å, C(9)-M-N 77.79(19)˚, C(9)-M-Cl(1) 86.32(14)˚, N(1)-M-Cl(1) 90.63(12)˚

The complex adopts the expected pseudo-octahedral structure, with the oxazoline ligand coordinated such that the isopropyl substituent adjacent to the imine nitrogen is pointing towards the chloride **(2.15b)**, rather than the Cp* ring **(2.14b)**, thus minimising unfavourable steric interactions. The configuration at the Rh centre is (*S*), based on priority Cp* > Cl > N_{ox} > C_{ph} ;[20] the configuration at the chiral carbon is also (*S*), as (*S*)-valinol was used in the ligand synthesis. The bond lengths and distances are discussed further below.

The corresponding reaction of L4 with $[RuCl_2(p\text{-cymene})]_2$ in the presence of NaOAc was attempted. The reaction mixture was stirred overnight, filtered through celite to remove NaCl by-product and then evaporated. The ^1H NMR spectrum of the yellow/brown oily residue contained a mixture of at least two (*p*-cymene)ruthenium species. The oily residue was recrystallised from a concentrated CH_2Cl_2/pentane solution to afford a crop of platelet crystals, which were then characterised. The ^1H NMR spectrum shows that the crystals are of a single diastereomer, which did not epimerise after a week in $CDCl_3$, indicating the thermodynamic diastereoselectivity may be very high. The ^1H NMR spectrum of the crystals shows four signals in the aromatic region. The CH of the isopropyl is shifted almost 0.7 ppm downfield compared to the free ligand (δ 2.55 and 1.86 respectively) attributed to the proton being in close proximity to the electronegative chlorine atom (see structure below). The isopropyl of the *p*-cymene gives rise to two doublets at δ 0.90 and at δ 1.04 and a septet at δ 2.47, the four aromatic protons are also inequivalent (two are overlapping) and are observed between δ 4.82 and 5.55. The NOESY spectrum contains NOE cross peaks between the signal at δ 4.19 H^9 and those at δ 4.98 and 5.55 (*p*-cymene signals) consistent with the *p*-cymene being on the same side of the oxazoline as H^9 i.e. the same isomer as found for **(2.15a)** and **(2.15b)** described above. There were no cross peaks that might be expected from the other isomer (i.e. isopropyl methyls and *p*-cymene). The FAB-MS of **(2.15c)** showed an ion (~60%) due to $[M]^+$ m/z 459, with a minor ion due to $[M\text{-}HCl]^+$ m/z 423. These data are consistent with formation of **(2.15c)**. Crystals of **(2.15c)** were suitable for X-ray diffraction and the structure is discussed below. (Note this experiment was carried out by Mr A.J. Davenport)

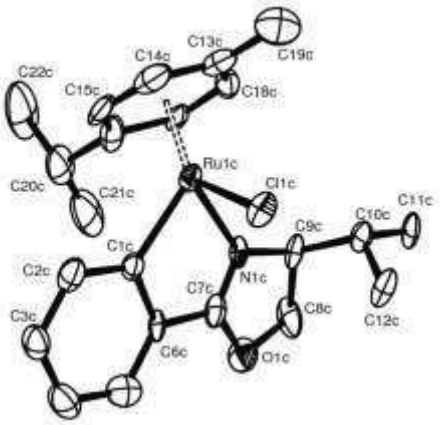

Fig. 2.7 Molecular Structure of one of the four independent molecules of **(2.15c).**

The structure contains four independent molecules however it confirms that the complex adopts the expected pseudo-octahedral structure, with the oxazoline ligand coordinated such that the isopropyl substituent adjacent to the imine nitrogen is pointing towards the chloride rather than the *p*-cymene ring **(2.15c)**.

It appears that even a monosubstituted oxazoline fails to cyclometallate easily under these conditions with $[RhCl_2Cp^*]_2$; even after heating, the reaction failed to go to completion. Note, one equivalent of acetic acid is liberated for each C-H bond activated, it is possible that an equilibrium is reached where the product can react with acetic acid to liberate the free ligand. A reduced reactivity for rhodium compared to iridium is in accordance with previous results for acetate-assisted C-H activation.[9] The reaction produced the same diastereomer as a major product for all three complexes **(2.15a,b,c)**, in the case of Ru and Rh the reaction was totally selective, whereas with Ir the minor diastereomer was also observed. A better conversion was observed in the case of Rh when a monosubstituted oxazoline was used in comparison to 4-dimethyl-2-oxazolinylbenzene,[9] which suggests that the reaction is sensitive to steric hindrance, a less crowded oxazoline led to an increased conversion in the case of rhodium.

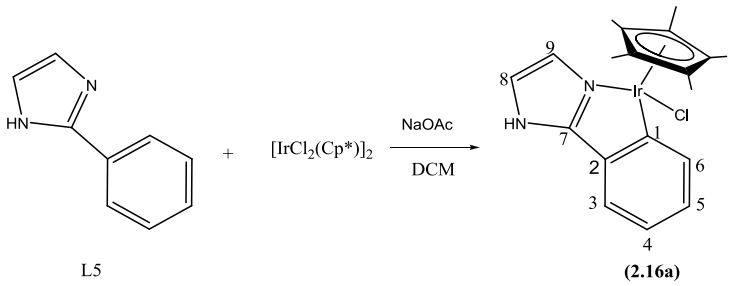

Scheme 2.23

Having shown that oxazoline (4,4 Dimethyl-2oxazolinylbenzene) and pyrazole can both act as directing groups the related heterocycle imidazole was tested. Phenylimidazole (L5) also offers the advantage over the oxazoline of reduced steric hindrance. The reaction of L5 with $[IrCl_2Cp^*]_2$ in DCM in the presence of NaOAc gave **(2.16a)** in 55% yield after 4 hours **(Scheme 2.23)**. The ^1H NMR spectrum of **(2.16a)** shows the expected signals for an orthometallated phenyl and an N–coordinated imidazole group. A 1:1 ratio of the ligand and the Cp* signal is also observed at δ 1.70. The imidazole gives rise to a broad singlet at δ 5.90 for H^8 and another broad singlet at δ 11.0 assigned to the NH. This very low field shift for the NH suggests that it is hydrogen bonded, possibly to solvent or to the chloride of another molecule. Addition of D_2O led to disappearance of this signal confirming its assignment as the NH proton. Unfortunately the signal for the other imidazole proton is overlapped with the phenyl proton H^4 a 2H multiplet being observed at δ 6.75. This assignment was easily confirmed by observation of cross peaks in the COSY and NOESY spectra. The other phenyl protons gives rise to a triplet at 7.02 assigned to H^5 and two doublets at δ 6.97 and 7.74 assigned to H^3 and H^6. The ^{13}C NMR spectra show the expected number of C-H and quaternary carbons for **(2.16a)** and the metallated carbon is at δ 158.07. The FAB-MS spectrum showed ions at *m/z* 506 and 471 due to $[M]^+$ and $[M\text{-}Cl]^+$ respectively. The X-ray structure of **(2.16a)** was determined and is shown with selected bond distances and angles in **Fig 2.8**.

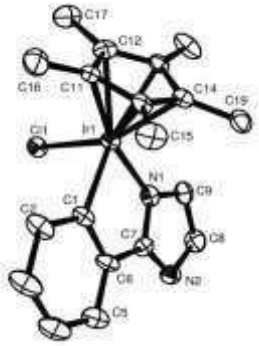

Fig. 2.8 Molecular structure with selected bonds and angles for **(2.16a)**

Selected bond lengths and angles: M-N 2.081(7) Å, M-C(1) 2.070(8) Å, M-Cl 2.429(2) Å, N(1)-C(7) 1.314(8) Å, C(7)-C(6) 1.456(11) Å, C(6)-C(1) 1.383(11) Å, C(1)-M-N 77.4(3)˚, C(1)-M-Cl(1) 86.6(2)˚, N(1)-M-Cl(1) 87.64(19)˚

The crystal structure of **(2.16a)** shows the expected structure for a half sandwich cyclometallated complex with a three legged piano stool structure. The M-N and M-C bond distances [2.081(7) and 2.070(8) Å respectively] are statistically the same as the corresponding bond lengths [2.073(7) and 2.061(9) Å] in the phenylpyrazole complex **(2.13a)**. An additional feature in the structure of **(2.16a)** is an intermolecular hydrogen bond between N(2)-H and the chloride of another molecule with an N–H...Cl distance of 3.266 Å.

The analogous reaction of phenylimidazole with $[RuCl_2(p\text{-cymene})]_2$ was attempted. The ^1H NMR spectrum showed three different sets of *p*-cymene peaks one of which can be assigned to [RuCl(OAc)(*p*-cymene)] furthermore there were no signals for unreacted phenylimidazole. The other species present have not been identified, the deprotonation on the N–H site after coordination of the ligand may stop the C-H activation process. Coordination of imidazole in half–sandwich complexes has been previously reported by Ozdemir[21] in 2005 and by Dyson. [22] In 2010 Pandey *et al.* reported the synthesis of coordinated N-phenylimidazole groups on Ru and Rh half sandwich complexes, which shows that imidazole can bind strongly to the metal hence a lack of coordinating ability of the imidazole is unlikely to be a cause of the failure of the cyclometallation.{Singh, 2010 #448}

Acetate assisted C-H activation of N-benzylidenemethylamine L6 with Rh and Ir half sandwich complexes in the presence of NaOAc has recently been reported by Jones *et al.* **(Scheme 2.24)**.[17] The expected products **(2.9a,b)** were formed in good yields (93%) and were also characterised by crystallography.[17] These results show that L6 is a good donor ligand for acetate assisted C-H activation as expected for N-alkyl imines.[9] Jones *et al.* also reported reactions of **(2.9a,b)** with alkynes. In order to allow comparison with ruthenium (see Chapter 4) the corresponding arene ruthenium complex **(2.9c)** was synthesised.

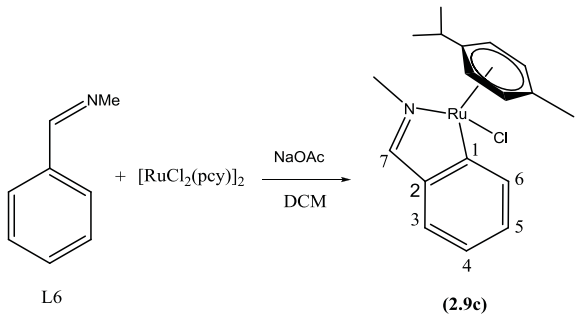

Scheme 2.24

L6 was reacted with $[RuCl_2(p\text{-cymene})]_2$ in DCM in the presence of NaOAc and gave **(2.9c)** as a green solid in 80% yield **(Scheme 2.24)**. The ^1H NMR spectrum of **(2.9c)** shows a 1:1 ratio between the *p*-cymene signal and the cyclometallated ligand. The methyl signal is observed as a singlet at δ 3.99 (cf δ 3.82 and 3.90 for **(2.9a)** and **(2.9b)** respectively)[17] and the imine proton is observed as a doublet at δ 7.97. The ligand shows signals for four aromatic protons with two doublets at δ 8.14 (H^6) and 7.39 (H^3), a triplet of doublets at δ 7.10 (H^5) and a triplet at δ 6.95 (H^4). The isopropyl of the *p*-cymene gives rise to two inequivalent doublets at δ 0.89 and at δ 1.07 and a septet at δ 2.51. All the four aromatic protons are also inequivalent with four doublets between δ 4.92 and 5.60. These data are consistent with the metal centre being chiral and epimerisation being slow on the NMR timescale. The ^{13}C NMR spectrum shows the expected number of signals with the metallated carbon and the imine carbon at δ 188.51 and 172.45 respectively. The FAB-MS spectrum showed ions at m/z 389

and 354 due to $[M]^+$ and $[M\text{-}Cl]^+$ respectively. Hence acetate assisted C-H activation can be extended to Ru with L6, this result confirms the earlier observation[9] that N-alkyl imines are good donor groups for C-H activation for all three metal complexes $[IrCl_2Cp^*]_2$, $[RhCl_2Cp^*]_2$, $[RuCl_2(p\text{-cymene})]_2$. Hence alkylimines are suitable to use as a directing group to probe the activation of different types of C-H bonds. Activation of a vinylic sp^2 C-H bond was then tried with L7 which contains an isopropyl substituent on the imine **(Scheme 2.25)**. L7 was synthesised according to known procedures.[23]

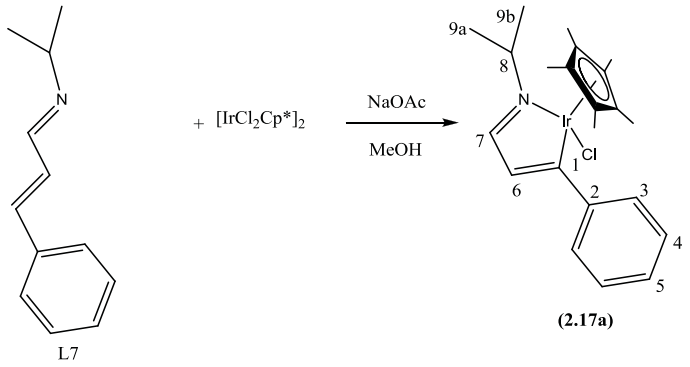

Scheme 2.25

L7 was reacted with $[IrCl_2Cp^*]_2$ in presence of NaOAc in MeOH and led to the formation of **(2.17a)** in 89% yield **(Scheme 2.25).** It is noticeable that the solvent is important in this case, when DCM was used clean conversion could not be achieved and broad signals were observed in the ^1H NMR spectrum suggesting probable coordination of L7 with $[IrCl_2Cp^*]_2$, also an isomerisation of the ligand is required for the C-H activation to proceed which may be solvent dependent.

The ^{1}H NMR spectrum of **(2.17a)** shows a 1:1 ratio between the Cp* and the cyclometallated ligand and the disappearance of one of the vinylic protons suggests the cyclometallation has occurred. The Cp* signal is observed at δ 1.48 and the isopropyl group of the imine shows two doublets at δ 1.45 and 1.49 (H^{9a} and H^{9b}) and a septet H^{8} at δ 4.23, 1.23 ppm downfield compared to L7 presumably due to coordination of the nitrogen. The imine proton H^{7} shows a broad singlet at δ 8.07 and H^{6} is observed as a doublet (*J* 2Hz) due to coupling with H^{7} at δ 6.77. The aromatic signals are observed as a 2H doublet at δ 7.42 for H^{3} and two triplets at δ 7.17 (1H) and 7.27 (2H) for H^{5} and H^{4} respectively. The signals for H^{3} and H^{4} integrate for 2 protons each which suggests that free rotation of the phenyl ring is occurring in solution and is fast on the NMR timescale. The expected number of C-H and quaternary carbons are observed in the ^{13}C NMR spectra with the metallated carbon being at δ 201.43 which is lower field than the aromatic metallated carbons observed earlier, between δ 144 and 167, for Ir complexes. The FAB-MS shows two signals at m/z 500 and 535 assigned as $[M\text{-}Cl]^{+}$ and $[M]^{+}$. The formation of **(3.17a)** shows that C-H activation is not restricted to aromatic and N–H bonds, vinylic C-H bonds can also be activated. The crystal structure of **(2.17a)** with selected bond distances and angles is shown in **Fig. 2.9** and is discussed below.

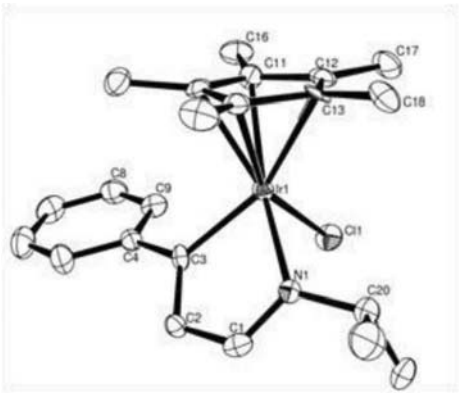

Fig. 2.9 Molecular structure of **(2.17a)**

Selected bond lengths and angles: Ir-N 2.084(5) Å, Ir-C(3) 2.031(5) Å, Ir-Cl 2.4048(16) Å, N(1)-C(1) 1.291(7) Å, C(1)-C(2) 1.412(8) Å, C(2)-C(3) 1.362(7) Å, C(3)-M-N 77.8(2)˚, C(3)-M-Cl(1) 91.23(15)˚, N(1)-M-Cl(1) 87.88(13)˚

The X-ray structure of **(2.17a)** shows the five-membered ring cyclometallated half sandwich complex. The Ir-C(3) and the Ir-N(1) bond lengths [2.031(5) Å] and [2.084(5) Å] are statistically the same as the respective ones of **(2.9a)** described by Jones *et al.*[17], [2.0374(16) Å] and [2.0884(14) Å] respectively. The chelate bond angle C(3)-M-N is [77.8(2)˚] as expected for a five membered ring half sandwich metallacycle.

The possibility to have a 1,2,3-triazole as a directing group for C-H activation was envisaged. The use of Click chemistry[24] to make 1,2,3-triazoles has been extensively studied and has a wide range of applications in material science and drug discovery.[25] Chelate complexes of (1,2,3) triazoles have been reported with lanthanides Eu[26] and Ln[27], Re[28] and Tc[29]. Recently a cyclometallated example with Ir was described by Ulbricht *et al.* with a non half sandwich system.[30] They showed the formation of cyclometallated triazole coordinated with the N(3) atom and acac as an ancillary ligand **(2.18a)(Fig 2.10)**, these complexes were used for luminescent studies. Ulbricht *et al.* showed that **(2.19a)** which is an isomer of **(2.18a)** could not be synthesised, moreover no example of complexes with the coordinated N(2) of a (1,2,3) triazole could be found in the book Comprehensive Organometallic Chemistry (1982-1994).[31]

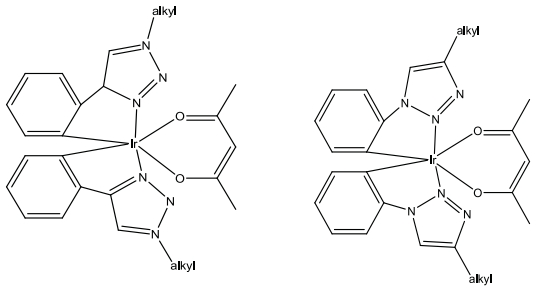

(2.18a) (2.19a)

Fig. 2.10

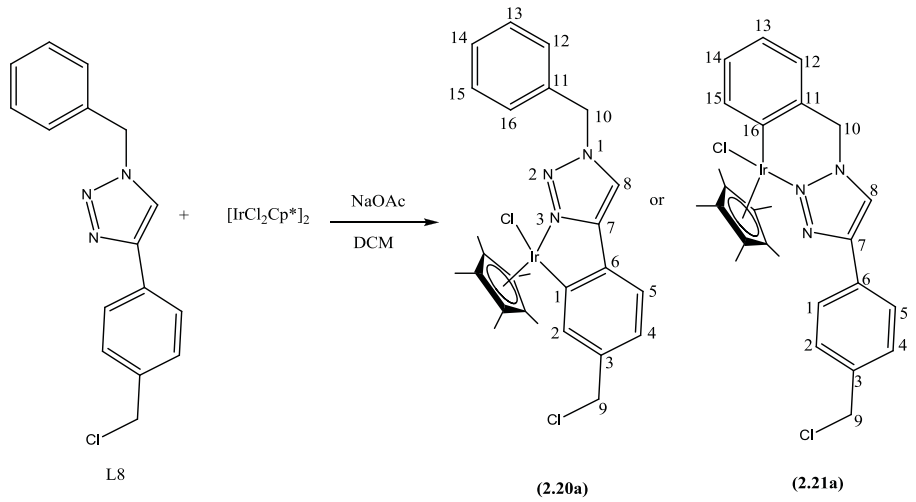

Scheme 2.26

L8 was synthesised by Graeme Stasiuk following a reported procedure.[26] The reaction of $[IrCl_2Cp^*]_2$ with L8 in presence of NaOAc could in principle lead to two possible isomers **(Scheme 2.26)**. A five-membered ring complex **(2.20a)** could be obtained if the N(3) of the triazole acts as the directing nitrogen, alternatively, a six-membered ring complex **(2.21a)** would be formed if N(2) is the directing atom **(Scheme 2.26)**. The example described by Ulbricht would suggest that the coordination of the N(2) of the triazole is less favourable, in addition, cyclometallation to form a six-membered ring is slower than to form a five-membered ring (see 2-benzylpyridine (L2) above) hence **(2.20a)** is the more likely product. The ^{1}H NMR spectrum of the reaction after 20 h showed one set of signals for the cyclometallated ligand and a Cp* signal observed at δ 1.76. Two singlets are observed at δ 7.54 and 7.76 which are assigned to H^8 and H^2 respectively. The observation of two singlets is characteristic for the formation of **(2.20a),** (**2.21a)** would be expected to show only one singlet for H^8. Four doublets at δ 4.57, 4.70, 5.36 and 5.49 are observed for the benzylic protons $H^{9a, 9b}$ and $H^{10a, 10b}$ respectively, these being diastereotopic since complexation makes the metal centre chiral. The assignment of H^2 and H^9 was determined by a NOESY experiment, cross peaks between H^2 and the Cp*and between H^2 and H^9 were observed, however H^5 and H^4 could not be differentiated since neither of them showed any NOE

correlation to any other proton in the complex. In the ^{13}C NMR spectrum the metallated carbon is observed at δ 159.89. In the FAB-MS spectrum a peak at m/z 610 is assigned to $[M\text{-}Cl]^+$. Hence, this reaction shows that (1,2,3)-triazole is a good directing group for aromatic C-H activation and the regioselectivity of the reaction shows that coordination of N3 and formation of a five-membered ring is favoured over the formation of a six-membered with the coordination of the less good donor N(2).

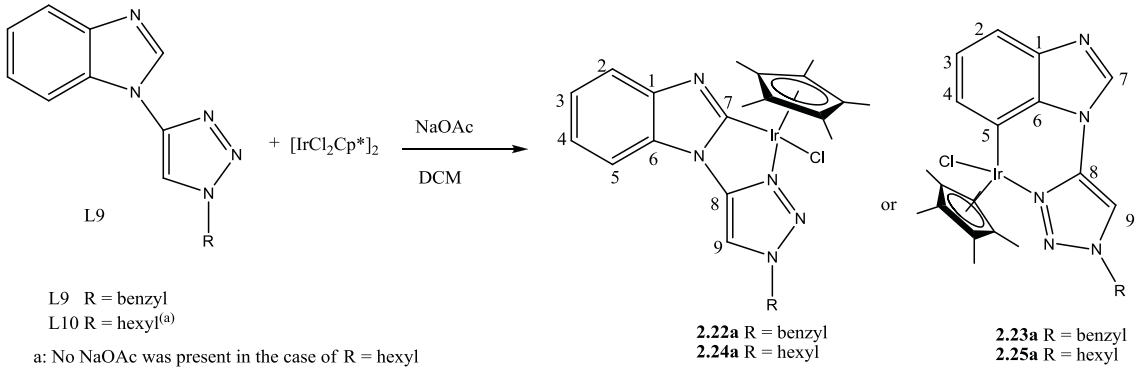

Scheme 2.27 Potential products from a C-H activation reaction.

The possibility to have a triazole as a donor group but having a competition between two types of C-H bond (aromatic and heteroaromatic) and two sizes of chelate ring (five-membered and six-membered) was investigated using L9 **(Scheme 2.27)** which was synthesised from reported procedures by Dr G.A. Burley.[32]

Two potential products were envisaged, both involving N(3) as the directing group, **(2.22a)** containing a five-membered ring formed by activation of the benzimidazole CH bond and, **(2.23a)** containing a six-membered ring by activation of an aromatic C-H bond. Other possible products derived from N(2) as a directing atom were considered less plausible in accordance with our observation from the reaction of L8 and the examples reported by Ulbricht.[30] The ligand L9 was reacted with $[IrCl_2Cp^*]_2$ in the presence of NaOAc in DCM. The reaction led to one product with one set of signals for the ligand and a Cp* (δ 1.66)

observed in the ^{1}H NMR spectrum. However, surprisingly no C-H activation had occurred, 13 protons of the ligand were still present though with different chemical shifts from the starting material. This is consistent with coordination of N(3) of the triazole or the imine N of the benzimidazole. The ^{1}H NMR spectrum showed three singlets assigned to H^{7}, H^{9} and H^{10} (2H) at δ 9.39, 8.01 and 5.31 respectively. A 0.89 downfield shift is observed for H7 in comparison to L9 which would suggest that the coordination occurs through the benzimidazole to produce **(2.26a)** shown in **Fig. 2.11**. The benzylic protons H^{10} are equivalent showing there is no chiral centre. Two doublets at δ 8.02 and 8.14 were assigned to H^{5} and H^{2} respectively. Assignments were determined by NOESY spectroscopy with a correlation between H^{9} and H^{5} in the spectrum. The expected number of C-H and quaternary carbons for the complex was observed in the ^{13}C NMR spectra.

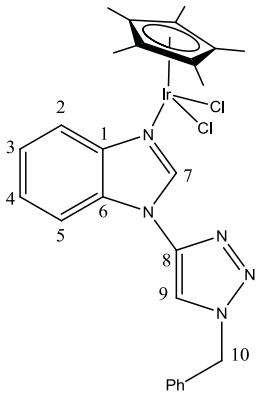

(2.26a)

Fig. 2.11

Crystallisation from DCM/Hexane gave suitable crystals for an X-ray analysis and the structure confirmed the coordination from the benzimidazole group. The structure is shown below in **(Fig 2.12)** with the selected bond distances and angles.

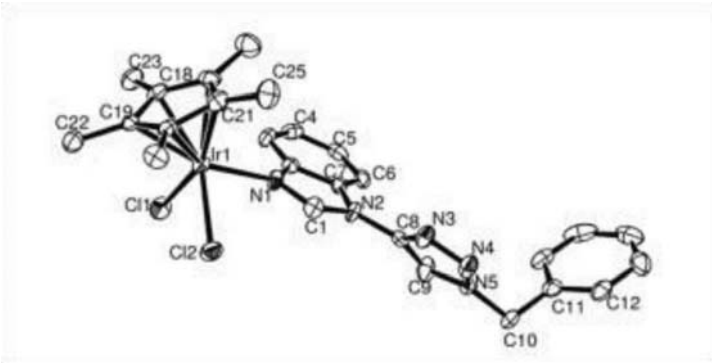

Fig 2.12 Molecular structure of **(2.26a)**

Selected bond lengths and angles: M-N(1) 2.135(5) Å, M-Cl(1) 2.4191(18) Å, M-Cl(2) 2.4124(18) Å, Ir(1)-C(21) 2.144(7) Å, Ir(1)-C(19) 2.152(6) Å, Ir(1)-C(18) 2.155(7) Å, Ir(1)-C(17) 2.156(7) Å, Ir(1)-C(20) 2.162(7) Å, N(1)-M-Cl(1) 88.52(15)˚, N(1)-M-Cl(2) 85. 71(16)˚

The X-ray structure confirms the coordination of L9 to the IrCp* *via* N1, with the all the Ir-C bonds lengths being the same (between 2.144(7) Å, and 2.162(7) Å).

L10 was reacted with $[IrCl_2Cp^*]_2$ in DCM. The analogue of **(2.26a)** with an hexyl chain instead of the benzyl group **(2.27a) (Fig 2.13)** was synthesised and fully characterised.

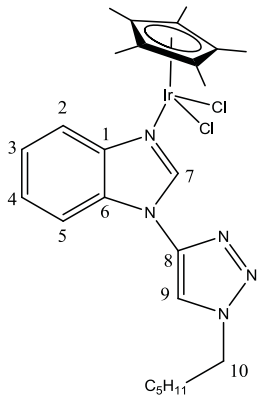

(2.27a)

Fig. 2.13

The ^1H NMR spectrum shows similar chemical shifts to **(2.27a)** with H^7 observed at δ 9.35 confirming the downfield shift due to coordination of the metal centre, the protons H^{10} are observed at δ 4.13 as a triplet integrating for 2 protons showing that these are equivalent and

confirming the absence of chirality as mentioned above coordination of an imidazole group to RhCp* and Ru(arene).[21, 22 33]

The conclusions from this section on the scope of acetate assisted C-H activation, are: (i) cyclometallation of a ortho substituted phenyl occurs at room temperature for a wide range of N-donor directing groups (pyrazole, pyridine, imine, oxazoline, imidazole, and triazole) with IrCp*; (ii) pyridine, alkylimines, and pyrazoles also work as directing groups for Cp*Rh and areneruthenium, (iii) Cp*Rh is not as effective as Cp*Ir or areneruthenium at promoting cyclometallation (iv); five-membered rings form more easily than six-membered ones, which is well established in palladium chemistry,[34] (v) acetate assisted C-H activation can be extended to vinyl sp^2 C-H bonds

Up until now the ligands tested could only bind through one heteroatom donor at a time. Some examples had a choice of two possible binding sites but no ligands had the possibility of chelation via two heteroatoms. Hence, in the next section ligands that can potentially chelate via two heteroatoms will be considered, to see how this may interfere with the C-H activation.

2.2 Cyclometallation of potentially chelating ligands

2.2.1 Introduction

Half sandwich complexes of chelating bifunctional ligands have been widely studied.[35-38] The most relevant to this work are N–N, N–O, N–C (discussed earlier), C–C and C–O ligands and some pertinent examples are presented below. Amino acids easily form N–O chelates with half sandwich complexes, for example those in **Scheme 2.28** reported by Koch *et al.* [39]

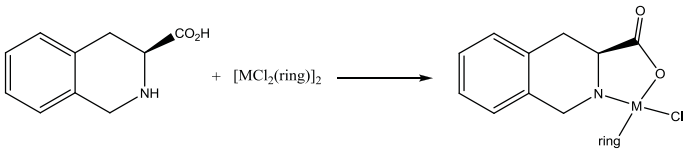

Scheme 2.28

Macchioni *et al.* reported the study of 2-acetylpyridine and 2-benzoylpyridine with Ru half sandwich complexes, in 2006.[40] They showed the formation of chelate complexes in the presence of N–O ligands **(Scheme 2.29)** and their aggregation in solution by PGSE (pulsed-gradient spin-echo) NMR experiments.

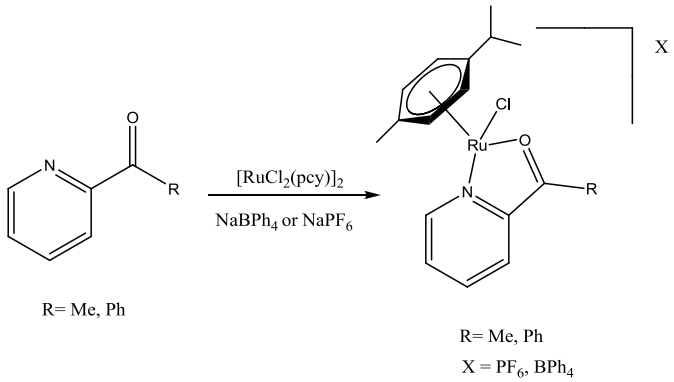

Scheme 2.29

Prasad *et al.* described the formation of Cp*M (M = Ir and Rh) half sandwich complexes with N–N and N–O chelates from heterocyclic functionalised naphthyridine ligands **(Scheme 2.30)**. N–N coordination was favoured over N-S coordination **(2.28a,b)** and coordination of furan is possible to form an N,O chelate complex **(2.29a,b)**.[41] Interestingly in the case of **(2.29a,b) (Scheme 2.31)** no C-H activation was observed even though the ligand has an intramolecular basic site. Hence in this case N,O coordination appears to be favoured over the C-H activation. This contrasts with the results reported by Tilset *et al.* as described (see section 2.1) where C-H activation was favoured over N–N chelate formation in the case of a diimine ligand **(Scheme 2.11)**.[13]

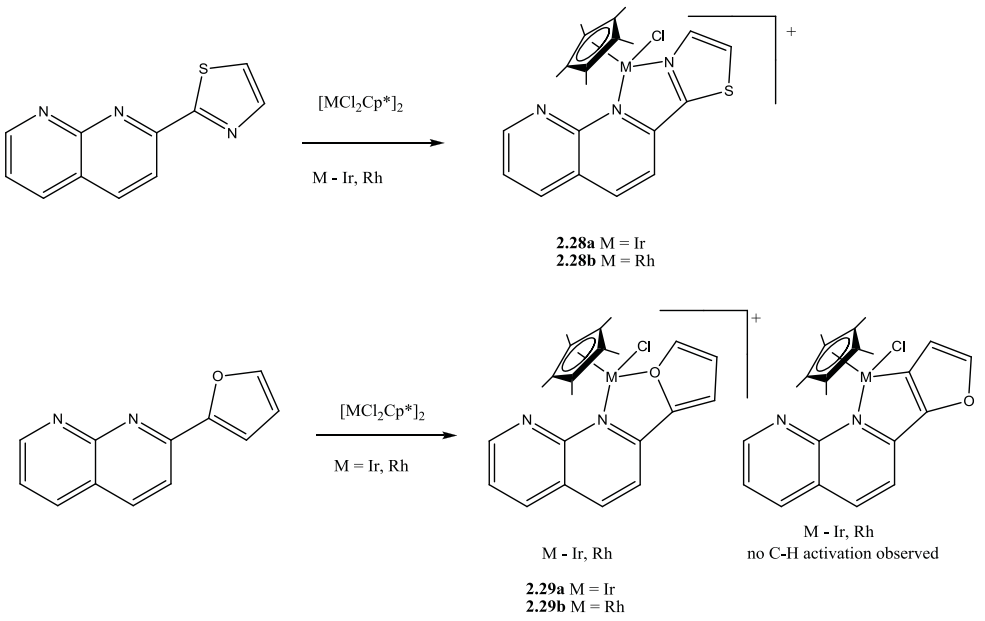

Scheme 2.30

N–heterocyclic carbenes are known and have been extensively studied over the last decade.[42, 43] They also have also been used as a directing group for C-H activation and metallacycle formation. In 2006, Peris *et al.* described the formation of a Cp*Ir cyclometallated carbene complex **(2.31a)** using acetate as a base.[44] Complex **(2.30a)**, a possible intermediate of this reaction was synthesised by transmetallation, however it is unstable at room temperature and spontaneously converts into **(2.31a)** without added base **(Scheme 2.31)**. No directing group is required in the C-H activation to produce the Ir-carbene bond, but this group then directs the next C-H activation which occurs spontaneously with loss of HCl.

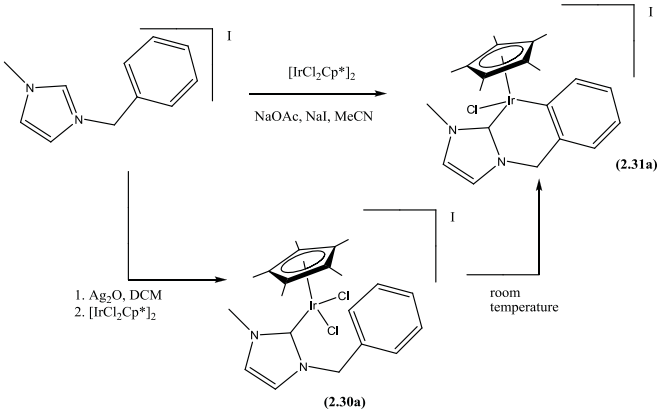

Scheme 2.31

The same year Yamaguchi used a similar system to describe aliphatic C-H activation using a weak base **(Scheme 2.32)**.[45] Peris investigated the competition between aliphatic and aromatic C-H activation using an asymmetric imidazolium ligand **(Scheme 2.33)**. When R = ^{i}Pr aromatic C-H activation occurred to form **(2.32a)** whereas when R = ^{t}Bu aliphatic C-H activation occurred exclusively to produce **(2.33a)**. The authors concluded that steric factors are very important for the selectivity of the reaction and commented that this contrasts with previous views where Ir(III) activates the stronger bonds .[46]

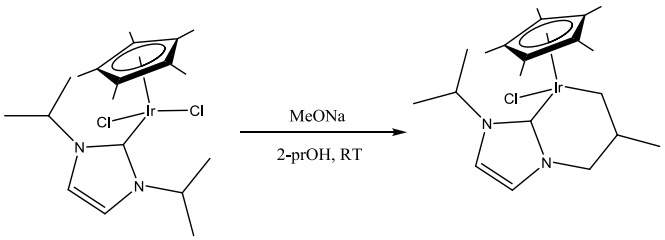

Scheme 2.32

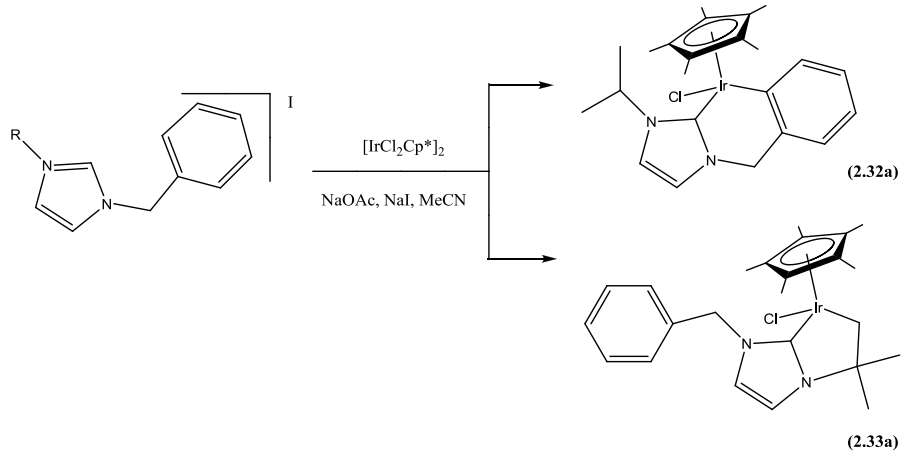

Scheme 2.33

2.2.2 Results and discussion

C-H activation was investigated with the carbene precursor benzimidazolium salt L11. Multiple pathways and products can be envisaged from the reaction of L11 with $[IrCl_2Cp^*]_2$ in the presence of NaOAc **(Scheme 2.34)**. The formation of the monodentate carbene complex **(2.34a)** is feasible as discussed above in **Scheme 2.31.**[44] From **(2.34a)** there may be a competition between the formation of the neutral N–C chelate **(2.37a)** and acetate assisted C-H activation to produce C,C cyclometallated complex **(2.36a) (Scheme 2.34)**. Alternatively, the triazole may coordinate first to form **(2.35a)** which could then undergo aromatic C-H activation to form the six-membered ring **(2.38a)** or carbene formation to form **(2.37a)**. Other possibilities involving coordination of N(2) have not been addressed, our previous observations from the reactions of L8 and L9 confirmed the low potential of coordination of the N(2) of the triazole.

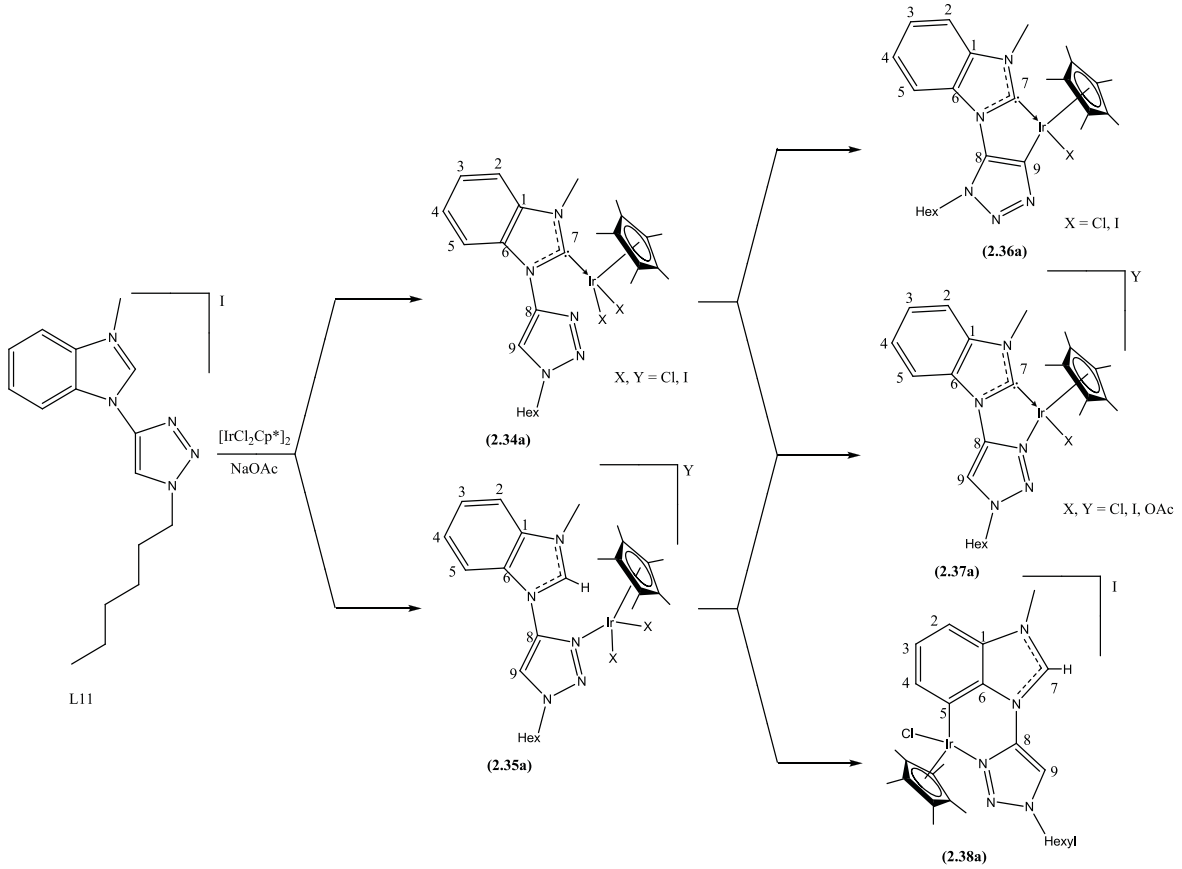

Scheme 2.34

L11 was reacted with $[IrCl_2Cp^*]_2$ in presence of NaOAc in DCM. The reaction was monitored by ^1H NMR spectroscopy and after 20 hours the ^1H NMR spectrum showed complete reaction, with one set of signals for the ligand and a Cp* suggesting that the reaction selectively produced one compound. The ^1H NMR spectrum showed signals integrating for 38 H (i.e. loss of one H) which suggests the formation of **(2.34a)** or **(2.37a)** or **(2.38a)**, and rules out the formation of **(2.35a),** which would show 39 H, and **(2.36a)** which would show 37 H **(Scheme 2.34)**. The spectrum shows only one singlet, integrating for 1 H at δ 10.94 this rules out the formation of **(2.38a)** because two singlets (H^7 and H^9) would be expected for **(2.38a)**. However the chemical shift of this proton is similar to H^7 in the free ligand (at δ 10.09) whereas H^9 in L11 is at δ 8.83. In the NOESY spectrum the singlet at δ 10.94 shows cross peaks with both H^5 and the hexyl chain which proves the assignment as H^9, this also confirms the loss of H^7 and the formation of a carbene. The carbene complex

(2.34a) is neutral so H^9 should be similar to free ligand L11. However, in **(2.37a)** the triazole is coordinated to the metal and the complex is cationic so H^9 is much more acidic and can hydrogen bond to the counterion (Cl^-, I^-) thus giving the lowfield NMR shift. The Cp* is observed as a singlet at δ 2.03 whilst the methyl is a singlet at δ 4.07 (cf δ 4.28 in L11). The aromatic protons show two doublets at δ 7.50 and 8.70 for H^2 and H^5 and two triplets for H^3 and H^4 at δ 7.44 and 7.59. NOE correlations between the methyl signal and the Cp* and the methyl and H^2 confirm the assignments. The ^{13}C NMR spectra show the expected number of carbons with the carbene C^7 at δ 173.00 which is similar to the chemical shifts observed by Yamaguchi (within 10 ppm). The ES-MS spectrum shows one peak at m/z 738 which agrees with the cation **(2.37a)** with X=I and the FAB-MS spectrum shows two signals at m/z 738 and 611 which agree with $[IrI(L11\text{-}H)Cp^*]^+$ and $[Ir(L11\text{-}H)Cp^*]^+$. The elemental analysis is also consistent with the formation of **(2.37a)** with iodide as a counter ion. This reaction shows that the formation of the chelate **(2.37a)** is favoured over **(2.36a)** or **(2.38a)**, however this product could be formed from **(2.34a)** or **(2.35a)**. Hence the order of reaction between N–coordination of triazole or the carbene formation could not be determined.

In order to further investigate the competition involved between chelate formation and C-H activation, L12 was used. L12 essentially replaces the carbene donor of L11 with another heterocyclic N-donor atom. The reaction of the dimer with L12 in presence of NaOAc could produce several products **(Scheme 2.35)**. Coordination of the indazole first gives **(2.39a)** as an intermediate, subsequent C-H activation would form a five-membered ring **(2.41a)** whilst N–N chelate formation would give **(2.42a)**. If N(3) of the triazole coordinates before the indazole, **(2.40a)** is the intermediate which can then give N–N chelate product **(2.42a)** or a less plausible aromatic C-H activation to form **(2.43a)**. In both cases there is a direct competition between coordination of a second N-atom to form a neutral chelate and C-H activation to form an N,C anionic chelate.

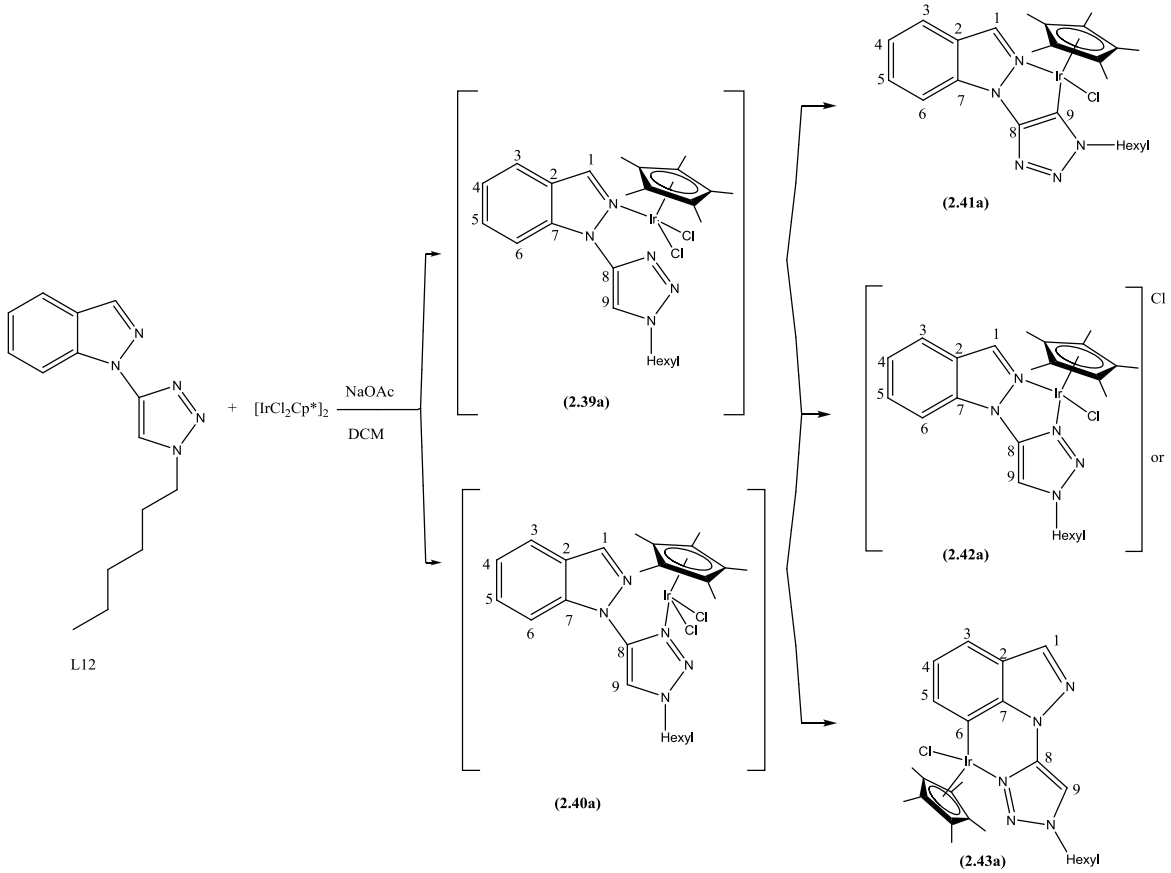

Scheme 2.35

The reaction of L12 with $[IrCl_2Cp^*]_2$ and NaOAc was carried out in DCM and after 23 hours, the ^1H NMR spectrum shows one Cp* signal and one set of signals for the ligand which integrated to 19 protons and shows that no C-H activation had occurred so neither **(2.41a)** or **(2.43a)** was formed, hence the product was **(2.42a)**. The ES-MS and FAB-MS showed a peak at m/z 632 assigned as the cation $[IrCl(L12)Cp^*]^+$. The reaction was repeated without NaOAc in presence of KPF_6, to afford **(2.42a)** as a PF_6 salt **(Fig. 2.14)**.

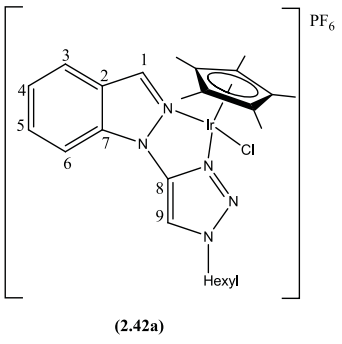

Fig. 2.14 Structure of (2.42a)* (* isolated as a PF_6 salt)

The ^{1}H NMR spectrum shows a singlet due to the Cp* at δ 1.83. Two singlets at δ 8.46 and 8.59 are observed and assigned to H^{1} and H^{9} respectively. H^{9} is 0.7 ppm downfield from the corresponding signal in L12 (δ 7.85). This is consistent with coordination of the triazole in a cationic complex making H^{9} more acidic, however it is not as low field as in **(2.42a)** (δ 10.94) presumably less hydrogen bonding to PF_6 than there is to chloride in **(2.42a)**. The other aromatic protons are observed as two doublets at δ 7.86 (H^{6}) and 7.88 (H^{3}) and two doublets of doublets at δ 7.37 (H^{4}) and 7.66 (H^{5}). The ^{13}C NMR spectra show the expected number of C-H and quaternary carbons with the imine carbon C^{1} at 138.68. The elemental analysis confirmed that the product contains PF_6 as a counterion.

This reaction proved that the formation of the N,N chelate and in particularly coordination of a second N-donor atom is favoured over the acetate assisted C-H activation in this case which contrasts with the example described by Tilset *et al*. where C-H activation was favoured over the formation of a diimine chelate complex.[13] Acetate assisted C-H activation appears to be an easy reaction with monodentate ligands however when multiple sites are present the formation of N–N and C–N neutral chelates are favoured over the acetate assisted C-H activation in the cases studied. Further investigation of the competition between multiple sites was carried out using potential neutral N–O chelates.

The competition between acetate assisted C-H activation and the formation of N–O chelates was attempted using pyridine as a directing group with 2-benzoylpyridine (L13) and 2-acetylpyridine (L14). The reaction of L13 with $[IrCl_2Cp^*]_2$ in presence of NaOAc could lead to the formation of **(2.44a)** by acetate assisted C-H activation, or **(2.45a) (Scheme 2.36)** *via* N–O chelate formation as observed by Macchioni *et al.*[40] in the case of Ru(*p*-cymene) and discussed earlier.

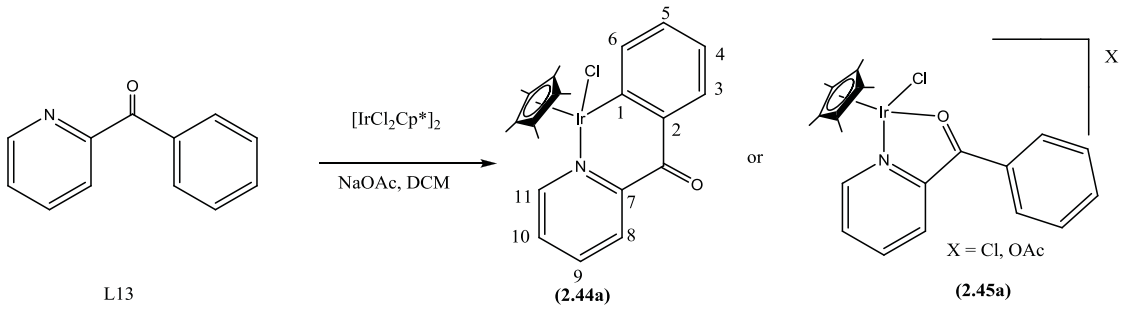

L13 **(2.44a)** **(2.45a)**

Scheme 2.36

The reaction of L13 with $[IrCl_2Cp^*]_2$ in the presence of NaOAc was attempted. The ^1H NMR spectrum of the mixture after 8 hours showed a Cp* signal at 1.67 and two sets of four aromatic signals, assigned by a COSY experiment, consistent with cyclometallation and formation of **(2.44a)**. The pyridine ring gives rise to three doublets of doublets of doublets at δ 8.14 (H^8), 9.12 (H^{11}) and 7.39 (H^{10}) and a triplet of doublets at δ 7.87 for H^9. The phenyl ring gives rise to four mutually coupled signals, in this case four doublets of doublets of doublets are observed at δ 7.00, 7.26, 7.80 and 7.84 for H^5, H^4, H^3 and H^6 respectively. The ^{13}C NMR spectra show the expected number of carbons for the cyclometallated product with the metallated carbon observed at δ 156.51. The product was crystallised from DCM/hexane and the structure was determined by X-ray crystallography and is shown in **Fig. 2.15** with selected bond distances and angles and is discussed below.

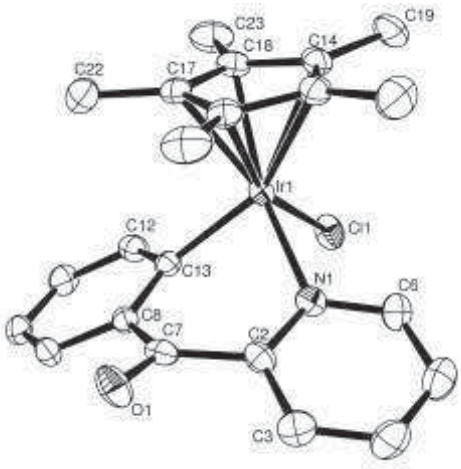

Fig. 2.15 Molecular structure of (2.44a)

Selected bond lengths and angles: Ir(1)-N(1) 2.083(4) Å, Ir(1)-C(13) 2.030(5) Å, Ir(1)-Cl(1) 2.4055(12) Å, N(1)-C(2) 1.365(2) Å, C(2)-C(7) 1.503(7) Å, C(7)-C(8) 1.487(6), Ir(1)-C(16) 2.146(4), Ir(1)-C(17) 2.166(5), Ir(1)-C(18) 2.167(5), Ir(1)-C(15) 2.256(5), Ir(1)-C(14) 2.265(5), C(8)-C(13) 1.402(6), C(13)-Ir(1)-N(1) 86.75(16)˚, C(13)-Ir(1)-Cl(1) 88.32(13)˚, N(1)-Ir(1)-Cl(1) 87.85(16)˚

The structure confirms the formation of the six-membered ring half sandwich complex. The metal-ligand bond lengths Ir(1)-C(13), Ir(1)-Cl(1) and Ir(1)-N(1), [2.030(5) Å] [2.4055(12) Å] [2.083(4) Å] respectively are very similar to the corresponding ones of **(2.12a),** [2.049(7) Å] [2.4084(18) Å] [2.109(5) Å] respectively, however the N-M-C angle 86.75(16)° is slightly bigger in **(2.44a)** than that, 84.4(2)°, in **(2.12a)**. This can be explained by the angle C(8)-C(7)-C(2) [120.3(4)°] being bigger for **(2.44)** due to the ketone, than for the corresponding angle in **(2.12a)** [112.7(6)°]. As observed for the previous IrCp* crystal structures and in the literature the Cp* ring is bonded asymmetrically to the metal centre with two long Ir-C bonds (ca. 2.26 Å) and three short ones (2.15 to 2.17 Å). This reaction showed that the C-H activation pathway to form a six-membered ring is favoured over N–O chelate formation. In a deliberate attempt to make the N,O chelate the reaction was repeated in the absence of NaOAc and in presence of KPF_6 in $CDCl_3$ however only starting materials were observed by ^1H NMR spectroscopy. In a more polar solvent (MeOH) the N,O complex forms easily[47]and

the ^{1}H, ^{13}C NMR data are the same as reported by Macchioni *et al.*[40] As discussed later bidentate N,O coordination requires liberation of Cl- which is solvent dependent.

The reaction of L13 with $[RhCl_2Cp^*]_2$ in the presence of NaOAc in DCM was also attempted **(Scheme 2.37)**. After 6 hours the ^{1}H NMR spectrum of the mixture showed two sets of signals for the ligand in a ratio of 1:3 with the major one corresponding to the free ligand, and many other Cp* signals between δ 1.00 and 2.00. After work up (filtration through celite and several washes with diethylether) more than one product is observed in the ^{1}H NMR spectrum, however a crystallisation from DCM/hexane afforded some crystals suitable for X-ray diffraction. A view of the structure and selected bond distances and angles is shown and discussed below **(Fig. 2.16)**.

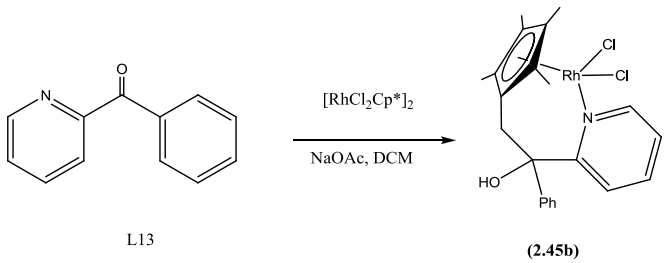

L13 (2.45b)

Scheme 2.37

The ^{1}H NMR spectrum of this batch of crystals showed four singlets (integrating for 3 H) at δ 2.10, 1.90, 1.70 and 1.55 and two 1H doublets at δ 2.95 and 2.53 which would agree with an activated Cp* **(2.45b) (Scheme 2.37)** however other Cp* impurities were observed. More than one set of signals were observed for the ligand. Further crystallisations did not afford pure product. The ES-MS spectrum shows two peaks at m/z 420 and 461 assigned to $[Rh(L13)Cp^*-H]^+$ and $[Rh(L13)Cp^*-H+MeCN]^+$.

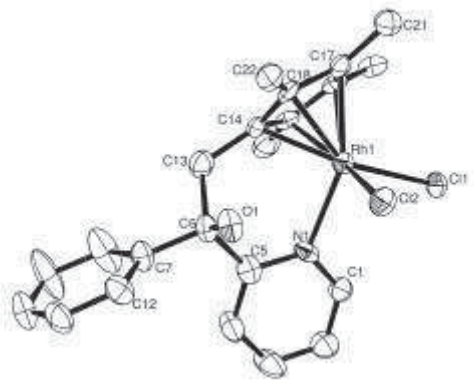

Fig. 2.16 Molecular structure of (2.45b)

Selected bond distances and angles: Rh(1)-C(14) 2.093(5) Å, Rh(1)-N(1) 2.195(5) Å, Rh(1)-Cl(1) 2.4057(16) Å, Rh(1)-Cl(2) 2.4147(16) Å, N(1)-C(5) 1.381(7) Å, C(5)-C(6) 1.533(8) Å, C(6)-C(13) 1.542(7) Å, C(13)-C(14) 1.485(7) Å, C(15)-C(19) 1.476(7) Å, C(16)-C(20) 1.504(7) Å, C(18)-C(22) 1.494(7) Å, C(17)-C(21) 1.490(7) Å, N(1)-Rh(1)-Cl(1) 94.16(14)°, N(1)-Rh(1)-Cl(2) 88.25(13)°

The structure of **(2.45b)** confirms that one arm of the Cp* is linked to the ligand. The N-Rh(1)-Cl(1) angle is substantially bigger [94.16(14)°] than the N-Rh(1)-Cl(2) angle [88.25(13)°]. It is noticeable that an intramolecular hydrogen bond is observed between Cl(2) and H(1) [3.214 Å], this could explain the fact that the N-Rh(1)-Cl(2) angle [94.16(14)°] is larger than the N-Rh(1)-Cl(1) angle [88.25(13)°].

Hence, in contrast to the observations of the corresponding reaction with Ir, with Rh the acetate assisted C-H activation to form **(2.45b)** was not the favoured pathway, however neither was N–O chelate formation, instead, only a low conversion was observed (30%), and more than one complex was formed, one of which showed an activated Cp*. It seems that activation of a methyl of the Cp* occurs which then attacks the ketone to link the Cp* to the ligand. Deprotonation of a Cp* with Rh and Ir complexes is well precedented.[48-50]

L13 was also reacted with $[RuCl_2(p\text{-cymene})]_2$ in the presence of NaOAc and no C-H activation was observed after 6 hours. In the ^1H NMR spectrum only [RuCl(OAc)(*p*-cymene)], which is from the reaction between $[RuCl_2(p\text{-cymene})]_2$ and NaOAc, and unreacted L13 were observed. In the ES-MS spectrum two peaks at m/z 418 and 459, assigned to $[RuCl(L13)(p\text{-cymene})]^+$ and $[Ru(MeCN)(L13)(p\text{-cymene})]^+$ respectively show that some reaction probably coordination of pyridine is occuring, as observed by Macchioni *et al.* **(Scheme 2.29)**.[40]

From these results with L13, the C-H activation pathway was favoured over N–O chelate formation with $[IrCl_2Cp^*]_2$ in DCM. In the case of $[RuCl_2(p\text{-cymene})]_2$ no C-H activation occurred though, as expected,[9] all the $[RuCl_2(p\text{-cymene})]_2$ reacted with NaOAc. The coordination of L13 did not compete with the reaction with NaOAc in this case. Macchioni observed the formation of the N–O chelates in the presence of larger counter ions than Cl^- such as PF_6 or BPh_4 in DCM **(Scheme 2.29)**.[40] In the case of $[RhCl_2Cp^*]_2$ the reaction was not clean and some of **(2.45b)** could be observed.

Further investigations of the competition between the N–O chelate formation and C-H activation were attempted with 2-acetylpyridine (L14). This ligand offers the possibility to probe sp^3 rather sp^2 C-H activation. A previous study on C-H activation of L14 was carried out in our group, thus L14 was reacted with $[RhCl_2Cp^*]_2$, $[IrCl_2Cp^*]_2$ and $[RuCl_2(p\text{-cymene})]_2$ in the presence of NaOAc. The reaction with $[IrCl_2Cp^*]_2$ produced a mixture of products where one of them is a cyclometallated complex, however in the presence of $[RhCl_2Cp^*]_2$, the reaction led to the cyclometallated product. The ^1H NMR spectrum of the product showed a Cp* signal at δ 1.57 and two mutually coupled 1H doublets at δ 2.84 and 3.84 proving that C-H activation had occurred. The four aromatic protons gave rise to three doublets at δ 8.65, 7.65 and 7.49 for H^6, H^3 and H^5 and a triplet of doublets at δ 7.89 assigned

to H^4. The ^{13}C NMR spectra showed the expected number of carbons with the metallated carbon observed as a doublet at δ 45.33 and an HMQC spectrum showed a correlation between the CH_2 and the metallated carbon which further proved the formation of **(2.46b) (Scheme 2.38)**. The reaction of L14 with $[RuCl_2(p\text{-cymene})]_2$ in presence of NaOAc did not afford the cyclometallated complex. These preliminary results showed that $[RhCl_2Cp^*]_2$ was most successful for preparation of the cyclometallated product, some cyclometallation was observed in the case of $[IrCl_2Cp^*]_2$ but no C-H activation occurred in the case of $[RuCl_2(p\text{-cymene})]_2$. This contrasts with the results with all the other N-donor ligands for which Ir was better than Rh or Ru for acetate assisted C-H activation.

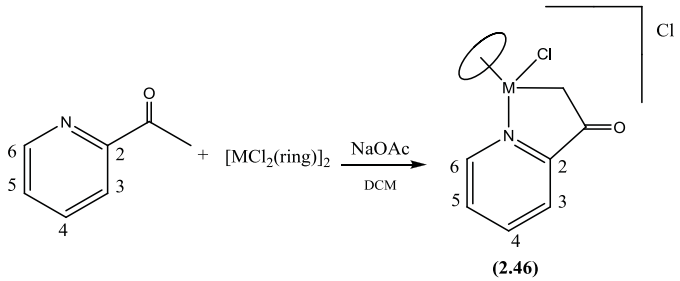

M = Rh, ring = Cp*, gives **(2.46b)** clean reaction
M = Ir, ring = Cp*, no clean reaction observed
M = Ru, ring = p-cymene, no reaction with L14 observed

Scheme 2.38

In order to investigate the different order of reactivity with L14, the interaction between the dimers $[IrCl_2Cp^*]_2$, $[RhCl_2Cp^*]_2$ and $[RuCl_2(p\text{-cymene})]_2$ and the ligand was tested. The coordination of L14 with the dimers $[IrCl_2Cp^*]_2$, $[RhCl_2Cp^*]_2$ and $[RuCl_2(p\text{-cymene})]_2$ was examined by ^1H NMR spectroscopy in CD_2Cl_2 at different temperatures. In the case of $[IrCl_2Cp^*]_2$, the ^1H NMR spectrum at room temperature showed the two starting materials ($[IrCl_2Cp^*]_2$ and L14) with five signals for L14, two doublets at δ 8.72 and 8.04 due to H^6 and H^3 and two triplets at δ 7.89 and 7.52 due to H^5 and H^4 respectively, the methyl signal was observed at δ 2.68 and the Cp* signal for $[IrCl_2Cp^*]_2$ at δ 1.53. Another set of signals integrating for ca 5% of the starting materials was also observed, with two singlets at δ 1.75

at δ 3.26 for the Cp* and the methyl signal and four broad multiplets at δ 8.11, 8.60, 8.86 and 8.99. This new species was assigned as **(2.47a) (Scheme 2.39)**, the downfield shift (between 0.22 and 1.04 ppm) observed for all the pyridine signals in comparison to free L14 would be consistent with the formation of a cation. The previous formation of the corresponding Ru(*p*-cymene) complex by Macchioni *et al.*[40] **(Scheme 2.29)** is also consistent with the formation of **(2.47a)**.

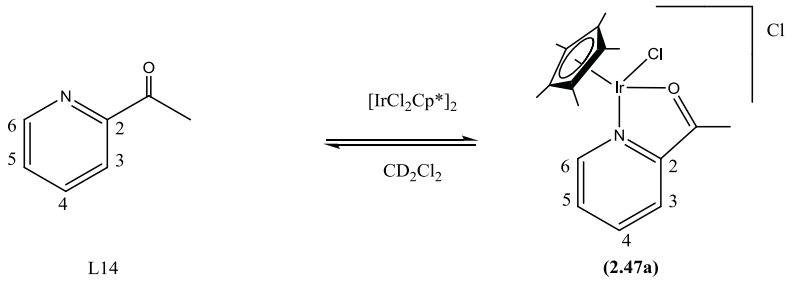

L14 **(2.47a)**

Scheme 2.39

Hence it appears that **(2.47a)** is in equilibrium with the starting materials. To confirm this hypothesis a variable temperature NMR study was undertaken and various spectra are shown in **Fig 2.17**. As the temperature was lowered, the rate of interconversion was slowed and the minor signals became more resolved showing two doublets at δ 8.96 H^6 and 9.13 H^3 and two triplets at δ 8.66 H^4 and 8.13 H^5 with two singlets for the methyl and the Cp* at δ 3.31 and 1.77 respectively. The amount of **(2.47a)** also increases as the temperature decreases with a 1:1 ratio at 243.5 K. At 211 K the equilibrium was slow on the NMR timescale and a 1:1 ratio was observed between the starting materials (L14 and $[IrCl_2Cp^*]_2$) and **(2.47a)** in the ^1H NMR spectrum. An NOE correlation between H^3 **(2.47a)** and the methyl signal would suggest that these two signals are close which implies that the oxygen atom is pointing to the metal centre and is consistent with the assignment as **(2.47a)**.

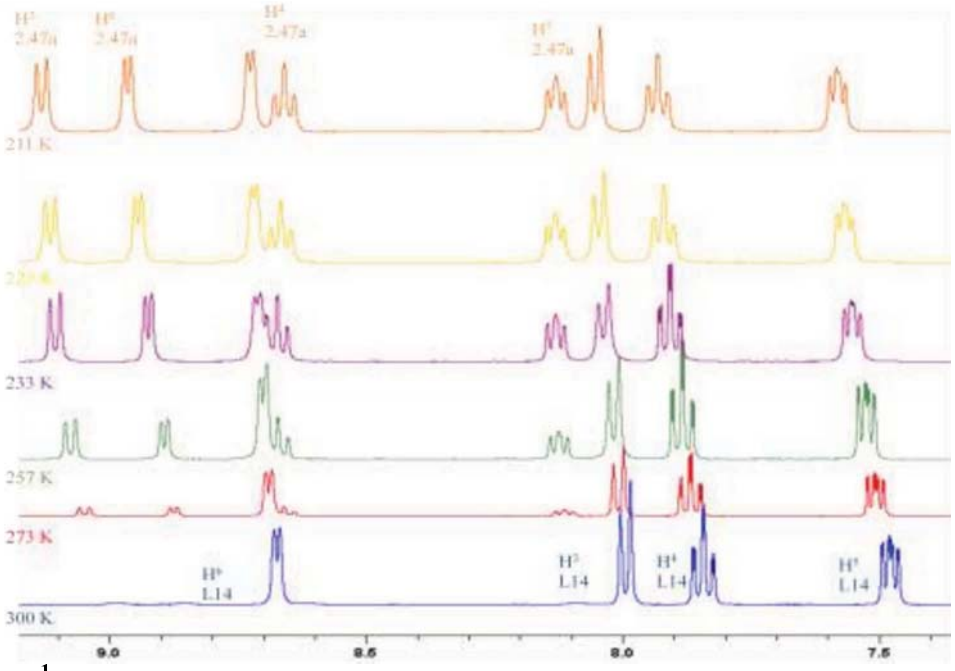

Fig. 2.17 ^{1}H NMR spectra at different temperatures from the reaction of $[IrCl_2Cp^*]_2$ with 2-acetylpyridine (L14) (400 MHz, in CD_2Cl_2)

The assignment was established with a ROESY experiment at 270 K **(Fig. 2.18)** showing a correlation between the signals for free and coordinated L14. The correlation between H^3 (L14) and H^3 **(2.47a)** shows that there is a substantial downfield shift for H^3 **(2.47a)** which may be due to hydrogen bonding with the chloride counterion.

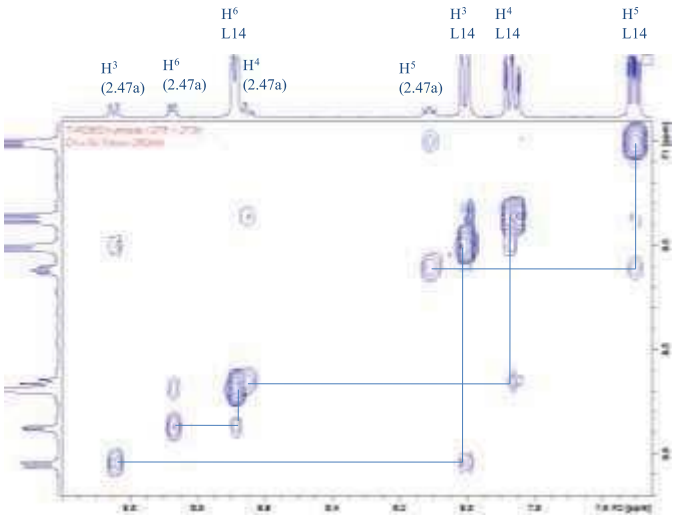

Fig. 2.18 ROESY NMR spectrum at 273 K from the reaction of $[IrCl_2Cp^*]_2$ with 2-acetylpyridine (L14) in CD_2Cl_2

The formation of **(2.47a)** requires Cl^- as a counterion which is likely to be poorly solvated in CD_2Cl_2. To test this d_4-methanol which is more polar was added to the mixture. The addition of d_4 methanol (20% by volume) changed the equilibrium position and the coordination of L14 increased from ca 5 to 70% at room temperature consistent with the better solvation of chloride favouring formation of **(2.47a)**.

The reaction of L14 with $[RhCl_2Cp^*]_2$ was also attempted but no sign of coordination was observed in the ^1H NMR spectrum even at low temperature (247 K). The spectrum showed a Cp* signal at δ 1.52 for $[RhCl_2Cp^*]_2$ and the signals for free L14.

The reaction of $[RuCl_2(p\text{-cymene})]_2$ with L14 was also attempted in an NMR tube in CD_2Cl_2 and the ^1H NMR spectrum at room temperature showed signals for starting materials ($[RuCl_2(p\text{-cymene})]_2$ and L14) and two new sets of *p*-cymene signals and one new set for coordinated L14 **(Scheme 2.40)**. The major ruthenium species formed (30%) showed signals for a coordinated *p*-cymene group with four doublets at δ 5.90, 6.03, 6.08 and 6.22 for the aromatic protons, a singlet at 2.30 for the methyl and signals for the isopropyl group. The associated coordinated ligand showed two doublets at δ 8.24 and 9.71 for H^3 and H^6 respectively, a multiplet at δ 8.08 for H^5 and a triplet at δ 8.14 for H^4. The acetyl signal was observed as a singlet at δ 2.94. As for the iridium reactions, the high frequency of the signals in comparison to the starting materials, is consistent with a cationic species and the inequivalence of the *p*-cymene signals shows a chiral metal centre also consistent with **(2.47c) (Scheme 2.40)**.

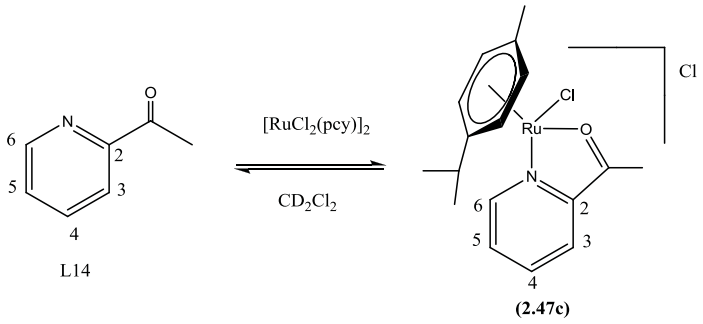

Scheme 2.40

The assignment was confirmed by a ROESY experiment where exchange between free and coordinated L14 was observed. The ^{1}H NMR spectrum also showed some [$RuCl_2$(*p*-cymene)]$_2$ and another set of *p*-cymene signals with two broad doublets at δ 5.15 and 5.40 for the aromatic protons and a singlet at δ 2.18 for the methyl group, no L14 signals were associated with this ruthenium-containing species. However, a ROESY experiment showed that this species was also exchanging with [$RuCl_2$(*p*-cymene)]$_2$ and with **(2.47c)**. The *p*-cymene protons were not all inequivalent which would suggest that the metal centre was not chiral. These signals have been assigned to [$RuCl_3$(*p*-cymene)]$^-$ where the extra Cl^- would come from the formation of the N–O chelate (i.e. the counterion for **(2.47c)** is a mixture of Cl^- and [$RuCl_3$(*p*-cymene)]$^-$. In order to confirm the formation of [$RuCl_3$(*p*-cymene)]$^-$, [$RuCl_2$(*p*-cymene)]$_2$ was reacted with NEt_4Cl in CD_2Cl_2. The ^{1}H NMR spectrum showed the signals for [$RuCl_2$(*p*-cymene)]$_2$ and NEt_4^+, but also the corresponding signals for [$RuCl_3$(*p*-cymene)]$^-$ observed earlier, moreover in the negative ion ES-MS spectrum a peak at m/z 343 [$RuCl_3$(*p*-cymene)]$^-$ was observed. In 1978, Robertson *et al.* reported the formation of Cs[$RuCl_3$(*p*-cymene)] however it was not fully characterised.[51] As for [$IrCl_2Cp^*$]$_2$, to probe the role of Cl^- in this process, d_4-methanol (10 equivalents) was added at room temperature to a solution of [$RuCl_2$(*p*-cymene)] and L14, the ^{1}H NMR spectrum showed an increase in the formation of **(2.47c)** confirming the importance of solvation of "free" Cl^-.

These results show that coordination of L14 to $[IrCl_2Cp^*]_2$ and $[RuCl_2(p\text{-cymene})]_2$ to form an N–O chelate is an equilibrium process which is more favoured toward the formation of the N–O chelate in the case of Ru than Ir. However, no coordination was observed in the case of $[RhCl_2Cp^*]_2$. The production of "free" Cl^- is an important factor in N–O chelate formation as is shown by using more polar solvents. To investigate if **(2.47a)** and **(2.47c)** are intermediates for the acetate assisted C-H activation, more stable salts are needed, hence the isolation of these as PF_6 salts was attempted.

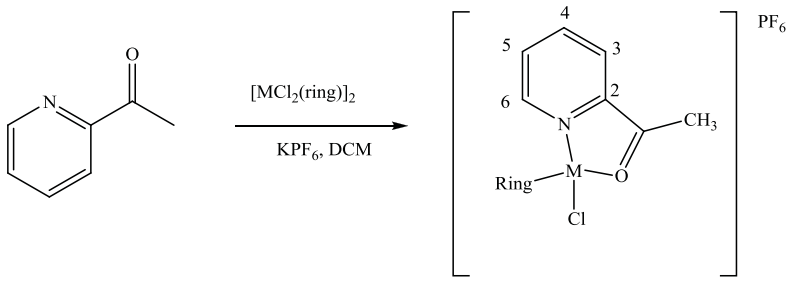

L14

(2.47a)* M = Ir ring= Cp*
(2.47c)* M = Ru ring = *p*-cymene
(2.47d)* M = Ru ring= mes

* isolated as PF_6 salts

Scheme 2.41

The reactions of (L14) with $[MCl_2Cp^*]_2$ (M = Ir, Rh) and $[RuCl_2(mes)]_2$ were carried out in DCM in the presence of KPF_6 **(Scheme 2.41)**. Complex **(2.47c)** was described previously by Macchioni *et al.*[40] The reaction of L14 with $[IrCl_2Cp^*]_2$ and KPF_6 in DCM led to the formation of **(2.47a)** in 74% yield. The ^1H NMR spectrum shows four different protons for the pyridine system and singlets at δ 4.00 and 1.79 for the methyl group and the Cp* respectively. The pyridine system is composed of three doublet of doublet of doublets at δ 8.91, 8.50 and 8.05 for H^6, H^3, and H^5 respectively and a doublet of triplets at δ 8.34 for H^4. The assignment was determined by NOESY experiments where a correlation between H^6 and the Cp*, and between H^3 and the methyl group were observed. The chemical shifts are similar to the ones observed with Cl^- as a counter ion, however H^3 is more upfield in this case (0.6 ppm) which could be explained by the absence of hydrogen bonding when PF_6 is used as

counter ion. The ^{13}C NMR spectrum shows the expected number of carbons, the CO is observed at δ 210.78 and the acetyl methyl at δ 26.04 (confirmed by a DEPT experiment). The FAB-MS spectrum showed a signal at *m/z* 484 due to the cation $[IrCl(L14)Cp^*]^+$. Crystals of this compound were obtained from DCM/hexane and were suitable for X-ray diffraction. The structure is shown in **Fig. 2.19** with selected bond distances and angles in **Table 2.3** and is discussed with the ruthenium analogue below.

An attempt to make the similar compound with $[RhCl_2Cp^*]_2$ under the same conditions failed. The ^1H NMR spectrum of the mixture showed that free ligand and $[RhCl_2Cp^*]_2$ were still present. To test the same reaction with ruthenium, $[RuCl_2(mes)]_2$ was chosen as a starting material in preference to $[RuCl_2(p\text{-cymene})]_2$ since it has much simpler ^1H NMR signals which makes identification much easier. Reaction of L14 with $[RuCl_2(mes)]_2$ and KPF_6 gave **(2.47d)** after 20 hours at in 87% yield. The ^1H NMR spectrum was similar to the one of **(2.47a)** showing 4 different proton signals for the pyridine ligand, a singlet for the methyl group at δ 3.01 and two singlets for the mesitylene at δ 2.33 and 5.37. The most downfield signal is H^6, observed as a doublet at δ 9.21, whilst H^3 is observed as a doublet at δ 8.30 with two doublets of doublets of doublets at δ 7.94 and 8.26 for H^5 and H^4 respectively. The chemical shifts are similar to **(2.47a)** (within 0.2 ppm) and those of **(2.47c)** described by Macchioni *et al.* with (arene = *p*-cymene).[40] The ^{13}C NMR spectrum shows the expected number of carbons with the CO at δ 211.0. The FAB-MS mass spectrum shows an ion at *m/z* 378 due to $[RuCl(L14)(Mes)]^+$. Crystals of this compound were obtained from DCM/hexane and were suitable for X-ray diffraction. The structure is shown below in **Fig. 2.19** with selected bond distances and angles in **Table 2.3** and discussed further below.

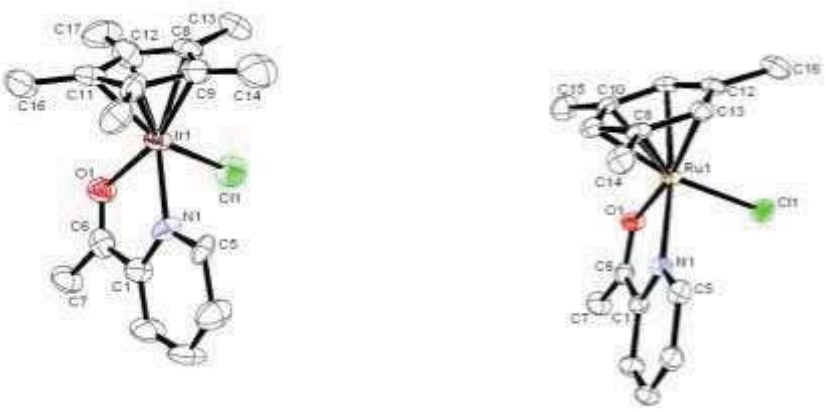

Fig. 2.19 Molecular structure of the cation in (2.47 a,d)

Table 2.3 Selected bond distances (Å) and angles(˚) for the cation in **(2.47a,d).**

	2.47a	**2.47d**
M-O	2.154(10)	2.105(3)
M-N	2.101(11)	2.106(4)
M-Cl	2.377(5)	2.3849(13)
O-C6	1.235(17)	1.234(5)
C6-C1	1.488(19)	1.469(6)
C1-N	1.384(18)	1.353(5)
M-C (ring)	2.108(16)	2.175(4)
	2.138(15)	2.175(4)
	2.161(14)	2.186(5)
	2.172(14)	2.190(4)
	2.179(14)	2.193(5)
		2.207(4)
Cl-M-N	82.8(3)	84.78(10)
Cl-M-O	84.7(3)	85.63(9)
N-M-O	76.1(4)	75.92(13)

Both cations show a similar three legged piano stool structure. For **(2.47d)**, the Ru-O [2.105(3) Å] and Ru-N [2.106(4) Å] bond lengths are statistically the same whereas for **(2.47a)** the Ir-O bond [2.154(10) Å] is longer than the Ir-N bond [2.101 (11) Å]. The two cations show similar O-M-N chelate angles namely 76.1(4)˚ and 75.92(13)˚ for **(2.47a)** and **(2.47d)** respectively. It is noticeable that the acetylpyridine is planar for both complexes with a small torsion angle N–C-C–O of less than 4 degrees.

From these reactions Ru and Ir complexes show similar behaviour, N–O chelates were easily formed with L14 but they do not undergo clean C-H activation in the presence of NaOAc. In contrast the Rh complex promoted the acetate assisted C-H activation but no N,O coordination could be observed even in the presence of KPF_6. In order to have a better understanding of these differences and to see if the N,O complexes are intermediates in C-H activation, the reactivity of **(2.47a)** and **(2.47d)** was investigated.

The acidity of the acetyl methyl was probed by adding D_2O to NMR samples of **(2.47a)** and **(2.47d)** in CD_2Cl_2, this led to a gradual disappearance of the signal for the acetyl methyl protons due to H-D exchange **(Scheme 2.42)**.

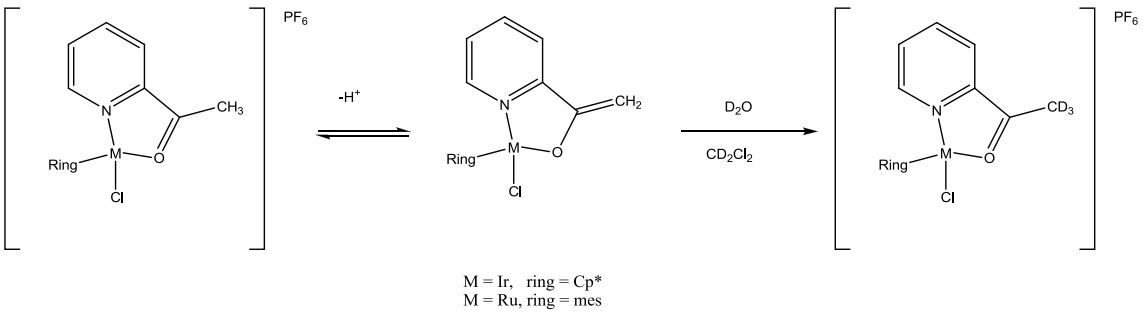

Scheme 2.42

This H-D exchange showed that a keto-enol equilibrium was occurring but the amount of enol complex was presumably small, since no signals for this species were observed. To test whether the N–O chelates (**2.47a** and **2.47d**) are intermediates in CH activation they were treated with NaOAc, however no reaction occurred after 4 hours, the ^1H NMR spectra of the mixture showed only the starting compounds. Note, within this time the reaction of $[RhCl_2Cp^*]_2$ with L14 would have been complete. A stronger base NaOMe, was reacted with **(2.47d)**. After 6 hours, the ^1H NMR spectrum showed two different sets of mesitylene signals in equal amounts, which would suggest either a 1:1 mixture of two species or the formation of an unsymmetric dimer. Three other signals at δ 1.96, 3.19 and 6.54 were observed with the

latter disappearing in the presence of D_2O which would be consistent with formation of an alcohol group. Unfortunately total purification was not possible, the product transforms to further products if left in solution for long periods. However, we have managed to get some crystals from the mixture, and the structure with selected bond distances and angles is shown in **Fig. 2.20**.

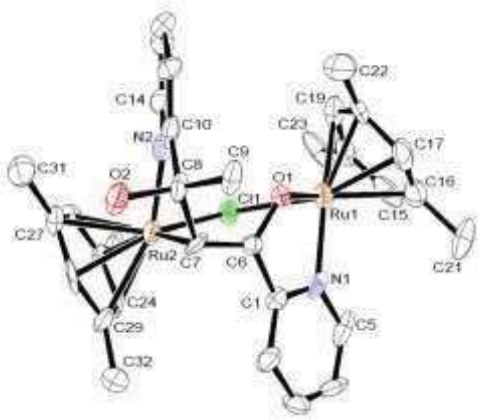

Fig. 2.20 Molecular structure of (2.48d)

Selected bond distances and angles of dication **(2.48d):** Ru(1)-N(1), 2.099(10) Å, Ru(1)-O(1), 1.995(9) Å, Ru(1)-Cl(1), 2.442(3) Å, Ru(2)-N(2), 2.080(11) Å, Ru(2)-C(7), 2.203(12) Å, Ru(2)-Cl(1), 2.441(3) Å, O(1)-C(6), 1.286(12) Å; O(2)-C(8), 1.442(13) Å; C(6)-C(7), 1.385(14) Å; C(7)-C(8), 1.540(15) Å, O(1)-Ru(1)-N(1), 77.4(4)°, Ru(1)-O(1)-C(6), 114.7(7)°, Ru(1)-N(1)-C(1), 113.1(8)°, C(6)-C(1)-N(1), 111.7(11)°; C(1)-C(6)-O(1), 116.1(10)°; C(7)-Ru(2)-N(2), 75.3(4)°, Ru(2)-C(7)-C(6), 108.7(8)°, Ru(2)-N(2)-C(10), 120.3(9)°; C(8)-C(10)-N(2) , 114.9(12)°, C(7)-C(8)-C(10), 109.7(11)°

The structure shows an unsymmetrical dicationic dimer, the two Ru centres are symmetrically bridged by one chloride. Ru(1) can be viewed as a cationic Ru(II) centre with an N,O chelate where the Ru(1)-(O1) bond is shorter than the Ru-N(1) bond [1.995(9) Å] and [2.099(10) Å] respectively. The Ru(2) centre has an N–C chelate with Ru(2)-N(2) shorter than Ru(2)-C(7), [2.080(11) Å] and [2.203(12) Å] respectively. There is some contribution from an enol resonance form for C(7)-C(6)-O(1) in the 2-acetylpyridine bonded to Ru(1).

Thus, C(7)-C(6) [1.385(14)Å] and Ru(1)-O(1) [1.995(9) Å] are somewhat shorter, and O(1)-C(6) [1.286(12) Å] somewhat longer than the corresponding bonds, [1.481(6) Å], [2.105(3) Å], and [1.234(5) Å], respectively, in the N,O chelate complex (**2.47d).** A plausible explanation of the formation of **(2.48d)** is that deprotonation of **(2.47d)** in the presence of NaOMe leads to a reactive enol which reacts with **(2.47d)** in an aldol-type reaction. Macchioni *et al.* also observed a related reaction on a Ru(*p*-cymene) N–O chelate complex in the presence of Ag^{+} **(Scheme 2.43)**.[40]

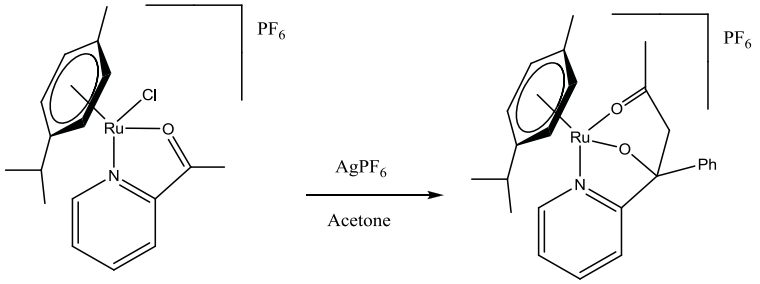

Scheme 2.43

The fact that reaction with NaOAc failed to produce the N–C complexes suggests that the N–O chelate products are not intermediates during an acetate assisted C-H activation process. However, the deuterium incorporation shows that the keto-enol equilibrium can occur and the dimerisation in the presence of NaOMe shows that the enol form is reactive. To further investigate the stability of C- or O-bound enolates, the dimers ($[IrCl_2Cp^*]_2$, $[RhCl_2Cp^*]_2$ and $[RuCl_2(p\text{-cymene})]_2$) were reacted with the lithium enolate of L14 .

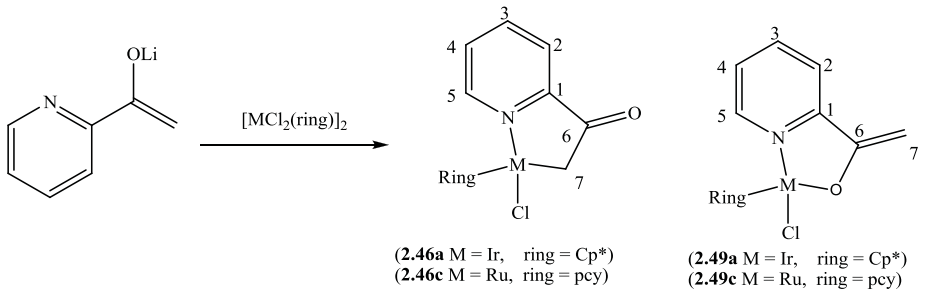

Scheme 2.44

The enolate was made *in situ* by the reaction of L14 with LiHMDS in THF at -80˚C. The enolate was then reacted with the relevant dimer **(Scheme 2.44)**. The reaction with $[RhCl_2Cp^*]_2$ gave the N,C chelate complex **(2.46b)** in 81% yield with identical spectroscopic data to the sample prepared by C-H activation.

The reaction with $[IrCl_2Cp^*]_2$ **(Scheme 2.44)** showed complete conversion, the ^{1}H NMR spectrum showed one set of signals for the cyclometallated ligand and one Cp* signal at δ 1.55. There was no methyl signal; and instead two mutually coupled doublets (*J* 7 Hz), were observed at *δ* 3.00 and 3.41, assigned to the metal-bound CH_2 in **(2.46a)**. These resonances are similar to **(2.46b)** and are consistent with the N–C chelate product **(2.46a)** rather than **(2.49a)** with the epimerisation being slow on the NMR timescale. Hence, the lithium enolate gave the N,C product **(2.46a)** rather than an isomeric N,O enolate complex **(2.49a)**. Furthermore, in a NOESY spectrum a correlation between the Cp* signal and one of the CH_2 protons at *δ* 3.00, confirms the assignment to **(2.46a)**. The ^{1}H NMR spectrum showed four signals for the pyridine group with two doublets of doublets of doublets at δ 8.51 and 7.54 for H^6 and H^3, a triplet of doublets at δ 7.86 for H^4 a doublet of doublets of doublets at δ 7.36 for H^5. All the chemical shifts are upfield in comparison the N–O chelate complex which may be due to the neutral nature of **(2.46a)**. The ES mass spectrum shows an molecular ion at *m/z* 448 $[M\text{-}Cl]^+$, a fragment at *m/z* 406 $[M\text{-}CH_2CO\text{-}Cl]^+$ and a signal at *m/z* 569 corresponding to $[M\text{-}Cl+L14]^+$ from the substitution of the chloride by a second L14. Crystals suitable for X-

ray diffraction were obtained and the structure with selected bond distances and angles is shown below **(Fig. 2.21)**.

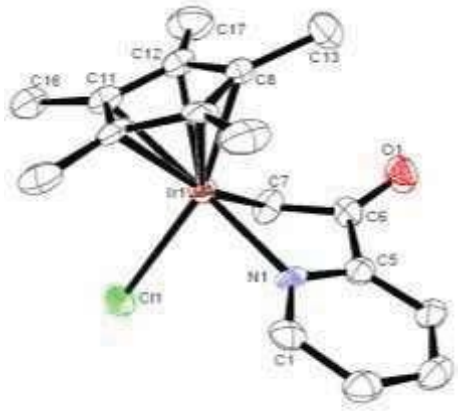

Fig. 2.21 Molecular structure of (2.46a)

Selected bond lengths and bond angles: Ir(1)-N(1), 2.094(6)Å, Ir(1)-C(7), 2.121(8)Å, Ir(1)-Cl(1), 2.424(2)Å, O(1)-C(6), 1.213(10)Å, C(7)-Ir(1)-N(1), 77.2(3)°, Ir(1)-C(7)-C(6), 102.1(5)°, Ir(1)-N(1)-C(5), 114.5(5)°, C(6)-C(5)-N(1), 111.6(6)°, C(5)-C(6)-C(7), 112.2(7)°.

The structure of **(2.46a)** confirmed the formation of the N–C chelate half sandwich complex. The bond distances Ir(1)-N(1) [2.094(6)Å], Ir(1)-C(7) [2.121(8)Å] and Ir(1)-Cl(1) [2.424(2)Å] are the same as those [2.112(2) Å], [2.138(3) Å], and [2.4294(8)Å] respectively in the corresponding rhodium complex **(2.46b).** The pyridine and acetyl groups are significantly non planar with a dihedral angle C(7)-C(6)-C(5)-N(1) of 26.7° whilst in the N–O chelate complexes **(2.47a)** and **(2.47d)** the pyridine is coplanar with the acetyl group.

The reaction of the enolate of L14 with $[RuCl_2(p\text{-cymene})]_2$ under similar conditions showed one major product in the ^1H NMR spectrum with some impurities. As observed for **(2.46a)** two mutually coupled doublets are present in the spectrum at δ 3.70 and at δ 3.10 which is consistent with a CH_2 group bonded to the metal. The *p*-cymene system shows four doublets for the aromatic protons at δ 5.30, 5.22, 5.02, 4.98, the isopropyl group gives rise to two doublets at δ 1.12, 1.08 and a septet at δ 2.57, the methyl of the *p*-cymene is observed at δ

1.78. The expected number of signals for the pyridine group is also present with two doublets at δ 8.90 and 7.49 due to H^5 and H^2 respectively and two doublets of doublets at δ 7.75 (H^3) and at δ 7.35 (H^4). Purification by crystallisation or chromatography failed to produce a pure sample of **(2.46c)**.

The formation of the N–C chelates **(2.46a,c)** with $[IrCl_2Cp^*]_2$ and $[RuCl_2(p\text{-cymene})]_2$ proved that these complexes are thermodynamically stable. Hence, the failure to get these by C-H activation with $[IrCl_2Cp^*]_2$ and $[RuCl_2(p\text{-cymene})]_2$ **(Scheme 2.38)** was not due to thermodynamic instability of the product. Moreover sp^3 C-H activation provided the N–C complex with $[RhCl_2Cp^*]_2$ which suggested that the acetyl proton was acidic enough to be activated by this process. The study of the coordination of L14 with $[IrCl_2Cp^*]_2$ and $[RuCl_2(p\text{-cymene})]_2$ suggests that the formation of the N–O chelate complexes occurs readily hence competes favourably with the reaction with NaOAc which is consistent with the failure of these to promote C-H activation. In the case of $[RhCl_2Cp^*]_2$ no coordination of L14 was observed and so acetate assisted C-H activation can proceed.

A further investigation of sp^3 C-H activation was carried out with 2-ethylpyridine with $[RhCl_2Cp^*]_2$ in the presence of NaOAc. No reaction was observed and the ^1H NMR spectrum of the mixture after 4 hours showed only starting materials. Coordination of 2-ethylpyridine with $[RhCl_2Cp^*]_2$ was investigated and no coordination was observed at room temperature, at 247 K broad signals (20% in intensity) at δ 1.38, 1.56, 7.37, 7.70, 9.30 would suggest that some reversible coordination is occurring. Coordination of 2-ethylpyridine with $[IrCl_2Cp^*]_2$ was observed by ^1H NMR spectroscopy at room temperature as evidenced by broad signals in the pyridine region. When the temperature was lowered to 233K sharp signals for coordinated 2-ethylpyridine were present with a Cp* at δ 1.51, two doublets of quadruplets at δ 2.96 and 3.70 for the CH_2 and a triplet for the CH_3 at δ 1.41. The pyridine signals showed two doublets

at δ 9.23 and 7.40 for $H^{6`}$ and $H^{3`}$ respectively, a triplet at δ 7.69 $H^{4`}$ and a doublet of doublets at δ 7.16 for $H^{5`}$. The chemical shifts for the pyridine signals are similar to the ones observed in the case of the coordination of 2-acetylpyridine. The fact that the CH_2 shows two inequivalent protons proves that the plane of the pyridine is not perpendicular to the Cp* and there is no mirror plane in the molecule **(Scheme 2.45)**.

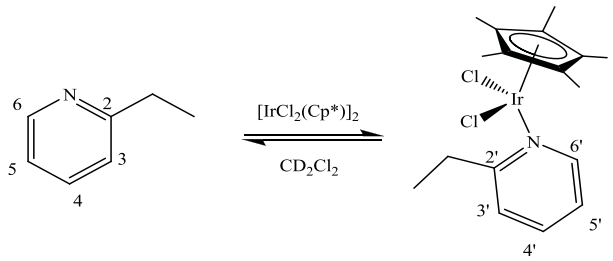

Scheme 2.45

The coordination of 2-phenylpyridine (L1) with $[MCl_2Cp^*]_2$ (M = Ir, Rh) was also investigated by ^1H NMR spectroscopy in CD_2Cl_2. No coordination was observed with both complexes $[MCl_2Cp^*]_2$ (M = Ir, Rh) even at low temperature (247 K).

In conclusion, in the case of 2-phenylpyridine the pyridine does not react until after the dimer has reacted with acetate, consistent with easy C-H activation of this substrate by $[MCl_2Cp^*]_2$ (M = Ir, Rh) and $[RuCl_2(p\text{-cymene})]_2$. In the case of 2-ethylpyridine, even though the reaction with acetate can occur first, there is no subsequent C-H activation. The decreased acidity of the proton to be activated in 2-ethylpyridine compared with 2-acetylpyridine may be a factor in the lower reactivity of 2-ethylpyridine. In addition, the need to include another sp^3 carbon in the metallacyclic ring may also make cyclometallation of 2-ethylpyridine less favourable. In the case of 2-acetylpyridine and $[RhCl_2Cp^*]_2$, reaction with acetate occurs first, leading to C-H activation product **(2.46b)**; however, for iridium and ruthenium the possibility of

forming an N,O chelate, **(2.47a,c)** provides an alternative reaction pathway that is competitive with the acetate assisted C-H activation.

2.3 Conclusion

From the study on the effect of the donor atom on monodentate ligands, the results confirmed that acetate assisted CH activation can occur for aromatic sp^2 C-H activation with Ir with all the N-donor directing groups attempted. Ir is better than Rh, Rh and Ru show similar behaviour depending on the ligand.[9] This scale of reactivity allowed us to assess the efficiency of the donor group according to the ability to cyclometallate with Ir, Rh or Ru. Thus, pyridine ~ pyrazole ~ alkylimine all cyclometallate with the three metal complexes ($[IrCl_2Cp^*]_2$, $[RhCl_2Cp^*]_2$ and $[RuCl_2(p\text{-cymene})]_2$) relatively quickly. Then come the oxazolines and aryl imine which cyclometallate with $[IrCl_2Cp^*]_2$ and either Rh or Ru depending on the substituents on the ligand and require longer reaction times (between 4 hours and few days), then imidazole where cyclometallation was only observed with $[IrCl_2Cp^*]_2$. This gives an overall order:

pyridine ~ pyrazole ~ alkylimine > oxazoline ~ aryl imine > imidazole.

Acetate assisted C-H activation has been extended to six-membered rings however this has only been observed with Ir. Acetate assisted C-H activation has been extended to different types of CH bonds (vinyl, sp^3). This study also investigated the effect of competing coordinating sites on the ligand and showed that the formation of chelates (N–C, N–N) or just N coordinated was favoured over the C-H activation pathways. In the case of competition with N–O chelate formation the C-H activation was the favoured pathway only in the case of $[RhCl_2Cp^*]_2$ with 2-acetylpyridine, and $[IrCl_2Cp^*]_2$ with 2-benzoylpyridine, showing dependence on the ligand-metal combination. The study of the coordination of 2-

acetylpyridine showed that acetate assisted C-H activation can be blocked by the formation of the N–O chelates however coordination of the ligand is not the only factor involved, 2-ethylpyridine did not coordinate with $[RhCl_2Cp^*]_2$ at room temperature and no C-H activation occurred in presence of NaOAc. For C-H activation to be the favoured pathway the coordination of the ligand has to be reversible, or NaOAc has to react before the ligand if coordination is irreversible. The order of these two steps was decisive to the product formed when multiple binding sites were present in the ligand. The influence of the carboxylate in the reaction and particularly the substituent on the carboxylate will be discussed in Chapter 3.

2.4 Experimental

The reactions described were carried out under nitrogen using dry solvents; however, once isolated as pure solids the compounds can be handled in air. ^{1}H, and ^{13}C-NMR spectra were obtained using Bruker 400 MHz spectrometers, with $CDCl_3$ as solvent unless otherwise stated. Chemical shifts were recorded in ppm (with tetramethylsilane as internal reference). FAB mass spectra were obtained on a Kratos concept mass spectrometer using NOBA as matrix. The electrospray (ES) mass spectra were recorded using a micromass Quattra LC mass spectrometer with DCM or acetonitrile as solvent. Microanalyses were performed by the Elemental Analysis Service (London Metropolitan University). All starting materials were obtained from Aldrich, with the exception of $[MCl_2Cp^*]_2$, (M = Rh, Ir)[52], and $[RuCl_2(p\text{-cymene})]_2$[53]. Ligands L4[53], L6[23], L7[23] were synthesised according to reported procedures, L8 was made by Dr G. J. Stasiuk[26] and L(9-12) were prepared by Dr G. A. Burley.

Preparation of [IrCl(L1-H)Cp*] **(2.10a)**

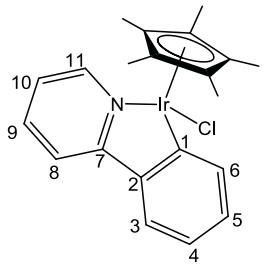

A mixture of $[IrCl_2Cp^*]_2$ (50 mg, 0.063 mmol), 2-phenylpyridine (L1) (24 mg, 0.15 mmol) and NaOAc (13 mg, 0.15 mmol), in DCM (5 ml) was stirred for 4 h at room temperature. The solution was filtered through celite and rotary evaporated to dryness. The product was crystallised from DCM/hexane to give (36 mg, 55%) as orange crystals. Anal Calc for $IrC_{21}H_{23}ClN$: C, 48.78, H, 4.48, N, 2.71. Found C, 48.69, H, 4.41, N, 2.73 %. ^{1}H NMR (300 MHz): δ 1.68 (s, 15H, C_5Me_5), 7.02 (td, 1H, *J* 7, 1, H^{10}), 7.07 (td, 1H, *J* 6, 1, H^{4}), 7.20 (td, 1H, *J* 7, 1, H^{5}), 7.65 (tm, 2H, *J* 8, H^{3} H^{9}), 7.82 (d, 2H, *J* 8, H^{8} H^{6}), 8.70 (d, 1H, *J* 5, H^{11}).^{13}C NMR: 8.91 (C_5Me_5), 88.51 (C_5Me_5), 118.87 (C^{8}), 122.04 (C^{4}), 122.24 (C^{10}), 123.83

(C^9), 131.00 (C^5), 135.8 (C^6), 136.93 (C^3), 144.07 (C^2), 151.32 (C^{11}), 163.33 (C^7), 167.36 (C^1). FAB-MS *m/z* 517 $[M]^+$, 482 $[M\text{-}Cl]^+$.

Preparation of [RhCl(L1-H)Cp*] **(2.10b)**

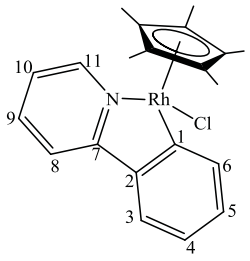

A mixture of $[RhCp^*Cl_2]_2$ (50 mg, 0.081 mmol), 2-phenylpyridine (L1) (31 mg, 0.20 mmol) and NaOAc (16 mg, 0.20 mmol), in DCM (5 ml) was stirred for 4 h at room temperature. The solution was filtered through celite and rotary evaporated to dryness and the product was crystallised from DCM /hexane to give (52 mg, 75 %) as orange crystals. Anal Calc for $RhC_{21}H_{23}ClN$: C, 58.96, H, 5.42, N, 3.27. Found C, 58.89, H, 5.33, N, 3.32 %. ^{1}H NMR (300 MHz): δ 1.68 (s, 15 H, $C_5\mathit{Me}_5$), 7.06 (td, 1 H, *J* 8, 1.2, H^{10}), 7.13 (td, 1 H,*J* 6, 1.6, H^4), 7.23 (td, 1H, *J* 7.5, 1.6, H^5), 7.60 (dd, 1H, *J* 7.5, 1.5, H^3), 7.70 (td, 1 H, *J* 7.5, 1.5, H^9),7.77 (d, 1 H, *J* 8, H^8), 7.81 (dd, 1 H, *J* 7.5, 1.5, H^6), 8.75 (d, 1 H, *J* 5.5, H^{11}). ^{13}C NMR: 9.17 ($C_5\mathit{Me}_5$), 96.97 (C_5Me_5, $J_{Rh\text{-}C}$ 24), 119.04 (C^8), 121.91 (C^4), 122.78 (C^{10}), 123.47 (C^3), 130.47 (C^5), 136.91 (C^9), 137.01 (C^6), 143.71 (C^2), 151.34 (C^{11}), 165.47 (C^7), 178.68 (C^1, $J_{Rh\text{-}C}$ *128*). FAB-MS: *m/z* 427 $[M]^+$, 392 $[M\text{-}Cl]^+$.

Preparation of [RuCl(L1-H)(*p*-cymene)] **(2.10c)**

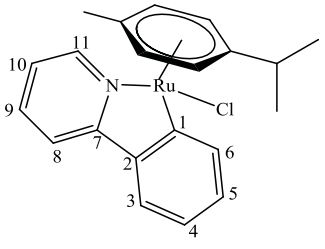

A mixture of $[RuCl_2(p\text{-cymene})]_2$ (50 mg, 0.081 mmol), 2-phenylpyridine (L1) (32 mg, 0.20 mmol) and NaOAc (17 mg, 0.20 mmol), in DCM (5 ml) was stirred for 4 h at room temperature. The solution was filtered through celite and rotary evaporated to dryness. The product was crystallised from DCM/hexane to give (42 mg, 61 %) as brown crystals. Anal Calc for $RuC_{21}H_{22}ClN$: C, 59.36, H, 5.22, N, 3.30. Found C, 59.19, H, 5.22, N, 3.25 %. ^{1}H NMR (300 MHz): δ 0.88 (d, 3 H, J 7, *Me'*Me*CH*), 0.97 (d, 3 H, *J* 7, Me'*Me*CH), 2.08 (s, 3 H, *Me*), 2.44 (sept, 1 H, *J* 7, C*H*MeMe'), 4.98 (d, 1 H, *J* 6, pcy), 5.17

(d, 1 H, *J* 6, pcy), 5.57 (t, 2 H, *J* 7, pcy), 7.02 (t, 1 H, *J* 7.5, H^4), 7.06 (t, 1 H, *J* 6, H^{10}), 7.19 (t, 1 H, *J* 7.5, H^5), 7.61 (d, 1 H, *J* 7.5, H^3), 7.69 (m, 2H, H^8 H^9), 8.15 (d, 1 H, *J* 7.5, H^6), 9.23 (d, 1 H, *J* 5, H^{11}). ^{13}C NMR: 18.75 (*Me*(pcy)), 21.72 (*Me*Me'CH), 22.51 (Me*Me'*CH(pcy)), 30.80 (MeMe'*C*H(pcy)), 82.18, 84.15, 89.64, 90.75 (4x*C*H,C_6H_4, Cy)), 100.52 (C (C_6H_4)), 100.68 (C (C_6H_4)), 118.78 (C^9), 121.35 (C^{10}), 122.51 (C^4), 123.48 (C^3), 129.47 (C^5), 136.58 (C^8), 139.59 (C^6), 143.32 (C^2), 154.32 (C^{11}), 165.41 (C^7), 181.40 (C^1). FAB-MS *m/z* 425 $[M]^+$, 390 $[M\text{-}Cl]^+$.

Preparation of $[IrCl(L2\text{-}H)Cp^*]_2$ **(2.12a)**

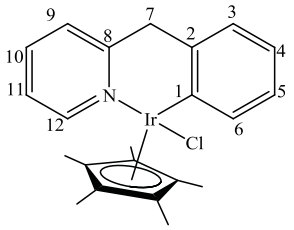

A mixture of $[IrCl_2Cp^*]_2$ (70 mg, 0.088 mmol), 2-benzylpyridine (L2) (37 mg, 0.22 mmol) and NaOAc (19 mg, 0.24 mmol) in DCM (5 ml) was stirred for 20 h, filtered through celite and evaporated to dryness. The product was crystallised from DCM/hexane to give (60.mg, 64%) as yellow crystals. Elemental analysis was not performed as Jones reported the synthesis of **(2.12a)** during the course of our study.[17] ^{1}H NMR: δ 1.56 (s, 15H, C_5Me_5), 3.76 (d, *J* 14.5, 1H, H^7), 3.88 (d, *J* 14.5, 1H, H7'), 6.81 (td, *J* 7, 1, 1H, H^4), 6.97 (t, *J* 7, 1H, H^5), 7.03 (t, *J* 7, 1 H, H^{11}), 7.07 (d,1 H, *J* 7.5, H^3), 7.31 (d, *J* 7.5, 1 H, H^9), 7.53 (td, 1 H, *J* 7.5, 1, H^{10}), 7.59 (d, 1 H, 7.5, H^6), 9.05 (d, 1H, *J* 5, H^{12}). ^{13}C NMR: 9.09 (C_5Me_5), 49.03 (C^7), 87.39 (C_5Me_5), 122.72 (C^4), 123.33 (C^9), 123.56 (C^3), 125.24 (C^{11}), 126.82 (C^5), 137.18 (C^2), 137.79 (C^6), 139.54 (C^{10}), 151.89 (C^8), 156.66 (C^{12}), 162.36 (C^1). ES-MS *m/z* 496 $[M\text{-}Cl]^+$ and 537 $[M\text{-}Cl+MeCN]^+$

Preparation of [IrCl(L3-H)Cp*] **(2.13a)**

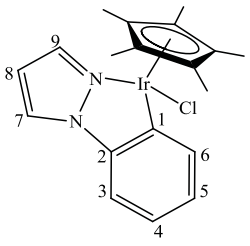

A mixture of $[IrCl_2Cp^*]_2$ (50 mg, 0.063 mmol), 2-phenylpyrazole (L3) (18 mg, 0.125 mmol) and NaOAc (13 mg, 0.15 mmol) in DCM (5 ml) was stirred for 4 h at room temperature. The solution was filtered through celite and rotary evaporated to dryness. The product was crystallised from chloroform /hexane to give (32 mg, 50 %) as yellow crystals. Anal Calc. for $IrC_{19}H_{22}ClN_2$: C, 45.09, H, 4.38, N, 5.54. Found C, 45.16, H, 4.44, N, 5.64 %. ^{1}H NMR (300MHz): δ 1.66 (s, 15 H, *Me*$_5$(Cp*)), 6.43 (t, 1 H, *J* 2.5, H^8), 6.93 (td, 1 H, *J* 7.5, 1, H^4), 7.02 (td, 1 H, *J* 7.5, 1, H^5), 7.18 (dd,1 H, *J* 7.5, 1, H^3), 7.60 (d,1H, *J* 2, H^9), 7.67 (dd,1H, *J* 7.5, 1, H^6), 7.81 (d, 1H, *J* 2.5, H^7). ^{13}C NMR: 7.98 (C$_5$*Me*$_5$), 87.06(*C*$_5$Me$_5$), 106.96 (C^8), 109.72 (C^3), 121.69 (C^4), 124.01 (C^7), 126.04 (C^5), 135.56 (C^6), 136.78 (C^9), 141.48 (C^2), 144.52(C^1). FAB-MS: *m/z* 471 [M-Cl]$^+$, 506 [M$^+$].

Preparation of [RhCl(L3-H)Cp*] **(2.13b)**

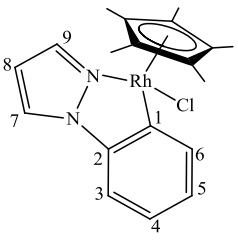

A mixture of $[RhCp^*Cl_2]_2$ (50 mg, 0.081 mmol), 2-phenylpyrazole (L3) (29 mg, 0.20 mmol) and NaOAc (16 mg, 0.20 mmol) in DCM (5 ml) was stirred for 4 hours at room temperature. The solution was filtered through celite and rotary evaporated to dryness. The product was crystallised from DCM /hexane to give (42 mg, 61 %), as orange crystals. Anal Calc for $RhC_{19}H_{22}ClN_2$: C, 54.76, H, 5.32, N, 6.72. Found C, 54.85, H, 5.27, N, 6.63.^{1}H NMR: δ 1.68 (s, 15 H, C$_5$*Me*$_5$), 6.50 (t, 1 H, H^8), 7.04 (td, 1 H, *J* 7.5, 2.5, H^4), 7.15 (m, 2 H, H^5 H^3), 7.76 (dd, 1 H, *J* 7.5, 1.5, H^6), 7.81 (d, 1 H, *J* 2, H^9), 7.95 (d, 1 H, *J* 2.5, H^7). ^{13}C NMR: 9.22 (C$_5$*Me*$_5$), 95.65 (*C*$_5$Me$_5$, $J_{Rh\text{-}C}$ 27), 107.99 (C^8), 111.00 (C^3), 123.28 (C^4), 124.99 (C^7), 126.92

(C^5), 137.40 (C^4), 138.87 (C^9), 141.75 (C^2), 159.17 (C^1, $J_{Rh\text{-}C}$ 129). FAB-MS *m/z* 416 $[M]^+$, 381 $[M\text{-}Cl]^+$.

Preparation of [RuCl(L3-H)(*p*-cymene)] **(2.13c)**

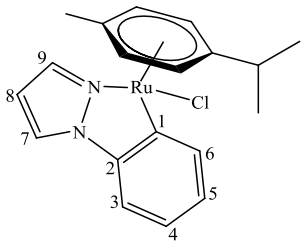

A mixture of $[RuCl_2(p\text{-cymene})]_2$ (50 mg, 0.081 mmol), 2-phenylpyrazole (L3) (29 mg, 0.20 mmol) and NaOAc (16 mg, 0.20 mmol), in DCM (5 ml) was stirred for 4 hours at room temperature. The solution was filtered through celite and rotary evaporated to dryness. The product was crystallised from DCM /hexane to give (42 mg, 64 %) as brown crystals. Anal Calc for $RuC_{19}H_{21}ClN_2$: C, 55.13, H, 5.11, N, 6.77. Found C, 55.14, H, 5.20, N, 6.70 %. ^{1}H NMR: δ 0.92 (d, 3H, *J* 7, CH*Me*Me'), 0.96 (d, 3H, *J* 7, CHMe*Me'*), 2.04 (s, 3 H, -*Me*), 2.44 (sept, 1H, *J* 7, C*H*MeMe'), 5.07 (d, 1H, *J* 7, pcy), 5.28 (d, 1H, *J* 7, pcy), 5.55 (d, 2 H, *J* 7, pcy), 6.48 (t, 1H, *J* 2.5, H^8), 7.03 (td, 1H, *J* 7.5, 1.5, H^4), 7.10 (td, 1H, *J* 7.5, 1.5, H^5), 7.17 (dd, 1H, *J* 7.5, 1.5, H^3), 7.90 (d, 1H, *J* 2.5, H^7), 8.05 (d, 1H, *J* 2, H^9), 8.13 (dd, 1H, *J* 7, 2, H^6). ^{13}C NMR: 17.74 (*C*HMeMe'), 20.89 (Me*Me'*), 21.34 (Me'*Me*), 29.63 (*Me*), 81.11, 83.01, 87.09, 87.54 (4xCH, C_6H_4, pcy)), 99.03 ($C(C_6H_4)$), 107.23 (C^8), 110.34 (C^3), 118,21 ($C(C_6H_4)$), 122.09 (C^4), 123.83 (C^7), 125.01 (C^5), 128.40 (C^2), 139.08 (C^6), 140.75 (C^1),141.09 (C^9). FAB-MS *m/z* 414 $[M]^+$, 379 $[M\text{-}Cl]^+$.

Preparation of [IrCl(L4-H)Cp*] **(2.15a)**

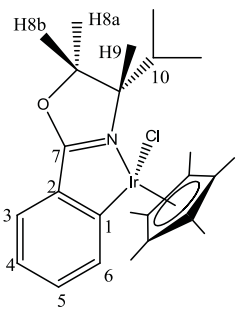

A mixture of $[IrCl_2Cp^*]_2$ (50 mg, 0.063 mmol), 4(S)-isopropyl-2-oxazolinylbenzene (L4) (25 mg, 0.13 mmol) and NaOAc (13 mg, 0.16 mmol) in DCM (10 ml) was stirred for 26 h. The mixture was filtered through celite and evaporated to dryness and washed with hexane. The product was crystallised from DCM/hexane to give yellow crystals (25 mg, 72%). Anal Calc for $IrC_{22}H_{29}ClNO{\bullet}CH_2Cl_2$: C, 43.43, H, 4.91, N, 2.21. Found C, 44.38,

H, 4.73, N, 2.28 %. ^{1}H NMR: δ 0.89 (d, 3 H, *J* 6.5, CHMe*Me*), 0.97 (d, 3 H, *J* 7.0, CH*Me*Me), 1.73 (s, 15 H, C_5Me_5), 2.31 (m, 1 H, H^{10}), 4.16 (m, 1 H, H^{9}), 4.63 (dd, 1 H, *J* 9`.5, 9.0, H^{8a}), 4.71 (dd, 1 H, *J* 8.9, 5.3, H^{8b}), 6.97 (t, 1 H, *J* 7.0, H^{4}), 7.20 (td, 1 H, *J* 7.5, 1, H^{5}), 7.36 (dd, 1 H, *J* 7.5, 1, H^{3}), 7.73 (d, 1 H, *J* 7.5, H^{6}). ^{13}C NMR δ 8.32 (C_5Me_5), 14.50 (CHMe*Me*), 18.80 (CH*Me*Me), 28.08 (C^{10}), 67.30 (C^{9}), 70.19 (C^{8}), 86.47 (C_5Me_5), 120.75 (C^{4}), 125.25 (C^{3}), 129.79 (C^{2}), 131.57 (C^{5}), 134.61 (C^{6}), 163.59 (C^{1}), 178.28 (C^{7}). FAB-MS *m/z* 551 $[M]^+$, 514 $[M-Cl]^+$

Attempted preparation of [RhCl(L4-H)Cp*] **(2.15b)**

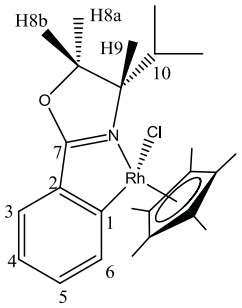

A mixture of $[RhCl_2Cp^*]_2$ (50 mg, 0.081 mmol), 4(S)-isopropyl-2-oxazolinylbenzene (L4) (34 mg, 0.18 mmol) and NaOAc (17 mg, 0.16 mmol) in MeOH (10 ml) was refluxed for 7 days. The mixture was filtered through celite, evaporated to dryness and washed with hexane to afford a brown solid (42 mg). Further attempts of purification by crystallisation failed, however **(2.15b)** could be seen to be present in the NMR spectrum. ^{1}H NMR: δ 0.88(d, 3 H, *J* 6.5, CH*Me*Me), 0.98 (d, 3 H, *J* 7.0, CHMe*Me*), 1.66 (s, 15 H, C_5Me_5), 2.24 (m, 1 H, H^{10}), 4.27 (m, 1 H, H^{9}), 4.60 (m, 2 H, H^{8a}, H^{8b}), 7.00 (td, 1 H, *J* 7.5, 1, H^{4}), 7.26 (td, 1 H, *J* 7.5, 1.5, H^{5}), 7.33 (dd, 1 H, *J* 7.5, 1.5, H^{3}), 7.74 (d, 1 H, *J* 7.5, H^{6}).Note additional broad signals for other Cp*Rh species were observed at 1.50 ^{13}C NMR: δ 9.38 (C_5Me_5), 15.40 (CH*Me*Me), 18.80 (CHMe*Me*), 29.94 (C^{10}), 67.59 (C^{9}), 70.83 (C^{8}), 94.92 (C_5Me_5, $J_{Rh\text{-}C}$ 6), 122.36 (C^{4}), 125.76 (C^{3}), 130.79 (C^{2}), 131.75 (C^{5}), 136.31 (C^{6})* (*spectrum too weak to see the signals for C^{1} and C^{7})

Preparation of [RuCl(L4-H)(*p*-cymene)] **(2.15c)**

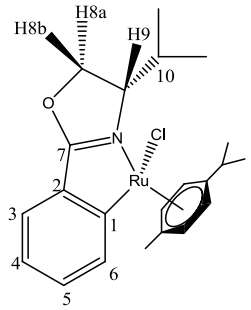

A mixture of $[RuCl_2(p\text{-cymene})]_2$ (200 mg, 0.327 mmol), 4(S)-isopropyl-2-oxazolinylbenzene (L4) (124 mg, 0.655 mmol) and NaOAc (13 mg, 0.16 mmol) in DCM (2 ml) was stirred overnight at room temperature. The mixture was filtered through celite and evaporated to dryness to give a brown/yellow oily residue. Crystallisation by slow diffusion of pentane into a dichloromethane solution gave yellow brown crystals (284 mg, 95%). Anal Calc for $RuC_{22}H_{28}ClNO$: C, 57.57, H, 6.15, N, 3.05. Found C, 57.00, H, 6.12, N, 3.02 %. ^{1}H NMR: δ 0.90 (d, 3H, *J* 7 Hz, CH*Me*Me'), 0.98 (d, 3H, *J* 6.5 Hz, CH*Me*Me'), 1.04 (d, 3H, *J* 3.5 Hz , CHMe*Me*'(pcy)), 1.07 (d, 3H, *J* 4 Hz, CHMe*Me*'(pcy)), 2.09 (s, 3H, *Me*(pcy)), 2.47 (m, 1H, (pcy)C*H*MeMe'), 2.55 (m, 1H, C*H*MeMe'), 4.19 (ddd, 1H, *J* 9, 7, 3 Hz, H^9), 4.59 (m, 2H, H^{8a}, H^{8b}), 4.82 (dd, 1H, *J* 6, 1 Hz, pcy), 4.98 (dd, 1H, *J* 6, 0.5 Hz, pcy), 5.55 (d, 2H, *J* 6 Hz, pcy), 6.97 (dt, 1H, *J* 7.5, 1.5 Hz, H^4), 7.21 (dt, 1H, *J* 7.5, 1 Hz, H^5), 7.32 (dd, 1H, *J* 7.5, 1.5 Hz, H^3), 8.08 (d, 1H, *J* 7.5 Hz, H^6). FAB-MS *m/z* 459 $[M]^+$, 423 $[M\text{-}HCl]^+$.(Note this experiment was carried out by Mr A.J. Davenport)

Preparation of [IrCl(L5-H)Cp*] **(2.16a)**

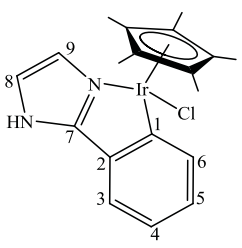

A mixture of $[IrCl_2Cp^*]_2$ (50 mg, 0.063 mmol), 2-phenylimidazole (L5) (20.3 mg, 0.14 mmol) and sodium acetate (13 mg, 0.15 mmol), in DCM (5 ml) was stirred for 4 h at room temperature. The solution was filtered through celite and rotary evaporated to dryness. The product was crystallised from chloroform /hexane to give (35 mg, 55 %) yellow crystals. Anal Calc for $IrC_{19}H_{22}ClN_2 \bullet CHCl_3$: 38.47, H 3.55, N 4.49. Found: C 38.77, H 3.52, N 4.47%. ^{1}H NMR: δ 1.70 (s, 15 H, C_5Me_5), 5.90 (br s,1 H, H^8), 6.75 (m, 2 H, H^4, H^9), 6.97 (d, 1 H, *J*

7.5, H^3), 7.02 (t, 1 H, *J* 7.5, H^5), 7.74 (d, *J* 7. 5, 1 H, H^6), 11.0 (br s, 1 H, N*H*). ^{13}C NMR: 9.13 (C_5Me_5), 117.61 (C_5Me_5), 117.61 (C^8), 122.03(C^3), 122.29 (C^4), 123.72 (C^9), 128.54 (C^5), 135.16 (C^2), 135.38 (C^6), 157.60 (C^7), 158.07 (C^1). FAB-MS: *m/z* 506 [M^+], 471 [M-Cl]$^+$.

Preparation of [RuCl(L6-H)(*p*-cymene)] **(2.9c)**

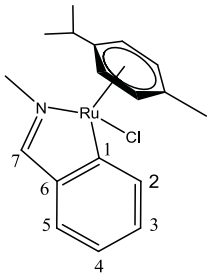

A mixture of [$RuCl_2$(*p*-cymene)]$_2$ (250 mg, 0.410 mmol), *N*-benzylidenemethylamine (L6) (95 mg, 0.897 mmol), NaOAc (84 mg, 0.16 mmol) and a drop of benzaldehyde in DCM (50 ml) was stirred for eight hours at room temperature. The mixture was filtered through celite washed with hexane and precipitated from $CHCl_3$/hexane to give a green powder (210 mg, 65%). Anal Calc for $RuC_{18}H_{22}ClN$•$CHCl_3$: C, 44.90, H, 4.56, N, 2.76. Found C, 44.83, H, 4.39, N, 2.76 %. ^{1}H NMR: δ 0.89 (d, 3 H, *J* 7, *Me'*Me*CH*), 1.07 (d, 3 H, *J* 7, Me'*Me*CH), 2.04 (s, 3 H, *Me*(pcy)), 2.51 (sept, 1 H, *J* 7, C*H*MeMe'), 3.99 (s, 3 H, N*Me*), 4.92 (d, 1 H, *J* 6, pcy), 5.12 (d, 1 H, *J* 6, pcy), 5.52 (d, 2 H, *J* 6, pcy),5.60 (d, 2 H, *J* 6, pcy), 6.95 (t, 1 H, *J* 7.5, H^4), 7.10 (td, 1 H, *J* 7.5, 1, H^5), 7.39 (d, 1 H, *J* 7, H^3), 7.97 (d, 1H, *J* 1, H^7), 8.14 (d, 1 H, *J* 7.5, H^6). ^{13}C NMR: 18.87 (*Me*(pcy)), 21.61 (*Me*Me'CH(pcy)), 22.81 (Me*Me'*CH(pcy)), 31.01 (MeMe'*C*H(pcy)), 53,24 (N*Me*), 81.17, 81.32, 90.02, 90.13 (4x*C*H,C_6H_4, pcy)), 100.86 (C (C_6H_4)), 100.79 (C (C_6H_4)), 122.16 (C^4), 128.31 (C^3), 129.24 (C^5), 139.07 (C^2), 145.49 (C^6), 172.45 (C^7), 188.51 (C^1). FAB-MS *m/z* 389 [M^+], 354 [M-Cl]$^+$.

Preparation of [IrCl(L7-H)Cp*] **(2.17a)**

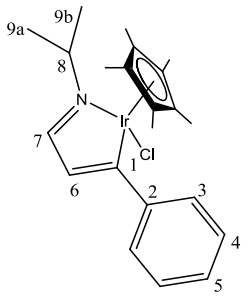

A mixture of $[IrCl_2Cp^*]_2$ (100 mg, 0.12 mmol), (Z)-N-(3-phenylallylidene)isopropylamine (L7) (48 mg, 0.27 mmol) and NaOAc (25 mg, 0.31 mmol), in MeOH (20 ml) was stirred for 20 h at room temperature. The solution was filtered through celite and rotary evaporated to dryness and washed with hexane to give a red powder (120 mg, 89 %). Anal Calc for $IrC_{22}H_{29}ClN$: C, 49.38, H, 5.46, N, 2.62. Found C, 49.28, H, 5.39, N, 2.57 %. ^{1}H NMR: δ 1.45 (d, *J* 7.0, 3 H, H^{9a}), 1.48 (s, 15 H, C_5Me_5), 1.485 (d, *J* 7.0, 3 H, H^{9b}), 4.23 (sep, *J* 7.0, 1H, H^8), 6.77 (d, *J* 2.0, 1H, H^6), 7.17 (t, *J* 7.5, 1 H, H^5), 7.27 (t, *J* 7.5, 2 H, $H^{4a,b}$), 7.42 (d, *J* 7.5, 2H, $H^{3a,b}$), 8.07 (br s, 1H, H^7). ^{13}C NMR: 8.87 (C_5Me_5), 24.00 (C^9), 24.54 ($C^{9'}$), 59.72 (C^8), 90.20 (C_5Me_5), 126.39 (C^3), 126.73 (C^5), 127.28 (C^4), 129.65 (C^6), 149.44 (C^2), 169.63 (C^7), 201.43 (C^1). FAB-MS *m/z* 500 $[M-Cl]^+$ and 535 $[M]^+$.

Preparation of [IrCl(L8-H)Cp*] **(2.20a)**

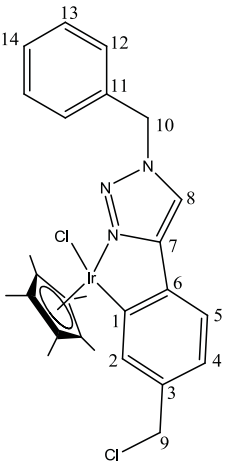

A mixture of $[IrCl_2Cp^*]_2$ (60 mg, 0.076 mmol), 1-benzyl-4-(4-(chloromethyl)phenyl)-1H-1,2,3-triazole (L8) (47 mg, 0.17 mmol) in DCM (5 ml) was stirred for 20 h. The mixture was filtered through celite and evaporated to dryness. The product was precipitated from DCM/hexane to produce a yellow powder (20 mg, 63%). Anal Calc. for $IrC_{26}H_{28}Cl_2N_3$: C, 48.37, H, 4.37, N, 6.51. Found C, 48.39, H, 4.41, N, 6.43 %. ^{1}H NMR: δ 1.76 (s, 15 H, C_5Me_5), 4.57 (d, 1 H, *J* 11.5, H^9), 4.70 (d, 1 H, *J* 11.5, $H^{9'}$), 5.36 (d, 1 H, *J* 11.5, H^{10}), 5.49 (d, 1 H, *J* 11.5, $H^{10'}$), 6.98 (d, 1H, *J* 7.5, H^{4or5}), 7.27 (m, 3 H, $H^{4or5, 12}$), 7.37 (m, 3 H, $H^{13, 14}$), 7.54 (s, 1 H, H^8), 7.76 (s, 1 H, H^2). ^{13}C NMR: 9.04 (C_5Me_5), 47.39 (C^9), 55.28 (C^{10}), 88.40 (C_5Me_5), 117.37 (C^8), 121.57,

122.75 (C^4, C^5), 128.19 (C^{12}), 129.08 (C^{13}), 129.25 (C^{14}), 136.40 (C^2), 133.82, 135.88, 137.35, 157.23, 159.89 (C^1, C^3, C^6, $C^{7,}$ C^{11}). FAB-MS *m/z* 610 $[M\text{-}Cl]^+$, ES-MS *m/z* 610 $[M\text{-}Cl]^+$, 651 $[M\text{-}Cl+MeCN]^+$.

Preparation of $[IrCl_2(L9)Cp^*]$ **(2.26a)**

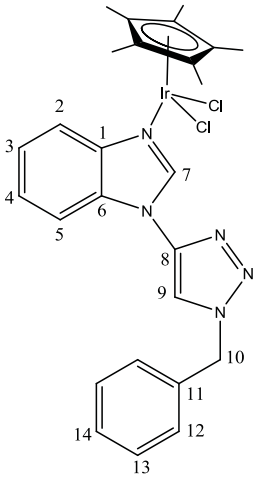

A mixture of $[IrCl_2Cp^*]_2$ (50 mg, 0.063 mmol), 1-(1-benzyl-1H-1,2,3-triazol-4-yl)-1H-benzimidazole (L9) (38 mg, 0.14 mmol) in DCM (5 ml) was stirred for 4 h. The mixture was filtered through celite and evaporated to dryness. The product was washed with hexane and precipitated from DCM/hexane to give a yellow powder (60.0 mg, 63%). The product was crystallised from DCM/hexane. Anal Calc. for $IrC_{26}H_{28}Cl_2N_5$: C, 46.36, H, 4.19, N, 10.40. Found C, 46.48, H, 4.06, N, 10.42 %. ^{1}H NMR: δ 1.66 (s, 15 H, C_5Me_5), 5.31 (s, 2 H, H^{10}), 7.32 (m, 7 H, $H^{3, 4, 12, 13, 14}$), 8.01 (s, 1 H, H^9), 8.02 (d, 1 H, *J* 7.5, H^5), 8.14 (d, 1 H, *J* 7.5, H^2), 9.39 (s, 1 H, H^7). ^{13}C NMR: 9.16 (C_5Me_5), 54.15 (C^{10}), 86.01 (C_5Me_5), 114.21 (C^9), 114.76 (C^5), 120.21 (C^2), 124.12 (C^4), 125.59 (C^3), 128.51 (C^{14}), 128.55 (C^{13}), 128.85 (C^{12}), 131.71 (C^{11}), 134.65 (C^6), 139.96 (C^1), 141.26 (C^8), 143.51 (C^7). FAB-MS 673 $[M]^+$, 638 $[M\text{-}Cl]^+$

Preparation of $[IrCl_2(L10)Cp^*]$ **(2.27a)**

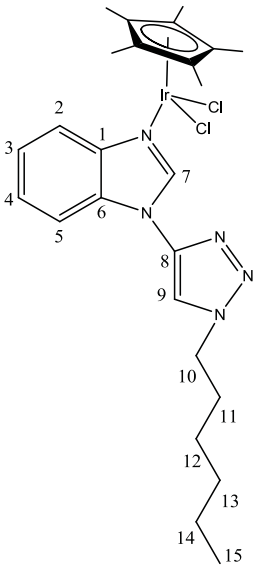

A mixture of $[IrCl_2Cp^*]_2$ (60 mg, 0.076 mmol), 1-(1-hexyl-1H-1,2,3-triazol-4-yl)-1H-benzimidazole (L10) (43 mg, 0.17 mmol) in DCM (5 ml) was stirred for 4 h. The mixture was filtered through celite and evaporated to dryness. The product was washed with hexane and precipitated from DCM/hexane to give a yellow powder (31.0 mg, 73%). Anal Calc. for $IrC_{25}H_{34}Cl_2N_5$: C, 44.97, H, 5.13, N, 10.49. Found C, 40.96, H, 5.05, N, 10.44 %. ^{1}H NMR: δ 0.85 (t, 3 H, *J* 7, H^{15}), 1.22 (m, 6 H,$H^{12, 13, 14}$),

1.66 (m, 17 H, C_5Me_5, H^{11}), 4.13 (t, 2 H, *J* 7.5, H^{10}), 7.36 (tt, 2 H, *J* 7.5, 8.0, $H^{3, 4}$), 7.97 (d, 1 H, *J* 8.0, H^5), 7.98 (s, 1 H, H^9), 8.10 (d, 1 H, *J* 7.5, H^2), 9.35 (s, 1 H, H^7). ^{13}C NMR: 8.16 (C_5Me_5), 12.97 (C^{15}), 21.38 (C^{14}), 24.96 (C^{13}), 29.21 (C^{11}), 30.14 (C^{12}), 49.95 (C^{10}), 84.94 (C_5Me_5), 112.94 (C^9), 114.00 (C^5), 119.26(C^2), 124.55 (C^3), 130.80 (C^6), 138.99 (C^1), 139.92 (C^8), 142.46 (C^7).

Praparation of [IrI(L11-H)Cp*]Cl **(2.37a)**

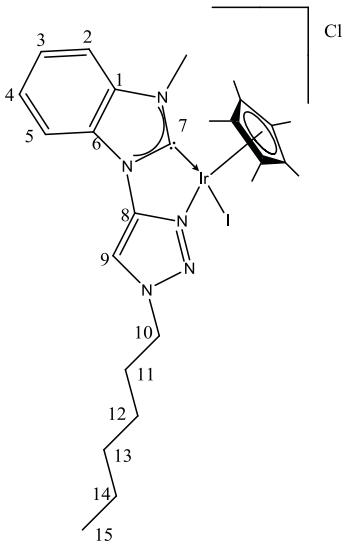

A mixture of $[IrCl_2Cp^*]_2$ (60 mg, 0.076 mmol), N-methyl-1-(1-hexyl-1H-1,2,3-triazol-4-yl)-1H-benzoimidazolium iodide (L11) (68 mg, 0.17 mmol) and NaOAc (15 mg, 0.19 mmol) in DCM (5ml) was stirred for 20 h. The mixture was filtered through celite and evaporated to dryness. The product was washed with hexane and precipitated from DCM/hexane to give a yellow powder (50 mg, 40%). Anal Calc. for $IrC_{26}H_{36}ClIN_5$: C, 40.39, H, 4.69, N, 9.06. Found C, 40.28, H, 4.60, N, 9.03 %. ^{1}H NMR: δ 0.87 (t, 3 H, *J* 7.0, H^{15}), 1.33 (m, 6 H, $H^{12, 13, 14}$), 2.03 (s, 15 H, C_5Me_5), 2.13 (m, 2H, H^{11}), 4.07 (s, 3H, Me), 4.77 (t, 2 H, *J* 7.0, H^{10}), 7.44 (t, 1 H, *J* 8.0, H^3), 7.50 (d, 1 H, *J* 8.0, H^2), 7.59 (t, 1 H, *J* 8.0, H^4), 8.70 (d, 1 H, *J* 8.0, H^5), 10.94 (s, 1 H, H^9). ^{13}C NMR: 10.30 (C_5Me_5), 13.99 (C^{15}), 22.51 (C^{14}), 26.02 (C^{13}), 29.97 (C^{11}), 31.07 (C^{12}), 35.54 (Me), 53.55 (C^{10}), 93.18 (C_5Me_5), 110.85 (C^2), 114.00 (C^5), 115.89(C^8), 125.10 (C^3), 126.76 (C^4), 129.27 (C^1), 144.91 (C^8), 173.00 (C^7). FAB-MS: *m/z* 738 $[M]^+$, 611 $[M-I]^+$, ES-MS: *m/z* 738 $[M]^+$

Preparation [IrCl(L12)Cp*]PF_6 **(2.42a)**

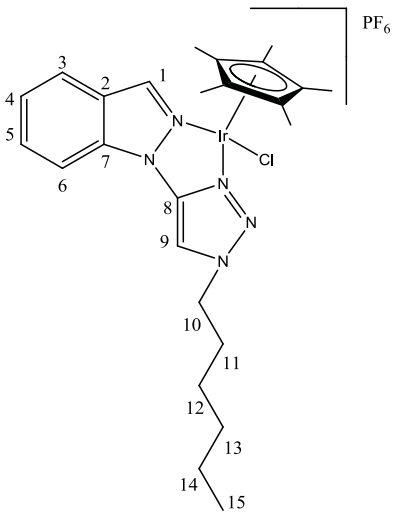

A mixture of [$IrCl_2Cp^*]_2$ (29 mg, 0.037 mmol), the ligand (L12) (22 mg, 0.083 mmol) and KPF_6 (27 mg, 0.15 mmol) in DCM (3 ml) was stirred for 20 h. The mixture was filtered through celite and evaporated to dryness. The product was washed with hexane and precipitated from DCM/hexane to give a yellow powder (38 mg, 65%). Anal Calc. for $IrC_{25}H_{34}Cl_2F_6N_5P$: C, 38.63, H, 4.41, N, 9.01. Found C, 38.72, H, 4.48, N, 8.93 %. ^{1}H NMR: δ 0.89 (m, 3H, H^{15}), 1.34 (m, 6 H,$H^{12, 13, 14}$), 1.83 (s, 15 H, C_5Me_5), 2.08 (m, 2 H,H^{11}),4.63 (t, 2 H, *J* 7.5, H^{10}), 7.37 (dd, 1 H, *J* 7.5, 8.0, H^4), 7.66 (dd, 1 H, *J* 7.5, 8.0, H^5), 7.86 (d, 1 H, *J* 8.0, H^6), 7.88 (d, 1 H, *J* 8.0, H^6), 8.46 (s, 1 H, H^1), 8.59 (s, 1 H, H^9). ^{13}C NMR: 9.02 (C_5Me_5), 13.94 (C^{15}), 22.42 (C^{14}), 26.00 (C^{13}), 29.66 (C^{11}), 30.99 (C^{12}), 53.72 (C^{10}), 89.51 (C_5Me_5), 110.63 (C^6), 111.19 (C^9), 122.34 (C^3), 124.81 (C^4), 124.91 (C^2), 132.30 (C^5), 136.62 (C^7), 138.68 (C^1), 142.64 (C^8). ES-MS: *m/z* 632 $[M]^+$; FAB-MS: *m/z* 632 $[M]^+$

Preparation [IrCl(L13-H)Cp*]PF_6 **(2.44a)**

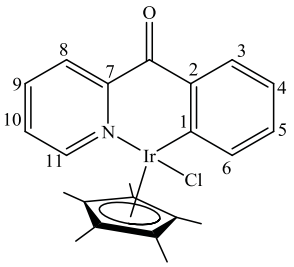

A mixture of [$IrCl_2Cp^*]_2$ (50 mg, 0.063 mmol), 2-benzoylpyridine (L13) (28 mg, 0.157 mmol) and NaOAc (12 mg, 0.157 mmol) in DCM (5 ml) was stirred for eight h, and evaporated to dryness. The product was crystallised from DCM /hexane to give (45 mg, 93%) as brown crystals. Anal Calc. for $IrC_{22}H_{23}ClNO$: C, 48.48, H, 4.25, N, 2.57. Found C, 48.38, H, 4.19, N, 2.51%. ^{1}H NMR: δ 1.37 (s, 15H, C_5Me_5), 7.00 (ddd, 1 H, *J* 8, 7, 1, H^4), 7.26 (ddd, 1 H, *J* 8, 7.5, 1.5, H^5), 7.39 (ddd, 1 H, *J* 8, 6, 1.5, H^{10}), 7.80 (ddd, 1 H, *J* 8, 1, 0.5 H^3), 7.84 (ddd, *J* 8, 1.5, 0.5, H^6), 7.87 (td, *J* 8, 1.5, H^9), 8.14 (ddd, *J* 8, 1.5, 1, H^8), 9.12 (ddd,

J 6, 1.5, 1, H^{11}). ^{13}C NMR: 8.26 (C_5Me_5), 89.12 (C_5Me_5), 123.33 (C^5), 124.97 (C^8), 127.78 (C^{10}), 127.96 (C^6), 132.48 (C^4), 137.23 (C^2), 137.96 (C^9), 140.36 (C^3), 155.87 (C^{11}), 156.37 (C^7), 156.51 (C^1), 192.04 (CO). FAB-MS: *m/z* 510 $[M\text{-}Cl]^+$, 545 $[M^+]$

Reaction of $[RhCl_2Cp^*]_2$ with L13 in the presence of NaOAc

A mixture of $[RhCl_2Cp^*]_2$ (50 mg, 0.081 mmol), 2-benzoylpyridine (L13) (37 mg, 0.202 mmol) and NaOAc (17 mg, 0.157 mmol) in DCM (5 ml) was stirred for six h. The mixture was evaporated to dryness and washed with hexane and diethylether. The ^1H NMR spectrum showed the presence of several species none of which could be completely identified. The significant features of the ^1H NMR and ES-MS spectra are described in the result and discussion section **(2.2.2)**.

Preparation of $[IrCl(L14)Cp^*]PF_6$ **(2.47a).**

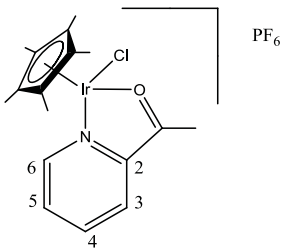

A mixture of KPF_6 (92 mg, 0.50 mmol), $[IrCl_2Cp^*]_2$ (100 mg, 0.13 mmol), and 2-acetylpyridine (L14) (30 mg, 0.25 mmol) in CH_2Cl_2 (10 ml) was stirred for 4 h. The solution was filtered through celite and rotary evaporated to dryness. The product was crystallised from chloroform to give (**2.47a)** (117 mg, 74%) as orange crystals. Anal. Calc for $IrC_{17}H_{22}ClF_6NOP$: C, 32.46, H, 3.53, N, 2.23. Found: C, 32.47, H, 3.43, N, 2.35 %. ^1H NMR (CD_2Cl_2, 400 MHz): δ 1.79 (s, 15H, C_5Me_5), 4.00 (s, 3H, CO*Me*), 8.05 (ddd, 1H, *J* 8.0, 5.5, 1.5, H^5), 8.34 (td, 1H, *J* 8.0, 1.5, H^4), 8.50 (ddd, 1H, *J* 8.0, 2.0, 1.5, H^3), 8.91 (ddd, 1H, *J* 5.5, 1.5, 1.0, H^6). ^{13}C NMR: δ 8.75 (C_5Me_5), 26.04 (CO*Me*), 88.80 (C_5Me_5), 131.43 (C^3), 133.17 (C^5), 140.90 (C^4), 151.27 (C^6), 152.19 (C^2), 210.78 (CO). ES-MS: *m/z* 484 $[M]^+$.

Preparation of [RuCl(L14)(mes)]PF_6 **(2.47d).**

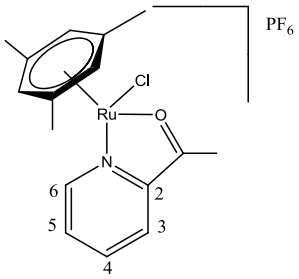

A mixture of KPF_6 (63.2 mg, 0.34 mmol), $[RuCl_2(Mes)]_2$ (50 mg, 0.08 mmol), and 2-acetylpyridine (L14) (20.8 mg, 0.17 mmol) in DCM (5 ml) was stirred for 20 h. The solution was filtered through celite and rotary evaporated to dryness. The product was crystallised from chloroform to give **(2.47d)** (78 mg, 87%) as brown crystals. Anal. Calc for $RuC_{16}H_{19}ClF_6NOP$: C, 36.76, H, 3.66, N, 2.68. Found: C, 36.86, H, 3.51, N, 2.66 %. ^{1}H NMR (CD_2Cl_2): δ 2.33 (s, 9H, $C_6H_3\mathit{Me_3}$), 3.01 (s, 3H, COMe), 5.37 (s, 3H, $C_6\mathit{H_3}Me_3$), 7.94 (ddd, 1H, *J* 7.5, 5.5, 2, H^5), 8.26 (ddd, 1H, *J* 8, 7.5, 1, H^4), 8.30 (d, 1H, *J* 8, H^3), 9.21 (d, 1H, *J* 5.5, H^6). 13C NMR: δ 18.7 ($C_6H_3\mathit{Me_3}$), 25.8 (COMe), 77.0 [C*H*($C_6H_3Me_3$)], 105.9 [CMe($C_6H_3Me_3$)], 130.1 (C^4), 131.7 (C^5), 140.2 (C^3), 151.7 (C^2), 154.1 (C^6), 211.0 (CO). FAB-MS: *m/z* 378 $[M]^+$.

Reaction of **(2.48d)** with NaOMe to give **(2.49d)**

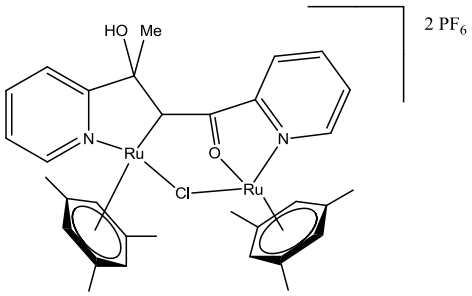

NaOMe (4.1 mg, 0.076 mmol) was added to a solution of complex **(2.48d)** (40 mg, 0.076 mmol) in DCM (5 ml), and the mixture was stirred for 6 days at room temperature. Another equivalent of MeONa (4.14 mg, 0.076 mmol) was added, and the reaction was stirred for a further day. The mixture was filtered through celite and rotary evaporated to dryness. Attempted crystallisation from DCM/hexane gave a black precipitate (25 mg) and a few crystals suitable for X-ray analysis. The ^{1}H NMR spectrum of the crystals was slightly impure, but the peaks for **(2.49d)** could be assigned as follows. ^{1}H NMR (CD_2Cl_2): δ 1.96 (s, 3H, *Me*C(OH)), 1.98 (s, 9H, $C_6H_3\mathit{Me_3}$), 2.01 (s, 9H, $C_6H_3\mathit{Me_3}$), 3.19 (s, 1 H, OH), 5.05 (s, 3H, $C_6\mathit{H_3}Me_3$), 5.10 (s, 3H, $C_6\mathit{H_3}Me_3$), 6.54 (s, 1 H, C*H*C(OH)), 7.47 (d, 1 H, *J* 7.5, Hpyr),

7.62 (dd, 1 H, *J* 6.0 Hpyr), 7.68 (dd, 1 H, *J* 5.5, Hpyr), 8.00 (t, 1 H, *J* 7.5, Hpyr), 8.05 (d, 1 H, *J* 7.5, Hpyr), 8.11 (t, 1H, *J* 7.5, Hpyr), 8.66 (d, 1 H, *J* 5.5, Hpyr), 9.01 (d, 1 H, *J* 5.5, Hpyr). FAB-MS: *m/z* 719 [M - H]+.

Preparation of [IrCl(L14-H)Cp*] **(2.46a)**

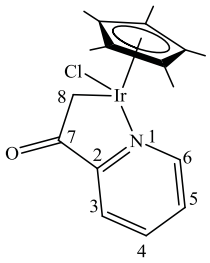

2-acetylpyridine (L14) (21.3 mg, 0.176 mmol) was added to a solution of LiHMDS (0.18 ml, 0.194 mmol) in THF (5ml) at -78˚C. After being stirred for one hour at the same temperature, $[IrCl_2Cp^*]_2$ (70 mg, 0.088 mmol) was added to the mixture. The mixture was allowed to warm up and stirred for four hours. The solution was filtered through celite and evaporated to dryness. The product was isolated as an orange precipitate (58 mg, 68%). Anal Calc. for $IrC_{17}H_{21}ClNO$: C, 42.27, H, 4.38, N, 2.90. Found C, 42.23, H, 4.28, N, 2.81 %. ^{1}H NMR (CD_2Cl_2, 300 MHz): δ 1.53 (s, 15H, C_5Me_5), 2.96 (d, 1H, *J* 9.5, H^8), 3.40 (d, 1H, *J* 9.5, H^8), 7.36 (ddd, 1H, *J* 8.0, 5.5, 1.5, H^5), 7.54 (ddd, 1H, *J* 8.0, 1.5,1.0, H^3), 7.86 (td, 1H, *J* 8.0, 1.5, H^4), 8.51 (ddd, 1H, *J* 5.5, 1.5, 1.0, H^6). ^{13}C NMR: δ 7.51 (C_5Me_5), 35.24 (C^8), 85.56 (C_5Me_5), 120.47 (C^3), 126.79 (C^5), 137.47 (C^4), 150.83 (C^6), 156.54 (C^2), 200.65 (C^7). FAB-MS: *m/z* 483 $[M]^+$, 448 $[M\text{-}Cl]^+$.

Preparation of [RuCl(L14-H)(*p*-cymene)] **(2.46c)**

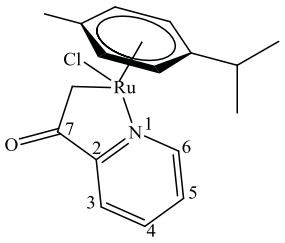

2-acetylpyridine (L14) (28 mg, 0.228 mmol) was added to a solution of LiHMDS (0.24 ml, 0.236 mmol) in THF (5 ml) at -78˚C. After being stirred for one hour at the same temperature, $[RuCl_2(p\text{-cymene})]_2$ (70 mg, 0.114 mmol) was added to the mixture. The mixture was allowed to warm up and stirred for four h, the solution was filtered through celite and evaporated to dryness (70 mg). The ^{1}H NMR spectrum showed a mixture but the signals for **(2.46c)** could be identified as follows. ^{1}H NMR ($CDCl_3$, 400 MHz): δ δ 1.04 (d,

3H, J 7.0, CHMe*Me'*), 1.13 (d, 3H, *J* 7.0, CH*Me*Me'), 1.77 (s, 3H, Me), 2.57 (sept, 1H, *J* 7.0, C*H*MeMe'), 3.08 (d, 1H, *J* 8.0, CH_2), 3.72 (d, 1H, *J* 8.0, CH_2), 4.97 (d, 1H, *J* 5.0, Cy), 5.02 (d, 1H, *J* 5.5, Cy), 5.25 (d, 1H, *J* 5.0, Cy), 5.31 (d, 1H, *J* 5.5, Cy), 7.35 (ddd, 1H, *J* 7.0, 5.5, 1.5, H^5), 7.47 (d, 1H, *J* 7.0, H^3), 7.74 (td, 1H, *J* 7.0, 1.0, H^4), 8.91 (d, 1H, *J* 5.5, H^6).ES-MS: *m/z* 394 $[M]^+$, 355 $[M\text{-}Cl]^+$, 314 $[M\text{-}CH_2CO]$.

Examination of the Coordination of Substituted Pyridines by ^{1}H NMR Spectroscopy:

A mixture of $[MCl_2Cp^*]_2$ (M = Ir, Rh) or $[RuCl_2(p\text{-cymene})]_2$ (15 to 20 mg) and an equimolar amount of the appropriate ligand (2-acetylpyridine, 2-ethylpyridine, or 2-phenylpyridine) was dissolved in CD_2Cl_2 (or $CDCl_3$). The ^{1}H NMR spectra were recorded using a Bruker DRX (400 MHz) at different temperatures. The description of the spectra is detailed in Section 2.B.2.

2.5 Bibliography

1 H. C. L. Abbenhuis, M. Pfeffer, J.-P. Sutter, A. de Cian, J. Fischer, H. L. Ji, and J. H. Nelson, *Organometallics*, 1993, **12**, 4464.

2 M. Pfeffer, J.-P. Sutter, and E. P. Urriolabeitia, *Inorg. Chim. Acta*, 1996, **249**, 63.

3 A. J. Davenport, D. L. Davies, J. Fawcett, and D. R. Russell, *J. Chem. Soc., Dalton Trans.*, 2002, 3260.

4 J.-P. Djukic, A. Berger, M. Duquenne, M. Pfeffer, A. de Cian, N. Kyritsakas-Gruber, J. Vachon, and J. Lacour, *Organometallics*, 2004, **23**, 5757.

5 Q.-F. Zhang, K.-M. Cheung, I. Williams, D, and W.-H. Leung, *Eur. J. Inorg. Chem.*, 2005, **2005**, 4780.

6 J. Vicente and J. A. Abad, *J. Chem. Soc. Dalton Trans.*, 1990, 1459.

7 S. Fernandez, M. Pfeffer, V. Ritleng, and C. Sirlin, *Organometallics*, 1999, **18**, 2390.

8 J. B. Sortais, N. Pannetier, A. Holuigue, L. Barloy, C. Sirlin, M. Pfeffer, and N. Kyritsakas, *Organometallics*, 2007, **26**, 1856.

9 D. L. Davies, O. Al-Duaij, J. Fawcett, M. Giardiello, S. T. Hilton, and D. R. Russell, *Dalton Trans.*, 2003, 4132.

10 C. Scheeren, F. Maasarani, A. Hijazi, J.-P. Djukic, M. Pfeffer, S. D. Zaric, X.-F. Le Goff, and L. Ricard, *Organometallics*, 2007, **26**, 3336.

11 G. C. Martin and J. M. Boncella, *Organometallics*, 1989, **8**, 2968.

12 J. Perez, V. Riera, A. Rodriguez, and D. Miguel, *Organometallics*, 2002, **21**, 5437.

13 B. J. Wik, C. Romming, and M. Tilset, *J. Mol. Catal. A Chem.*, 2002, **189**, 23.

14 W. Bauer, M. Prem, K. Polborn, K. Sunkel, W. Steglich, and W. Beck, *Eur. J. Inorg. Chem.*, 1998, 485.

15 S. Arita, T. Koike, Y. Kayaki, and T. Ikariya, *Organometallics*, 2008, **27**, 2795.

16 K. Ishiwata, S. Kuwata, and T. Ikariya, *Organometallics*, 2006, **25**, 5847.

17 L. Li, W. W. Brennessel, and W. D. Jones, *J. Am. Chem. Soc.*, 2008, **130**, 12414.

18 D. L. Davies, S. M. A. Donald, O. Al-Duaij, J. Fawcett, C. Little, and S. A. Macgregor, *Organometallics*, 2006, **25**, 5976.

19 L. Carter, D. L. Davies, J. Fawcett, and D. R. Russell, *Polyhedron*, 1993, **12**, 1123.

20 K. Stanley and M. C. Baird, *J. Am. Chem. Soc.*, 1975, **97**, 6598.

21 B. Çetinkaya, B. Alici, I. Özdemir, C. Bruneau, and P. H. Dixneuf, *J. Organomet. Chem.*, 1999, **575**, 187.

22 C. A. Vock, C. Scolaro, A. D. Phillips, R. Scopelliti, G. Sava, and P. J. Dyson, *J. Med. Chem.*, 2006, **49**, 5552.

23 P. Mangeney, T. Tejero, A. Alexakis, F. Grosjean, and J. Normant, *Synthesis*, 1988, 255.

24 C. K. Hartmuth, M. G. Finn, and K. B. Sharpless, *Angew. Chem., Int. Ed.*, 2001, **40**, 2004.

25 J. E. Moses and A. D. Moorhouse, *Chem. Soc. Rev.*, 2007, **36**, 1249.

26 G. J. Stasiuk and M. P. Lowe, *Dalton Trans.*, 2009, 9725.

27 M. Jauregui, W. S. Perry, C. Allain, L. R. Vidler, M. C. Willis, A. M. Kenwright, J. S. Snaith, G. J. Stasiuk, M. P. Lowe, and S. Faulkner, *Dalton Trans.*, 2009, 6283.

28 M. Obata, A. Kitamura, A. Mori, C. Kameyama, J. A. Czaplewska, R. Tanaka, I. Kinoshita, T. Kusumoto, H. Hashimoto, M. Harada, Y. Mikata, T. Funabiki, and S. Yano, *Dalton Trans.*, 2008, 3292.

29 T. L. Mindt, H. Struthers, L. Brans, T. Anguelov, C. Schweinsberg, V. Maes, D. Tourwac, and R. Schibli, *J. Am. Chem. Soc.*, 2006, **128**, 15096.

30 B. Beyer, C. Ulbricht, D. Escudero, C. Friebe, A. Winter, L. Gonzalez, and U. S. Schubert, *Organometallics*, 2009, **28**, 5478.

[31] P. J. H. In:, E.W. Abel, F. G. A. Stone, and G Wilkinson, *Editors, Comprehensive Organometallic Chemistry: A Review of the Literature 1982–1994 ,Vol 12, Pergamon Press, Oxford (1995) Chap. 8.2.*
[32] G. A. Burley, D. L. Davies, G. A. Griffith, M. Lee, and K. Singh, *J. Org. Chem.*, 2010, **75**, 980.
[33] A. K. Singh, P. Kumar, M. Yadav, and D. S. Pandey, *J. Organomet. Chem.*, 2010, **695**, 567.
[34] J. Vicente, I. Saura-Llamas, J. Cuadrado, and M. C. Ramirez de Arellano, *Organometallics*, 2003, **22**, 5513.
[35] Y.-F. Han, W.-G. Jia, W.-B. Yu, and G.-X. Jin, *Chem. Soc. Rev.*, 2009, **38**, 3419.
[36] I. Omae, *Chem. Rev.*, 1979, **79**, 287.
[37] M. Saporita, G. Bottari, G. Brancatelli, D. Drommi, G. Bruno, and F. Faraone, *Eur. J. Inorg. Chem.*, 2007, **2008**, 59.
[38] C. Ganter, *Chem. Soc. Rev.*, 2003, **32**, 130.
[39] D. Koch, K. Polborn, K. Sünkel, and W. Beck, *Inorg. Chim. Acta*, 2002, **334**, 365.
[40] D. Zuccaccia, G. Bellachioma, G. Cardaci, C. Zuccaccia, and A. Macchioni, *Dalton Trans.*, 2006, 1963.
[41] K. T. Prasad, B. Therrien, and K. M. Rao, *J. Organomet. Chem.*, 2008, **693**, 3049.
[42] D. Bourissou, O. Guerret, F. P. Gabbai, and G. Bertrand, *Chem. Rev.*, 1999, **100**, 39.
[43] C. M. Crudden and D. P. Allen, *Coord. Chem. Rev.*, 2004, **248**, 2247.
[44] R. Corberan, M. Sanau, and E. Peris, *J. Am. Chem. Soc.*, 2006, **128**, 3974.
[45] F. Hanasaka, Y. Tanabe, K.-i. Fujita, and R. Yamaguchi, *Organometallics*, 2006, **25**, 826.
[46] R. Corberan, M. Sanau, and E. Peris, *Organometallics*, 2006, **25**, 4002.
[47] D. L. Davies and R. C. Jones, *unpublished results*, 2009.
[48] M. Bernechea, J. R. Berenguer, E. Lalinde, and J. Torroba, *Organometallics*, 2008, **28**, 312.
[49] L. P. Barthel-Rosa, V. J. Catalano, K. Maitra, and J. H. Nelson, *Organometallics*, 1996, **15**, 3924.
[50] O. V. Gusev, S. Sergeev, I. M. Saez, and P. M. Maitlis, *Organometallics*, 1994, **13**, 2059.
[51] D. R. Robertson, T. A. Stephenson, and T. Arthur, *J. Organomet. Chem.*, 1978, **162**, 121.
[52] C. White, A. Yates, and P. M. Maitlis, *Inorg. Synth.*, 1992, **29**, 228.
[53] M. A. Bennett and A. K. Smith, *J. Chem. Soc., Dalton Trans.*, 1974, 233.

Chapter Three

Mechanistic study: Effect of carboxylate in the C-H activation

3 Chapter 3

3.1 Introduction

Chapter 3 will focus on the mechanism of acetate-assisted C-H activation in half sandwich complexes $[MCl_2Cp^*]_2$ (M = Ir, Rh), $[RuCl_2(p\text{-cymene})]_2$ and in particular the role of the carboxylate. A brief introduction to half sandwich carboxylate chemistry is provided below.

Maitlis *et al.* reported that excess silver acetate reacts with $[MCl_2(PMe_3)Cp^*]$ (M = Rh, Ir) to produce bis acetato complexes **(3.1)(Scheme 3.1)**. In the presence of KPF_6 in water these lose acetate to form **(3.2)**.[1]

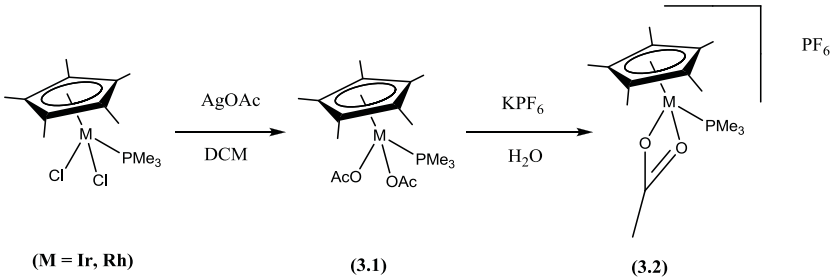

(M = Ir, Rh) **(3.1)** **(3.2)**

Scheme 3.1

Further studies by Maitlis *et al.* showed that silver benzoate reacts with $[RhCl_2(DMSO)Cp^*]$ **(3.3)** with loss of DMSO to give **(3.4)** which is sensitive to H_2O **(Scheme 3.2)** for which a crystal structure was obtained. The reaction of the iridium analogue of **(3.3)** only produced the cyclometallation of the benzoate **(3.5)(Scheme 3.2)**.[2]

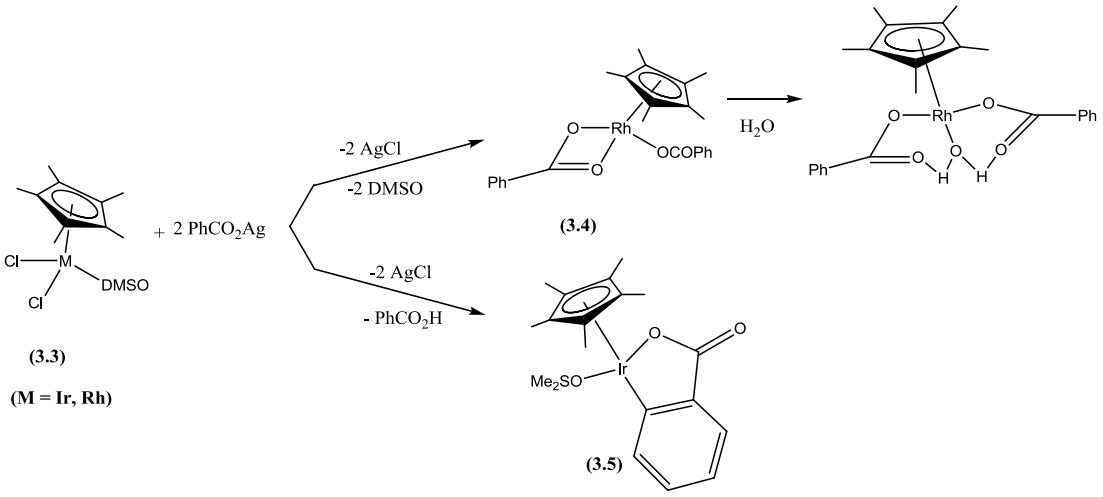

Scheme 3.2

Merola *et al.* described the reaction of silver acetate with $[RhCl_2Cp^*]_2$ to form **(3.6)** which easily transforms to **(3.7)** in the presence of water **(Scheme 3.3)**. They also reported the crystal structures of **(3.6)** and **(3.7).**[3]

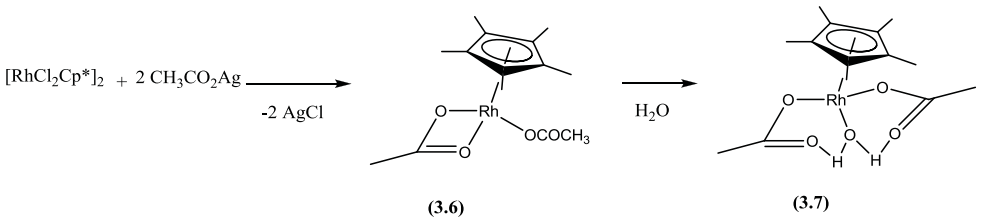

Scheme 3.3

As mentioned in Chapter 1 $[Pd(OAc)_2]$ is a very good starting material for cyclometallation and acetate was suggested to play a role in the C-H cleavage step. In Chapter 2 the scope of acetate assisted C-H activation with half-sandwich complexes $[MCl_2Cp^*]_2$ (M = Rh, Ir) and $[RuCl_2(p\text{-cymene})]_2$ was described. In 2003 Davies *et al.* proposed a mechanism for these reactions **(Scheme 3.4)**.[4]

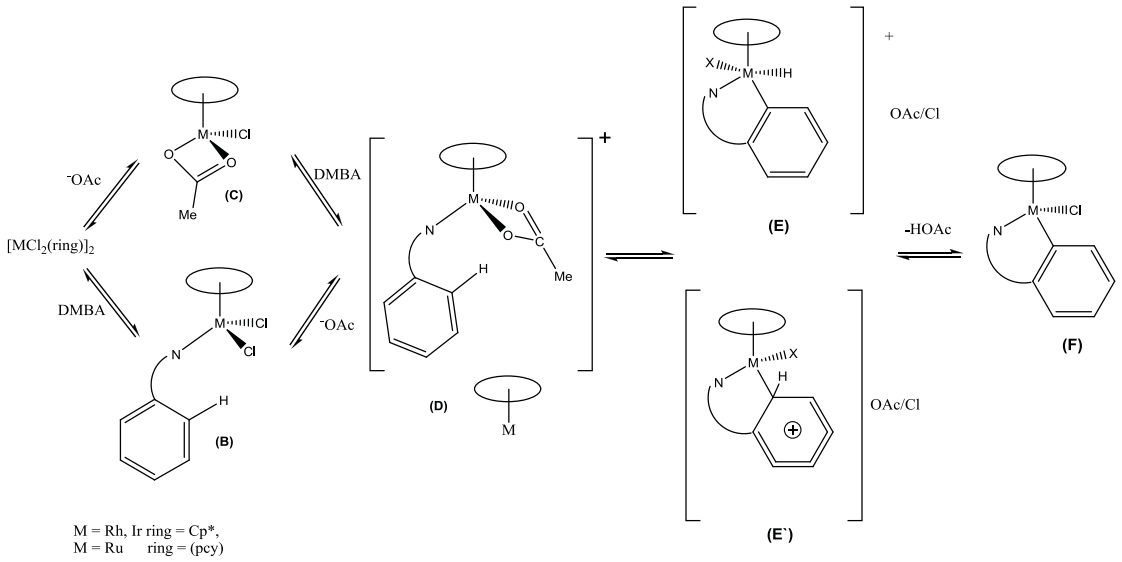

Scheme 3.4 Proposed mechanism for the acetate assisted C-H activation

The C-H activation step was assumed to start from a key intermediate **(D)**. The formation of **(D)** can be envisaged by two different routes, (i) the dimer could react with acetate to form **(C)** and then coordination of the ligand would occur, (ii) the reaction of the dimer with the ligand occurs first and then acetate would coordinate. Isolation of the intermediate **(B)** failed whereas an intermediate of type **(C)** [RuCl(OAc)(*p*-cymene)] was isolated for ruthenium. No reaction was observed between the ligands and the dimers whereas all the dimers reacted with acetate. Hence, all the experimental data agreed with the reaction going *via* **(C)**. The authors concluded that acetate played a number of different roles, (i) opening the dimer and (ii) as a intramolecular base (as originally proposed by Ryabov for cyclopalladation[5]). They also noted that intramolecular hydrogen bonding between monodentate acetate and a coordinated ligand is certainly feasible, as shown in the X-ray structure of **(2.7)**.[3] Conversion of a monodendate acetate to a bidentate one creates a vacant site in **(D)**. Two possible mechanisms were then considered for the C-H activation step. An oxidative addition of the metal into the aryl C-H bond to give a M(V) (M = Ir, Rh) or Ru(IV) **(E)** followed by

the loss of HX to form **(F)**, or an electrophilic activation which would go *via* a Wheland intermediate **(E`)** followed by a loss of a proton.

The authors suggested that the failure of DMBA which is a good donor but not a π-acceptor to cyclometallate with $[RhCl_2Cp^*]_2$ and $[RuCl_2(p\text{-cymene})]_2$ was consistent with an electrophilic mechanism. However, cyclometallation of DMBA with $[RuCl_2(C_6H_6)]_2$ starting from a more electrophilic cationic precursor $[RuCl(NCMe)_2(C_6H_6)]PF_6$ and using a stronger base such as NaOH has been described.[6] Hence, coordination of the ligand before reaction with a base is also possible with stronger bases than acetate and higher temperatures. More recently Pfeffer *et al*. isolated **(3.8)**, which is an analog of **(B)** in **Scheme 3.4**, and they showed that cyclometallation could occur from **(3.8)** in the presence of NaOH to produce **(3.9)** **(Scheme 3.5)**.[7]

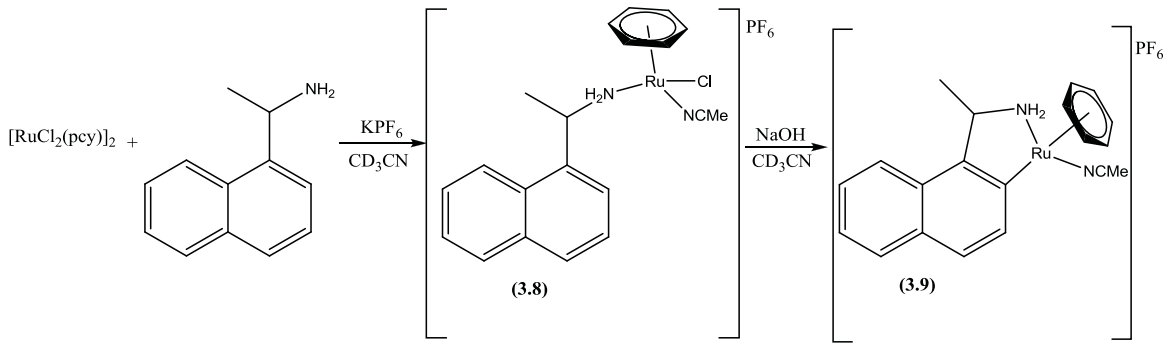

Scheme 3.5

Further investigations of the mechanism of acetate assisted C-H activation were carried out by Davies and Macgregor who reported computational studies of cyclometallation of DMBA with $Pd(OAc)_2$, (see chapter 1 section 1.3.4.1). The same group subsequently reported a computational study of the mechanism of acetate assisted cyclometallation of DMBA with $[IrCl_2Cp^*]_2$ **(Scheme 3.6)**.[8] This focussed on the C-H activation step i.e. starting from intermediate **(D)** in **Scheme 3.4**.

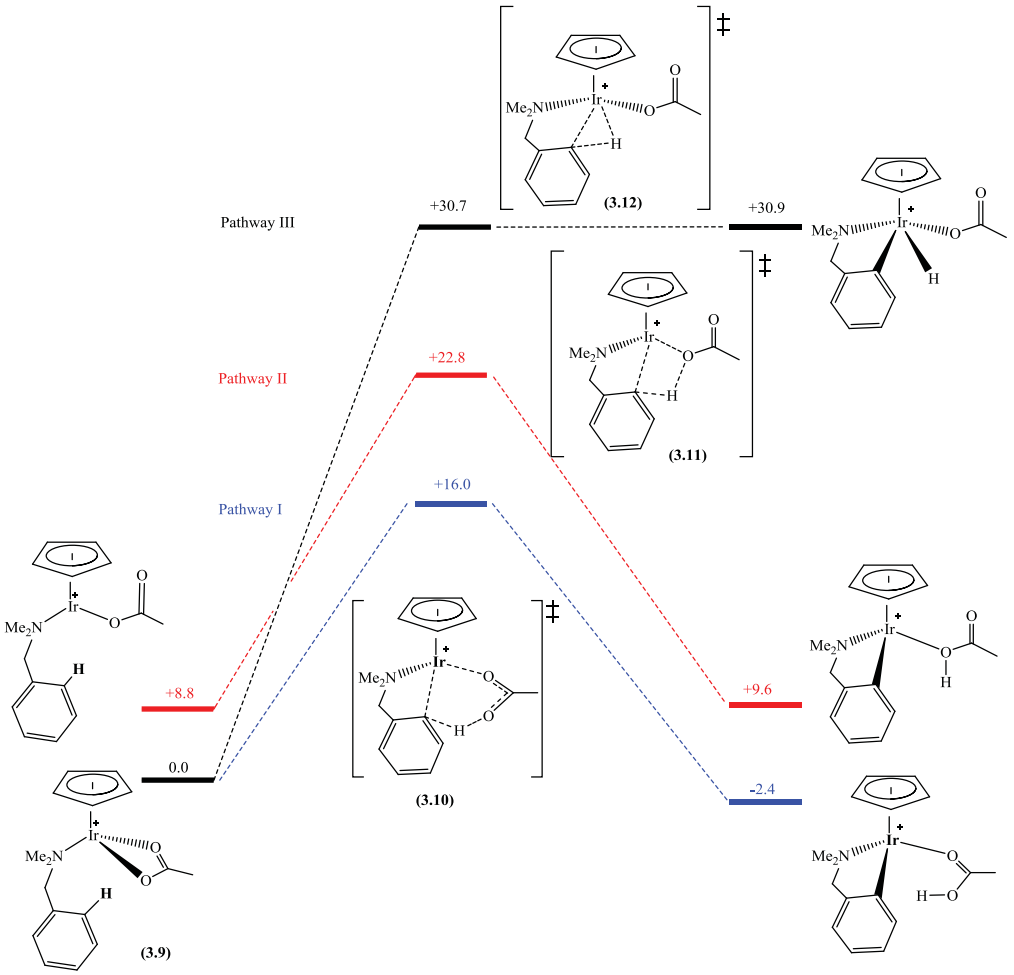

Scheme 3.6 Computed reaction profile (kcal mol^{-1}) for C−H activation via OA, SBM and EA

Three possible mechanisms i.e. (i) pathway I an ambiphilic type of mechanism {AMLA(6)}, (ii) pathway II a SBM {AMLA(4)} and (iii) OA (pathway III) were considered **(Scheme 3.6)**. The oxidative addition pathway going *via* **(3.12)** had the highest activation energy barrier as might be expected for formation of a cationic iridium (V) species, though a similar species had been proposed by Bergman *et al.* [9] for C-H activation by [IrMe(OTf)(PMe_3)Cp*] and was supported by theoretical studies as described in chapter 1 section 1.3.1.[10] Pathway I, AMLA(6) C-H activation, proceeded via a single, low energy transition state **(3.10)** corresponding to displacement of the proximal OAc arm by the incoming C-H bond. The actual C-H activation then occurred

with no significant activation energy barrier. Pathway II, AMLA(4), was initiated by dissociation of the distal OAc arm to give a 16 e^- complex. In this case C-H activation occurred *via* a four-membered transition state **(3.11)** with H transfer to the Ir-bound oxygen. The four-membered transition state (AMLA(4)) had a higher activation barrier than the six-membered transition state (AMLA(6)) (22.8 and 16.0 kcal mol^{-1} respectively).

Very recently Jones *et al*. reported kinetic studies on the acetate assisted C-H activation of a N-phenyl imine with $[RhCl_2Cp^*]_2$.[11] The reaction of the dimer with acetate was very fast, and the mono and bis acetate Rh complexes were in equilibrium. They postulated a mechanism shown in Scheme 3.7 and confirmed earlier suggestions that **D (Scheme 3.4)** is a key intermediate.

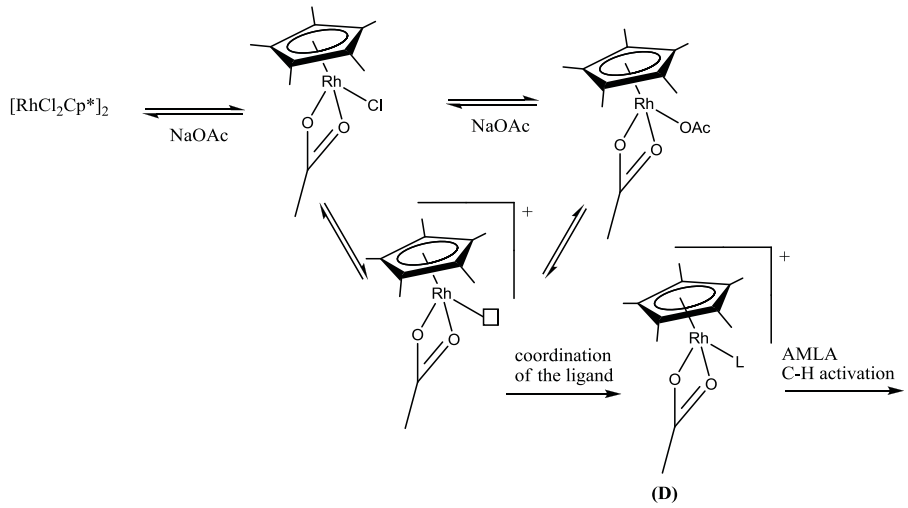

Scheme 3.7

Further kinetic experiments by the same group showed that the reaction with $[Cp^*IrCl_2]_2$ was 3 to 4 times faster than the reaction with $[Cp^*RhCl_2]_2$ for a given substrate; moreover the reaction with substrates bearing *m*-methoxy substituents were over 10 times faster than the reactions with substrates bearing *m*-trifluoromethyl substituents, which was consistent with an electrophilic activation.[11] Further kinetic

studies using partially deuterated phenylimine-d_5 under similar reaction conditions showed a large primary isotopic effect (>5) which contrasts with the small KIE observed by Ryabov[12] and computed by Macgregor *et al.* for cyclopalladation of DMBA.[8] Jones *et al.* concluded that acetate assisted C-H activation was occurring *via* an electrophilic activation with the C-H activation step being the rate determining step. They proposed a similar transition state to the one reported by Davies and Macgregor **(3.10)(Scheme 3.6).**

3.2 Results and discussion

3.2.1 Role of the base

In order to investigate the role of the base in the cyclometallation of DMBA with $[IrCl_2Cp^*]_2$, different bases were selected covering a wide range of pKa values **(Table 3.1)**. A stronger base should favour deprotonation however it is also a stronger ligand, hence opening of the chelate ring may be disfavoured.

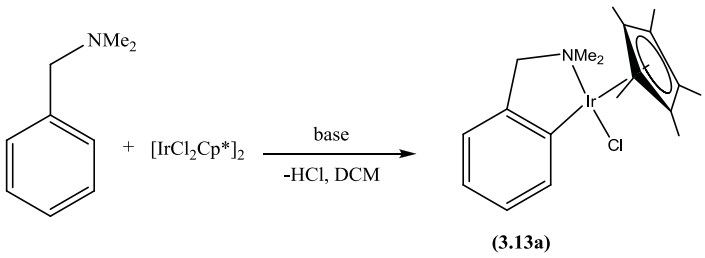

(3.13a)

Scheme 3.8

Table 3.1 Table of the pK_a values for the carboxylates tested

pK_a	10.32	4.76	4.31	3.83	0.65	-0.23
Base	CO_3^{-2}	$CH_3CO_2^-$	$PhCO_2^-$	$HOCO_2^-$	$CCl_3CO_2^-$	$CF_3CO_2^-$

Following the procedure reported by Davies *et al*, $[IrCl_2Cp^*]_2$ was reacted with DMBA (1 equiv. per Ir) and the corresponding base (1.25 equiv. per Ir) in DCM (10 ml) for 4h

at room temperature (method A).[8] After filtration through celite and evaporation to dryness the ^{1}H NMR spectrum showed mixtures of Cp* signals between δ 0.5 and 2.0 ppm. The product **(3.13a)** shows a singlet for the Cp* at δ 1.63 and the NMe_2 group gives rise to two singlets at δ 2.90 and 3.03. The benzyl protons are also inequivalent giving two mutually coupled doublets at δ 3.26 and 4.38. The phenyl group shows four inequivalent protons as expected for the orthometallated product. $[PhCH_2NHMe]^+$ was also observed and depending on the ratio of DMBA/$DMBAH^+$ the chemical shifts for N*Me*$_2$ (singlet) varied between δ 2.32 and 2.73 and the benzylic protons between δ 3.30 and 3.37. The yields are estimated by ^{1}H NMR spectroscopy, and by measuring the ratio between the Cp* signal of **(3.13a)** at δ 1.63 and the total integral of all the Cp* signals observed**.** Unfortunately, the signal for H_2O in $CDCl_3$ also occurs in this range so it can affect the overall integral and hence the calculated yield. To check the accuracy of these results a second set of experiments was run (Method B). This method used 1.25 eq of base and DMBA per Ir over 18 hours and the concentration of the reaction was reduced by a factor 2.5 (20 mg of $[IrCl_2Cp^*]_2$ in 10 ml of DCM) in order to facilitate the dissolution of the base in DCM. The yields of the reaction were determined by ^{1}H NMR spectroscopy by measuring the ratio of the integration of the Cp* singlet of **(3.13a)** with the Me signal of mesitylene used as an internal standard (0.05 mmol/L), the results are shown in **Table 3.2**.

Table 3.2 Yields of the reaction using different bases with the method A and B.

Base	Method A	Method B
NaOAc	70%[8]	65%
$CaCO_3$	0	_
$PhCO_2Na$	40%	29%
$NaHCO_3$	_	0
Cl_3CO_2Na	_	28%
CF_3CO_2Na	38%	55%
CF_3SO_3Na	_	Traces

The reaction of $[IrCl_2Cp^*]_2$ and DMBA (1.26 eq) with NaO_2CMe in DCM was reported to give **(3.13)** in 70% yield after four hours using method A.[4] A similar yield (65%) was observed using method B. NaO_2CCPh and NaOAc have a similar pKa, using NaO_2CCPh as base (method A) gave **(3.13a)** in 40% yield after 4 hours. The ^1H NMR spectrum showed, in addition to **(3.13a),** signals for $[PhCH_2NHMe_2]^+$ cation and other unidentified "IrCp*" compounds. The FAB-MS showed ions at *m/z* 847 and 449 assigned as $[(IrClCp^*)_2O_2CPh]^+$ and $[IrCp^*O_2CPh]^+$ respectively. In order to understand if these "IrCp*" products are intermediates in the reaction, the solid was redissolved in DCM and another equivalent of DMBA was added. The reaction mixture was left for another four hours. The ^1H NMR spectrum showed an increased yield (54%) but the other products were still present. Doing the reaction using method B gave a decreased yield of 29%.

In the presence of carbonate or bicarbonate no reaction occurred. The ^1H NMR spectrum only showed a signal due to the starting dimer and DMBA, this may be explained by the low solubility of these salts in DCM suggesting the necessity of

"organic" bases, however this confirmed that DMBA does not react with $[IrCl_2Cp^*]_2$ on its own as observed previously.[4]

The use of less basic carboxylates was attempted with NaO_2CCCl_3 (pKa = 0.65) and NaO_2CCF_3 (pKa = -0.23). In the case of NaO_2CCCl_3 the reaction using method B gave **(3.13)** in 28% yield. As for benzoate the ^1H NMR spectrum showed the formation of other "IrCp*" products and $[PhCH_2NHMe_2]^+$, hence the reaction had not gone to completion in 18 hours. Trifluoroacetate was then tried; using method A **(3.13a)** was produced with a 38% yield, though other "IrCp*" signals were observed. Hence at the end of the 4 hours the reaction mixture was redissolved in DCM and another equivalent of DMBA was added. The mixture was left stirring for four more hours. After this time the ^1H NMR spectrum showed an increased yield (50%) but other "IrCp*" products were still present. Using method B, an improved yield was found (55%). Hence, there is no simple correlation between the pKa of the base and the yield of the reaction, and a high pKa is not a prerequisite for the reaction to proceed.

To try and clarify the role of the base in the reaction, acetate was reacted with $[IrCl_2Cp^*]_2$. After 15 min the ^1H NMR spectrum showed no $[IrCl_2Cp^*]_2$ remained, however broad signals at δ 1.65 and δ 1.95 were observed probably due to a dynamic equilibrium between mono and bis acetate complexes, as observed by Jones *et al.* in the case of rhodium.[11] A similar reaction was attempted with a large excess of NaO_2CPh, the ^1H NMR spectrum showed that complete reaction between $[IrCl_2Cp^*]_2$ and benzoate had occurred within 15 min. Broad signals were observed in the ^1H NMR spectrum suggesting dynamic processes were occurring, and the ES-MS spectrum showed ions at m/z 404, 761 and 811 corresponding to $[IrCl(MeCN)Cp^*]^+$, $[Ir_2Cl_3Cp^*]^+$ and

$[Ir_2ClHO_2CCPhCp^*_2]^+$ respectively. The results suggest that benzoate and acetate can break the dimer and that [IrCl(carboxylate)Cp*] is not the only species present.

The observations that $[IrCl_2Cp^*]_2$ reacts rapidly with carboxylates combined with the failure of DMBA to react with the dimer in the absence of acetate[4] is further evidence that the reaction goes via pathway **(C) (Scheme 3.4)**. Ikariya *et al.* described cyclometallation of benzylamines with "$Ir(OAc)_2Cp^*$" formed *in situ* in from $[IrCl_2Cp^*]_2$ and NaO_2CMe.[13]

To gain further insight into the mechanism of acetate assisted C-H activation, the energy profile for cyclometallation of DMBA by $[IrCl_2Cp^*]_2$ was computed by our collaborators using DFT calculations **(Scheme 3.9)** with slightly corrected energy levels in comparison to Scheme 3.6, different conformation of the DMBA-H ligand leads to a stabilization of all stationary points along the three computed pathways.[14] In all cases, the rate limiting step is the displacement of one arm of the acetate ligand from the metal. A separate C-H cleavage step is only observed in some cases ($MeCO_2$, $PhCO_2$ and CCl_3CO_2), and even then, the activation barrier is very low (ca ΔE = 0.9 Kcal/mol in the case of $MeCO_2$). The results of the DFT calculations show only a weak correlation between the pK_a and the computed energy barrier **(Table 3.3)**, according to the calculations weak bases slightly enhance the reactivity through an easier displacement of one arm of the carboxylate.

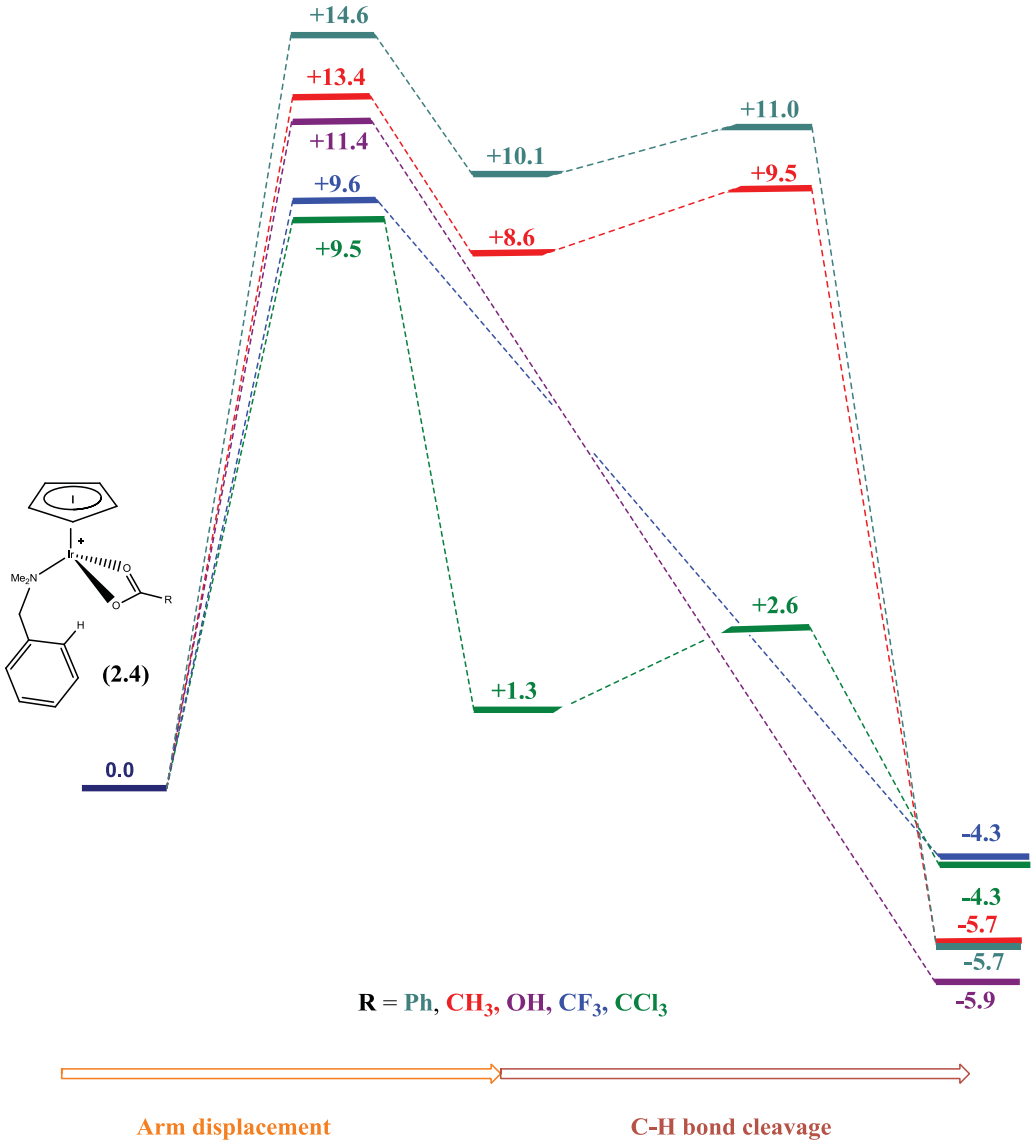

Scheme 3.9 Computed reaction profile (kcal mol^{-1}) for C−H activation with different carboxylates

Table 3.3 Computed energies of activation and pK_a values for the carboxylates studied.

Base	$^-O_2CCCl_3$	$^-O_2CCF_3$	HCO_3^-	^-O_2CPh	^-OAc
E^{act}	9.5	9.6	11.4	14.6	13.4
pk_a	0.65	0.23	3.83	4.31	4.76

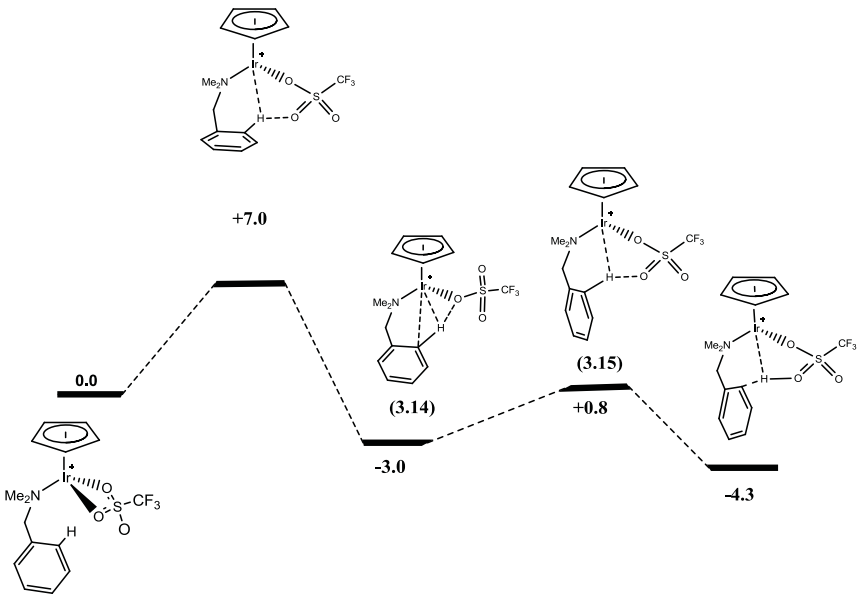

Scheme 3.10 Computed reaction profile (kcal mol^{-1}) for C−H activation with triflate

Since a weak base is likely to enhance reactivity through a less strong bidentate interaction with the metal, the reaction profile was computed with triflate **(Scheme 3.10)**. The κ^2–κ^1 displacement step is very facile and has the smallest barrier computed so far ($\Delta E^{\ddagger}$ = 7.0 kcal/mol). Moreover, the intermediate formed, [Ir(DMBA)(κ^1-CF_3SO_3)Cp]$^+$, **(3.14)**, is actually 3.0 kcal/mol more stable than [Ir(DMBA)(κ^2-CF_3SO_3)Cp]$^+$. Unlike these analogues, however, in this case the κ^1-isomer, **(3.14)**, would be expected to be the dominant form in solution. As such, the C-H activation step becomes rate-determining with $\Delta E^{\ddagger}$ = 3.8 kcal/mol **(3.15)**, the smallest value for the overall barrier found so far. The triflate system is a promising target for experiment as the barrier to C−H activation is still small.

The reaction with NaO_3SCF_3 was attempted using method B. After 18 hours, the ^{1}H NMR spectrum showed only traces of **(3.13)**, the major signals were assigned as $[PhCH_2NHMe_2]^+$. However, no starting $[IrCl_2Cp^*]_2$ was observed which suggests that triflate reacted with the dimer but C-H activation did not occur within 18hours When

the reaction was left stirring for 4 days a 50% yield was observed in the ^{1}H NMR spectrum suggesting that the process was incomplete after 18 hours and that the reaction was considerably slower than the one using NaOAc. The fact that the reaction with triflate as a base was the slowest and showed the smallest yield after 18 hours suggests that C-H activation (arm displacement + C-H bond cleavage) is not the rate determining step in this case. Hence, the steps for the formation of **(3.14)** have to be considered.

Opening the dimer by the base has been computed by DFT for the extreme cases of triflate and acetate. The results showed that the initial opening of the dimer is exothermic in both cases but is significantly more favourable for acetate (ΔE = -27.1 kcal/mol) than triflate (ΔE = -9.1 kcal/mol) **(Scheme 3.11)**. The next step, substitution of Cl by the second arm of the base, is energetically favourable for acetate (E = -32.5 kcal/mol) but is not for triflate (E = 1.8 kcal/mol). Hence a η^2 complex is more stable for acetate whereas an η^1 is more stable for triflate. In the subsequent steps for the acetate system, addition of DMBA is slightly uphill (E = −24.3 kcal mol^{-1}) but is followed by exothermic C−H activation and displacement of HOAc by Cl such that the overall process is highly exothermic (ΔE = −34.0 kcal mol^{-1}). In contrast, with triflate, ligand addition and subsequent C−H activation are both uphill events and even though the final displacement of CF_3SO_3H by Cl is thermodynamically favourable, the overall reaction is approximately thermo-neutral (ΔE =−0.2 kcal mol).

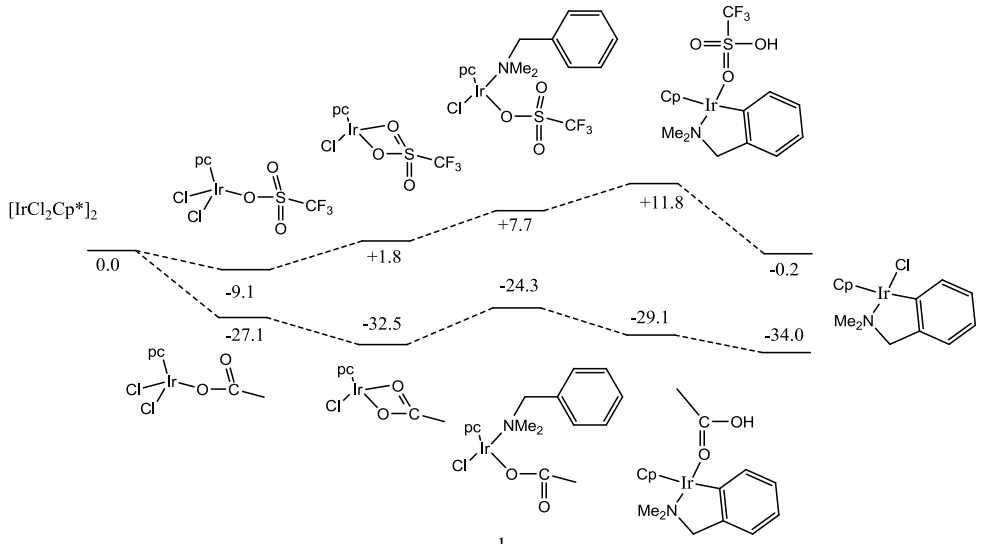

Scheme 3.11 Computed energies (kcal mol^{-1}) for key intermediates in the cyclometallation of DMBA by $[IrCl_2Cp]_2$ in the presence of acetate and triflate.

To conclude, DFT computations have provided a better understanding of the mechanism of the overall reaction. The reaction is dependent on many factors, including the ability of the base to generate the key intermediate **(D) (Scheme 3.4)** from the dimer and the ease of displacement of one carboxylate arm from the bidentate form. The experimental study showed that the solubility was also an important factor, for example bicarbonate gives no conversion because of its low solubility. The base plays a dual role in the process, breaking the dimer, and as an intramolecular base, the best yields are obtained with a compromise between these factors. The fact that DMBA did not react with the dimer also showed that the base reacted prior to the coordination of the ligand to produce a bidentate carboxylate as proposed for palladium by Sakaki,[15] and Fagnou,[16] and for RhCp* complexes by Jones, [11] and by us for 2-acetylpyridine activation described in Chapter 2.

3.3 Experimental

All reactions were carried out at room temperature under nitrogen; however, the workup was carried out in air unless stated otherwise. ^{1}H NMR spectra were obtained using a Bruker ARX 400 MHz spectrometer, with $CDCl_3$ as solvent unless otherwise stated. Chemical shifts were recorded in ppm (on δ scale for ^{1}H NMR, with tetramethylsilane as internal reference). FAB-MS spectra were obtained on a Kratos concept mass spectrometer using NOBA as matrix, and ES-MS spectra were recorded using a micromass Quattro LC mass spectrometer in acetonitrile. $[IrCl_2Cp^*]_2$[17] was made by literature methods; other compounds were obtained from Aldrich and Alfa Aesar.

General procedure for cyclometallation of DMBA with different bases:

Procedure A:

A mixture of $[IrCl_2Cp^*]_2$ (100 mg, 0.125 mmol), the appropriate base ($NaCF_3CO_2$, $NaPhCO_2$, $CaCO_3$, NaOTf) and DMBA (34 mg) in DCM (20 ml) was stirred for 4 h, and was filtered through Celite. The reactions were monitored by ^{1}H NMR spectroscopy and the yields were estimated from the ^{1}H NMR spectra by integration.

Procedure B:

A mixture of $[IrCl_2Cp^*]_2$ (20 mg), the appropriate base ($NaCF_3CO_2$, $NaPhCO_2$, $CaCO_3$, NaOTf) and DMBA (8 mg) in DCM (10 ml) was stirred for 18 h and was filtered through Celite. The solid was dissolved in 0.5 ml of a $CDCl_3$ solution containing mesitylene (0.05 mmol/L) as an internal standard and the yields were estimated from the ^{1}H NMR spectra by integration.

Reaction with $NaCF_3CO_2$ using procedure A

This was prepared with $NaCF_3CO_2$ (43 mg, 0.315 mmol). After 4h, the ^1H NMR spectrum showed no unreacted $[IrCl_2Cp^*]_2$ and only 38% yield of product **(3.13a)**.

In an attempt to form more of **(3.13a)**, the solid was dissolved in DCM (20 ml) and another equivalent of DMBA (34 mg, 0.252 mmol) was added. After stirring for a further 4 h, the solution was filtered through celite and evaporated to dryness. The ^1H NMR spectrum showed an increased yield of 50%.

Reaction with $NaPhCO_2$ using procedure A

This was prepared with $NaPhCO_2$ (45 mg, 0.315 mmol); the ^1H NMR spectrum showed no unreacted $[IrCl_2Cp^*]_2$ and 40% yield of product **(3.13a)**.

In an attempt to form more product the solid was dissolved in DCM (20 ml) and another equivalent of DMBA (34 mg, 0.252 mmol) was added. After stirring for a further 4 h the solution was filtered through Celite and evaporated to dryness. The ^1H NMR spectrum showed a yield of 54%.

Reaction with $CaCO_3$ using procedure A

This reaction was attempted using $CaCO_3$ (45 mg, 0.315 mmol); after 4 h the ^1H NMR spectrum showed signals for $[IrCl_2Cp^*]_2$ and DMBA.

Reaction with NaOAc using procedure B

This was prepared with NaOAc (5 mg, 0.063 mmol); the ^1H NMR spectrum showed a yield of 65%.

Reaction with $NaCF_3CO_2$ using procedure B

This was prepared with $NaCF_3CO_2$ (8 mg, 0.063 mmol); the ^1H NMR spectrum showed **(3.13)** had been formed in 55% yield.

Reaction with $NaPhCO_2$ using procedure B

This was prepared with $NaPhCO_2$ (9 mg, 0.063 mmol); the ^1H NMR spectrum showed a yield of 29% of **(3.13a)**.

Reaction with $NaHCO_3$ using procedure B

This was attempted with $NaHCO_3$ (11 mg, 0.063 mmol); the ^1H NMR spectrum showed signals for $[IrCl_2Cp^*]_2$ and DMBA.

Reaction with NaOTf using procedure B

This was prepared with NaOTf (11 mg, 0.063 mmol); the ^1H NMR spectrum showed traces of **(3.13a)**.

Reaction with $NaCCl_3CO_2$:

This was prepared from $[IrCl_2Cp^*]_2$ (20 mg, 0.025 mmol), DMBA (8 mg, 0.063 mmol) and $NaCCl_3CO_2$ (11 mg, 0.063 mmol); after stirring for 18 hours the solution was filtered through Celite and evaporated to dryness. The mixture was dissolved in dry $CDCl_3$ and mesitylene (7.03 μl) added. The ^1H NMR spectrum showed a yield of 29%.

3.4 Bibliography

[1] K. Isobe, P. M. Bailey, and P. M. Maitlis, *J. Chem. Soc., Dalton Trans.*, 1981, 2003.

[2] J. M. Kisenyi, G. J. Sunley, J. A. Cabeza, A. J. Smith, H. Adams, N. J. Salt, and P. M. Maitlis, *J. Chem. Soc., Dalton Trans.*, 1987, 2459.

[3] P. M. Boyer, C. P. Roy, J. M. Bielski, and J. S. Merola, *Inorg. Chim. Acta*, 1996, **245**, 7.

[4] D. L. Davies, O. Al-Duaij, J. Fawcett, M. Giardiello, S. T. Hilton, and D. R. Russell, *Dalton Trans.*, 2003, 4132.

[5] A. D. Ryabov, *Chem. Rev.*, 1990, **90**, 403.

[6] S. Fernandez, M. Pfeffer, V. Ritleng, and C. Sirlin, *Organometallics*, 1999, **18**, 2390.

[7] J. B. Sortais, N. Pannetier, A. Holuigue, L. Barloy, C. Sirlin, M. Pfeffer, and N. Kyritsakas, *Organometallics*, 2007, **26**, 1856.

[8] D. L. Davies, S. M. A. Donald, O. Al-Duaij, S. A. Macgregor, and M. Polleth, *J. Am. Chem. Soc.*, 2006, **128**, 4210.

[9] S. R. Klei, T. D. Tilley, and R. G. Bergman, *J. Am. Chem. Soc.*, 2000, **122**, 1816.

[10] D. M. Tellers, C. M. Yung, B. A. Arndtsen, D. R. Adamson, and R. G. Bergman, *J. Am. Chem. Soc.*, 2002, **124**, 1400.

[11] L. Li, W. W. Brennessel, and W. D. Jones, *Organometallics*, 2009, **28**, 3492.

[12] A. D. Ryabov, I. K. Sakodinskaya, and A. K. Yatsimirsky, *J. Chem. Soc., Dalton Trans.*, 1985, 2629.

[13] S. Arita, T. Koike, Y. Kayaki, and T. Ikariya, *Organometallics*, 2008, **27**, 2795.

[14] Y. Boutadla, D. L. Davies, S. A. Macgregor, and A. I. Poblador-Bahamonde, *Dalton Trans.*, 2009, 5887.

[15] B. Biswas, M. Sugimoto, and S. Sakaki, *Organometallics*, 2000, **19**, 3895.

[16] M. Lafrance, D. Lapointe, and K. Fagnou, *Tetrahedron*, 2008, **64**, 6015.

[17] C. White, A. Yates, and P. M. Maitlis, *Inorg. Synth.*, 1992, **29**, 228.

Chapter Four

Applications of the acetate assisted C-H activation reaction

4 Chapter 4

4.1 Introduction

As discussed in chapter 1, in recent years tremendous strides have been made in catalytic functionalisation of C-H bonds.[1-4] Direct C–H activation in catalysis has its roots in the pioneering work reported by Murai *et al.* involving C-C and C-X (X = heteroatom) bond formation.[5] This introduction will focus on C–H activation followed by insertion reactions, with the three metals studied earlier (Ir, Rh, Ru).

Murai *et al*. described the first examples of direct activation of C–H bonds of aromatics and their addition to internal alkynes with ketones as the directing group. **(Scheme 4.1).**[5, 6]

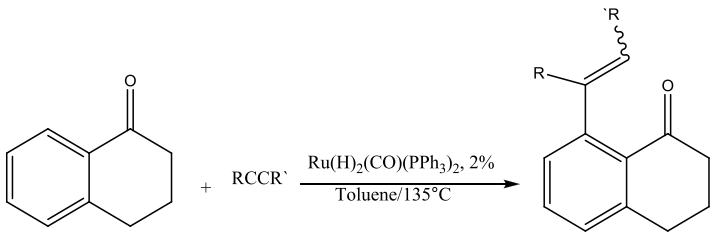

Scheme 4.1

A similar Ru-catalysed reaction of aromatic imines with alkenes also occurs **(Scheme 4.2)**, but in this case the reaction leads to by-products arising from dehydrogenative coupling *via* β-H eliminations.[7] Investigations of the corresponding reaction with imidates showed that the nature of the directing group has a major influence on the product formed.[8]

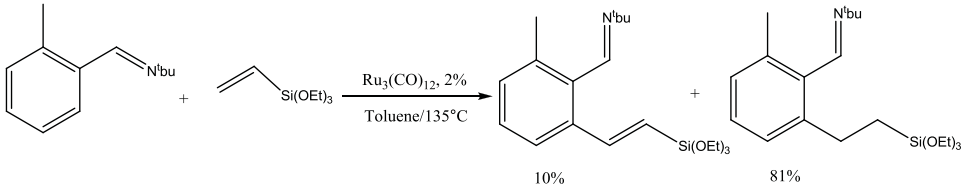

Scheme 4.2

The first step of these Ru-catalysed reactions is C–H activation by oxidative addition which forms both an M–H and M–C bond, either of these can potentially react, hence in some cases competing pathways are possible **(Scheme 4.3)**. With N-donor atoms, carbometallation and hydrometallation (Pathway 1 and 2) both occur, while in the case of O-donor atoms, only hydrometallation (Pathway 1) is observed. The reactivity of **(4.1A)** is decisive, if the formation of **(4.1D)** does not occur no **(4.1E)** is formed and the reaction only forms **(4.1C)** via **(4.1B)**.[8]

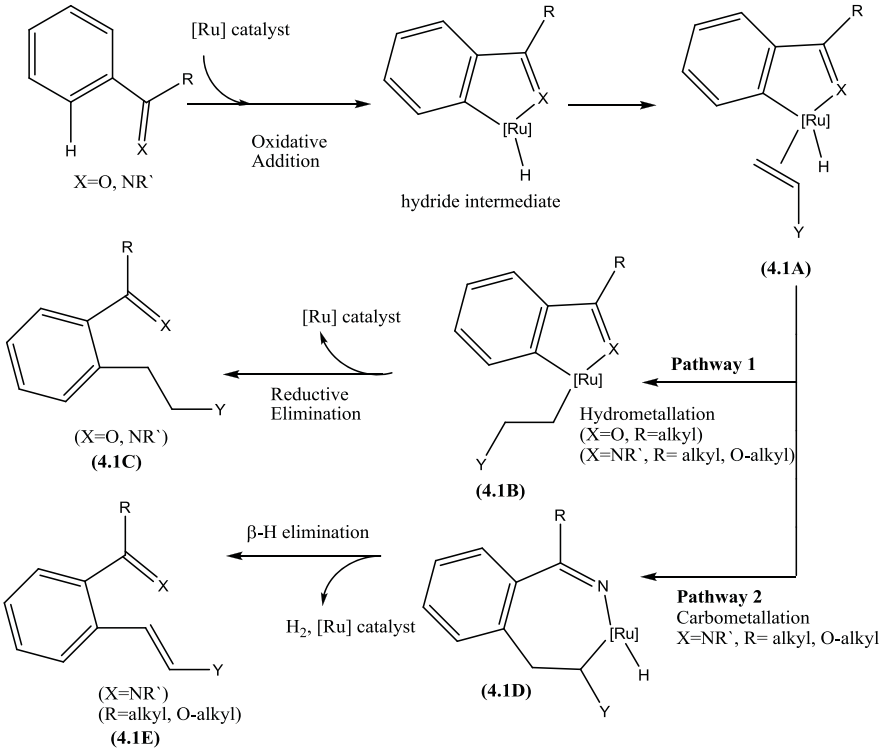

Scheme 4.3 Proposed catalytic cycle for the ruthenium catalysed coupling of aromatic C-H bond with olefins.

As mentioned above, the problem with this approach is that oxidative addition of the C–H bond forms both a M–H and M–C bond, either of which can potentially react, hence competing pathways may occur. An alternative strategy would be to use electrophilic or AMLA C–H bond activation where just a M-C bond is formed with no M–H bond, hence having only one subsequent reaction pathway. This introduction will focus on C–H activation by electrophilic activation or AMLA followed by insertion of alkynes.

Miura *et al.* developed several catalytic systems in which an AMLA C–H bond activation is likely to be the first step.[9-17] For example, C–H activation followed by insertion of alkynes with O-donor directing group ligands was investigated with $[MCl_2Cp^*]_2$ (M = Ir, Rh) **(Scheme 4.4)**.[11, 12]

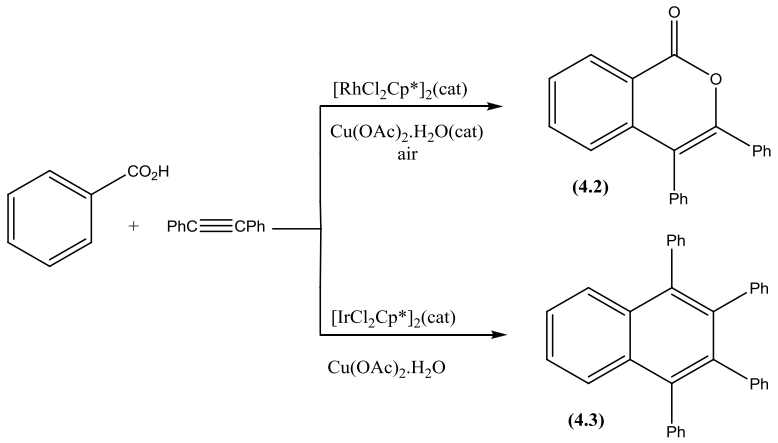

Scheme 4.4

Changing the metal in this reaction has a dramatic effect, the Rh catalyst gives heterocycle **(4.2)** whereas the Ir-catalyst leads to the formation of carbocycle **(4.3).** The proposed mechanism is shown in **Scheme 4.5**. In both cases, the carboxylate acts as a directing group for the C–H activation to form **(4.4)** which undergoes an alkyne insertion to form **(4.5).** In the case of Rh, **(4.5)** undergoes C–O reductive elimination to form the isocoumarin **(4.2)** whilst in the case of Ir decarboxylation of **(4.5)** is favoured and a second insertion occurs before a C–C reductive elimination to produce the naphthalene derivative **(4.3)**.[11, 12] Consistent with this, Jones *et al.* have observed that reductive elimination is more favourable for Rh(III) than Ir(III) (see below).[18]

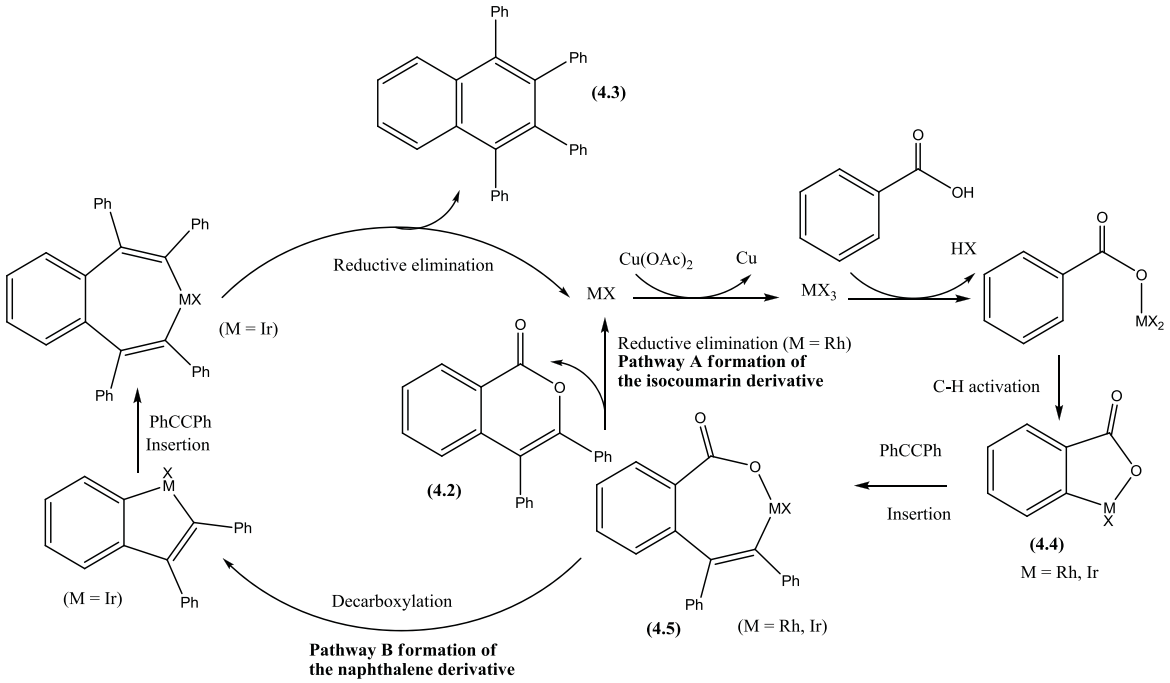

Scheme 4.5 Postulated mechanism for the formation of the coumarin derivative (pathway A) and the naphthalene derivative (pathway B).[11, 12]

Further mechanistic investigation of pathway B showed that when the benzoic acid was ortho substituted by Cl, two regioisomers **(4.7)** and **(4.10)** were observed **(Scheme 4.6)**.[12] The authors suggested a mechanism where before the second insertion a protonation equilibrium was occurring which allowed isomerisation of **(4.6)** into **(4.9)** *via* **(4.8).**

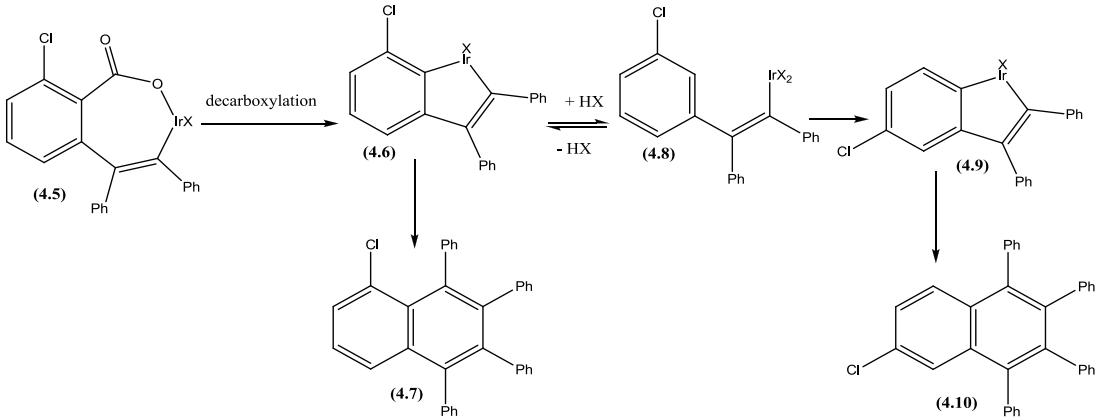

Scheme 4.6

An analogous effect of the nature of the metal on a catalytic reaction of indoles has been reported by the same group **(Scheme 4.7)**.[11, 17] With $[RhCl_2Cp^*]_2$ as catalyst heterocycle formation occurs whilst no catalysis is observed with $[IrCl_2Cp^*]_2$ whereas with $Pd(OAc)_2$ a carbocycle is formed (presumably by a decarboxylation mechanism similar to that in **Scheme 4.5**).[11,17]

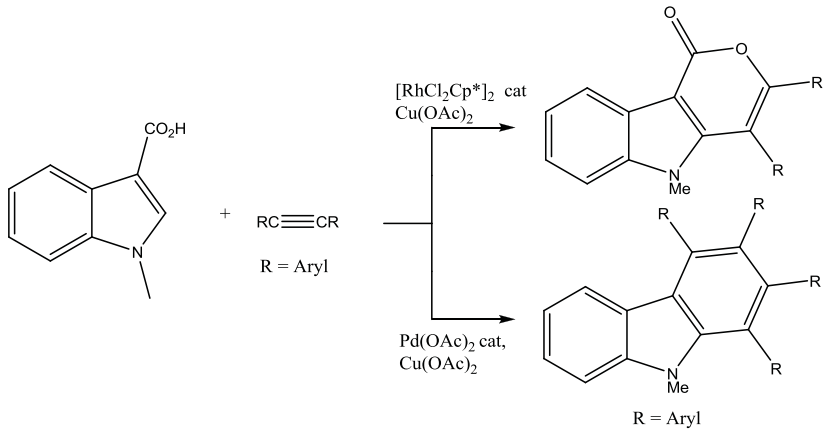

Scheme 4.7

The oxidation state of the metal is also important as illustrated in **Scheme 4.8**.[16] Rh(III) gives the expected heterocycle **(4.11)** by a mechanism analogous to pathway A in **Scheme 4.5**. However, when Rh(I)/$C_5H_2Ph_4$ was used **(4.12)** was produced *via* a decarboxylation reaction, this suggests that not only the identity of the metal but also its oxidation state is important in determining the products. These processes can be extended to vinylic C-H bonds, for example the expected heterocycle **(4.13)** is formed from methacrylic acid **(Scheme 4.9)**.[15]

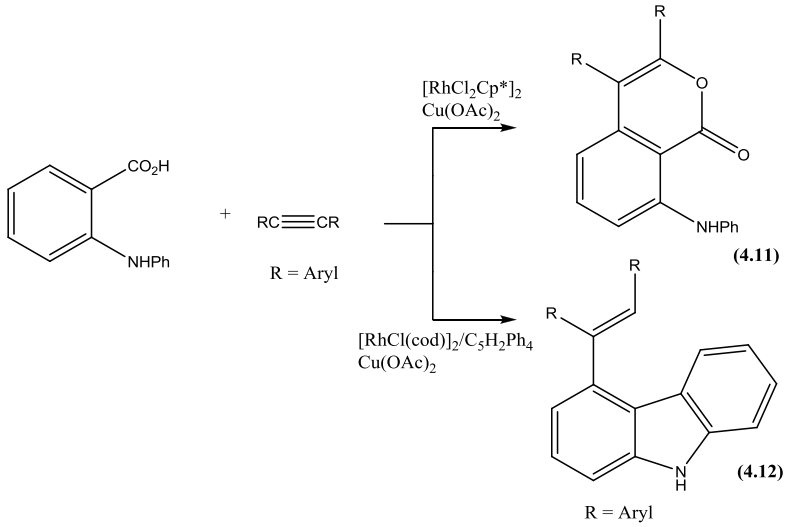

Scheme 4.8

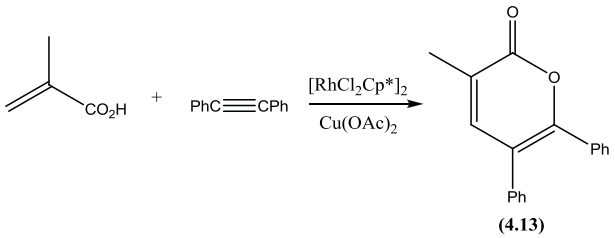

Scheme 4.9

C–H activation and insertion are only postulated as steps in these catalytic cycles. To investigate if these are intermediates, stoichiometric studies of cyclometallated complexes with alkynes maybe useful. Pfeffer *et al*. have previously synthesised cyclometallated arene ruthenium complexes **(4.14)** by C–H activation (see Chapter 1 section 2). They showed that these complexes react with internal alkynes in MeOH, in the presence of $NaPF_6$ to produce the isoquinolinium complexes **(4.16) (Scheme 4.10)**.[19]

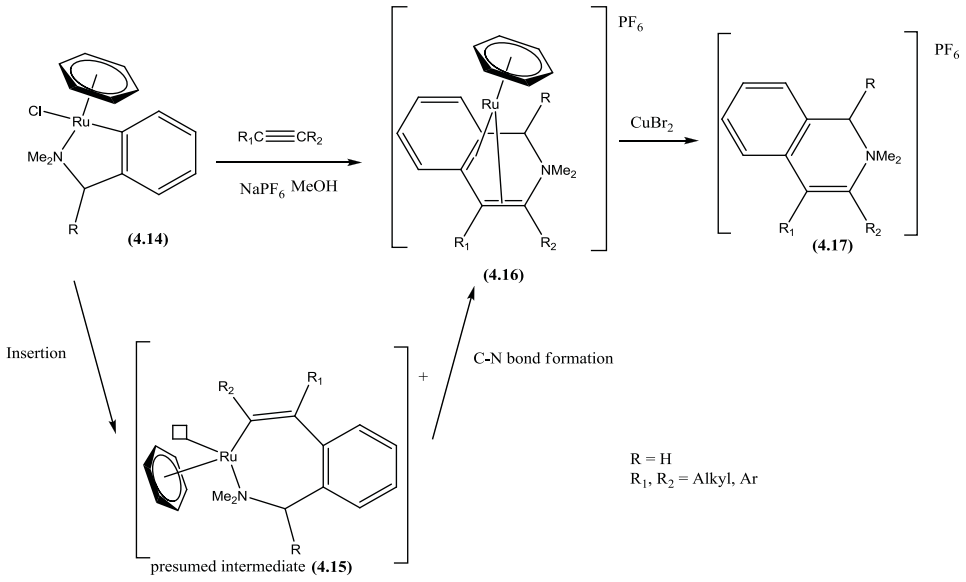

Scheme 4.10

Bulky substituents on the alkyne lead to slower rates of reaction. The reactions are postulated to go *via* **(4.15)** followed by spontaneous reductive elimination from Ru(II) to Ru(0) to give **(4.16).** Addition of an oxidising agent such as $CuBr_2$ is necessary for the liberation of heterocyclic cations **(4.17)**. The reactions did not take place in DCM. The authors suggested that the addition of PF_6 and methanol as solvent aid loss of Cl^- to give more reactive cationic complexes **(4.15)**.[19] Pfeffer suggested that insertion occurred into the M–C bond rather than the M–N bond and this has been found in all other half-sandwich cases to date and further examples of insertion are discussed below. Pfeffer showed that in contrast to electron rich alkynes which give the isoquinolium complexes **(4.16),** with the electron deficient alkyne, DMAD, the reaction stopped after the insertion step.[20] When asymmetrical alkynes were used the regioselectivity of the insertion was mainly due to steric factors, the smaller alkyne substituent ending up on the metallated carbon. However, if $PhCCCF_3$ was used, two products were formed. Hence, with CF_3 next to the metal, the reaction stopped at the insertion stage whereas with Ph next to the metal C–N bond formation occurred and the coordinated heterocycle was observed**.**

In conclusion, insertion of the alkyne into the Ru-C bond occurred in all cases, but the reductive elimination was governed by the electronic effect at the metallated carbon. Pfeffer suggested that the reductive elimination needed an electron rich substituent on the metallated carbon to be able to attack the coordinated electrophilic amine.[20]

Subsequently, Jones *et al*. reported the insertion of DMAD into RhCp* and IrCp* cyclometallated complexes of imines **(2.9 a,b)** and 2-phenylpyridine **(2.10 a,b)** and in these cases also the reaction stopped after the alkyne insertion **(Scheme 4.11)**.[18]

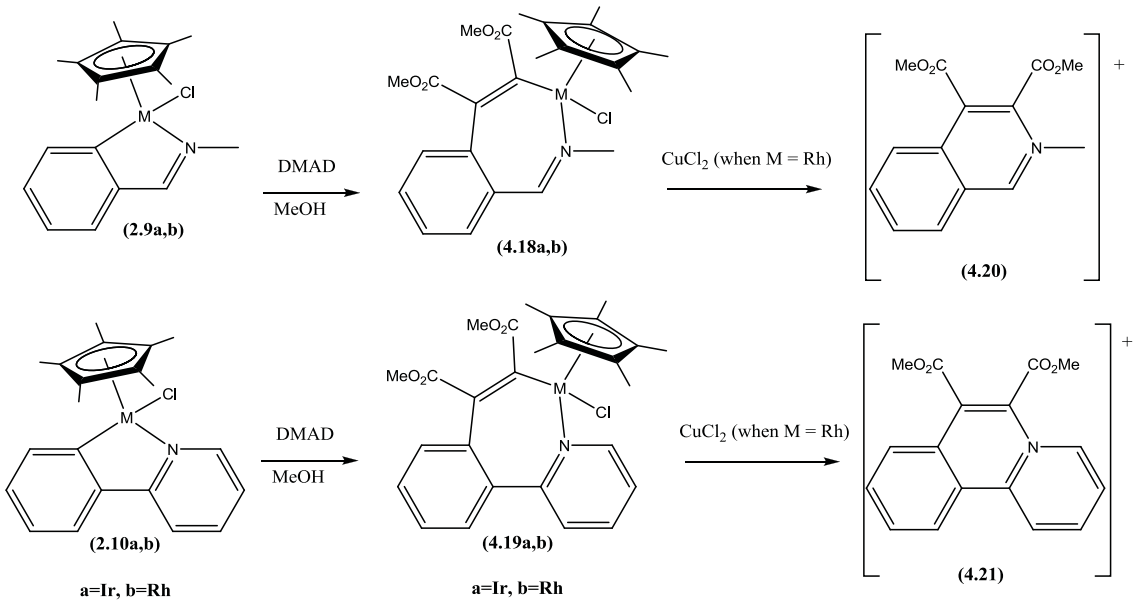

Scheme 4.11

The rhodium products **(4.18b)** and **(4.19b)** reacted with $CuCl_2$, to form the heterocyclic cations **(4.20)** and **(4.21)**. Whereas, **(2.9a)** and **(2.10a)** did not react with $CuCl_2$ at ambient temperature. Jones *et al*. attempted to make heterocyclic formation catalytic but the reaction was very slow.[18] They suggested that this was because the insertion needed a polar solvent whereas the reaction with $CuCl_2$ needed a non polar solvent. Hence, it was difficult to find one solvent that suited the entire catalytic cycle. In the case of ruthenium half sandwich complexes Pfeffer *et al.* showed that when DMAD was

inserted (**4.15** $R_1 = R_2 = CO_2Me$), the heterocyclic derivative was not formed even after reaction with $CuBr_2$.[20]

In contrast to iridium and ruthenium complexes, presumably Cu oxidises Rh(III) to Rh(IV) which then spontaneously reductively eliminates to form the C–N bond. The ease of the reductive elimination is dependent on the metal centre.

2-Phenylpyridine has also been used in catalytic C–H activation/insertion reactions, Zhang *et al.* reported the alkenylation of 2-phenylpyridine with $RuCl_3$ **(Scheme 4.12)**.[21] This process was postulated to go *via* a base assisted C–H activation to form **(4.22)**, followed by regiospecific insertion of the terminal alkyne **(4.24) (Scheme 4.12)**.[21] No C–N bond formation occurred, however the presence of benzoic acid provides an alternative route to liberate an organic product by protonation of the metallated carbon to form an alkene, thereby allowing the catalytic system to turn over without an oxidising agent **(Scheme 4.12)**. This was the first example of a chelation assisted C–H activation followed by insertion of a terminal alkyne in the literature. The advantage of this catalytic reaction was the use of $RuCl_3$ with no preactivation of the metal required.

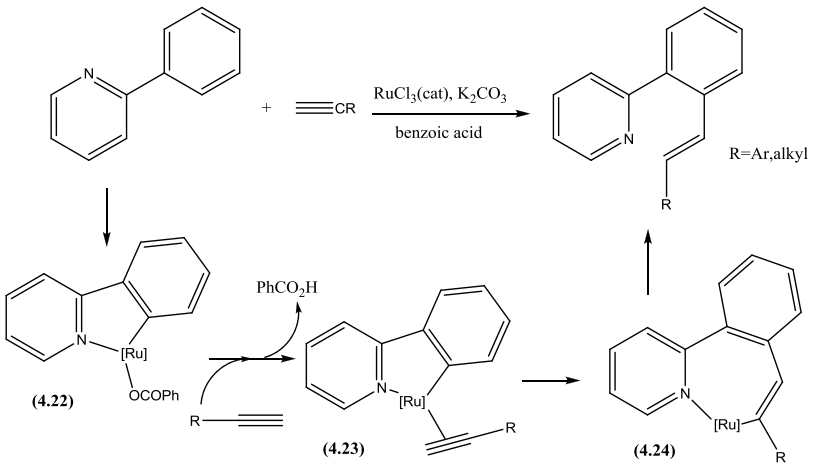

Scheme 4.12

Other N-donor ligands can act as a directing group for AMLA type C–H activation in catalytic cycles. The reactions of 2-phenylpyrazole and 2-phenylimidazole with internal

alkynes have been described by Miura.[13] 2-phenylpyrazole in the presence of diphenylacetylene, a catalytic amount of $[RhCl_2Cp^*]_2/C_5H_2Ph$ and $Cu(OAc)_2$ produced a carbocycle **(4.25)(Scheme 4.13).**

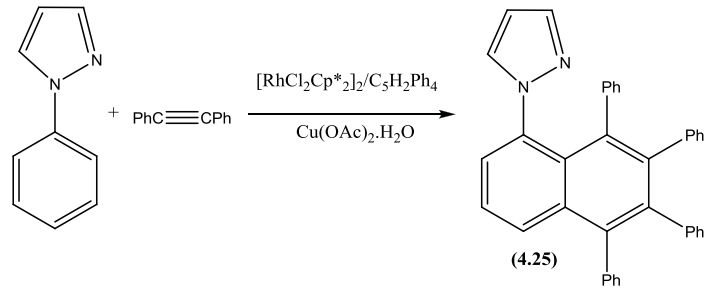

Scheme 4.13

In the case of 2-phenylimidazole only one insertion followed by C–N bond formation was observed (i.e. similar to pathway A in **Scheme 4.6**) to form the heterocycle **(4.26) (Scheme 4.14),** however, with the N-methylated analogue the carbocycle **(4.27)** was formed.

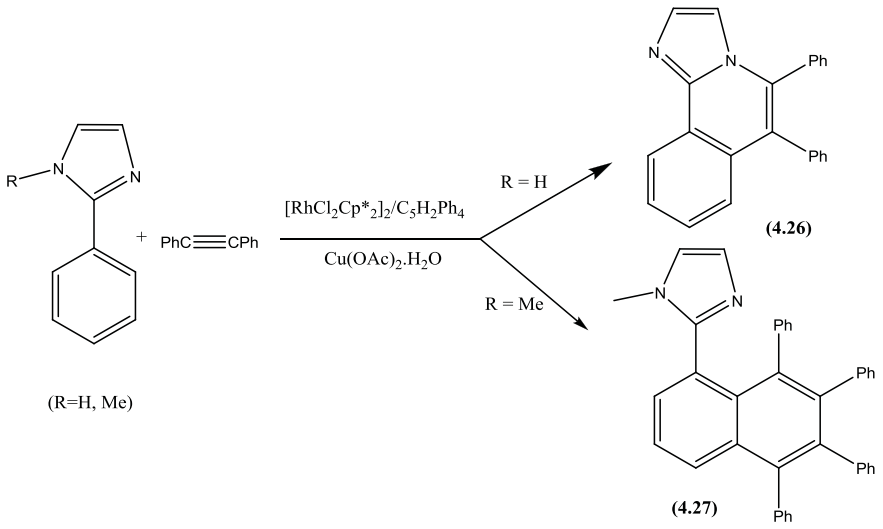

Scheme 4.14

The possible competition between C–N and C–C bond formation is also relevant in the reaction of imines **(Scheme 4.15)**.[14] In these cases the outcome depends on the substituent on nitrogen and on the imine carbon. In the case of N-phenylbenzylidene **(4.28)**, an indene **(4.29)** is produced by a C–C bond formation, as opposed to the

formation of a pyridinium salt observed by Jones *et al*. described earlier **(Scheme 4.11)**.[18]

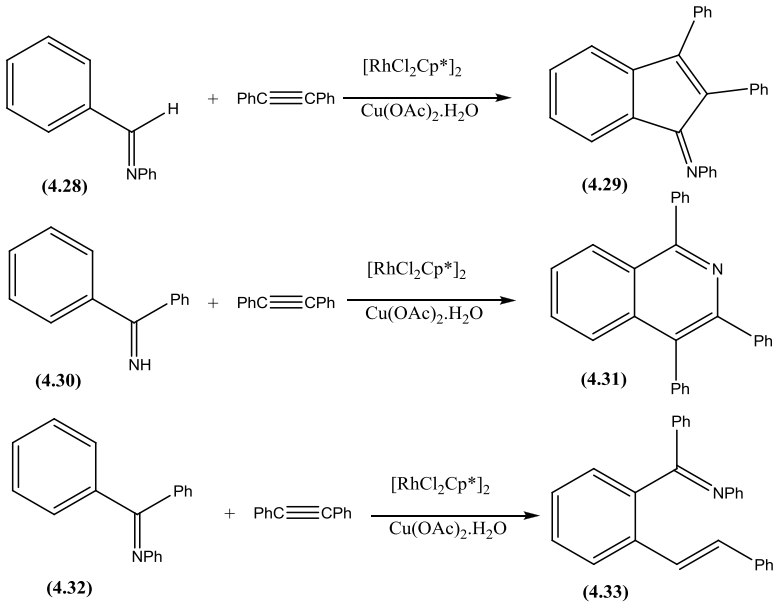

Scheme 4.15

When **(4.30)** was used, C–N bond formation occurred to give the isoquinoline **(4.31)**. However when the corresponding N–Ph derivative **(4.32)** was used, formation of alkenyl product **(4.33)** occurred rather than N–C or C–C bond formation **(Scheme 4.15)**. Subtle variations in the substituents gave large differences in the product selectivity.

A recent study by Fagnou *et al.* used N–^{t}Bu imines **(4.34)** and showed the formation of the isoquinoline derivative with a loss of the ^{t}Bu substituent on the imine to form **(4.35)** **(Scheme 4.16)**.[22]

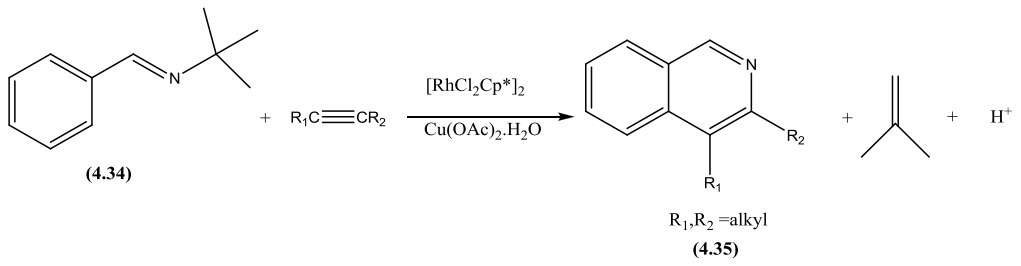

Scheme 4.16

Fagnou originally considered two possible mechanisms based on previous precedents, **(Scheme 4.17)** (i) a reductive elimination from a Rh(IV) moiety related to the mechanism proposed by Jones *et al.*[18], and (ii) an electrocyclisation /oxidation related to previous work by Bergman *et al* [23] involving C–H activation by oxidative addition. The first mechanism (reductive elimination from Rh(IV)) was tested by using the same reaction conditions without $Cu(OAc)_2$. The product was formed in a low yield (stoichiometric amount of product) however when $Cu(OAc)_2$ was added, the yield increased. Since some conversion was observed without $Cu(OAc)_2$ it is not essential for the reductive elimination step.

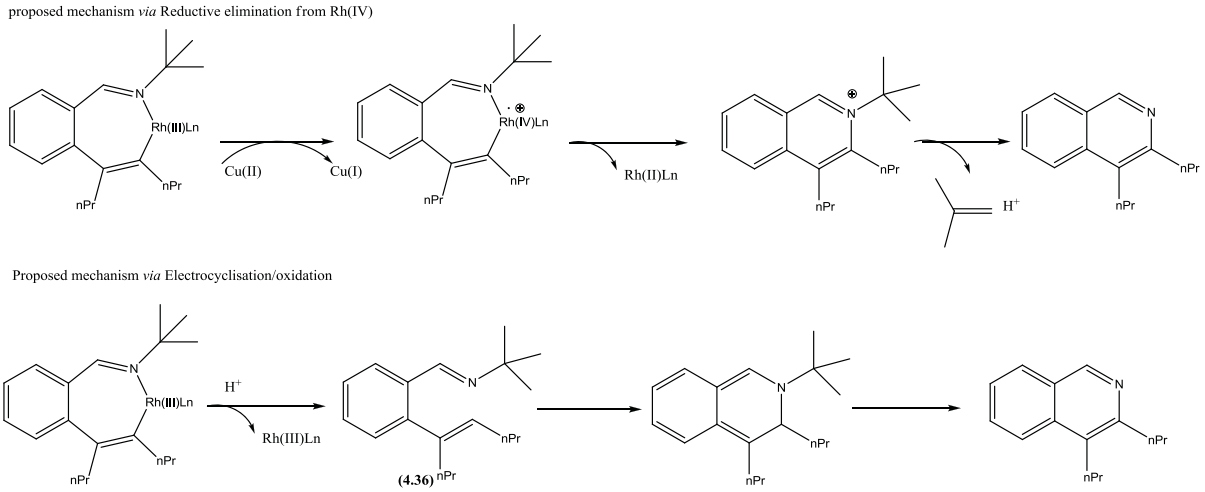

Scheme 4.17 Possible mechanisms considered by Fagnou *et al.* for the formation of isoquinoline.[22]

The electrocyclisation/oxidation mechanism was investigated by synthesizing the alkenyl intermediate **(4.36)** separately. The reaction of **(4.36)** under catalytic conditions did not afford the expected product **(Scheme 4.18)**. Furthermore the reaction of **(4.36)** with an alkyne formed a pyridine derivative product **(4.37)** arising from a new C–H activation **(Scheme 4.18).**

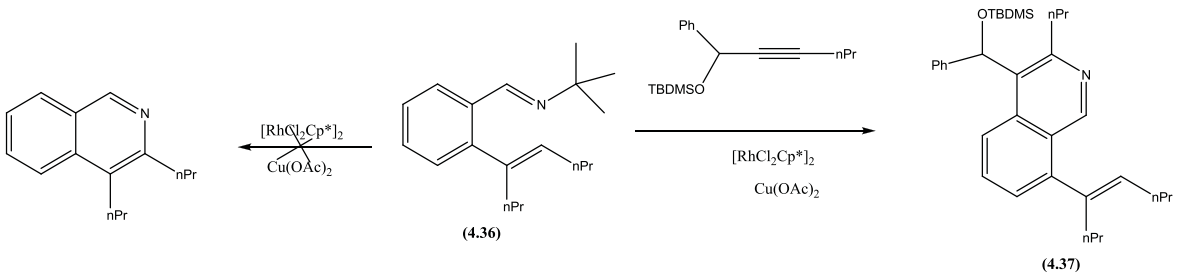

Scheme 4.18 Investigation of the electrocyclisation/oxidation mechanism by Fagnou et al.[22]

Hence Fagnou concluded that C–N bond formation is happening directly from the Rh(III) complex **(Scheme 4.19)**, which contrasts with the system examined by Jones *et al.* where oxidation of the metal occurs before reductive elimination.[18]

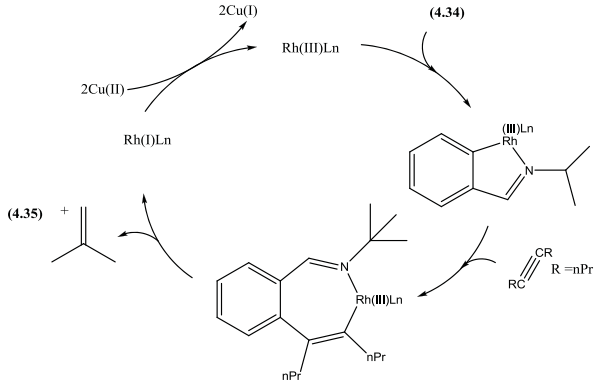

Scheme 4.19 Mechanism proposed by Fagnou for the formation of isoquinolines.[22]

In conclusion AMLA C–H activation can be applied for catalytic reactions involving insertions of alkynes. As discussed above, the C–H activation seems to be easy with a range of O–donor and N–donor directing groups. The outcome of the reaction is largely dependent on the ease of the reductive elimination step; if C–X (X = O, N) bond formation is not favoured other pathways may occur and further insertions and/or protonation can take place. In the case of iridium so far, C–X (X = O, N) bond formation has not been observed, this is probably due to a higher activation barrier than the C–C bond formation. For rhodium C–X (X = O, N) bond formation is easier than iridium and can occur spontaneously depending on substituents on the alkyne and on the ligand. In the case of ruthenium only one type of ligand was studied for half sandwich

complexes. C–N bond formation occurs spontaneously except when there is an electron withdrawing group on the metallated carbon after insertion. Even though reductive elimination is spontaneous the Ru(0) complex formed is very stable and oxidation of the metal is required for the dissociation of the organic fragment.

In the examples described by Pfeffer *et al.*[19, 20, 24] and Fagnou *et al.*[22, 25] the oxidising agent reacts after the C-N bond formation (reductive elimination) whereas in those described by Jones *et al.*[18] the oxidising agent reacts prior to the reductive elimination. The order of these steps and the possibility of alternative routes described by Miura *et al.*[11, 12, 15-17] depends on the nature of the metal complex, the directing ligand, the substituents on the alkyne, the solvent and the oxidising agent. In most of these examples Miura and co-workers have proposed plausible mechanisms but there has been no detailed study of the mechanism of catalysis. Mechanistic investigations are needed to be able to understand how the different substituents and other factors affect the process and hence design more efficient catalysts. This chapter will describe the insertion of alkynes into cyclometallated complexes with Ir, Rh and Ru and factors affecting C–N bond formation will be discussed.

4.2 Results and discussion

4.2.1 Insertions of alkynes into cyclometallated 2-phenylpyrazole (2.13a,b,c)

4.2.1.1 Reaction of DMAD with (2.13a-c)

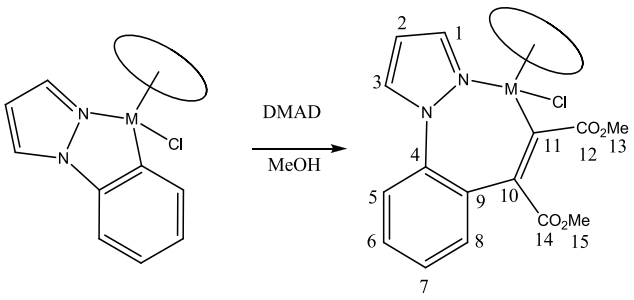

(2.13a) M= Ir, ring = Cp*
(2.13b) M= Rh, ring = Cp*
(2.13c) M= Ru, ring = *p*-cymene

(4.38a) M = Ir, ring = Cp*
(4.38b) M = Rh, ring = Cp*
(4.38c) M =Ru, ring = *p*-cymene

Scheme 4.20

The reaction of **(2.13a)** with DMAD in MeOH **(Scheme 4.20)** was monitored by ES-MS spectrometry and after 1 hour, only one peak was observed at *m/z* 613 [**(4.38a)**-Cl]$^+$ as expected for one insertion of DMAD. After work-up, **(4.38a)** was isolated in 51% yield. The ^{1}H NMR spectrum of **(4.38a)** shows a 1:1:1 ratio of the Cp*, the cyclometallated 2-phenylpyrazole and DMAD. Three singlets are observed at δ 1.31, 3.64 and 3.69 due to the Cp* and the two different OMe groups respectively. The Cp* signal is shifted 0.35 ppm to higher field than in the starting complex **(2.13a)** at δ 1.66, this can be explained by a ring-current effect of the Cp* lying over the original cyclometallated phenyl ring of the 2-phenylpyrazole (see X-ray structure later). Similar ring current effects have been observed for cyclometallated bisoxazoline benzene complexes which also have seven-membered chelate ring.[26] Similar chemical shifts for the Cp* signal are observed by Jones *et al.* for the related DMAD insertion products **(4.18a)** and **(4.19a)** at δ 1.34 and δ 1.27 respectively.[18] The pyrazole gives rise to two

doublets at δ 7.81 (H^3) and δ 8.21 (H^1), and a triplet at δ 6.51 (H^2). The cyclometallated phenyl system is composed of four protons, H^7 and H^8 show a multiplet which integrates for two protons at δ 7.43, H^5 is coupled to H^6 and H^7 and gives rise to a doublet of doublets at δ 7.17. Proton H^6 is coupled to H^5, H^7, H^8 and appears as a triplet of doublets at δ 7.34. The signals for H^1 and (OMe^{13}) were assigned by NOESY spectroscopy, both of which show a NOE correlation to the Cp* signal, H^5 is also correlated to H^3. In the ^{13}C NMR spectra, the expected number of quaternary and C–H carbons is seen and the metallated carbon C^{11} is observed at δ 176.15 which is lower field than the metallated carbon for **(2.13a)** at δ 167.36. This shift of the metallated carbon is close to the ones for **(4.18a)** at δ 176.26, and **(4.19a)** at δ 176.16 observed by Jones *et al.*[18] The FAB-MS spectrum shows ions at *m/z* 613 due to $[M\text{-}Cl]^+$ and 648 for $[M]^+$. Crystallisation from DCM/hexane gave crystals suitable for X-ray diffraction and the structure is discussed below with that of **(4.38b)** and **(4.38c)**.

The reaction of the analogous cyclometallated rhodium complex **(2.13b)** with DMAD was also investigated **(Scheme 4.20)**. The reaction was monitored by ES-MS spectrometry, and after 5 hours, the ES-MS spectrum showed only one peak at *m/z* 523 assigned as $[\textbf{(4.38b)}\text{-}Cl]^+$. After work-up **(4.38b)** was isolated in 81% yield. The ^1H NMR spectrum of **(4.38b)** is very similar to that of **(4.38a)**. As for **(4.38a)** the Cp* signal is observed at δ 1.30 and shifted upfield (0.38 ppm) compared to the starting material **(2.13b)**. Two singlets are observed, at δ 3.64, and 3.69 due to the two different OMe groups. The pyrazole signals are observed at δ 7.82 (H^3), 8.27 (H^1) and 6.50 (H^2). In the ^{13}C NMR spectra, the expected number of quaternary and C–H carbons is seen. The metallated carbon C^{11} is easily identified due to coupling with Rh and is observed as a doublet at δ 181.60 ($J_{Rh\text{-}C}$ 135 Hz), similar to those at δ 176.01 and 177.16 for the metallated carbon for **(4.18b)** and **(4.19b)** observed by Jones *et al.*[18] The FAB-MS mass spectrum shows an ion at *m/z* 523 $[M\text{-}Cl]^+$. Crystallisation of **(4.38b)** from DCM/hexane

gave crystals suitable for X-ray diffraction and the structure is discussed below with the related complexes **(4.38a)** and **(4.38c)**.

The corresponding reaction of the cycloruthenated complex **(2.13c)** with DMAD was also attempted **(Scheme 4.20).** Monitoring by ES-MS spectrometry showed a decrease of the starting material peaks at *m/z* 379 [**(2.13c)**-Cl)]$^+$ and 411 [**(2.13c)**-Cl+MeCN]$^+$ and appearance of a new peak at *m/z* 521 [**(4.38c)**-Cl]$^+$. After 18 hours, the peaks at *m/z* 379 and 411 were no longer visible and the reaction was assumed to have finished. After work-up, **(4.38c)** was isolated in 78% yield.

The ^{1}H NMR spectrum of the product **(4.38c)** shows two singlets for the two different OMe groups at δ 3.63 and 3.64. The isopropyl of the *p*-cymene gives rise to two inequivalent doublets at δ 1.06 and at δ 1.16 and a septet at δ 2.64, the Me signal is observed at δ 2.11. The four aromatic protons of *p*-cymene are also inequivalent and give four doublets at δ 4.12, 4.44, 4.54 and 5.52. The aromatic protons are shifted 0.03-0.95 upfield from **(2.13c)**, consistent with a ring current effect due to the *p*-cymene lying over the original cyclometallated phenyl ring of 2-phenylpyrazole. These data are also consistent with the metal centre being chiral and epimerisation being slow on the NMR timescale. The pyrazole gives rise to two doublets at δ 7.78 H^3 and δ 8.38 H^1 and a triplet at δ 6.47 (H^2). As in **(4.38a)** the C_6H_4 group shows four inequivalent and mutually coupled protons at δ 7.51 (H^7, H^8), δ 7.19 (H^5) and δ 7.41 (H^6). The assignments were confirmed by a cross peak between H^3 and H^5 in the NOESY spectrum. The ^{13}C NMR spectrum shows the expected number of C–H and quaternary carbons, the metallated (C^{11}) is observed at δ 190.94. The FAB-MS spectrum shows a ions at *m/z* 556 [M]$^+$ and 521 [M-Cl]$^+$. Crystallisation from DCM/hexane gave crystals suitable for X-ray diffraction and the structure is shown in **Fig. 4.1** with selected bonds distances and angles in **Table 4.1**, and discussed below with that of **(4.38a)** and **(4.38b).**

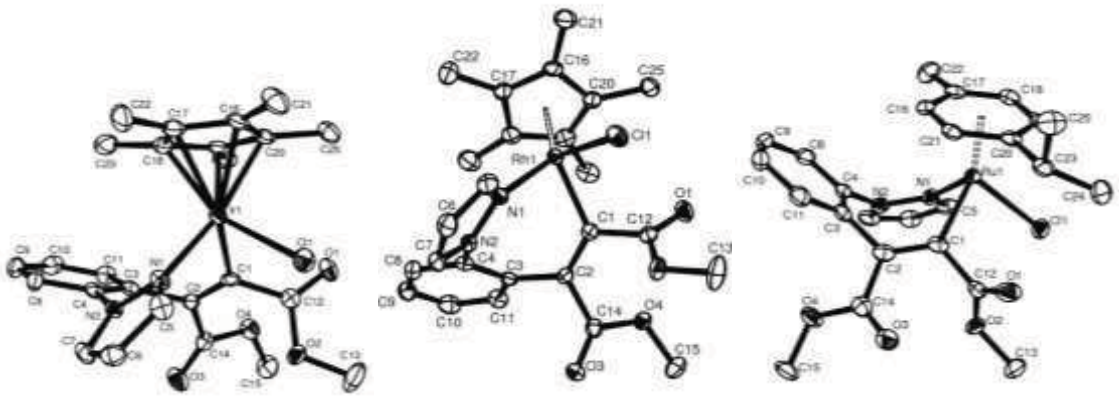

(4.38a) **(4.38b)** **(4.38c)**

Fig. 4.1 Molecular structures and atom-numbering schemes for **(4.38a)**, **(4.38b)** and **(4.38c).** H atoms have been omitted for clarity.

Table 4.1 Selected bond distances [Å] and bond angles [°] for **(4.38a), (4.38b)** and **(4.38c)**

	(4.38a)	**(4.38b)**	**(4.38c)**
M(1)-N(1)	2.086(4)	2.093(2)	2.097(4)
M(1)-Cl(l)	2.418(1)	2.4131(7)	2.4183(17)
M(1)-C(1)	2.050(5)	2.040(3)	2.070(4)
C(3)-C(2)	1.498(6)	1.487(3)	1.480(6)
C(2)-C(1)	1.346(6)	1.339(4)	1.360(7)
N(1)-M(1)-C(1)	85.08(16)	85.67(9)	83.35(16)
N(1)-M(1)-Cl(1)	86.84(11)	88.61(6)	85.94(11)
Cl(1)-M(1)-C(1)	88.51(13)	89.92(8)	89.37(14)

The complexes all adopt a pseudo octahedral structure. The structures confirm that the alkyne has inserted into the M–C bond rather than the M–N bond, to form a seven-membered ring. No C–N bond formation has occurred in contrast to ruthenium cyclometallated complexes described earlier.[19, 20, 24] In all three structures the π-bound ligand (Cp* and *p*-cymene) is lying over the originally cyclometallated phenyl ring consistent with the ring current effects discussed above. The three structures also show

similar bond lengths and angles to **(4.18a)** and **(4.19b)** described by Jones *et al.*[18] In each complex the M–C(1) bond length [2.050(5), 2.040(3) and 2.070(4) Å for **(4.38a), (4.38b)** and **(4.38c)** respectively] is slightly shorter than the M–N(1) bond [2.086(4) 2.093(2) and 2.097(4) Å respectively]. Both the M–C(1) and the M–N(1) bond lengths are statistically the same in **(4.38a)** and **(4.38b)** [2.050(5) and 2.086(4) Å in **(4.38a)** and 2.040(3) and 2.093(2) Å in **(4.38b)** respectively]. The chelate angles C(1)–M–N(1) of **(4.38a) (4.38b)** and **(4.38c)** [85.08(16), 85.67(9) and 83.35(16)° respectively] are bigger than those of **(2.13a) (2.13b)** and **(2.13c)** [77.5(3), 78.5(3) and 77.38(12)° respectively], due to the increased size of the cyclometallated ring. The formation of a seven membered ring also requires a non-planar arrangement of the phenyl and pyrazole rings. Thus in **(4.38a-c)** the angle between the mean last squares plane of the phenyl and pyrazole varies between 51.35° **(4.38b)** and 54.52° **(4.38c)**, whilst in the five membered ring precursors **(2.13a-c)** the corresponding angle varies between only 3.42° **(2.13c)** and 5.05° **(2.13b)**. To conclude the insertion of DMAD into the M–C bond occurs for all three complexes **(2.13a,b,c)** and no evidence for the N–C bond formation was found.

4.2.1.2 Reaction of diphenylacetylene with (2.13a-c)

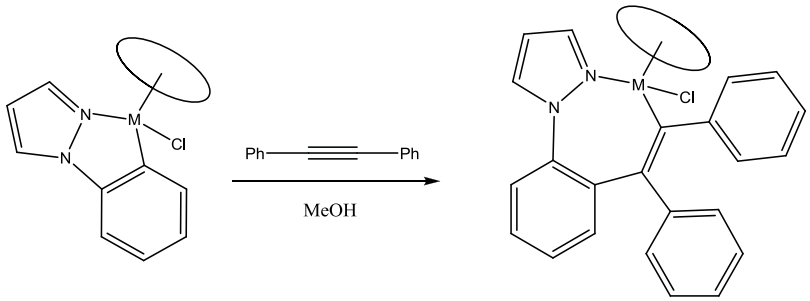

(2.13a) M= Ir, ring = Cp*
(2.13b) M= Rh, ring = Cp*
(2.13c) M= Ru, ring = *p*-cymene

(4.39a) M = Ir, ring = Cp*
(4.39b) M = Rh, ring = Cp*
(4.39c) M = Ru, ring = *p*-cymene

Scheme 4.21

The reaction of **(2.13a)** with diphenylacetylene in MeOH was attempted **(Scheme 4.21)**. Monitoring by ES-MS spectrometry showed a decrease of the peaks at *m/z* 379

[**(2.13a)**-Cl]$^+$ and 420 [**(2.13a)**+MeCN]$^+$ and appearance of a new peak at *m/z* 647 [**(4.39a)**-Cl]$^+$. After 3 hours, only one peak was observed at *m/z* 649 [**(4.39a)**-Cl]$^+$, and the reaction was assumed to be complete. After evaporation and washing with hexane, **(4.39a)** was isolated in 62% yield.

The ^{1}H NMR spectrum of **(4.39a)** shows a Cp* signal at δ 1.36 with an upfield shift of 0.30 ppm compared to **(2.13a)** at δ 1.66. This can be explained by a ring current effect of the Cp* lying over the cyclometallated phenyl of the 2-phenylpyrazole group, as observed for complexes **(4.38a-c)**. The pyrazole group gives rise to two doublets at δ 7.91 (H^3) and δ 8.41 (H^1), and a triplet at δ 6.56 (H^2). These chemical shifts are close to the ones observed for **(4.38a)** at δ 7.81 (H^3), 8.21(H^1) and 6.51(H^2). In the ^{13}C NMR spectrum, the expected number of quaternary and C–H carbons is seen and the metallated carbon is observed at δ 161.23 (C^{11}) which is higher field than the metallated carbon in **(4.38a)** at δ 176.15. The FAB-MS spectrum showed ions at *m/z* 647 [M-Cl]$^+$ and 684 [M]$^+$. Crystallisation of **(4.39a)** from DCM/hexane gave crystals suitable for X-ray diffraction and the structure is discussed below with the related complex **(4.39b)** and **(4.39c)**.

Reaction of **(2.13b)** with diphenylacetylene in MeOH was attempted **(Scheme 4.21)**. After 3 hours the mixture was evaporated and washed with hexane and **(4.39b)** was isolated in 62% yield. The ^{1}H NMR spectrum of **(4.39b)** showed similar signals to the ones observed for **(4.39a)** with one Cp* signal at δ 1.35 (cf δ 1.36 for **(4.39a)**). The pyrazole group gives rise to two doublets at δ 8.56 (H^1) and 7.92 (H^3) and a triplet at δ 6.56 for H^2. In the ^{13}C NMR spectrum, the expected number of quaternary and C–H carbons is seen and the metallated carbon is observed at δ 176.08 (C^{11}) as a doublet (J_{Rh-C} 30.5 Hz). The FAB-MS spectrum showed an ion at *m/z* 559 [M-Cl]$^+$.

Crystallisation of **(4.39b)** from DCM/hexane gave crystals suitable for X-ray diffraction and the structure is discussed below with the related complexes **(4.39a)** and **(4.39c)**.

Ruthenium complex **(4.39c)** was obtained similarly from the reaction of **(2.13c)** with diphenylacetylene in MeOH **(Scheme 4.21)**. The reaction was monitored by ES-MS spectrometry. Peaks from **(2.13c)** namely *m/z* 379 [**(2.13c)**-Cl]$^+$ and 420 [**(2.13c)**-Cl+MeCN]$^+$ decrease over time and a new peak at *m/z* 557 [**(4.39c)**-Cl]$^+$ increases. After 1 hour the peaks at *m/z* 379 and 420 were no longer visible and the reaction was assumed to have finished. Removal of the solvent and washings with hexane to remove diphenylacetylene gave **(4.39c)** as a brown solid in 42 % yield.

The ^{1}H NMR spectrum of **(4.39c)** shows the expected signals an inserted diphenylacetylene complex and is very similar to **(4.39a)** with a *p*-cymene replacing the Cp*. A singlet integrating for 3 H for the Me of the *p*-cymene is observed at δ 2.44, the isopropyl group gives rise to two doublets at δ 1.08 and 1.23 and a septet at δ 2.79. The four aromatic protons of the *p*-cymene are also inequivalent and four doublets of doublets are observed at δ 3.48, 4.49, 4.63 and 5.54, similar to **(4.38c)** (between δ 4.12 and 5.52). These data are consistent with the metal centre being chiral and epimerisation being slow on the NMR timescale. The pyrazole gives rise to two doublets at δ 8.57 (H^1), δ 7.85 (H^3) and a triplet at δ 6.50 (H^2). The cyclometallated phenyl system is composed of four protons, three multiplets at δ 7.26, 7.29 and 7.34 for H^7, H^6 and H^5 respectively and a doublet of triplet for H^8 at δ 7.22. The assignment is confirmed by a cross peak between (H^3) and (H^5) in the NOESY spectrum. The ^{13}C NMR spectrum shows the expected number of C–H and quaternary carbons, the metallated (C^{11}) is observed at δ 183.19, relatively close to the corresponding signal in **(4.38c)** at δ 190.94. The FAB-MS spectrum showed a peak at *m/z* 557 assigned as [M-Cl]$^+$.

Crystallisation of **(4.39c)** from DCM/hexane gave crystals suitable for X-ray diffraction, however it has two molecules in the unit cell and the Ru–C and Ru–N bond lengths vary in the two molecules therefore bond lengths and angles are not discussed below. The X-ray structure is shown with that of **(4.39a)** and **(4.39b)** in **Fig 4.2** with selected distances and angles in **Table 4.2**.

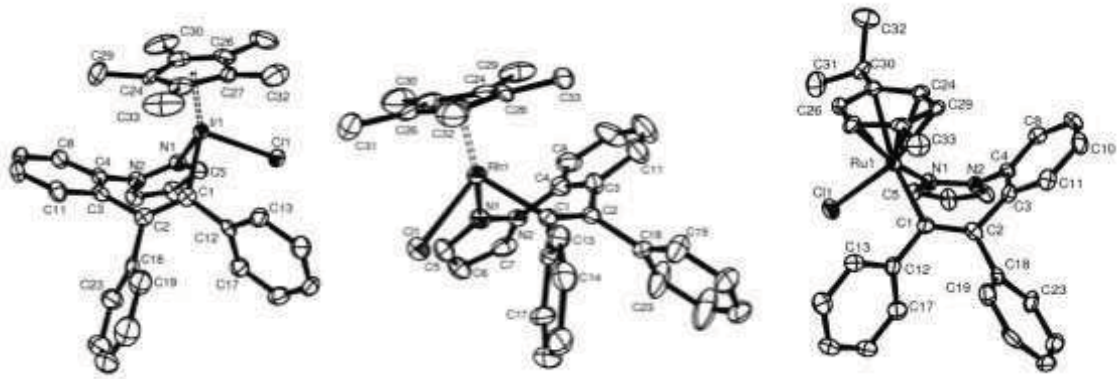

(4.39a) **(4.39b)** **(4.39c)**

Fig 4.2 Molecular structures for **(4.39a)**, **(4.39b)** and **(4.39c).** H atoms have been omitted for clarity.

Table 4.2 Selected bond distances [Å] and bond angles [°] for **(4.39a), (4.39b).**

	(4.39a)	**(4.39b)**
M(1)-N(1)	2.088(5)	2.096(6)
M(1)-Cl(l)	2.4254(15)	2.411(2)
M(1)-C(1)	2.069(6)	2.061(7)
C(3)-C(2)	1.505(8)	1.452(10)
C(2)-C(1)	1.341(8)	1.355(10)
N(1)-M(1)-C(1)	82.9(2)	84.5(2)
N(1)-M(1)-Cl(1)	86.45(14)	87.29(19)
Cl(1)-M(1)-C(1)	89.67(16)	91.5(2)

Complexes **(4.39a,b,c)** have a similar structure to **(4.38 a,b,c)** and confirm that the alkyne has inserted into the M-C bond rather than the M-N bond, to form the seven-membered ring. The M–C bond lengths of **(4.39a)** and **(4.39b)**, [2.069(6) and 2.061(7) Å respectively] are shorter than the M–N bond lengths **[**2.088(5) and 2.096(6) Å] respectively as found for **(4.38a,b)**. The chelate angles of **(4.39a,b)** [82.9(2) and 84.5(2)° respectively] are slightly less than those in **(4.38a,b)** [85.08(16) and 85.67(9)° respectively] . This is presumably due to the increased size of the phenyl substituent in **(4.39a,b)** compared with a CO_2Me substituent in **(4.38a,b)**. As found in **(4.38a-c)** the phenyl and pyrazole are not coplanar, the angles between the planes of the pyrazole and original cyclometallated phenyl are 52.66° and 45.55° in **(4.39a)** and **(4.39b)** respectively.

These results showed that diphenylacetylene inserts into the M-C bond of the three complexes **(2.13a-c)** and no evidence for N–C bond formation was observed with pyrazole as a directing group with either DMAD or diphenylacetylene. This again suggests that the two first steps of the postulated mechanism of catalytic C–H activation/insertion are certainly feasible with Ir, Rh and Ru complexes **(Scheme 4.5)**.[13]

4.2.1.3 Reaction of phenylacetylene with (2.13a-c)

There are few examples of stoichiometric insertion reactions with terminal alkynes,[27, 28, 29, 30, 31] and in the case of half sandwich complexes only two examples have been reported with insertion of terminal alkynes, one with [CoI(DMBA)Cp][32] and recent work from our group on a Cp*Ir cyclometallated oxazoline.[33]

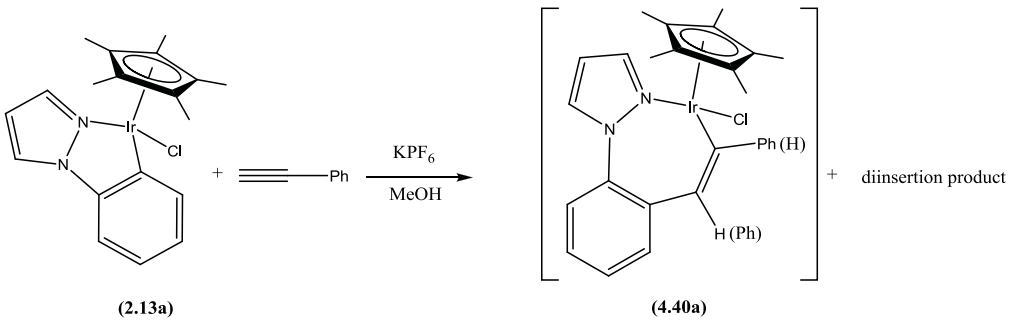

(2.13a) (4.40a)

Scheme 4.22

The complex **(2.13a)** was reacted with phenylacetylene in MeOH in the presence of KPF_6 **(Scheme 4.22)**. The reaction was monitored by ES-MS spectrometry and after 5 min, three signals were observed at *m/z* 471, 573 and 675 which were assigned as [**(2.13a)**-Cl]$^+$, [**(2.13a)**-Cl+PhCCH]$^+$, [**(2.13a)**-Cl+2PhCCH]$^+$. The reaction appears to give a mixture of mono and diinsertion products with the second insertion occurring at least with a similar rate as the first one, so that it is not possible to get clean conversion into the monoinserted product. Therefore a second equivalent of phenylacetylene was added to drive the reaction to the diinsertion product. After 3 hours, only one peak was observed in the ES-MS spectrum at *m/z* 675 [**(2.13a)**-Cl+2 PhCCH]$^+$. The ^{1}H NMR spectrum showed a mixture of 2 Cp* signals at δ 1.71 and 1.65 with a ratio 1:5 suggesting a mixture of two products. The ratio between the integrals of the Cp* and the aromatic signals for the major product agreed with 2 molecules of phenylacetylene inserted into one complex. Phenylacetylene can insert two ways round for the first and the second insertion which can produce a complex mixture of isomers and multiple insertions are known for cyclopalladated complexes[34-37] and Ir half sandwich complexes.[33] Attempts to purify the mixture by crystallisation and chromatography were not successful, hence no products could be unambiguously characterised.

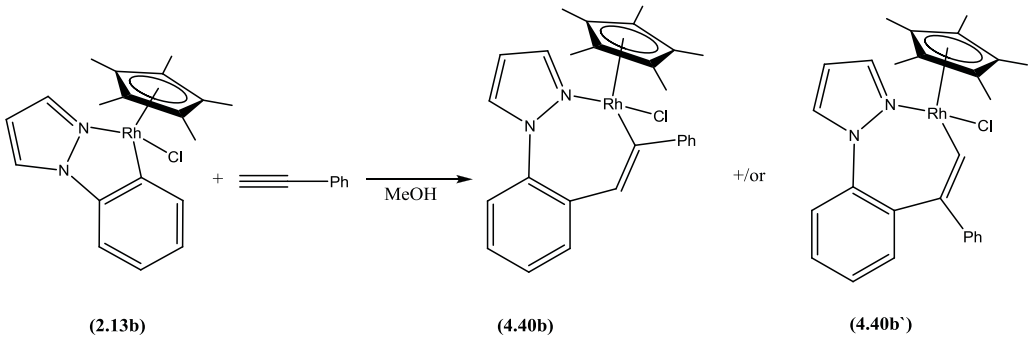

(2.13b) (4.40b) (4.40b`)

Scheme 4.23

The insertion of phenylacetylene was also tried with **(2.13b) (Scheme 4.23)**. Monitoring by ES-MS spectrometry showed the reaction was complete after 5 hours with only one product peak being observed at *m/z* 483 [**(4.40b)**-Cl]$^+$ or [**(4.40b`)**-Cl]$^+$. This suggests that the reaction is slower for rhodium than for iridium, and the monoinsertion product is significantly less reactive than the starting complex **(2.13b)** so that the monoinserted product can be isolated.

The ^{1}H NMR spectrum of the product shows one set of signals with a 1:1:1 ratio of Cp* to the cyclometallated 2-phenylpyrazole and phenylacetylene which suggests only one regioisomer was obtained. The Cp* signal is observed at δ 1.30, which is the same chemical shift as that observed for **(4.38b)**. The pyrazole gives rise to two doublets of doublets at δ 7.76 (H^3) and δ 8.46 (H^1), both signals showing a mutual $^4J_{H\text{-}H}$ coupling of 1 Hz, and a triplet at δ 6.48 for H^2. In the ^{13}C NMR spectrum, the expected number of quaternary and C–H carbons for insertion of one phenylacetylene is seen. The metallated carbon is easily identified due to coupling with rhodium and is observed as a doublet at δ 178.64 ($J_{Rh\text{-}C}$ 125 Hz). A DEPT spectrum shows that the metallated C is a quaternary carbon rather than a C–H which allows us to assign the product as **(4.40b)** rather than **(4.40b`).** This regioselectivity is identical to that observed for a Cp*Ir cyclometallated oxazoline complex.[33] The FAB-MS spectrum showed an ion at *m/z* 483 [M-Cl]$^+$.

The same reaction has also been investigated with the cycloruthenated complex **(2.13c) (Scheme 4.24).** The reaction was monitored by ES-MS spectrometry, and after 1 hour one peak was observed at *m/z* 481 [**(2.13c)**-Cl+PhCCH]$^+$. The ^{1}H NMR spectrum showed three sets of *p*-cymene signals, one of which was assigned to the starting complex. To try to convert more of the starting complex into product another equivalent of phenylacetylene was added. Unfortunately instead of leading to more conversion, decomposition was complete after two days exposed to air and light. The ^{1}H NMR spectrum showed broad signals and liberation of non-coordinated *p*-cymene with a septet at δ 2.90 and a doublet at δ 1.35 for the isopropyl group, a singlet at δ 2.40 for the Me and a (4 H) multiplet for the aromatic protons at δ 6.90. The excess of phenylacetylene could displace the *p*-cymene instead of converting the starting complex into the inserted product.

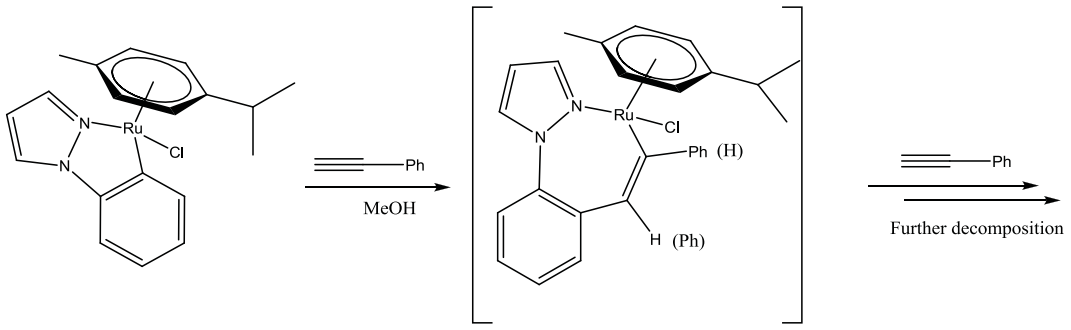

(2.13c) **(4.40c)**

Scheme 4.24

To conclude, with the insertions of phenylacetylene, in the case of **(2.13b)** a mono insertion is observed with the selective formation of one isomer **(4.40b)**. In the case of **(2.13a)** mono and diinsertion occurs with the possibility of having multiple isomers; diinsertions with half sandwich complexes of IrCp* have recently been reported.[33] In the case of **(2.13c)** more than one product is formed and further reactions led to loss of the *p*-cymene ligand. The outcome of the reaction is different from one metal to the other which suggests that the metal plays an important role in the insertions of

phenylacetylene. These results contrast with the insertions of DMAD where only one alkyne inserts in each case and all three products are stable. The reactions with diphenylacetylene and DMAD demonstrate that for the postulated mechanism proposed by Miura *et al.* the C–H activation/insertion steps are certainly reasonable.[13]

4.2.2 Reactions of alkynes with (2.10a)

Insertion of DMAD into the M-C bond of **(2.10a) (Scheme 4.11)** to form **(4.19a,b)** has been reported by Jones *et al.* (see section 4.1).[18] Addition of copper acetate was necessary to promote C–N bond formation and release of the isoquinoline salt. The formation of **(4.19a)** has been repeated and full assignment is avalaible in the experimental section. The reactivity of **(2.10a)** towards diphenylacetylene and phenylacetylene is discussed below.

The reaction of **(2.10a)** with diphenylacetylene was monitored by ES-MS spectrometry, and after 5 min only one peak was observed at *m/z* 660 [**(2.10a)**-Cl+PhCCPh]$^+$. The ^{1}H NMR spectrum showed a mixture of **(2.10a)** with a Cp* signal at δ 1.59, and two other products with Cp* signals observed at δ 1.40 and 1.25. The ratio of these three products being 0.1:1:0.7. This mixture was left in $CDCl_3$ and further changes were observed. After 10 days, the major product disappeared leaving only two remaining Cp*Ir signals with a ratio 0.1:1. The FAB-MS spectrum at this stage showed three peaks at *m/z* 332, 482 and 660 assigned as the isoquinolinum salt [**4.41C**]$^+$, [**(2.10a)**-Cl]$^+$ and [**(2.10a)**-Cl+PhCCPh]$^+$ respectively. A plausible explanation for these data would be the formation of the diphenylacetylene-inserted complex **(4.41 A)** which then undergoes N–C bond formation to give **(4.41B)** which then decoordinates from the metal to give the isoquinolinum salt **(4.41C) (Scheme 4.25).** Both **(4.41A)** and **(4.41B)** would be expected to show ions at *m/z* 660 in the FAB-MS spectrum. Further purification (chromatography and crystallisations) was not successful.

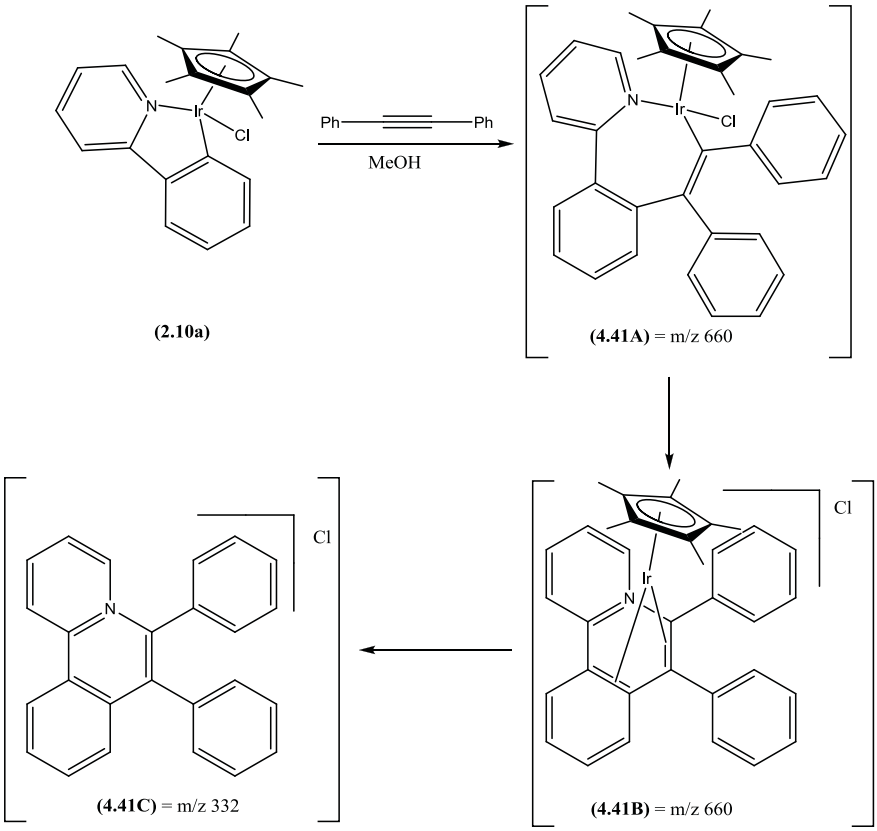

Scheme 4.25 Plausible interpretation of the reaction of **(2.10a)** with diphenylacetylene

The same complex **(2.10a)** was reacted with one equivalent of phenylacetylene and the reaction was monitored by ES-MS spectrometry. After 1 hour the ES-MS spectrum showed 2 peaks at *m/z* 482 [**(2.10a)**-Cl]$^+$ and 686 [**(2.10a)**-Cl+2PhCCH]$^+$. The reaction appears to give only diinsertion products, with the second insertion occurring faster than the first one, so that it is not possible to get clean conversion into the monoinserted product. Therefore a second equivalent of phenylacetylene was added to drive the reaction to the diinsertion product. After one more hour, only one peak was observed in the ES-MS spectrum at *m/z* 686 [**(2.10a)**-Cl+2PhCCH]$^+$. This is similar to the observations of the reaction of **(2.13a)** with phenylacetylene discussed earlier (section 4.2.1.3)**.**

The ^{1}H NMR spectrum showed a mixture of products and three significant Cp* signals observed at δ 1.59 **(2.10a)**, 1.55 and 1.22 with a ratio of 0.3:0.5:1 respectively. Further evidence of a mixture of three products is observed in the FAB-MS spectrum with three

signals at *m/z* 482 [**(2.10a)**-Cl]$^+$, 582 [**(2.10a)**-Cl+HCCPh]$^+$, 686 [**(2.10a)**-Cl+2HCCPh]$^+$. The peak at *m/z* 582 is an evidence for a monoinsertion product (Note, if the loss of Cl^- is not favoured it may be difficult to see this ion by ES-MS spectrometry), furthermore no isoquinoline fragment was observed which suggests that the ring closure process is not involved **(Scheme 4.26)**. Attempts to isolate any pure product by crystallisation and chromatography failed.

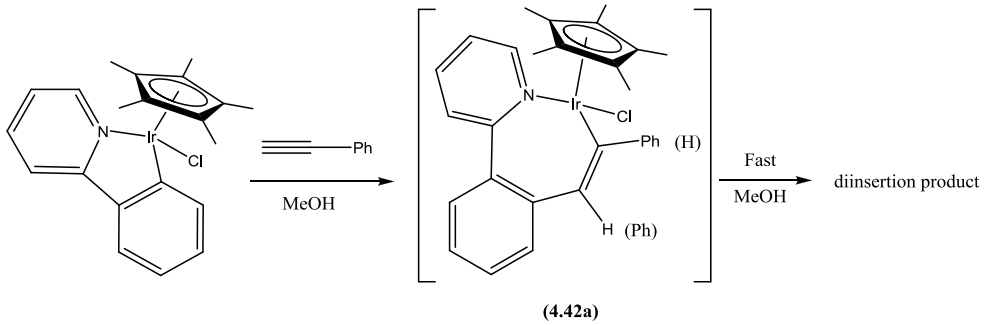

(4.42a)

Scheme 4.26 Plausible interpretation of the reaction of **(2.10a)** with phenylacetylene

In conclusion **(2.10a)** reacts with diphenylacetylene however the results are different to those obtained by Jones *et al.* with DMAD.[18] The ES-MS spectrum suggests that mono insertion occurs but that this product is unstable. From the reaction with diphenylacetylene, the presence of a peak at the mass of the isoquinolinium cation in the FAB-MS spectrum suggests that reductive elimination can take place without an oxidising agent, as observed by Fagnou *et al.*(see section 4.1).[22] This would mean that C–N bond formation is observed when the substituent changes from an electron withdrawing (CO_2Me) to a phenyl group consistent with the results reported by Pfeffer *et al.* (see section 4.1).[19, 20, 24]

4.2.3 Insertion of alkynes into cyclometallated imine complex (2.9b)

Further investigations of the effect of the substituent on the alkyne and the parameters involved in the ring closure were carried out with the rhodium complex **(2.9b)** reported

by Jones *et al.*[18] The reaction of **(2.9b)** with DMAD was repeated, and afforded the expected product. The description of the ^{1}H NMR and ^{13}C NMR of **(4.18b)** is available in the experimental section.

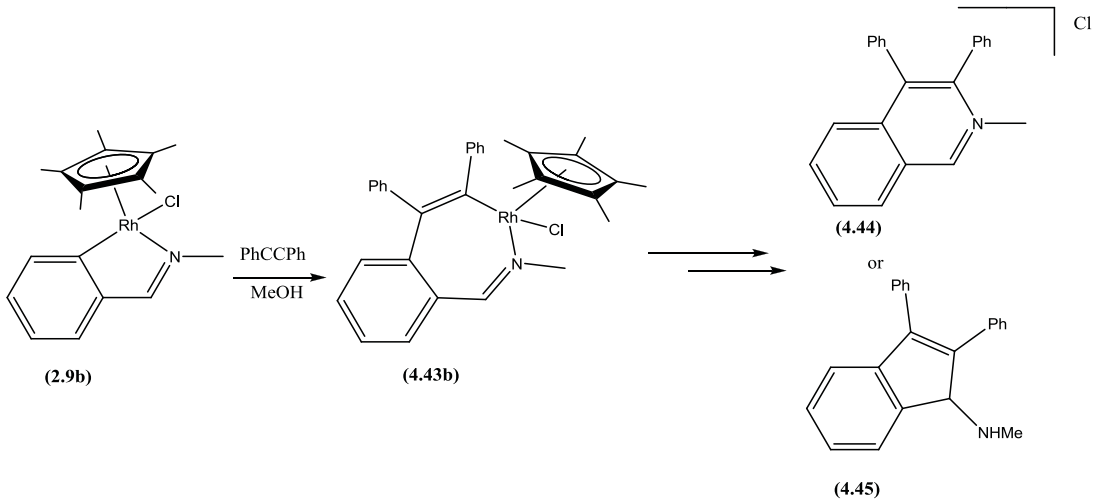

Scheme 4.27

The reaction of **(2.9b)** with diphenylacetylene was then attempted **(Scheme 4.27)**. After 5 min the ES-MS spectrum showed three signals at *m/z* 356 [**(2.9b)**-Cl]$^{+}$, 397 [**(2.9b)**-Cl+MeCN]$^{+}$ and 534 [**(2.9b)**-Cl+PhCCPh]$^{+}$. After 45 min a precipitate was formed, ES-MS and FAB-MS spectra of the solid showed a peak at *m/z* 296 [isoquinolinum salt]$^{+}$ implying C–N formation and dissociation of **(4.44)** from the metal has taken place. However C–C bond formation to form a carbocycle **(4.45)** cannot be ruled, though C–C bond formation has so far only been observed with N-aryl substituents.[14] The ^{1}H NMR spectrum of the precipitate shows a mixture of products with two broad and intense signals in the Cp* region at δ 1.58 and 1.55 and one set of signals for the cyclometallated ligand with an NMe signal at δ 3.36. The ratio of the signals for the ligand and the two Cp* peaks is 1:4:0.8 respectively. This could imply that the isoquinoline salt is liberated however purification by crystallisation or chromatography was not successful.

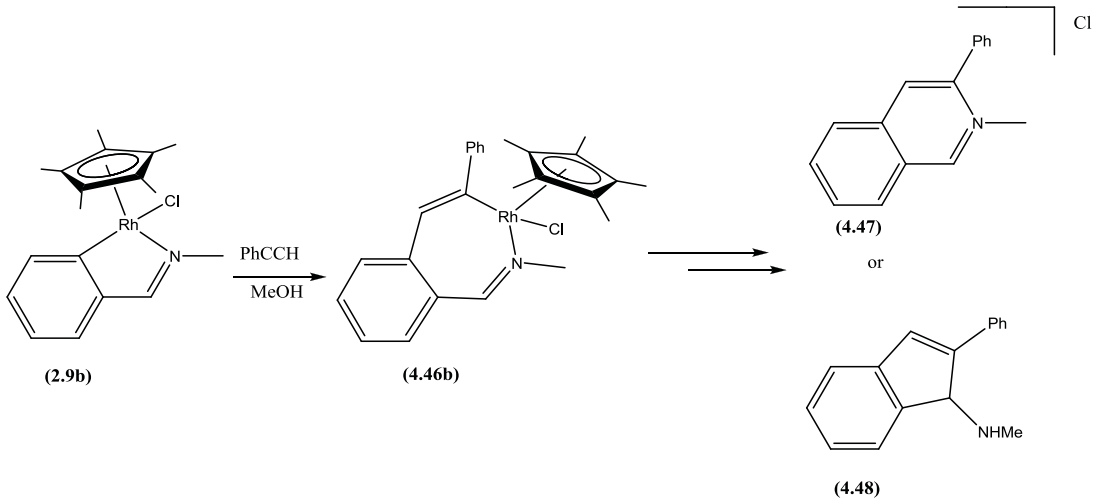

Scheme 4.28

Reaction of **(2.9b)** with phenylacetylene was also examined **(Scheme 4.28).** After 5 min the ES-MS spectrum showed three signals at *m/z* 356 [**(2.9b)**-Cl]$^+$, *m/z* 397 [**(2.9b)**+MeCN]$^+$ and 458 [**(2.9b)**+PhCCH]$^+$, a solid precipitated after 30 min and after 45 min only one peak was observed at *m/z* 458 [**(2.9b)-**Cl+PhCCH]. The ^{1}H NMR spectrum of the solid shows a 1:1:1 ratio of signals due to the Cp*, the cyclometallated N-methylbenzylidene and phenylacetylene fragments. Only one set of signals is observed which implies that only one regioisomer is observed. Two singlets at δ 1.35 and 3.89 were assigned, to a Cp* and an NMe signal respectively. An upfield shift of 0.34 ppm is observed for the Cp* in comparison to **(2.9b)** at δ 1.69, consistent with the formation of a monoinsertion complex **(4.46b)** by analogy to **(4.40b)**. The regioselectivity was further confirmed by X-ray diffraction see below. After a few hours in $CDCl_3$, further reaction occurs and a new set of signals is observed. The Cp* signal is observed at δ 1.63, and the NMe signal is observed at δ 3.43. The FAB-MS spectrum at this stage shows two peaks at *m/z* 220 [isoquinolinum salt]$^+$ and 458 [**(2.9b)-**Cl+PhCCH]$^+$. Further purification by crystallisation and chromatography failed. A proposal for the interpretation of these data would be that the first product formed is **(4.46b)** which reacts further in solution. C–N[19, 20, 24] or C–C[11] bond formation occurs to

produce **(4.47)** or **(4.48)**. A discussed above for diphenylacetylene, C–C is less likely than C–N bond formation. The signal for the isoquinolinium salt **(4.47)** in the FAB-MS spectrum suggests that reductive elimination and dissociation from the metal is possible without Cu. A crystal structure of the complex **(4.46b)** was obtained and is shown in **Fig 4.3** with selected bond distances and angles and is discussed below.

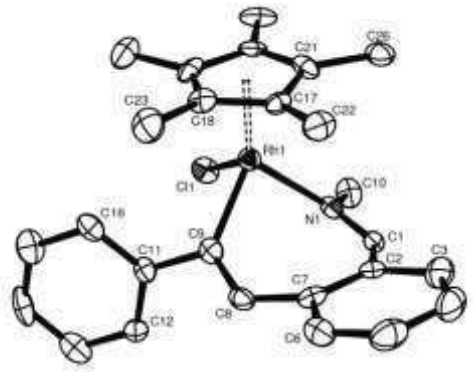

Fig.**4.3** Molecular structure of **(4.46b).** H atoms have been omitted for clarity.

Selected bond distances and angles for **(4.46b)**: M(1)-N(1), 2.059(6) Å; M(1)-Cl(l), 2.4130(19) Å; M(1)-C(9), 2.029(7) Å; C(9)-C(8),1.365(9) Å; C(8)-C(7), 1.484(9) Å, N(1)-M(1)-C(9), 87.6(3)°; N(1)-M(1)-Cl(1), 89.63(16)°; Cl(1)-M(1)-C(9), 90.00(2)°

The complex **(4.46b)** adopts a pseudo octahedral structure and shows the expected 7 membered ring and that C–N or C–C bond formation has not occurred yet. The regioselectivity is the same as for **(4.40b)** with the phenyl from the phenylacetylene on the metallated carbon. The M–C and M–N bond lengths in **(4.46b)**, [2.029(7) and 2.059(6) Å respectively] are shorter than the corresponding bonds for **(4.39b)** [2.061(7) and [2.096(6) Å respectively] and the angle C-M-N is larger for **(4.46b)** than **(4.39b)**, [87.6 (3)°] and [84.5(2)°] respectively.

From this limited study with the cyclometallated imine complex **(2.9b)**, the same observations can be made as with 2-phenylpyridine as ligand. Simple insertion of DMAD occurs to provide the expected products **(4.18b)** and **(4.19a)** as observed

previously.[18] The reactions of diphenylacetylene and phenylacetylene seem to lead to the inserted compounds but these are unstable probably undergoing reductive elimination, as evidenced by peaks consistent with the free organic fragments being observed in the ES-MS spectra.

4.2.4 Insertion reactions of alkynes with (3.13a)

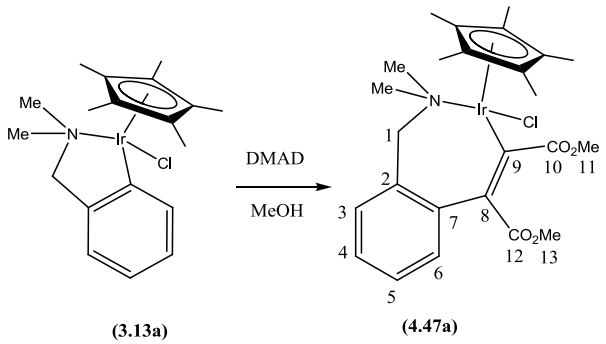

(3.13a) (4.47a)

Scheme 4.29

As mentioned in section 4.1 Pfeffer *et al*. have carried out an extensive study of the reaction of cyclometallated DMBA Ru-complex **(4.14)**. However, similar reactions with the corresponding Cp*Ir-complex have not been reported though preliminary studies have been carried out in our group.[38] Hence, complex **(3.13a)** was reacted with DMAD in MeOH **(Scheme 4.29)**. After one hour the ES-MS spectrum showed only one peak at *m/z* at 604 [**(4.47a)**-Cl]$^+$. The ^{1}H NMR spectrum showed a ratio 1:1:1 between the Cp*, the cyclometallated DMBA and DMAD. The Cp* is observed at δ 1.13, 0.5 ppm upfield from the starting complex **(3.13a)** at δ 1.63. This is consistent with the Cp* lying over the cyclometallated phenyl ring hence being affected by a ring current, as observed for **(4.38a)** and **(4.39a)**. The NMeMe` group shows two singlets at δ 2.70 and δ 3.09, and two mutually coupled doublets at δ 2.94 and 3.96 are assigned to the benzyl protons, the inequivalence of these is consistent with the metal being a chiral centre and epimerisation being slow on the NMR timescale. The OMe signals are observed at δ 3.66 and δ 3.78, these are close to the chemical shifts observed for the OMe signals of Ir

complex **(4.38a)**. The aromatic protons show two doublets at δ 7.29 and 7.46 for H^3 and H^6 respectively whilst H^4 and H^5 show triplets of doublets at δ 7.39 and at δ 7.23 respectively. This assignment is confirmed by a cross peak between one of the benzyl protons and H^3 in a NOESY spectrum. The ^{13}C NMR spectrum shows the expected number of signals for C–H and quaternary carbons. The metallated C^9 is observed at δ 180.43 which is again very close to the ones observed before and reported by Jones *et al.*[18] The FAB-MS spectrum shows a peak at *m/z* 604 [**(2.47a)**-Cl]$^+$, and crystallisation from DCM/hexane gave crystals suitable for X-ray diffraction. The X-ray structure is shown in **Fig 4.4** with selected distances and angles and is discussed below**.**

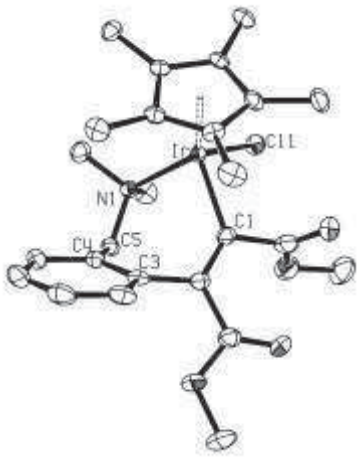

Fig. 4.4 Molecular Structure of **(4.47a).** H atoms have been omitted for clarity.

Selected bond distances and angles for **(4.47a) :**Ir(1)-N(1), 2.250(4) Å; Ir(1)-Cl(l), 2.4197(16) Å; Ir(1)-C(1), 2.039(5) Å; C(1)-C(2), 1.359(7) Å; C(2)-C(3), 1.493(7) Å, N(1)-Ir(1)-C(1), 87.78(17)° ; N(1)-Ir(1)-Cl(1) 90.65(10)°; Cl(1)-Ir(1)-C(1), 90.85(13)°

The structure of **(4.47a)** confirms that the alkyne has inserted into the Ir-C to form the seven-membered ring. The chelate bite angle [87.78(17)°] is bigger for **(4.47a)** than that [78.48(18)°] for **(3.13a)**[38], consistent with an increased size of the cyclometallated ring in **(4.47a)**. The M-C bond in **(4.47a)** [2.039(5) Å], is the same as that [2.050(5) Å] in

the other DMAD insertion product **(4.38a)**. On the other hand the M-N bond distance is significantly longer [2.250(4) Å vs 2.086(4) Å] as expected for an sp^3 N atom compared with an sp^2 one, it is also longer than that [2.186(4) Å] in starting complex **(3.13a)**.[38] No ring closure has occurred in this case consistent with all other alkyne insertions involving DMAD described above and those published by Pfeffer and Jones.[18, 20]

Previously in our group, **(3.13a)** was reacted with diphenylacetylene in MeCN in the presence of KPF_6 to form **(4.48a)**, which was identified by X-ray crystallography in 85% yield **(Scheme 4.30)**.[38]

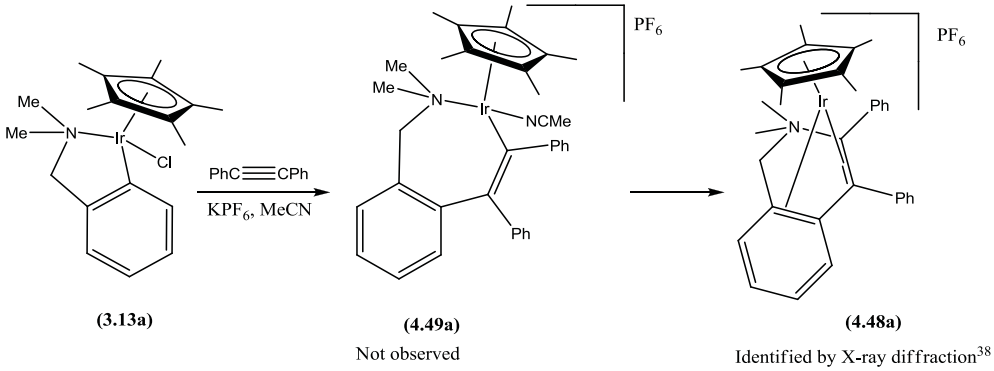

Scheme 4.30

The reaction of **(3.13a)** with diphenylacetylene was repeated in MeOH without KPF_6, unfortunately no product was isolated, and it appears that decomposition occurred as soon as the solvent was evaporated. Hence, the reaction was repeated using the original conditions. The ^1H NMR spectrum in $CDCl_3$ showed one major species, and a second minor Cp*Ir complex. The major product showed a Cp* signal at δ 1.51. The NMe_2 group gave rise to two sharp signals at δ 2.50 and 2.82, with the benzyl protons being observed as mutually coupled doublets at δ 3.26 and 3.82, these signals are consistent with **(4.48a)** however the original data were recorded in MeCN so direct comparison is not possible. The minor species appeared to be an isomer with two 3H singlets, two mutually coupled 1H doublets and notably a Cp* resonance shifted to higher field at δ 1.70 , this last shift perhaps suggesting a seven-membered insertion product consistent

with a small amount of **(4.49a)** which is the presumed intermediate on the way to **(4.48a)**.

The solid was not very soluble in $CDCl_3$ so the spectrum was run again in CD_3CN. The ^1H NMR spectrum in CD_3CN showed only one species present. The Cp* signal was observed at δ 1.28 i.e. 0.23 ppm upfield from **(4.48a)**. Two singlets at δ 2.81 and 3.21 were assigned as NMeMe` signals, and the benzyl protons showed two mutually coupled doublets at δ 3.29 and 4.42, which is consistent with the metal being a chiral centre and epimerisation being slow on the NMR timescale. This data is very close to that recorded earlier[38] and the high field shift for the Cp* makes this more consistent with it being **(4.49a)**. The ^{13}C NMR spectrum shows the expected number of C–H and quaternary carbons, notably, all six quaternary carbons are between δ 133.59 and 154.30, the last of which is assigned to the metallated carbon. These are quite low field shifts, complexes of type **(4.48a)** in which C_2 and $C_{7\text{-}9}$ are bonded in a π–fashion to the metal usually have shifts much less than this, as observed by Pfeffer for Ru-analogues and in complex **(4.53a)** below.[19,20] Hence this complex is assigned as **(4.49a)**. Interestingly, if the CD_3CN is removed and replaced with $CDCl_3$ the spectrum reverts to that observed originally i.e. **(4.48a)** with varying amounts of **(4.49a)**, presumably dependent on the amount of residual CD_3CN. This could be cycled two times with no other signals appearing. Unfortunately, attempted crystallisations of **(4.49a)** were not successful.

The results above suggest that **(4.48a)** can react with MeCN to convert back into **(4.49a)**. To investigate further, MeCN (ca 10 equivalents) was added to a solution of **(4.48a)** in $CDCl_3$, and the ^1H NMR spectrum, showed growth in signals of the minor species, which is consistent with the compound reacting with MeCN, as shown in **Scheme 4.31**.

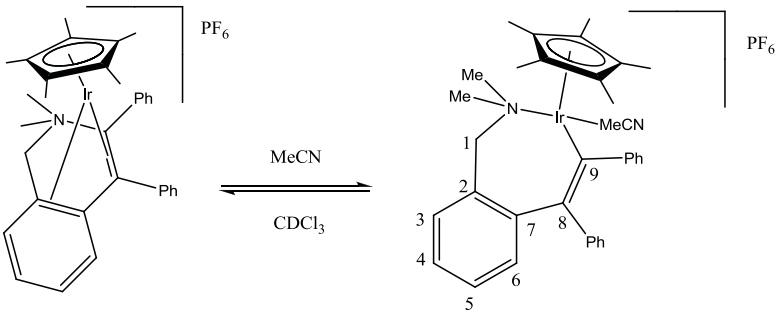

(4.48a) (4.49a)

Scheme 4.31

The ^{1}H NMR spectrum showed a Cp* signal at δ 1.28, two singlets for NMeMe` at δ 2.71 and 3.15, and two mutually coupled benzyl protons at δ 3.10 and 4.28, the ratio between **(4.48a)** and **(4.49a)** being 1.5:1 respectively. No signal for coordinated MeCN can be seen, it is either exchanging or under the signal for free MeCN at δ 1.94.

In this case it appears that the C–N bond formation is reversible, and dependent, on the presence of a coordinating ligand. In order to try and prove, the identity of **(4.49a)** substituting the MeCN by other ligands was attempted.

Addition of isopropylamine to a solution of **(4.48a)** did not cause any change to the complex so the reaction with PMe_3 was investigated. The complex **(4.48a)** was reacted with PMe_3 in DCM **(Scheme 4.32)**. The reaction was monitored by ES-MS spectrometry and after 5 min two peaks were observed at *m/z* 716 [**(4.48a)**+PMe_3]$^+$ and at *m/z* 515 [$IrCl(PMe_3)_2Cp^*$]$^+$. The ^{1}H NMR spectrum shows a mixture of two different products with a ratio 1:3. Integration suggests that the major product contains a Cp*, cyclometallated DMBA, diphenylacetylene and a PMe_3. It shows two doublets, one at δ 1.34 (9 H) assigned to the PMe_3, and one at δ 1.52 (15 H) assigned to a Cp* signal which couples with phosphorus, a broad singlet for NMeMe` at δ 2.33 and two mutually coupled benzyl protons at δ 3.48 and 4.07 and signals in the aromatic region. The minor product contains a doublet at δ 1.62 and a triplet at δ 1.78 in a ratio of 6:5 (i.e. $(PMe_3)_2$:Cp*), and no other signals hence this set is assigned to $[IrCl(PMe_3)_2Cp^*]PF_6$.

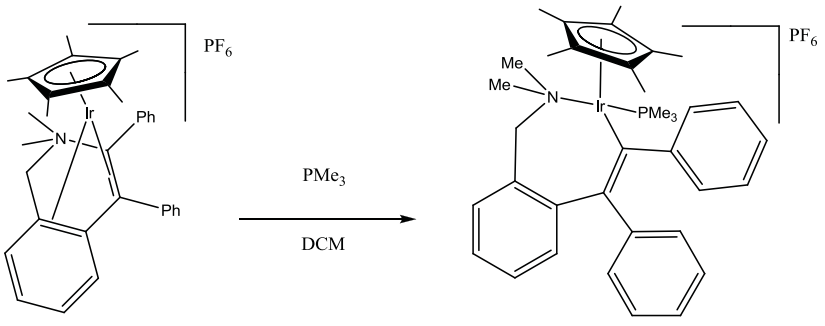

(4.48a) **(4.50a)**

Scheme 4.32

The ^{31}P NMR spectrum shows two signals at δ -45 assigned as $[IrCl(PMe_3)_2Cp^*]PF_6$ and at δ -37 for **(4.50a)**. Further purification of **(4.50a)** was difficult and crystallisation from DCM/hexane led to decomposition, with more of $[IrCl(PMe_3)_2Cp^*]PF_6$ being observed in the ^{31}P and ^{1}H NMR spectra.

4.2.5 Insertion of DMAD with (2.17a)

Up to this point all the insertion reactions studied have involved insertion into a cyclometallated phenyl group. Miura has shown that insertion into a cyclometallated vinyl is also possible (see **Scheme 4.9**); hence the reaction of **(2.17a)** with DMAD was investigated. The complex **(2.17a)** was reacted with DMAD in MeOH and the reaction was monitored by ES-MS spectrometry. Surprisingly, after 48 hours no reaction was observed so the mixture was heated at 50 °C for a further 48 hours but still no reaction was observed. Substitution of the chloride seems to be much more difficult with this complex. Hence to provide a more reactive complex, **(2.17a)** was reacted with $AgPF_6$ in MeCN to produce the corresponding MeCN cation **(4.51a)** as shown in **Scheme 4.33**.

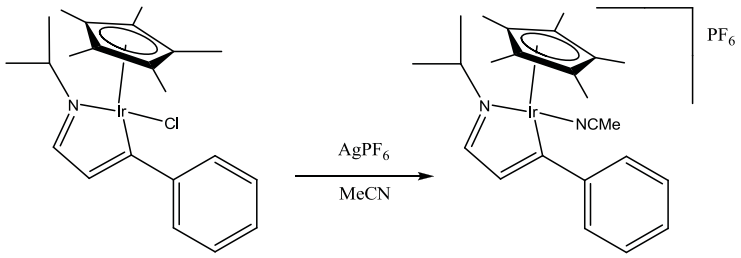

(2.17a) (4.51a)

Scheme 4.33

The ^{1}H NMR spectrum of **(4.51a)** shows a 1:1 ratio of the Cp* and the cyclometallated imine ligand with the Cp* signal at δ 1.55 which is 0.07 downfield compared to that of **(2.17a)**. The isopropyl group shows two doublets at 1.40 and 1.51 for the Me signals and a septet at δ 4.17 and all these chemical shifts are close to those observed for **(2.17a)**. The singlet for the coordinated MeCN appears at δ 2.59 as a sharp singlet. The imine signal was observed as a broad singlet at δ 8.12 which is similar to the imine proton of the starting complex **(2.17a)**. The ^{13}C NMR spectrum showed the expected number of C–H and quaternary carbons, the metallated C being at δ 197.13 further downfield than the metallated C on the starting complex **(2.17a)** at δ 173.00.

Complex **(4.51a)** was then reacted with DMAD in DCM, the reaction was monitored by ^{1}H NMR spectroscopy, and ES-MS spectrometry. At room temperature no reaction was observed after 4 hours but at 50°C the reaction was complete after 20 hours evidenced by a single peak at *m/z* 500 [**(4.51a)**-MeCN+DMAD]$^{+}$ in the ES-MS spectrum. The ^{1}H NMR spectrum of the product shows a 1:1:1 ratio between Cp*, the imine and DMAD but no MeCN. Three singlets are observed at δ 1.81, 3.80 and 3.88 for the Cp* and the two OMe signals. The isopropyl group gives rise to two doublets at δ 1.12 and 1.51 and a septet at δ 4.17. The imine proton is observed as a doublet at δ 8.68 and there is no evidence for a coordinated MeCN signal. Presumably MeCN has been liberated during the reaction and evaporated with the solvent, which suggests that N–C bond formation

has occurred to form **(4.53a)**. Note the relatively low field shift of the Cp* is also more consistent with **(4.53a)** than **(4.52a)** for which a shift to higher field is expected. The complex **(4.52a)** is presumably an intermediate during the reaction **(Scheme 4.34)**. The ^{13}C NMR spectrum showed the expected number for C–H and quaternary carbons. Crystallisation of **(4.53a)** from dichloromethane/hexane gave crystals suitable for X-ray diffraction. The X-ray structure is shown in **Fig 4.5** with selected distances and angles and discussed below.

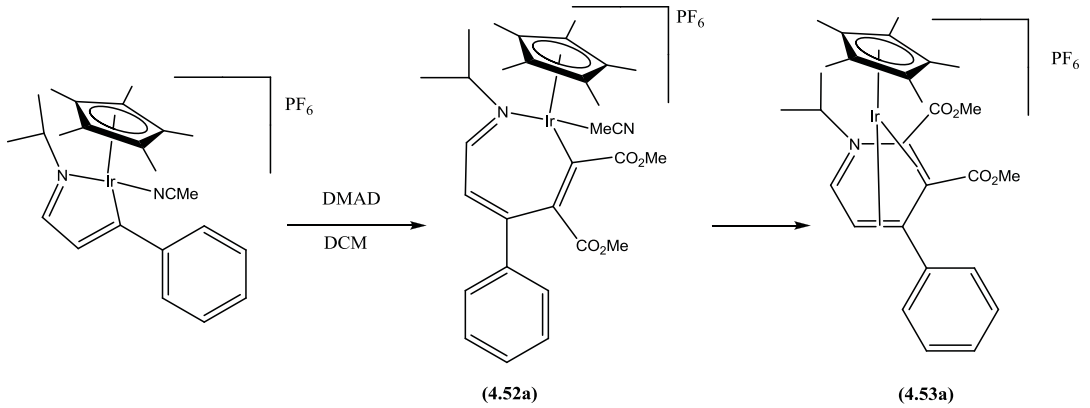

(4.52a) **(4.53a)**

Scheme 4.34

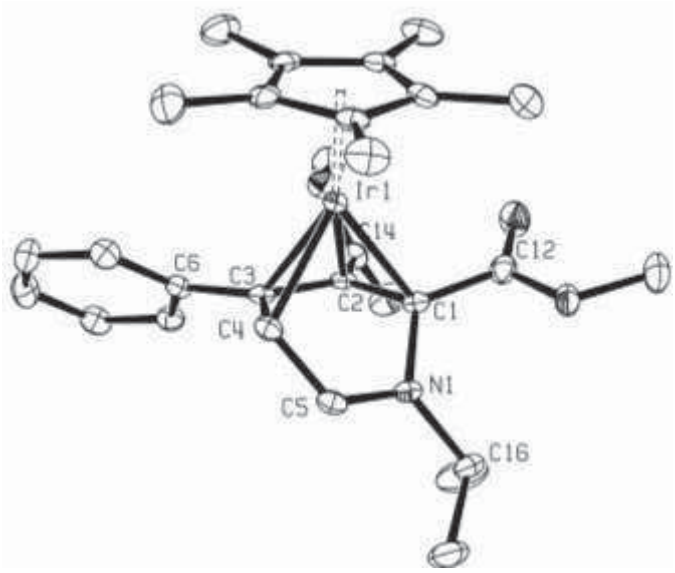

Fig. 4.5 Molecular structure of **(4.53a).** H atoms have been omitted for clarity.

Selected bond distances for the cation **(4.53a):** Ir(1)-C(1), 2.128(3) Å; Ir(1)-C(2) Å, 2.125(3); Ir(1)-C(3), 2.136(3) Å; Ir(1)-C(4), 2.130(3) Å; C(1)-C(2), 1.484(9) Å; C(2)-C(3), 1.426(4) Å; C(3)-C(4), 1.482(4) Å; C(1)-N(1), 1.479(3) Å, C(5)-N(1), 1.283(4) Å

The crystal structure of **(4.53a)** confirms that as predicted from the ^{1}H NMR spectrum N–C bond formation has occurred. The complex has a sandwich structure involving η^5-coordination of a Cp* ligand and an η^4-coordination of a pyridinium cation to a formally Ir(I) centre. The Ir–C(1) and Ir–C(4) lengths are statistically the same [2.128(3) and 2.130(3) Å respectively], the formal double bonds i.e. C(3)–C(4) [1.482(4) Å] and C(1)–C(2) [1.484(9) Å] are longer than the formal single bond C(2)–C(3) [1.426(4) Å] which is typical for a coordinated diene.[39]

In the case of **(2.17a)**, the insertion of DMAD was not observed even after heating the reaction, however insertion of DMAD was observed starting from a more reactive cation **(4.51a)**. The reductive elimination took place spontaneously, suggesting that this step is feasible even with electron withdrawing substituents on the alkyne. The ease of the reductive elimination is not only dependent on the substituent on the alkyne but also on the cyclometallated ligand.

4.3 Conclusion

This study shows that insertion of DMAD and diphenylacetylene into cyclometallated 2-phenylpyrazole complexes of Ir, Rh and Ru **(2.13a-c)** produces the 7 membered ring complexes in all cases. This demonstrates that the first two steps of the postulated mechanism described by Miura *et al.*[17] are certainly feasible. In agreement with Miura's results no C–N bond formation is observed on reaction of the pyrazole complexes with DMAD or diphenylacetylene.[13] However in contrast insertion of diphenylacetylene with cyclometallated 2-phenylpyridine **(2.10a)** and NMeimine **(2.9b)** complexes leads to a mixture of products and mass spectral evidences suggested that C–N bond formation is occuring. Reductive elimination and dissociation occur spontaneously without requiring a prior oxidation step in these cases.

Insertion of phenylacetylene leads to mixtures of mono and diinserted products with **(2.10a)**, **(2.13a)** and **(2.13c)** whereas a monoinserted complex was observed with **(2.13b)**. In the reactions of phenylacetylene with cyclometallated NMeimine **(2.9b)**, the ES-MS spectrum showed clear evidence for an insertion product however these initial products were unstable and the mass spectral evidence suggests that C–N bond formation and dissociation from the heterocycle has also occurred in this case.

Finally, this study shows, for the first time, that even with electron withdrawing substituents on the alkyne (DMAD), spontaneous C–N bond formation is feasible, hence the pyridinium complex **(4.53a)** has been characterised. This contrasts with Jones's results where Ir complexes containing DMAD would not form a C–N bond even after treatment with $CuCl_2$. Surprisingly, in the case of the isoquinolinium complex **(4.48a)**, preliminary results showed that the C–N bond formation is reversible, just by addition of MeCN. Overall, the ease of reductive elimination is dependent on the

combination of four factors (i) the metal, (ii) the cyclometallated directing group and (iii) the substituents on the alkyne, and (iv) the type of CH bond activated.

4.4 Experimental

The spectroscopic techniques/instruments used were as described in Chapter Two All starting materials were obtained from Aldrich, or prepared as described in Chapter 2 and Chapter 3 with the exception of complexes **(2.9b)**[18], **(3.13a)**[40] according to literature methods.

Preparation of **(4.18b)**

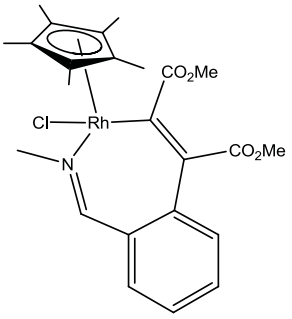

This was prepared in 74% yield as described in reference 18 from **(2.9b)** (15 mg, 0.038 mmol) and DMAD (17 mg, 0.12 mmol). The NMR data are the same as reported but are listed here for comparison with the other complexes.[1]H NMR: δ 1.31 (s, 15H, C_5Me_5), 3.66 (s, 3H, OMe), 3.71 (s, 3H, OMe), 3.83 (s, 3H, NMe), 7.28 (d, 1H, *J* 7.6, H^{Ph}), 7.29 (d, 1H, *J* 7.6, H^{Ph}), 7.35 (dd, 1H, *J* 7.6, 7.4, H^{Ph}), 7.45 (dd, 1H, *J* 7.6, 7.4, H^{Ph}), 8.60 (s, 1H, HCN). ^{13}C NMR: δ 8.52 (s, $C_5\mathit{Me}_5$), 50.40 (NMe), 51.91, 55.97, (2x OMe), 96.60 (d, $J_{Rh\text{-}C}$ 26.0 Hz, C_5Me_5), 126.74, 130.55, 132.04, 132.46, (4x C^{ph}), ,132.57, 133.06 (2x C^{q}), 138.62 ($\mathit{C}CO_2Me$), 174.27 (HC-N), 170.47, 167.55 (2x $\mathit{C}O_2Me$), 176.01 (d, $J_{Rh\text{-}C}$ 131.2 Hz, Rh-C).

Preparation of **(4.19a)**

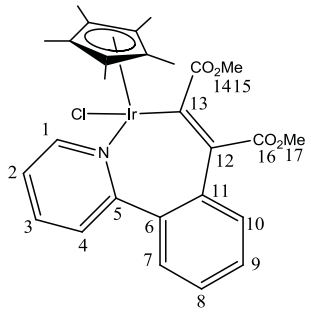

This was prepared in 86% yield as described in reference 18 from **(2.10a)** (15 mg, 0.038 mmol) and DMAD (17 mg, 0.12 mmol). The NMR data are the same as reported but are listed here for comparison with the other complexes.[1]H NMR: δ 1.27 (s, 15H,$C_5\mathit{Me}_5$), 3.64 (s, 3H, COO*Me*), 3.67 (s, 3H, COO*Me*), 7.17 (m, 2H, H^2, H^{10}), 7.27 (dd, 1H, *J* 8.0, 7.5 H^8), 7.30 (dd, 1H, *J* 8.0, 1.5, H^7), 7.42 (dd, 1H, *J* 8.0, 1.5, H^9), 7.49 (dd, 1H, *J* 8.0, 1.5, H^4), 7.75 (ddd, 1H, *J* 8.0, 7.5, 1.5, H^3), 9.40 (dd, 1H, *J* 6.0, 1.5 Hz, H^1). ^{13}C NMR: δ 8.29 ($C_5\mathit{Me}_5$) 50.95 (*Me*OOC)

51.70 (*Me*OOC) 88.94 (C_5Me_5) 123.98 (C^2) 126.42 (C^8) 127.42 (C^4) 128.87 (C^9) 131.68 (C^7) 133.51 (C^{10}) 134.28, 138.08, 138.52 (3x C^q), 140.98 (C^3), 155.31 (C^1), 163.70 (C^q), 164.23, 168.69 (2x CO_2Me) 176.37 (C^{13}).

Preparation of **(4.38a)**

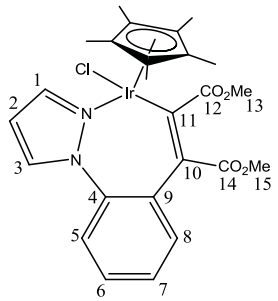

A mixture of **(2.13a)** (50 mg, 0.099 mmol) and DMAD (17 mg, 0.12 mmol) in MeOH (5 ml) was stirred for 1 h at RT. The solution was rotary evaporated to dryness. The solid was washed with hexane and recrystallised from DCM/hexane to give **(4.38a)** (30.0 mg, 51%) as yellow crystals. Anal Calc. For $IrC_{25}H_{28}ClN_2O_4$: C, 46.33, H, 4.35, N, 4.32. Found C 46.33, H 4.41, N 4.25%. ^{1}H NMR: δ 1.31 (s, 15 H, C_5Me_5), 3.64 (s, 3 H, OMe^{13}), 3.69 (s, 3 H, OMe^{15}), 6.51 (t, 1 H, *J* 2.5, H^2), 7.17 (dd, 1 H, *J* 8.0, 1.0, H^5), 7.34 (td, 1 H, *J* 8.0, 2.0, H^6), 7.43 (m, 2 H, H^7, H^8), 7.81 (dd, 1 H, *J* 2.5, 0.5, H^3), 8.21 (dd, 1 H, *J* 2.5, 0.5, H^1). ^{13}C NMR: δ 8.33 (C_5Me_5), 50.14 (OMe), 51.80 (OMe), 89.34 (C_5Me_5), 108.84 (C^2), 127.29 (C^5), 127.49, 128.68 ($C^{7,8}$), 133.21 (C^6), 134.37 (C^3), 132.30, 136.88, 138.45 ($C^{4,9,10}$), 145.48 (C^1), 167.64, 168.08 (2 x CO_2Me), 176.15 (C^{11}). ES-MS *m/z* 613 $[M\text{-}Cl]^+$, FAB-MS *m/z* 613 $[M\text{-}Cl]^+$, 648 $[M]^+$.

Preparation of **(4.38b)**

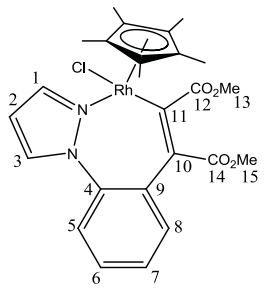

A mixture of **(2.13b)** (50 mg, 0.12 mmol) and DMAD (14 mg, 0.12 mmol) in MeOH (5 ml) was stirred for 5 h at RT. The solution was rotary evaporated to dryness. The product was washed with hexane and recrystallised from DCM/hexane to give **(4.38b)** (55.0 mg, 81%) as yellow crystals. Anal Calc. for $RhC_{25}H_{28}ClN_2O_4$: C 53.73, H 5.05, N, 5.01 found C 53.53, H 5.18, N 4.81%.^{1}H NMR: δ 1.30 (s, 15H, Cp*), 3.64 (s, 3H, OMe^{13}), 3.67 (s, 3H, OMe^{15}), 6.50 (t, 1H, *J* 2.5, H^2), 7.20 (dd, 1H, *J* 8.0, 1.0, H^5), 7.36 (ddd, 2H, *J* 8.0, 6.0, 2.0, H^6), 7.46 (m, 2H, H^7 H^8), 7.82 (dd, 1H, *J* 2.5, 0.5, H^3),

8.27 (dd, 1H, *J* 2.5, 0.5, H^1).^{13}C NMR (500Mhz): 8.57 (C_5Me_5), 50.35 (OMe^{13}), 51.88 (OMe^{15}), 96.89 (d, J_{RhC} 25, C_5Me_5), 108.94 (C^2), 127.44 (C^5), 127.68 (C^6), 128.61, 133.20 ($C^{7,8}$), 134.53 (C^3), 130.94, 136.99, 137.10 ($C^{4,9,10}$), 146.26 (C^1), 166.37, 174.39 (2 x CO_2Me), 181.60 (d, J_{RhC} 135, C^{11}). ES-MS *m/z* (M-Cl) 523, FAB-MS *m/z* 523 $[M-Cl]^+$

Preparation of **(4.38c)**

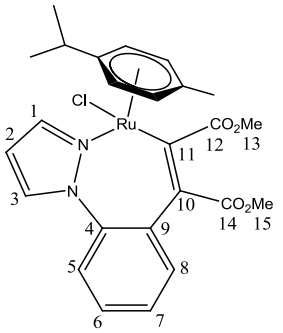

A mixture of **(2.13c)** (39 mg, 0.09 mmol), DMAD (16 mg, 0.13 mmol) in MeOH (5 ml) was stirred for 18 hours at room temperature, under N_2. The solution was rotary evaporated to dryness. The product was crystallised from DCM/hexane to give **(4.38c)** (41.0 mg, 78%) as brown crystals. Anal Calc. for $RuC_{25}H_{27}ClN_2O_4 \bullet CH_2Cl_2$: C 49.74, H 4.50, N 4.55 found C 49.89, H 3.53, N 4.13%. ^{1}H NMR: δ 1.06 (d, *J* 7.0, 3H, CH*Me*Me`), 1.16 (d, *J* 7.0, 3H, CHMe*Me'*), 2.11 (s, 3H, Me(Cy)), 2.64 (sept, *J* 7.0, 1H C*H*MeMe′), 3.63 (s, 3H, OMe), 3.64 (s, 3H, OMe), 4.12 (d, 1H, *J* 5.5, pcy), 4.44 (d, 1H, *J* 5.5, pcy), 4.54 (d, 1H, *J* 5.5, pcy), 5.52 (d, 1H, *J* 5.5, pcy), 6.47 (t, 1H, *J* 2.0, H^2), 7.19 (d, 1H, *J* 8.0, H^5), 7.41 (td, 1H, *J* 8.0, 1.5, H^6), 7.51 (m, 2H, H^7, H^8), 7.78 (d, 1H, *J* 1.5, H^3), 8.38 (d, 1H, *J* 1.5, H^1), ^{13}C NMR: δ 18.80 (*Me*(Cy)), 22.64 (*Me*Me'CH), 22.97 (Me*Me'*CH), 30.94 (MeMe'*C*H), 50.10, 51.78 (2 x OMe), 80.71, 82.40, 83.07, 92.81 (4 x *C*H, pcy), 102.84 (C^q, pcy), 108.35 (C^3), 109.37 (C^q, pcy), 126.38 (C^5), 127.45 (C^6), 128.54, 132.90 ($C^{7,8}$), 134.22 (C^2), 130.66, 137.41, 139.68 ($C^{4,9,10}$), 145.25 (C^1), 164.69, 175.47 (2 x CO_2Me), 190.94 (C^{11}). ES-MS *m/z* 521 $[M-Cl]^+$, FAB-MS *m/z* 556 $[M]^+$, 521 $[M-Cl]^+$.

Preparation of **(4.39a)**

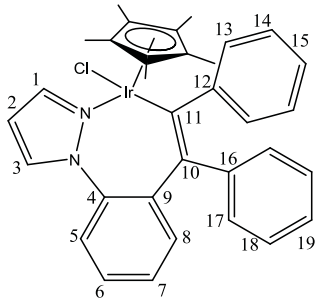

A mixture of **(2.13a)** (50 mg, 0.099 mmol) and diphenylacetylene (19 mg, 0.11 mmol) in MeOH (5 ml) was stirred for 3 h at RT. The solution was rotary evaporated to dryness. The product was washed with hexane and recrystallised from $CHCl_3$/hexane to give **(4.39a)** (42.0 mg, 62%) as yellow crystals. Anal Calc. for $IrC_{33}H_{32}N_2Cl{\bullet}CHCl_3$; C 50.81, H 4.14, N 3.49 found C 50.81, H 4.28, N 3.40%. ^{1}H NMR: δ 1.36 (s, 15H, Cp*), 6.56 (t, 1H, *J* 2.5, H^2), 6.67 (t, 1H, *J* 7.0, Ph), 6.71 (dd, 2H, *J* 8.0, 1.5, Ph), 6.83 (tt, 1H, *J* 7.5, 1.5, Ph), 6.91 (td, 2H, *J* 7.0, 1.0, Ph), 7.18 (m, 1H, Ph), 7.20 (t, 1H, *J* 2.0, Ph), 7.22 (d, 1H, *J* 1.0, Ph), 7.24 (dd, 1H, *J* 5.0, 5.5, Ph), 7.26 (t, 1H, *J* 2.5, Ph), 7.34 (m, 2H, Ph), 7.52 (m, 1H, Ph), 7.91 (dd, *J* 2.5, 1.0, 1H, H^3), 8.41 (dd, J 2.5, 1.0, 1H, H^1). ^{13}C NMR: δ 8.79 ($C_5\mathit{Me}_5$), 88.46 (C^{18}), 108.36 (C^2), 122.79, 124.34, 125.43, 126.51, 126.64, 131.60, 131.80 (CH, Ph), 133.77 (C^3), 134.45 (CH, Ph), 136.82, 138.54 (Ar C^q or C^{10}), 144.62 (C^1), 145.19, 147.65, 154.22, (Ar C^q or C^{10}), 161.23 (C^{11}). ES-MS *m/z* 647 $[M\text{-}Cl]^+$, FAB-MS *m/z* 649 $[M\text{-}Cl]^+$, 684 $[M]^+$

Preparation of (**4.39b)**

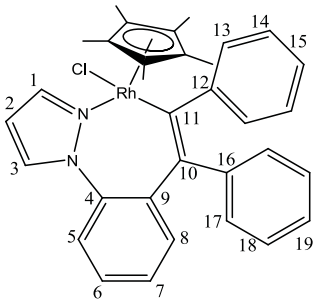

A mixture of **(2.13b)** (70 mg, 0.17 mmol) and PhC≡CPh (33 mg, 0.18 mmol) in MeOH (7 ml) was stirred at room temperature for 3 h. The solution was rotary evaporated to dryness and the solid was dissolved in DCM and filtered through celite. The filtrate was evaporated to dryness and the solid was washed with hexane to give **(4.39b)** (80 mg, 81 %) as an orange solid. Anal.Calc for $RhC_{33}H_{32}ClN_2$: 66.62, H 5.42, N 4.71. Found: C 66.53, H 5.41, N 4.79%.

^{1}H NMR: δ 1.35 (s, 15H, Cp*), 6.56 (t, 1H, *J* 2.5, H^{2}), 6.72 (m, 4H, Ph), 6.85 (m, 2H, Ph), 6.92 (m, 3H, Ph), 7.25 (m, 5H, Ph), 7.92 (dd, 1H, *J* 3, 0.5, H^{3}), 8.56 (dd, 1H, *J* 2, 1, H^{1}). ^{13}C NMR: δ 9.07 (C_5Me_5), 96.09 (d, J_{RhC} 6.5, C_5Me_5), 108.40 (C^{2}), 123.10, 124.55, 125.92, 126.57, 127.01, 128.40, 131.13 (CH, Ph), 133.77 (C^{3}), 134.54 (CH, Ph), 136.89, 137.04, 143.25 (Ar C^{q} or C^{10}), 145.78 (C^{1}), 146.71, 152.66 (Ar C^{q} or C^{10}), 176.08 (d, J_{RhC} 30.5, C^{11}). ES-MS: *m/z* 559 $[M\text{-}Cl]^{+}$. MS-FAB: *m/z* 594 $[M]^{+}$, 559 $[M\text{-}Cl]^{+}$.

Preparation of **(4.39c)**

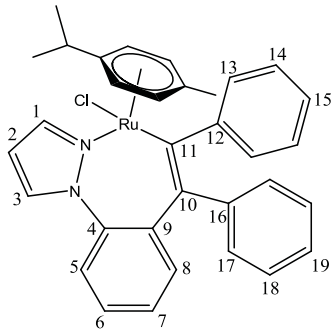

A mixture of **(2.13c)** (50 mg, 0.12 mmol) and diphenylacetylene (23 mg, 0.13 mmol) in MeOH (5 ml) was stirred for 1 h at RT. The solution was rotary evaporated to dryness. The product was washed with hexane and recrystallised from DCM/hexane to give **(4.39c)** (30.0 mg, 42%) as brown crystals. Anal Calc. for $RuC_{33}H_{31}N_2Cl$ % C 66.94, H 5.28, N 4.73 found C 66.95, H 5.34, N 4.65%. ^{1}H NMR: δ 1.08 (d, *J* 7.0, 3H, CH*Me*Me'), 1.23 (d, *J* 7.0, 3 H, CHMe*Me'*), 2.44 (s, 3H, Me, pcy), 2.79 (sept, 1H, *J* 7.0, C*H*MeMe'), 3.48 (dd, 1H, *J* 6.0, 1.0, pcy), 4.49 (dd, 1H, *J* 6.0, 1.0, pcy), 4.63 (dd, 1H, *J* 6.0, 1.0, pcy), 5.54 (dd, 1H, *J* 6.0, 1.0, pcy), 6.50 (t, 1H, *J* 2.5, H^{2}), 6.75 (m, 4H, Ph), 6.86 (tt, 1H, *J* 7.0, 1.5, Ph), 6.93 (tm, 3H, *J* 7.0, Ph), 7.22 (dt, 1H, *J* 7.0, 1.0, H^{8}), 7.26 (m, 1H, $H^{6,7}$), 7.29 (m, 1H, $H^{6,7}$), 7.30 (m, 2H, Ph), 7.34 (m, 1H, H^{5}), 7.85 (dd, 1H, *J* 2.5, 1.0, H^{3}), 8.57 (dd, 1H, *J* 2.5, 1, H^{1}) ^{13}C NMR δ 19.48 (*Me,* Cy), 23.04 (*Me*Me'CH), 23.46 (Me*Me'*CH), 31.21 (MeMe'*C*H), 75.14, 78.71, 80.91, 96.25 (4 x *C*H, pcy), 103.65 (Cq, pcy), 107.69 (C^{2}), 110.22 (Cq, pcy), 122.99, 124.53 , 125.36, 125.76, 126.19, 127.04, 128.00, 128.34, 131.41 (CH, Ph), 133.24 (C^{3}), 133.55 (C^{5}), 137.40, 137.57 (Ar C^{q} or C^{10}), 143.98 (C^{1}), 145.90, 146.62, 152.32 (Ar C^{q}, or C^{10}), 183.19 (C^{11}). ES-MS *m/z* 557 $[M\text{-}Cl]^{+}$, FAB-MS *m/z* 557 $[M\text{-}Cl]^{+}$

Reaction of **(2.13a)** with phenylacetylene in the presence of KPF_6

The complex **(2.13a)** (20.0 mg, 0.03 mmol) was dissolved in MeOH (5 ml), and KPF_6 (14.4 mg, 0.07 mmol) and phenylacetylene (4.0 mg, 0.03 mmol) were added under N_2. The reaction was monitored by ES-MS spectrometry. After 2 h. another equivalent of phenylacetylene was added and the reaction was stirred for a further 2h. The solution was rotary evaporated and washed with hexane. Crystallisation and chromatography failed to give any pure product. The ^{1}H NMR spectrum and ES-MS spectra showed a mixture of species were formed and significant features are discussed in the results and discussion section.

Preparation of **(4.40b)**

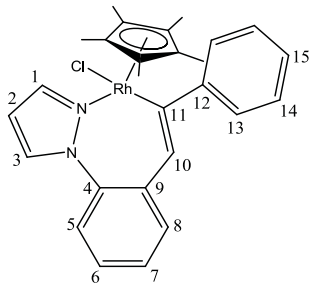

A mixture of **(2.13b)** (66 mg, 0.16 mmol) and PhC≡CH (18 mg, 0.17 mmol) in MeOH (7 ml) was stirred at room temperature for 2 h. The solution was rotary evaporated to dryness. The solid was dissolved in DCM and filtered through celite. The filtrate was evaporated to dryness and the crude product was purified by passing through a short silica column, using DCM as the first eluent and MeOH/DCM (1:9) as the second eluent. The second fraction was rotary evaporated to dryness to give **(4.40b)** (30 mg, 36 %) as an orange solid. Anal.Calc for $RhC_{27}H_{28}ClN_2$: C 62.50, H 5.44, N 5.40. Found: C 62.58, H 5.34, N 5.36%. ^{1}H NMR: δ 1.30 (s, 15H, Cp*), 6.48 (t, 1H, *J* 2.5, H^2), 7.05 (m, 1H, H^{15}), 7.07 (s, 1H, H^{10}), 7.15 (m, 4H, H^{13} H^{14}), 7.24 (m, 2H, H^5, H^6), 7.39 (ddd, 1H, *J* 8.0, 6.0, 2.0, H^7) 7.46 (dt, 1H, *J* 8.0, 1.0, H^8), 7.76 (dd, 1H, *J* 2.5, 1.0, H^3), 8.46 (dd, 1H, *J* 2.5, 1.0, H^1).^{13}C NMR: 9.21 ($C_5\mathit{Me}_5$), 95.82 (d, J_{RhC} 25, C_5Me_5), 108.41 (C^2), 124.77 (C^{15}), 125.57, 126.17 ($C^{5,6}$), 126.68, 126.88 ($C^{13,14}$), 128.10 (C^7), 128.35 (C^{10}), 132.81 (C^8), 134.26 (C^3), 135.27, 138.38, 152.85 (C^q, $C^{4,9,12}$), 145.48 (C^1), 178.64 (d, J_{RhC} 125, C^{11}). ES-MS *m/z* 483 $[M\text{-}Cl]^+$

Reaction of **(2.13c)** with phenylacetylene

The complex **(2.13c)** (50 mg, 0.12 mmol) was dissolved in MeOH (5 ml). Phenylacetylene was then added (12.2 mg, 0.12 mmol) and the mixture was stirred for one hour. The ^{1}H NMR spectrum showed the presence of several species none of which could be completely identified. The significant features of the ^{1}H NMR and ES-MS spectra are described in the result and discussion section (**4.2.1.3)**.

Reaction of **(2.10a)** with diphenylacetylene

The complex **(2.10a)** (50 mg, 0.09 mmol) was dissolved in a mixture of DCM (2 ml) and MeOH (2 ml). Diphenylacetylene was then added (17.2 mg, 0.09 mmol) and the mixture was stirred for 30 min. The ^{1}H NMR spectrum showed the presence of several species none of which could be completely identified. The significant features of the ^{1}H NMR and ES-MS spectra are described in the result and discussion section (**4.2.2)**.

Reaction of **(2.10a)** with phenylacetylene

The complex **(2.10a)** (50.0 mg, 0.09 mmol) was dissolved in a mixture of DCM (2 ml) and MeOH (2 ml), and phenylacetylene (9.9 mg, 0.09 mmol) was added. The reaction was monitored by ES-MS spectrometry. After an hour another equivalent of phenylacetylene was added and the ES-MS spectrum showed mostly double inserted product m/z 686. The significant features of the ^{1}H NMR and ES-MS spectra are described in the result and discussion section (**4.2.2)**

Reaction of **(2.9b)** with diphenylacetylene

The complex **(2.9b)** (50 mgs, 0.13 mmol) was dissolved in MeOH (5ml) and diphenylacetylene was added (22.7 mgs, 0.13 mmol). The reaction was monitored by ES-MS and a peak at *m/z* 296 [isoquinolinum salt]$^{+}$ was observed after 45 min. After 90 min the mixture was then filtered to give a green precipitate (48mg). The significant features of the ^{1}H NMR and ES-MS spectra are described in the result and discussion section (**4.2.2)**

Reaction of **(2.9b)** with phenylacetylene

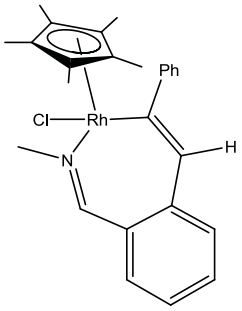

PhC≡CH (10 mgs, 0.09 mmol) was added to a solution of complex **(2.9b)** (50 mgs, 0.13 mmol) in MeOH (5 mL). The reaction was monitored by ES-MS, and after 5 min showed mostly m/z 458 (mono insertion), and traces of **(2.9b)**. Over a period of 30 min an orange precipitate formed which was collected by filtration (12 mgs, 19%). No microanalysis was obtained on this complex. ^{1}H NMR: δ 1.35 (s, 15H, Cp*), 3.89 (s, 3H, Me), 7.11 (m, 2H, H^{Ph}), 7.22 (m, 6H, H^{Ph}), 7.32 (d, 1H, *J* 7.5, H^{6}), 7.40 (dd, 1H, *J* 6.0, 7.0, H^{3}), 8.63 (s, 1H, NCH).

Preparation of **(4.47a)**

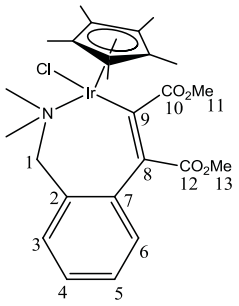

A mixture of **(3.13a)** (50 mg, 0.10 mmol), DMAD (17 mg, 0.12 mmol) in MeOH (5 ml) was stirred for 2 h. The solution was rotary evaporated to dryness and the solid washed with hexane. The product was crystallised from DCM/hexane to give **(4.47a)** (57.0 mg, 88%) as yellow crystals. Calculated $IrC_{25}H_{33}NO_4Cl$ % C 46.98, H 5.20, 2.19 found C 47.11, H 5.29, N 2.11%, ^{1}H NMR: δ 1.13 (s, 15 H, C_5Me_5), 2.70 (s, 3 H, N*Me*Me'), 2.94 (d, *J* 12, 1 H, H^{1}),3.09 (s, 3 H, NMe*Me'*), 3.66 (s, 3 H, OMe^{13}), 3.78 (s, 3 H, OMe^{11}), 3.96 (d, 1 H, *J* 12, H^{1}), 7.23 (td, 1 H, *J* 7.5, 1.0, H^{5}), 7.29 (d, 1 H, *J* 7.5, H^{6}), 7.39 (td, 1 H, *J* 7.5, 1.0, H^{4}), 7.46 (d, 1 H, *J* 7.5, H^{3}).^{13}C NMR: 8.84 (C_5Me_5), 44.88 (C^{11}), 51.72 (C^{13}), 58.18 (C^{15}), 58.44 (C^{14}), 70.44 (C^{1}), 90.41 (C_5Me_5), 126.00 (C^{5}), 128.07 (C^{4}), 131.62 (C^{6}), 131.80 (C^{3}),, 133.19, 134.62, 144.09 (3x C^{q}), 167.48, 176.90 (2x CO_2Me), 180.43 (C^{9}).

Preparation of **(4.48a)**

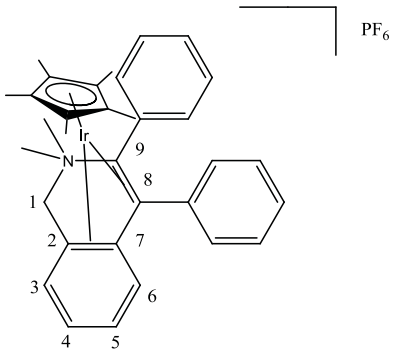

This was prepared following a previous method.[38] A mixture of **(3.13a)** (70 mg, 0.15 mmol), KPF_6 (50 mg, 0.28 mmol) and diphenylacetylene (25 mg, 0.15 mmol) in MeCN (10 ml) was stirred for 24 h. The solution was filtered through celite and rotary evaporated to dryness and gave a of brown solid (90 mg). ^{1}H NMR($CDCl_3$): δ 1.51 (s, 15 H, C_5Me_5), 2.50 (s, 3 H, NMe*Me'*), 2.82 (s, 3 H, N*Me*Me'), 3.26 (d, 1 H, *J* 13.5, H^1), 3.82 (d, 1 H, *J* 13.5, H^1), 6.15 (d, 1 H, *J* 7.8 H^{ph}), 6.74 (m, 1 H, H^{ph}), 6.79 (m, 2 H, H^{ph}), 6.87 (m, 1 H, H^{ph}), 7.02 (t, 2H, J 7.5, H^{Ph}), 7.28 (m, 2 H, *J* 7.5, 1.5, H^4), 7.43 (m, 4 H, H^{Ph}), 7.71 (d, 1 H, *J* 7.5, H^{Ph}). This is not in agreement with the NMR data reported previously in CD_3CN (see below).

Preparation of **(4.49a)**

The complex **(4.48a)** was dissolved in CD_3CN (0.5 ml).

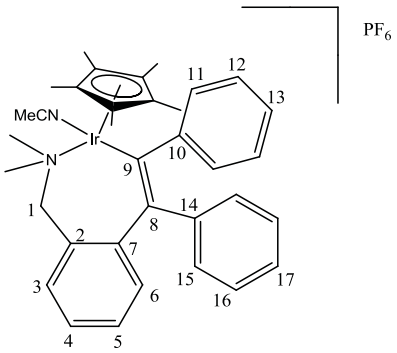

^{1}H NMR(CD_3CN): δ 1.28 (s, 15 H, C_5Me_5), 2.81 (s, 3 H, NMe*Me'*), 3.21 (s, 3 H, N*Me*Me'), 3.29 (d, 1 H, *J* 11.5, H^1), 4.42 (d, 1 H, *J* 11.5, H^1), 6.87 (m, 3 H, H^{ph}), 6.94 (tt, 1 H, *J* 7.5, 1.5, H^{ph}), 7.04 (t, 2 H, *J* 8.0, H^{ph}), 7.09 (m, 3 H, H^{ph}), 7.23 (td, 1 H, *J* 7.5, 1.5, H^4), 7.32 (td, 1 H, *J* 7.5, 1.5, H^5), 7.44 (m, 1 H, H^3), 7.48 (dd, 1 H, *J* 7.5, 1.0, H^6), 7.57 (m, 1 H, H^{ph}). ^{13}C NMR: 8.43 (C_5Me_5), 57.90 (CH_2NMeMe'), 58.52 (CH_2NMeMe'), 69.98 (CH_2NMeMe'), 92.57 (C_5Me_5), 125.18 (CH, ph), 125.47 (C^4), 126.74, 127.28 (2x CH, Ph), 129.22 (C^5), 129.32 (C^3),130.64, 131.68 (2x CH, ph), 132.20(C^6), 132.86 (CH, Ph), 133.59, 141.62, 147.17, 148.72, 152.93 (5x C^q), 154.30 (C^9)

Preparation of **(4.50a)**

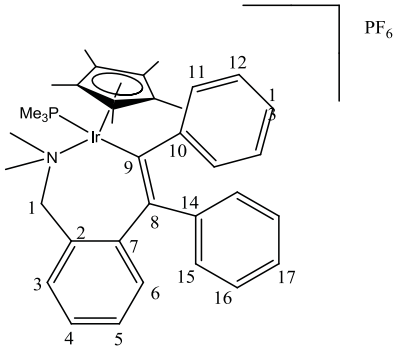

To **(4.48a)** (44mg, 0.05 mmol) in DCM (5 ml), PMe_3 (4.9 mg, 0.06mmol) was added. The mixture was stirred for 1h. The solvent was evaporated and the mixture washed with hexane. 20 mg of brown solid was collected. Further attempts of crystallisation DCM/hexane led to decomposition. ^{1}H NMR: δ 1.34 (d, 9 H, *J* 10.1, PMe_3), 1.52 (d, 15 H, *J* 1.5, C_5Me_5), 2.33 (s, 6 H, NMe_2), 3.48 (d, 3 H, *J* 13, H^1), 4.07 (d, 1 H, *J* 11.5, H^1), 6.68 (t, 1 H, *J* 7.5, H^1), 6.76 (m, 4 H, H^{ph}), 6.88 (m, 1 H, H^{ph}), 6.96 (t, *J* 7.5, 1 H, H^{ph}), 7.14 (m, 2 H, H^{ph}), 7.35 (m, 1 H, H^{ph}), 7.41 (d, 1 H, *J* 7.5, H^{ph}), 7.48 (d, 1 H, *J* 7.0, H^{ph}) ^{31}P NMR δ -37. ES-MS *m/z* 716 $[M]^+$

Preparation of **(4.51a)**

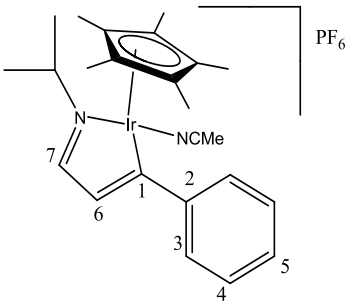

(2.17a) (50mg, 0.09mmol) was dissolved in DCM (5 ml), MeCN (49 µl) and $AgPF_6$ (35mg, 0.14 mmol) were added. The mixture was stirred for 4 h at RT and filtered through celite. The product **(4.51a)** was precipitated as a black solid (50mg, 78%) from DCM/Hexane. Anal. Calc. for $IrC_{24}H_{32}F_6N_2P$: C, 42.04, H, 4.70, N, 4.09. Found C, 41.95, H, 4.60, N, 3.84%. ^{1}H NMR: δ 1.40 (d, 3 H, *J* 7.0, CH*Me*Me), 1.51 (d, 3 H, *J* 7.0, CHMe*Me*), 1.55 (s, 15 H, C_5Me_5), 2.59 (s, 3 H, *Me*CN), 4.17 (sep, 1 H, *J* 7.0, C*H*MeMe), 6.83 (d, 1H, *J* 2.0, H^6), 7.21 (br s, 1 H, H^4), 7.23 (br d, 1 H, *J* 7.0, H^4), 7.29 (tt, 1 H, *J* 7.5, 1, H^5), 7.38 (d, 1 H, *J* 7.5, H^3), 7.40 (d, 1 H, *J* 7.5, H^3), 8.12 (br s, 1H, H^7). ^{13}C NMR: 3.57 (Me*CN*), 8.63 (C_5Me_5), 22.69 (CH*Me*Me), 24.04 (CHMe*Me*), 59.91 (C*H*MeMe), 31.07 (*Me*CN), 92.67 (C_5Me_5), 120.81 (Me*C*N), 126.30 (C^4), 128.28

(C^5), 128.32 (C^3), 132.03 (C^6), 146.63 (C^2), 172.88 (C^7), 197.13(C^1). ES-MS *m/z* 500 $[M\text{-}MeCN]^+$, 541 $[M]^+$, FAB-MS *m/z* 500 $[M\text{-}MeCN]^+$, 541 $[M]^+$.

Preparation of **(4.53a)**

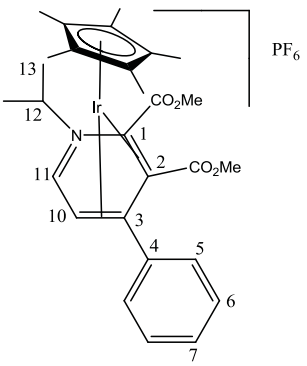

(4.51a) (55mg, 0.08 mmol) was dissolved in DCM (15 ml), DMAD was added (17 mg, 0.12 mmol) and the mixture was refluxed for 20 h. The solvent was evaporated to dryness and the mixture washed with hexane. The product **(4.53a)** was crystallised from DCM/hexane (20 mg, 40%). Anal. Calc. for $IrC_{24}H_{32}F_6N_2P$: C, 42.04, H, 4.70, N, 4.09 Found C, 42.81, H, 4.50, N, 1.67%. ^{1}H NMR: δ 1.12 (d, 3 H, *J* 6.5, CH*Me*Me), 1.51 (d, 3 H, *J* 6.5, CHMe*Me*), 1.81 (s, 15 H, C_5Me_5), 3.80 (s, 3 H, OMe), 3.88 (s, 3 H, OMe), 4.55 (m, 2 H, $H^{10,12}$), 7.41 (m, 3 H, $H^{6,7}$), 7.47 (m, 2 H, H^5), 8.68 (d, 1 H, *J* 4.5, H^{11}). ^{13}C NMR: 8.93 (C_5Me_5), 20.86 (CHMe*Me*), 22.76 (CH*Me*Me), 52.28 (C^{12}), 52.39, 53.48 (2xOMe), 55.68 (C^{10}), 74.01 (C^3), 94.70 (C_5Me_5, C^2), 95.68 (C^1), 129.00, 129.26, 129.95, 132.25 (C^{Ph}), 165.76, 167.76 (2x *C*O_2Me), 173.83 (C^{11}). ES-MS *m/z* 642 $[M]^+$, FAB-MS *m/z* 642 $[M]^+$.

Crystallography

Data for all the complexes were collected on a Bruker APEX 2000 CCD diffractometer. Details of data collection, refinement and crystal data are listed in the attached CD. The data were corrected for Lorentz and polarisation effects and empirical absorption corrections applied. Structure solution by Patterson methods and structure refinement on F^2 employed SHELXTL version 6.10. Hydrogen atoms were included in calculated positions (C-H = 0.96 Å) riding on the bonded atom with isotropic displacement parameters set to 1.5 U_{eq}(C) for methyl H atoms and 1.2 U_{eq}(C) for all other H atoms. All non atoms were refined with anisotropic displacement parameters.

4.5 Bibliography

[1] D. Alberico, M. E. Scott, and M. Lautens, *Chem. Rev.*, 2007, **107**, 174.

[2] F. Kakiuchi and T. Kochi, *Synthesis*, 2008, 3013.

[3] J. C. Lewis, R. G. Bergman, and J. A. Ellman, *Acc. Chem. Res.*, 2008, **41**, 1013.

[4] V. Ritleng, C. Sirlin, and M. Pfeffer, *Chem. Rev.*, 2002, **102**, 1731.

[5] S. Murai, F. Kakiuchi, S. Sekine, Y. Tanaka, A. Kamatani, M. Sonoda, and N. Chatani, *Nature*, 1993, **366**, 529.

[6] F. Kakiuchi, Y. Yamamoto, N. Chatani, and S. Murai, *Chem. Lett.*, 1995, 681.

[7] F. Kakiuchi, M. Yamauchi, N. Chatani, and S. Murai, *Chem. Lett.*, 1996, 111.

[8] F. Kakiuchi, T. Sato, M. Yamauchi, N. Chatani, and S. Murai, *Chem. Lett.*, 1999, 19.

[9] M. Miura, T. Tsuda, T. Satoh, and M. Nomura, *Chem. Lett.*, 1997, **26**, 1103.

[10] M. Miura, T. Tsuda, T. Satoh, S. Pivsa-Art, and M. Nomura, *J. Org. Chem.*, 1998, **63**, 5211.

[11] K. Ueura, T. Satoh, and M. Miura, *Org. Lett.*, 2007, **9**, 1407.

[12] K. Ueura, T. Satoh, and M. Miura, *J. Org. Chem.*, 2007, **72**, 5362.

[13] N. Umeda, H. Tsurugi, T. Satoh, and M. Miura, *Angew. Chem., Int. Ed.*, 2008, **47**, 4019.

[14] T. Fukutani, N. Umeda, K. Hirano, T. Satoh, and M. Miura, *Chem. Commun.*, 2009, 5141.

[15] S. Mochida, K. Hirano, T. Satoh, and M. Miura, *J. Org. Chem.*, 2009, **74**, 6295.

[16] M. Shimizu, K. Hirano, T. Satoh, and M. Miura, *J. Org. Chem.*, 2009, **74**, 3478.

[17] M. Yamashita, H. Horiguchi, K. Hirano, T. Satoh, and M. Miura, *J. Org. Chem.*, 2009, **74**, 7481.

[18] L. Li, W. W. Brennessel, and W. D. Jones, *J. Am. Chem. Soc.*, 2008, **130**, 12414.

[19] H. C. L. Abbenhuis, M. Pfeffer, J.-P. Sutter, A. de Cian, J. Fischer, H. L. Ji, and J. H. Nelson, *Organometallics*, 1993, **12**, 4464.

[20] M. Pfeffer, J. P. Sutter, and E. P. Urriolabeitia, *Bull. Soc. Chim. Fr.*, 1997, **134**, 947.

[21] K. Cheng, B. Yao, J. Zhao, and Y. Zhang, *Org. Lett.*, 2008, **10**, 5309.

[22] N. Guimond and K. Fagnou, *J. Am. Chem. Soc.*, 2009, **131**, 12050.

[23] D. A. Colby, R. G. Bergman, and J. A. Ellman, *J. Am. Chem. Soc.*, 2008, **130**, 3645.

[24] W. Ferstl, I. K. Sakodinskaya, N. Beydoun-Sutter, G. Le Borgne, M. Pfeffer, and A. D. Ryabov, *Organometallics*, 1997, **16**, 411.

[25] D. R. Stuart, M. Bertrand-Laperle, K. M. N. Burgess, and K. Fagnou, *J. Am. Chem. Soc.*, 2008, **130**, 16474.

[26] D. L. Davies, J. Fawcett, S. A. Garratt, and D. R. Russell, *Organometallics*, 2001, **20**, 3029.

[27] C. Cao, L. R. Fraser, and J. A. Love, *J. Am. Chem. Soc.*, 2005, **127**, 17614.

[28] H. Kuniyasu, F. Yamashita, T. Hirai, J.-H. Ye, S.-i. Fujiwara, and N. Kambe, *Organometallics*, 2005, **25**, 566.

[29] H. Kuniyasu, T. Kato, S. Asano, J.-H. Ye, T. Ohmori, M. Morita, H. Hiraike, S.-i. Fujiwara, J. Terao, H. Kurosawa, and N. Kambe, *Tetrahedron Lett.*, 2006, **47**, 1141.

[30] R. Hua, H. Takeda, S.-y. Onozawa, Y. Abe, and M. Tanaka, *J. Am. Chem. Soc.*, 2001, **123**, 2899.

[31] H. Kuniyasu, A. Ogawa, S. Miyazaki, I. Ryu, N. Kambe, and N. Sonoda, *J. Am. Chem. Soc.*, 1991, **113**, 9796.

[32] M. R. Meneghetti, M. Grellier, M. Pfeffer, and J. Fischer, *Organometallics*, 2000, **19**, 1935.

[33] D. L. Davies, O. Al-Duaij, J. Fawcett, and K. Singh, *Organometallics*, 2010, **29**, 1413.

[34] J. Vicente, I. Saura-Llamas, J. Turpin, D. Bautista, C. R. r. de Arellano, and P. G. Jones, *Organometallics*, 2009, **28**, 4175.

[35] K. R. Reddy, K. Surekha, G.-H. Lee, S.-M. Peng, and S.-T. Liu, *Organometallics*, 2001, **20**, 5557.

[36] J. Dupont, M. Pfeffer, J. C. Daran, and J. Gouteron, *J. Chem. Soc., Dalton Trans.*, 1988, 2421.

[37] A. M. LaPointe and M. Brookhart, *Organometallics*, 1998, **17**, 1530.

[38] O. Al-Duaij, *PhD thesis, University of Leicester*, 2005.

[39] J. P. Collman, L. S. Hegedus, J. R. Norton, and R. G. Finke, *Principles and Applications of Organotransition Metal Chemistry; University Science Books: Mill Valley, CA,*, 1987

[40] D. L. Davies, O. Al-Duaij, J. Fawcett, M. Giardiello, S. T. Hilton, and D. R. Russell, *Dalton Trans.*, 2003, 4132.

Postgraduate activities

Internal seminars-External speakers

22/11/06 Mini symposium "Aspects of Green Chemistry"

Dr Neil Winterton (University of Liverpool)

"Ionic Liquids: Hype or Help"

Dr Peter Licence (University of Nottingham)

"Ionic Liquids in-vacuo"

Dr Paul Watts (University of Hull)

"The application of micro reactors for improving atom efficient chemical reactions"

30/04/07 Mini symposium *"Metals in Medicine"*

Dr Sofia Pascu (University of Oxford)

"Designing Small Molecule-based Probes for In Vitro Fluorescence Imaging"

Prof. Nils Metzler-Nolte (Rhur-Universitaet Bochum, Germany)

"Labelling of Bioactive Peptide with organometallic Compounds: From Basic Chemistry to Biomedical Application"

Dr Gareth Williams (Durham University)

"Sensing and Imaging with Cell-permeable Luminescent Platinium and Iridium Complexes"

Prof. Chris Orvig (University of British Columbia, Canada)

"Carbohydrate Conjugates in Medicinal Inorganic Chemistry"

09/05/07 Mini-symposium "Aspects of catalysis"

Dr Ian Fairlamb (University of York)

"*Ligand effects in Pd catalysed processes: Importance of conformational flexibility and the exploitation of non-innocent alkene ligands"*

Prof. Simon Woodward (University of Nottingham)

"Organic 'Couplings'via New Metallic Chemistry of Al, Ni, Cu and Zn"

Dr David Willock (University of Cardiff)

"Simulation of adsorption and Reaction at catalyst surfaces"

06/05/08 The RSC Centenary Lecture by Professor Don Tilley (University of California Berkeley)

"New bond activations at transition metal centres: Fundamental studies and applications to Catalysis"

27/06/08 Anniversary research day in university of Leicester

Dr Rob Brown (University of Huddersfield)

"Cleaner Chemistry with Solid Acid Catalysts"

Dr Kevin Hughes (University of Leeds)

"*Mechanism Reduction: Methodologies and Examples"*

Dr Peter Holliman (University of Wales, Bangor)

"Super leaves - using materials chemistry to make clean up with solar energy"

Dr Karl Coleman (University of Durham)

"Chemistry of Carbon Nanotubes"

Dr Craig Rice (University of Huddersfield)

"Reprogrammable Ligands"

Dr Bill Henderson (Waikato University)

"180 Degrees of Coordination Chemistry"

Dr Mike Coogan (Cardiff University)

"Design and Application of Luminescent Rhenium Complexes in Cell Imaging"

Prof Emma Raven (University of Leicester)

"The reactivity of heme in biological systems"

Dr Andrew Russell (University of Reading)

"Symmetry in Synthesis; Obvious and Hidden"

Dr Sean Bew (University of East Anglia)

"Small Rings to Big Rings: Adventures in Asymmetric Synthesis"

Dr Sally Freeman (University of Manchester)

"Phosphorus Chemistry-To Leicester and Beyond"

29/10/08 Dr George Britovsek (Imperial College)

"Tuning the Reactivity of Non-heme Iron Catalysts for the Oxidation of Alkanes"

05/11/08 Dr Paul Davies (Birmingham)

"Organic Synthesis by Gold Catalysed Alkyne Activation"

25/02/09 Prof Martin Wills (University of Warwick)

"Asymmetric Catalysts for the Asymmetric Reduction of Ketones and Imines"

11/03/09 Prof Joe Harrity (University of Sheffield)

"'Development of New Strategies for the Synthesis of Functionalised Synthetic Intermediates"

06/05/09 James Clark (University of York)

"Green Chemistry and the Biorefinery"

Symposia, Conferences and Poster sessions attended

18/03/07 - 20/03/07 **Royal Society of Chemistry – Inorganic Reactions Mechanism Subject Group Meeting**

Three Day Conference at The University of York.

03/09/07 – 07/09/07 **Liverpool Centre for Materials and Catalysis Summer School on Catalysis**

Poster title: "Mechanistic Studies On Cyclometallation"

13/07/08 – 18/07/09 **XXIII international conference on organometallic chemistry Rennes (FR)**

Poster title: "C-H Activation of Pyridine Derivatives by Ir, Rh and Ru, Synthesis and Mechanism"

List of publications

1- Y. Boutadla, O. Al-Duaij, D. L. Davies, G. A. Griffith, and K. Singh, *Organometallics*, 2009, **28**, 433

2- Y. Boutadla, D. L. Davies, S. A. Macgregor, and A. I. Poblador-Bahamonde, *Dalton Trans.*, 2009, 5887.

3- Y. Boutadla, D. L. Davies, S. A. Macgregor, and A. I. Poblador-Bahamonde, *Dalton Trans.*, 2009, 5820.